Università
Ca'Foscari
Venezia

Corso di Dottorato di ricerca

in Scienze dell'Antichità

ciclo XXXI

Tesi di Ricerca

A Reassessment of the Debate on Late Minoan I and interlinked chronologies through Radiocarbon and Comparative Analysis

SSD: L-ANT 01

Coordinatore del Dottorato
ch. prof. Luigi Sperti

Supervisore
ch. prof. Filippo Maria Carinci

Dottorando
Tiziano Fantuzzi
Matricola 825926

Index

Foreword

The present work was done in fulfillment of a Ph.D course at "Scuola Dottorale Interateneo in Scienze dell'Antichità", jointly organised by the Universities of Venice (Ca' Foscari), Udine and Trieste. The work consisted in two separate parts.

1) The first part consisted in the critical re-analysis (and collation) of the available bibliography on the relevant arguments for the dating of the Late Minoan I A eruption at Thera/Santorini and their implications in/for the chronologies of the Aegean, the Levant and (northern) Egypt.
2) The second part consisted in the development of a possible new approach to the analysis of radiocarbon results through the following steps:
    a) critical review of the limits of Bayesian high-precision radiocarbon dating;
    b) development of an alternative algorithm for calibration of sample ^{14}C dates and sequences, based on notions from quantum physics;
    c) creation of an open-source package for rapid and intuitive application of such calibration method (and initial validation).

The "Quantum/Contingency" method developed in the present work (which is fundamentally a derivation of the method described by Weninger, 1986) has then been applied to the radiocarbon record from selected sites of high importance for the debate on the absolute date of the Minoan eruption at Thera/Santorini and of the interlinked MBA/LBA transition and early LBA in Egypt and the Aegean.

All the algorithms developed are/will be online and open-access for users on the site http://c14.bpinfo.org

Acknowledgments

The present author would like to express his greatest gratitude to all the scholars who have contributed in this work with useful comments and discussion, starting from Filippo M. Carinci and Paolo Biagi. A very special thank to Dr. Malcolm Hewitt Wiener and Dr. Judith Weingarten, whose support, comments and advising have been most fundamental in this work and beyond. Special thanks go also to Prof. Bernhard Weninger, Prof. Manfred Bietak, Prof. Christine Lilyquist, Prof. Peter Warren, Prof. Luca Girella, Dr. Kathryn Eriksson, Prof. Francesco Tiradritti, Prof. Irmgard Hein, Prof. Daphna Ben-Tor, Dr. Felix Höflmayer, Dr. Elisabetta Starnini, Prof. Charlotte Pearson, Prof. Renato Nisbet, Dr. Francesco Valletta, Prof. R.S. Merrillees, Prof. Claude Vandersleyen, Prof. James Weinstein, Prof. Dario Calimani, Dr. Gianmarco Alberti, Dr. Sandro Donadi, Dr. Cesare Ravazzi, Dr. Alberto Lezziero, Dr. Michela Leonardi, Dr. Marsia Bealby, Mr. Alejandro Magnoler Gonzalez and Mr. Christopher Lowe for very interesting discussion and confrontation of ideas. A special effort was paid to the choice of the best graphical representation, scaling and graphics as understandability was one of the basic aims of this work (following Weninger, 1986). This was done with the important contribution of Miss Valentina Campagnolo.

The methods and program developed for this study wouldn't have been obtained without the huge work of Dr. Federico Antolini who has supervised all the mathematics and statistics and also wrote a significant part of the code, and Mr. Luca Bertuol who has enhanced the program, found the best methods and approaches to open-source packages programming for the project and developed all the informatics underlying.

Last but not for importance, many thanks to Dr. Veronica Tabaglio who has patiently and painstakingly read the proofs and supported the author in all of his uneasy moments.

Chapter I

Introduction

I.1 Summary

The chronology of the Minoan eruption which occurred at Santorini-Thera (the southernmost island of the Cyclades) in the early Late Bronze Age is a central point for the study of the whole Eastern Mediterranean Bronze Age. The topic has been under discussion since the 1930s (Evans, 1935), and became the object of one of the most-discussed and controversial debates in the history of archaeology since the development of modern radiocarbon dating techniques (see f.e. Kemp and Merrillees, 1980). The present study is aimed at presenting a summary of the many arguments involved and a critical review of the basic sources for both the archaeological and the hard-sciences' interpretation of the available (i.e. published) data.

A detailed description of the arguments for the reconstruction of the relationships on the *longue durée* between Minoan Crete and Egypt (and the Levant), and the possible presence of Minoan specialists (from artisans to diplomatic envoys) in Egypt, is reported on Chapter II. Within this chapter, Paragraph II.1 provides a summary of the arguments and history of the debate over the first contacts between Minoan Crete and Egypt in the Early-Middle Bronze Age and the (hypothetical) african-levantine origin of the Minoan palatial culture(s).

The following Paragraphs II.2-4 describe the evolution of the Minoan-Egyptian interrelations on the basis of the main archaeological evidence so far available, with a detailed description of the Minoan "envoys" represented in the (early) XVIII dynasty Theban tombs (Paragraph II.3) and of the Minoan (and/or minoanizing) paintings found in palatial contexts belonging to the Egyptian and Levantine Middle-to-Late Bronze age (Paragraph II.4).

Chapter III deals with the archaeological arguments and the debate on the absolute

chronology of LM I A and the S.I.P.-N.K. transition in Egypt. As reported by P.M. Warren (2009:181):

> in order to write the history of international relations of the later Middle and the Late Bronze Age in the eastern Mediterranean we need to establish whether, at the time of the Minoan eruption of Santorini, the Egypt which was linked to the Aegean, Cyprus and the Levantine region was that of late Dyn. XIII or earlier Second Intermediate Period on the one hand or that of the early New Kingdom (early Dyn. XVIII) on the other.

A summary of the history of the debate on Aegean LM I A chronology since the late 1970s is reported in Paragraph III.1, while Paragraphs III.2.1-4 discuss the three chronologically most significant Egyptian imports from Aegean LM/LH I A contexts. They consist of three reworked stone vases, one from Akrotiri (Akr* 1800, Paragraph III.2.1), the other two from Mycenae Shaft Graves IV (NM592, Paragraph III.2.2) and V (NM829, Paragraph III.2.3). The chronological conclusions which can be drawn so far from this evidence are discussed in Paragraph III.2.4; the pertaining figures are shown in Appendix II.

The second most important argument for the archaeological dating of the Minoan eruption in the wider eastern Mediterranean context is represented by the pumice lumps that originate from the volcanic event found on the seashores and ancient workshops of northern Egypt and the Levant. The samples, the contexts of the findings and their chronological implications, are discussed in Paragraph III.3.

The third, and probably most important, argument for interlinking the chronology of the final phases of occupation at Akrotiri and Egypt consists in the distribution of Middle Cypriote III to Late Cypriot I A2 wares found in the Aegean, Egypt and several Levantine sites, and in particular Proto-White Slip (PWS) and White Slip I (WS I) ceramic classes. Paragraph III.4 starts with a description of the (now lost) WS I bowl found at Akrotiri and the debate on its relative and absolute dating. A chronological description of the stylistic evolution of PWS to WS I is reported below, along with a detailed summary of the most chronologically significant Cypriot imports from Tell el Dab'a, Egypt, and Levantine sites (in particular Tell el Ajjul), and a discussion of the controversial interpretations in the bibliography. Chronological conclusions follow on Paragraph III.5.

The archaeological arguments for the chronology of Tell el Dab'a, a multi-stratiphied tell

site in north-eastern Egypt, which, through its many interlinkages with Cyprus and the Levantine coast, has become one of the most important – and discussed – topics in the recent debate and the controversial interpretations, are discussed in Chapter IV.

The re-analysis of radiocarbon dating for the two key-sites Tell el Dab'a and Akrotiri is the subject of Chapter V.

Paragraph V.1.1 provides a summary and a critical review of the Bayesian-based radiocarbon chronology suggested for Tell el Dab'a (Kutschera et al., 2012), which constitutes one of the pivotal arguments for the supporters of the Aegean High Chronology (AHC). The whole radiocarbon dataset available for Tell el Dab'a is re-analysed in Paragraph V.1.2, while Paragraph V.1.3 discusses the possibility that the 120 years shift in the absolute chronology of the site advocated by the supporters of the AHC may simply be a reflection of the presence in the samples of residual (stratigraphically reworked) charred seeds from the preceding phases. This reworking could well be both a consequence of ancient re-excavation, mud brick decay and pit digging, as well as an artificial function of the statistical priors applied to reduce the uncertainty in the results. A new quantum-based calibration (see below) is consequently applied to the dataset, and a possible new chronological model for the Tell el Dab'a sequence is suggested.

The radiocarbon dataset for the final phases of occupation of Akrotiri on Santorini ("late" LM I A to Volcanic Destruction Level-VDL) is discussed in Paragraphs V.2.1-2. Paragraph V.2.1 is a summary and a critical review of the Bayesian chronology proposed for the VDL, while Paragraph V.2.2 reports the whole dataset (available) for Akrotiri LM I A contexts and suggests that 1) χ^2 test-based statistic tools which artificially reduce the uncertainty in the results have been inaccurately applied to the dataset, and that 2) a new approach which applies quantum-based calibration in combination with the recently published dendrochronological data by Pearson et al. (2018) provides strong evidence in favour of an eruption date in the early-middle XVI century BC. The radiocarbon dataset for the much-discussed Theran olive tree branch is re-analysed in Paragraph V.2.3 and new results possibly supporting an eruption date as late as 1525 BC (1sigma) are reported.

The systematic differences between the new Pearson et al. (2018) calibration data and the long-established and internationally recommended INTCAL-data for the time-period under study (3450-3649 calBP) are so large (20-50 BP on the ^{14}C-scale) that we must now raise serious doubts as to the interlaboratory integrity of the published INTCAL-data sets, also for other sections of the Holocene.

Final conclusions are outlined in Chapter VI, and the program python code used for the development of the methods and models proposed in this thesis is reported in Appendix I, along with the worked-example including the relevant datasets for Tell el Dab'a and Akrotiri.

I.2 Radiocarbon dating and quantum-based calibration

I.2.1 Radiocarbon dating

^{14}C is one of the three isotopes of carbon which are naturally present on Earth. While the other two (^{12}C and ^{13}C) are stable isotopes, ^{14}C decays radioactively – hence the name *radiocarbon* (Libby, Anderson and Arnold, 1949). The rate of this decay – which Libby and colleagues ultimately estimated at an half-life (t ½) of 5730±30[1] years – does not, as is widely misunderstood, constitute the basis of the dating method. Instead, all so-called *conventional* radiocarbon measurements are based on the (error-free) Libby half-life of 5570 years, whereby the [BP]-scale is defined by convention to be dimensionless: [BP]=1).

^{14}C is produced in the high stratosphere by interaction of nitrogen (^{14}N) with cosmic-rays (see below) following the reaction:

$^{14}N + n \Rightarrow {}^{14}C + p$

(where n is a neutron, and p a proton)

After oxidation to $^{14}CO_2$, radioactive carbon enters the food chain by photosynthesis. Organisms (plants and animals) thus absorb ^{14}C all through their lifetime. When an organism dies, radiocarbon uptake ceases and only decay remains, so the amount of ^{14}C in the organics starts to decrease in a measurable manner. After 10 half-lives (about 50-60.000 years) the amount of radioactive carbon is so reduced that it is no longer measurable, and other dating techniques are to be used. As ^{14}C decays, it emits a weak (160 keV) beta particle and is transformed back into nitrogen by the following reaction:

[1] Known as the empirical half-life, not to be mistaken with the (error-free) so-called *conventional Libby half-life* of 5570 years. In the last decades, it has been observed that the real half-life should be closer to 5700±30 years (Taylor and Bar-Yosef, 2014, with references), but this is irrelevant for radiocarbon dating.

$^{14}C \Rightarrow {}^{14}N + \beta$

Since the decay is constant but spontaneous (i.e. the probability of decay for an atom of ^{14}C in a discrete sample is constant), the analysis of counting data requires the application of statistical methods.

I.2.2 Radiocarbon Calibration

^{14}C age determinations are obtained by measuring the amount of ^{14}C in a sample and comparing that value against the ^{14}C concentration in an appropriate standard (NBS-Oxalic Acid). Since it is impossible to measure *all* of the ^{14}C contained in a sample (or standard), it is necessary to consider the statistical constraints that define the precision of a measurement (Taylor and Bar Yosef, 2014:127). From a physical point of view, radiocarbon decay is a random process (i.e. there is no way of knowing when an individual ^{14}C nucleus will decay), therefore the repetition of measurements of the decay of a large number of ^{14}C nuclei over a relatively long-counting period is required to allow patterns to emerge (Taylor and Bar-Yosef, 2014:128). A great achievement in regard to the amount of carbon required for ^{14}C-measurement was obtained in the late 70's with the introduction of Accelerator Mass Spectrometry (also known as High Energy Mass Spectrometry) which combines the use of a particle accelerator with mass spectrography, allowing direct measurement of the number of ^{14}C nuclei in a sample (i.e. without the need to wait for spontaneous decay), with the result of significantly reducing the counting time and – most importantly – the size of samples required.

^{14}C age values are cited in a format that expresses the calculated age along with an estimate of the experimental or analytical precision (which is sometimes improperly referred to as measurement error). The term *conventional radiocarbon age* applies to ^{14}C age expressions that have been calculated under the assumption that ^{14}C concentration in living organisms in each carbon reservoir have remained constant over the ^{14}C time scale[2]. This means that conventional

[2] «A fundamental assumption of the ^{14}C method is the requirement that natural ^{14}C concentrations in living or

^{14}C values are *not calibrated* (Taylor and Bar Yosef, 2014:26). Earth's natural radiocarbon is produced (mainly) by the collision of cosmic radiations with gaseous components of the atmosphere at the stratospheric level. As a consequence, the ^{14}C activity in a living or zero age organism on a worldwide basis has not remained constant through the ^{14}C time-scale, producing offsets between the measured (conventional) age and the real (calendar vel solar) age[3]. The term "calibration" refers to the conversion of conventional into calendar ages by comparison with known-age proxy data (most importantly dendrochronologically dated tree-rings sequences) that are used to construct the calibration curves (presently: IntCal13, Marine13, SH13).

The reliability of the final results depends on both the degree of accuracy – how close the ^{14}C age estimate is to the true BP-age of the sample – and precision – meant as both experimental (reproducibility of the results) *and* overall precision (taking in account the full range of factors which could influence the results) achievable. Overall accuracy and precision of radiocarbon age determinations may be influenced by four major elements as summarized in Taylor and Bar-Yosef (2014:131):

1) «Contextual elements: anomalies produced by failure to define accurately and precisely the physical relationship between dated samples and target object or phenomenon for which temporal placement [is] sought» (as inaccurate/incomplete geomorphological/stratigraphic analyses, undetected bioturbation, etc.);

---

zero age organisms in a particular carbon reservoir be equivalent to that which has been characteristic of living organisms in that same reservoir over the entire effective dating range of the ^{14}C method. This assumption implies that, over that time interval, there had existed an approximate equilibrium, steady-state, or constant relationship between ^{14}C production and decay rates […] the principal planetary-wide parameters affecting preindustrial ^{14}C concentrations primarily involve (1) changes in the atmospheric production rate of ^{14}C and/or (2) variations in the physical characteristics or exchange rates in various components of the cycle» (Taylor and Bar-Yosef, 2014:44).

[3] «[…] major variations in ^{14}C production rates reflect changes in the cosmic-ray flux in the vicinity of our solar system as well as solar magnetic field changes that modulate the cosmic-ray concentrations within our solar system. Radiocarbon production rate variations are also influenced by changes in the strength or intensity of the dipole magnetic field of our planet, which affects the interaction of cosmic-rays in the vicinity of the earth with the earth's upper atmosphere. Factors that can influence changes in the parameters affecting the movement of ^{14}C within different parts of the earth's carbon cycle include carbon reservoir sizes and rates of transfer of ^{14}C between different carbon reservoirs, the most important being exchange rates of various carbon species between the atmosphere and marine environments» (Taylor and Bar-Yosef, 2014:44).

2) «Compositional elements: anomalies produced by variability in ^{14}C concentrations in carbon-containing components and failure of physical/chemical pre-treatment(s) to isolate indigenous organics and/or successfully exclude exogenous organics» (as undetected natural or post-excavation organics applied);

3) «Systemic elements: anomalies produced by failure to detect violation of one or more physical assumptions on which the ^{14}C dating model rests and/or failure to appropriately calibrate, correct, or normalize values obtained as applied to to a given sample material» (as in undetected reservoir effects, local variations in atmospheric ^{14}C content, inter and intra specific variations in carbon absorption);

4) «Measurement elements: anomalies produced by laboratory-based errors» (as measurement and/or instrumental errors).

Since these conditions are not always all verifiable at the first stage, any attempt to use statistic tools which artificially reduce the variability in the dataset (as is the case of R_Combine applied to the Theran eruption data below, Chapter V.2) will not only run the risk of resulting in «*unrealistic chronological expectations and a spurious precision*» (Taylor and Bar-Yosef, 2014:160; emphasis in the original), but also mask the real properties of the data and make it difficult to turn back to the specific contextual information (archaeological, biochemical, environmental conditions) that need to be reviewed to address the explanation of apparent (or real) offsets.

Moreover, in recent years it has become increasingly clear that the mathematical operation of age-calibration for radiocarbon dates is more complicated than previously anticipated. This is due to the existence of many alternative (i.e. multiple) age-readings for each ^{14}C-date on the tree-ring calibration curve, but which are all logically exclusive. Hence, ^{14}C-ages have some very special statistical properties that are otherwise only expected to occur in quantum systems (e.g. atoms, elementary particles). Such "quantum" properties include the artificial clustering of dates and ages on both time-scales, the existence of multiple chronological solutions even for very large data sets, and – last not least – the seemingly contradictory yet natural (system-inherent) inversion of ages, on both time-scales (cfr. Weninger, 1986; Weninger et al., 2011, 2015).

I.2.3 Quantum calibration methods in http://c14.bpinfo.org

In practical terms, the mere application of traditional statistics, whether in its inferential or Bayesian form, to determine the probability distribution of a set of dates (particularly when the dating target is a single event, or relatively short time-period) results in an oversimplification of the problem. The approach proposed here is to look at a date in terms of *range* (or interval) rather than *probability distribution function* (*pdf*). This implies verifying the *compatibility* of dates believed to be contemporary, both on the uncalibrated and the calibrated scale (henceforth "contingency"), instead of *combining* those same dates to produce a unique synthetic result.

Each radiocarbon determination is hereby represented as a uniform pdf. ^{14}C laboratories usually produce a mean and a standard deviation for radiocarbon determinations (see above). These parameters uniquely identify a normal pdf for the uncalibrated date. The majority of current calibration algorithms use area-normalised pdfs in their analysis. However, due to the multiple readings of all ^{14}C-ages the very concept of classical probability becomes problematic, for which reason we now put focus on the overall range of the ^{14}C measurements/dates, on the calendric scale. In this approach, the mean and standard deviations of the dates are used to determine the range, which consists of a certain number of standard deviations that are older, and younger, than the mean value. In detail, the method is as follows.

The uncalibrated interval, which develops along the *y* direction, is projected onto the calibration curve and down to the *x*-axis to determine the corresponding calibrated interval. The calibrated interval consists of all the calibrated years (bins) that, when back-calibrated, fall in the uncalibrated range hypothesized initially (Figs 1-5 below). Other calibration software like OxCal start from an uncalibrated normal pdf to produce a calibrated pdf during the calibration process. The vertical dimension of the calibrated pdf, i.e. the curve height at each point, is related to probability as in any pdf curve. However, such curve height is due not just to the initial shape of the normal pdf curve, with higher probability around the mean value, but also to the many changes of slope and uncertainties ("thickness") of the calibration curve. Therefore, the calibration curve substantially influences the distribution of probability of date. The methods presented here produce a graphically similar result, i.e. a multi-modal curve, but, since the differences in height are an artifact of the differences in the "thickness" of the calibration curve, curve heights have a very different meaning (i.e. the differences in height depend on how

much of the calibration curve is “intercepted” by the uncalibrated interval).

Basically, the calibrated interval curve gives for each year a rough estimate of the likelihood that a sample dating to that year has the ^{14}C content measured for the sample, as compared to other years of the calibrated interval.

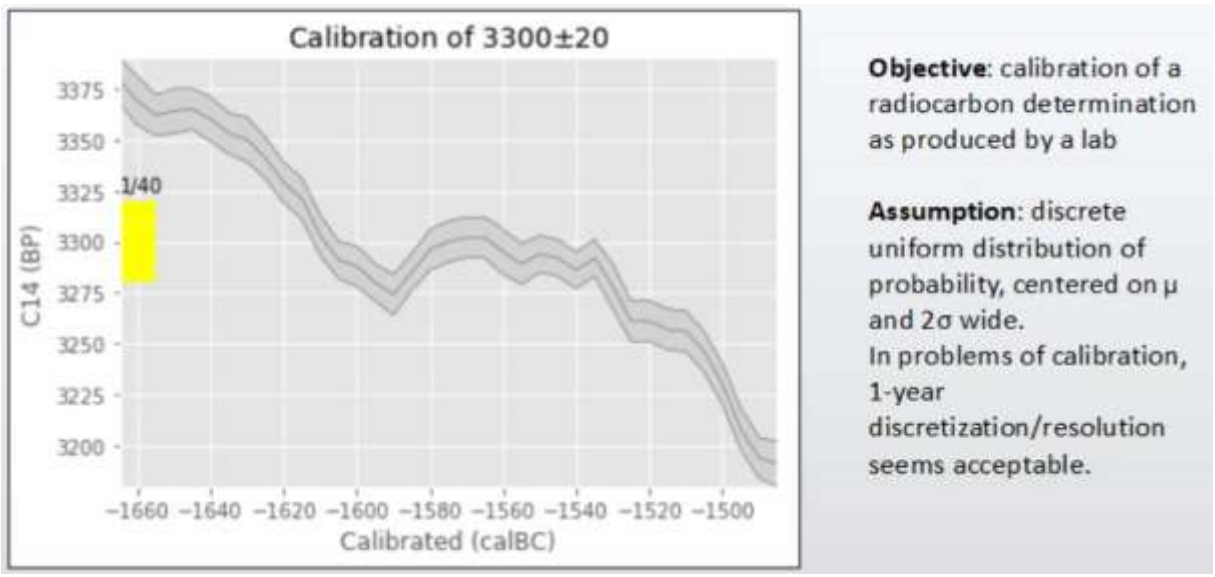

Fig. 1

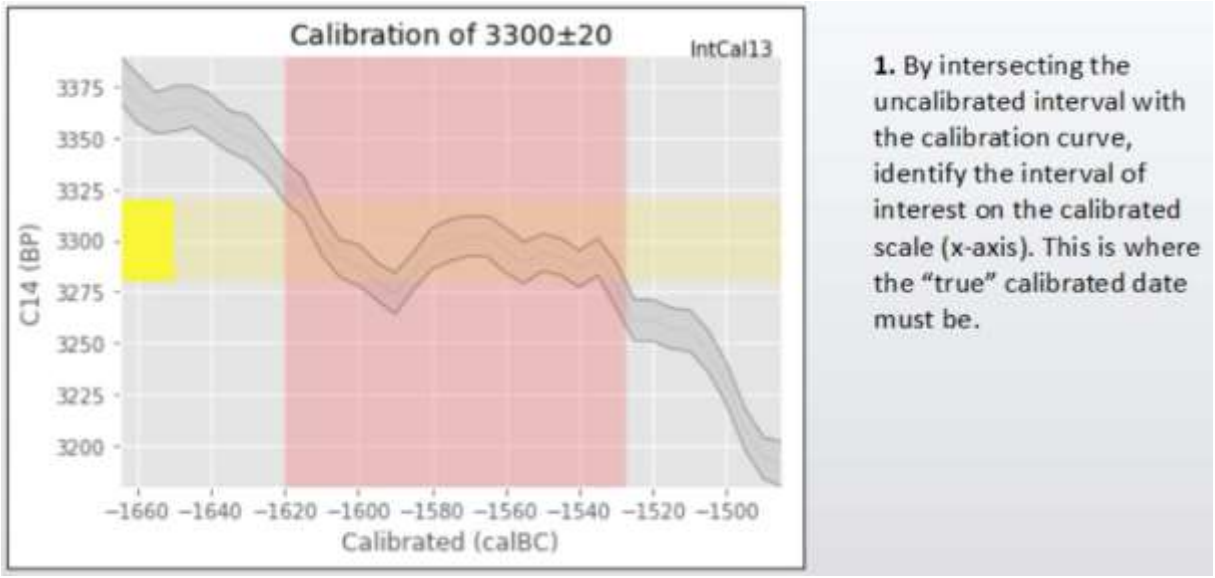

Fig. 2

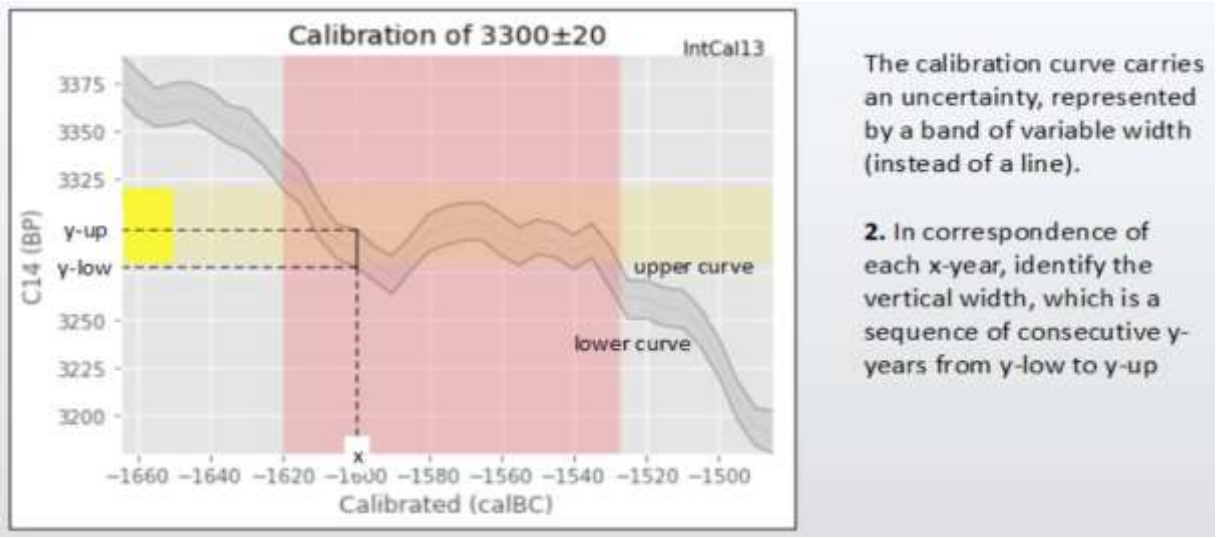
Calibration of 3300±20
IntCal13
3375
3350
3325
y-up
y-low
C14 (BP)
3250
3225
3200
upper curve
lower curve
x
−1660 −1640 −1620 −1600 −1580 −1560 −1540 −1520 −1500
Calibrated (calBC)
The calibration curve carries an uncertainty, represented by a band of variable width (instead of a line).
2. In correspondence of each x-year, identify the vertical width, which is a sequence of consecutive y-years from y-low to y-up

Fig. 3

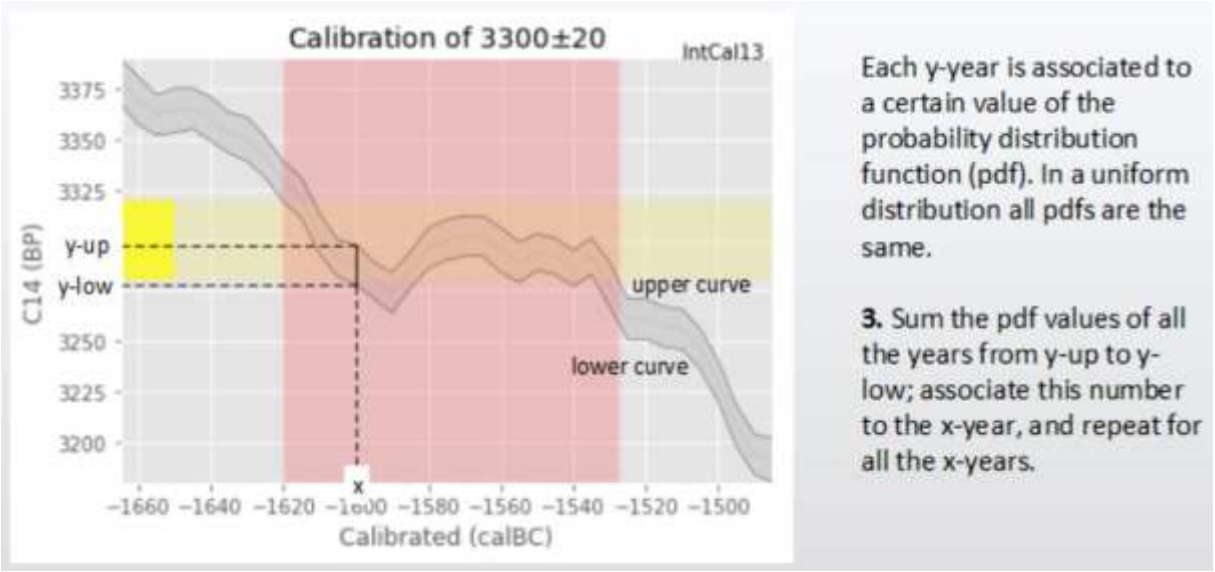
Calibration of 3300±20
IntCal13
3375
3350
3325
y-up
y-low
C14 (BP)
3250
3225
3200
upper curve
lower curve
x
−1660 −1640 −1620 −1600 −1580 −1560 −1540 −1520 −1500
Calibrated (calBC)
Each y-year is associated to a certain value of the probability distribution function (pdf). In a uniform distribution all pdfs are the same.
3. Sum the pdf values of all the years from y-up to y-low; associate this number to the x-year, and repeat for all the x-years.

Fig. 4

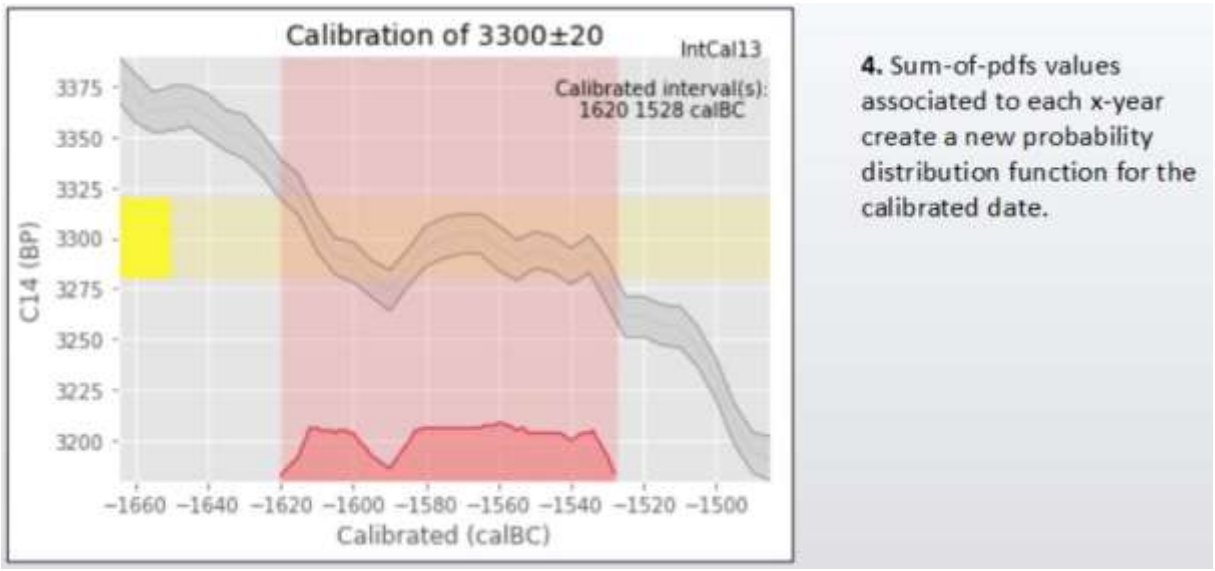

Fig. 5

The result of calibration is an interval on the calibrated time scale for each ^{14}C determination. Calibrated intervals are usually quite wide, especially in correspondence of plateaus in the calibration curve, and can only provide relatively limited information. Such an approach results very conservative, but on the other side it leaves the door open for a high degree of interpretation.

This is particularly important because calibration is based exclusively on ^{14}C measurements and the calibration curve, whereas stratigraphy, context, and other archaeological features concur to date (or mis-date) a target object/event (see above). Thus, a researcher can use calibrated intervals and data of different nature to formulate more specific hypotheses or elaborate scenarios. This might be precluded if the scope of calibration is dating precision, although Bayesian statistics-based analysis allows to hypothesize different priors and produce internally-coherent results. The main difference between a statistics-based approach and the approach proposed here lies in the scope of calibration. Statistics-based calibration aims to achieve an accurate and precise result and quantify its likelihood, leaving the user to decide whether to accept the result "as is" or reject it. The methodology illustrated here, instead, simply sets a few boundaries, without quantifying or suggesting likelihood, and lets the user further explore possible options.

We suggest that the two approaches are not mutually exclusive but should instead be paired in order not only to achieve better information, but also not to lose any information.

CHAPTER II

Interrelations between Minoan Crete and Egypt in the Bronze Age

II.1 Interrelations between Crete and Egypt in Pre and Proto-Palatial times (EM III- MM II B)

The earliest certain contexts in Crete which have yielded significant elements for the archaeology of contact between Minoan culture and Egypt are datable only to the end of the III millennium BC. From an archaeological point of view, Egyptian Protodynastic and Old Kingdom stone vessels found in Early Minoan (EM) contexts (together with local Final Neolithic wares, Evans, 1935; Warren, 1969), and several other (hypothetical) parallels in material culture, including the similarities between some typologies of Early Minoan/Cycladic figurines and earlier Predynastic Egyptian types, between the Minoan codpiece and the Libyan phallic astouche and between the EM tholoi and Halaf tholoi, the symbolism of double-axes and of horns of consecration, as well the later adoption of Egyptian faience technology and religious symbolism have been advocated as arguments hinting to this supposed influence (cfr. Warren, 1969; Branigan, 1969; Rutter, 1997; Treuil, 2008).

None of these arguments allows an actual "African" influence on the development of Minoan Pre-Protopalatial culture: for instance, concerning the origins of the Minoan tholoi, the

hypothesis of a Levantine inspiration from Halaf culture is strongly counterdicted not only by the very significant chronological gaps between the contexts, but also by the completely different destination of usage of such structures in the two different cultures (Vercoutter, 1954, 1956; Branigan, 1969; Renfrew, 1972). Similar chronological problems seem to affect the supposed parallels between the usage of Minoan codpieces and Libyan phallic astouches as well as the adoption of symbolic elements as the double-axe (Vercoutter, 1956; Rutter, 1997). However, some (minor) similarities between Early Minoan Crete and the Levantine maritime cultures are indeed noticeable, and were (re)advocated on the base of a wide range of arguments, from the mixed political-commercial-redistributive role of palatial centers to the adoption of the usage of pithoi and larnakes for burials, linking Early Minoan culture to the Palestinian tradition from Ghassul on. The debate on the origin of Minoan Palaces does still remain open, but actual proof for a true external "inspiration" – let alone a "colonisation" of any sort – are by far too exiguous to be taken seriously, at least at the present state of our knowledge.

Moreover, a much more significant continuity is clearly recognizable in the development of Minoan palaces from preceding Early Minoan "articulated" buildings (as for example at Mallia and at Knossos) as well as in the general development of typical Minoan architectural features in all of the palatial sites (for example: deplaced "central" courts, centrifugal disposition, lustral basins, ashlar building). This internal coherence seems to show a local development, stemming from the gradual concentration in a single architectural complex of all the different productive, administrative and political activities.

This process may be seen as the "natural" evolution of the preceding Early Minoan "articulated buildings" such as those of Vasiliki and Myrtos. Some kind of contact between Minoan Crete and Egypt starts to be more clearly identifiable by the first centuries of the II millennium BC: apart from the above mentioned Pre-Protodynastic imported stone vessels from Early Minoan contexts (Warren, 2000; Bevan, 2004), a number of Egyptian faience objects, scarabs, amulets and other imports are attested on Crete, most notably at the sites of Mochlos, Knossos and Archanes, and in some tholoi of the Mesara plain. A stone cup bearing the cartouche of King Userkaf comes from Kythera, in the Cyclades (Karetsou, 2000; Phillips, 2018).

Unfortunately, none of these contexts was proven to be safely datable, and the chronological value of these findings is ambiguous (Pomerance, 1978). It must be observed that

the actual number of Aegyptiaca found so far in Early Minoan contexts on Crete is very small (Cline, 1994; Phillips, 2008), but it nonetheless seems to correspond to more or less the time when the knowledge of a land named "Keftiw" reaches Egypt the other way round (Vercoutter, 1956; Strange, 1980; Wachsmann, 1987; Duhoux, 2003; but see Vandersleyen 1999, 2018 for a completely different interpretation of the name "Keftiw").

The local development of production technologies originally borrowed from Egypt on Crete (as f. e. stone vessel production and Egyptian blue technologies) fits into the framework of early Bronze Age interrelations across the Mediterranean. However, it is hard to figure out whether these exchanges may have been the result of direct contacts between Minoans and Egypt or, on the contrary, of indirect, multi-level exchanges probably mediated by the Levantine trading élites (Vercoutter, 1956; Strange, 1980; Wiener, 1984; Cline, 1994; Niemeier and Niemeier, 1998; Crowley, 1998). Only after the beginning of the Middle Bronze Age, during MM I A-B, do the interlinkages between Minoan culture and Egypt become much more abundant and clearly documented within the wide Protopalatial Minoan and Egyptian MK international trading networks. By the MM period, Egyptian influence becomes well attested in Crete, but it appears to be characterized by a total lack of interest by Minoan élites for the possible adoption of Egyptian symbolism of royalty and power in general (Phillips, 2006, 2008), something which makes it very different from what is observable in many other "Egyptianising" centers such as Byblos.

Moreover, the adoption of Egyptian traditional symbolism by Minoan élites seems to show a deliberate choice of specific themes felt as particularly fitting to Minoan religious/symbolic sensibility and to be soon "Minoanised" and transformed into a different local tradition (Carinci, 2000; Weingarten, 1991, 2000).

To sum up, the first contacts between Minoan culture and Egypt may be safely dated to the late Early Bronze Age, when Minoan Prepalatial culture starts to reflect external influence, which appears to be systematically and consciously "Minoanised" and re-elaborated in a local tradition already by Protopalatial times (Carinci, 2000).

The absolute periodisation of Middle Minoan Crete is very uncertain for many reasons: the start of the MM I A period is variously attributed to a range between 2000 and 1800 BC, while MM I B- II (the period to which the majority of Minoan vessels found in Egypt and the Levant

are dated) is relatively well-defined in the stratigraphies of some palatial and cult sites (Knossos, Mallia, Kamares, Mt. Iouktas), but very poor or absent at other sites, where MM III seems to directly follow MM I (cfr. Warren and Hankey, 1989; Rutter, 1997; Poursat, 2008). As a result, different chronological hypotheses have been put forward and debated in the last decades (cfr., for example, Kemp and Merrillees, 1980; Warren and Hankey, 1989; Ward, 1992; Girella, 2010). The situation is not much clearer for what concerns the absolute chronology of the fall of Protopalatial centers by the late Middle Bronze Age. A date between 1750 and 1720 BC for the destruction levels (DL) at Knossos and a slightly later date for the DL at Mallia is generally held as valid, but the situation becomes much more problematic when it comes to the end of the Middle Bronze Age, and the subsequent MM III – LM I A periods (Girella, 2010; see detailed chapters below).

By env. 1800 BC Minoan Kamares ware is attested in funerary contexts at several sites along the Nile valley (Kemp and Merrillees, 1980), including el-Lisht (T.879), Abydos (T.416), Qubbet el-Hawa (T.88), where a local Minoanising production is also attested, and futher to the south at Buhen (T.K5). Some other fragments of Minoan origin have been found in domestic contexts at el-Lisht (a total of 6 sherds from a XII-XIIIth Dynasty domestic context), el-Haraga (20 sherds from House 530, cutting through an earlier MK necropolis), Kahun (19 sherds of clearly MM I-II origin and 4 sherds of local Minoanising production from a domestic context, Kemp and Merrillees, 1980).

Similarly to el-Lisht, Tell el Dab'a – Avaris was by Middle Kingdom times a multi-ethnical town which hosted a large number of Asiatics (cfr. below, Bietak, 1999, 2004, 2013, 2018; Bietak et al., 2007) and also yielded some sherds of Minoan origin, including a MM II B Kamares cup (TD 7255, probably of Knossian origin, in an early XIII Dynasty context, Walberg, 1991), fragments of oval-mouth Aegean ware (Bagh, 1998), plus a golden pendant representing two opposed canids which has parallels in some productions from Mallia and Aegina (Crowley, 1998). Other parallels between Minoan imported objects in Egypt and the artistic productions from Mallia MM I are also to be found in some of the specimens from the Montu treasure at Tod (Kemp and Merrillees, 1980; Niemeier, 1998). Although MM III materials in Egypt seem to be very scarce (Kemp and Merrillees, 1980), some MM III – LM I A sherds have also come to light at Tell el Dab'a, as well as, in the Thutmoside period, 150 arrowheads of Helladic tradition (Bietak et al., 2011:87, fig. 43), locally produced Minoanising rhyta and Minoan fresco paintings (Bietak, 1992, 1999; Bietak et al., 2007, cfr. below).

The presence of Aegean imports at Tell el Dab'a may be linked to the role played by this important port center in the international trading network built at an early stage by the XII Dynasty kings and then taken over by the growing Asiatic influence and wider Mediterranean trading network, and finally by the Thutmoside rulers. It seems quite likely at this regard that the subsequent growing interest for the Aegean by the Egyptian Thutmoside courts of the XVIII Dynasty, leading to an actual "Minoan fashion" under the reigns of Hatshepsut and Thutmosis III, may be a reflection and a consequence of a historical process.

The adoption of Egyptian and/or Egyptianising elements in Minoan Crete becomes increasingly significant from the Protopalatial to the Neopalatial periods. Alongside with the above-mentioned introduction of the Egyptian blue and faience production technologies on Crete, a number of actual Egyptian imported objects has been found at several centers all through the island, although the only findings that hint to official contact between Egyptian and local élites are quite doubtful. The main elements consist of 1) a broken inscribed statuette bearing the name of User from a (disturbed) MM I B context at Knossos (which may be the result of looting), and 2) an alabaster lid bearing the cartouche of the Hyksos King Khyan from a MM III context at Knossos (cfr. Karetsou, 2000, with bibliography). The actual meaning and the reliability of those findings' contexts are not safely interpretable, as the objects may have been kept in use for a long time before their deposition, and their stratigraphical contexts show traces of later re-excavations (Evans, 1935), but they can be seen as the reflection of the increasing Minoan maritime trading network from at least MM I (Watrous, 1998). Already by MM I, Nilotic-type paraphernalia start to show up in funerary contexts in Crete, including cosmetic palettes, clay larnakes, systra, alabastra, goblets, double-vessels, miniature juglets and clay models reproducing bread loaf offers, showing a growing interest by Minoan élites for their specific symbolic value.

One of the most significant elements underlying a deliberated and conscious choice of specific Egyptian themes and ideas as fitting to specific Minoan ideological needs (something which implies a deep understanding of their original meaning) is to be seen in the transformation of the Egyptian birthgoddess Taweret into the Minoan Genius. This evolution has been clearly observed and discussed by M. Gill (1964) and J. Weingarten (1991) through the analysis of Knossian and Phaistian seals (particularly HM 202 and CMS II.S 321-322, Weingarten, 1991,

2000), and is more or less contemporary to the adoption of other Egyptian (and/or Levantine) themes in Crete such as the sphinx and the griffin, soon "Minoanised" and reinterpreted in a local tradition as shown in some masterpieces from Mallia (cfr. Karetsou, 2000; Morgan, 2010a, 2010b). Some much less clear forms of Egyptian influence have also been hypothesized for some MM architectural features in contexts such as the Chrysolakkos tomb (where an Egyptian imported cup was actually found), and the "feasting halls" in some MM II buildings (Watrous, 1998).

As Egyptian imports and influence on Crete become more abundant and clearly recognizable, the absence of almost any typical element of traditional "official" Egyptian foreign relationship becomes very striking. No other element linkable to the Egyptian royal or power symbolism has been found so far, with the possible exception of a Phaistian seal (CMS II.S, 268) representing a bull charging a fortified town (Gill, 1970). The comparison between the adoption and re-elaboration of some specific themes and the deliberate exclusion of others shows again a sort of consciousness of the original meaning and the explicit choice of the ones that would best fit into the specific needs of an originally Minoan tradition (Carinci, 2000; Phillips, 2001, 2006). Minoan élites imported from Egypt iconographic themes (Taweret, the sphinx, the crocodile, the "sacred monkeys", the cats, ...) as well as finished objects (e.g. stone and ceramic vessels, ostrich eggs, amulets, faience objects) and raw materials (alabaster, amethyst, carnelian, ivory, gold, blue frit, glass), but showed no interest for a much higher number of importable items. No reference to any of the Egyptian principal divinities and no hint of Egyptian symbolism of royalty and power is attested on Crete by the time, and the same "selective" adoption may be also reflected in the absence in the import records observable within material goods such as 182 examples of Egyptian stone vessels, 8 types of glass vessels (out of a total 10), the absence of almost all common Egyptian wares, all other typologies of Egyptian seals apart from scaraboids, and many other luxury objects and semi-precious materials as for example turquoise or jasper. J. Phillips, who extensively investigated the subject, has postulated four different (but not alternative) explicative scenarios, depending on the nature and typology of the imported goods (Phillips, 2006):

1) luxury finished products such as alabaster and glass vessels found in funerary contexts that were probably imported as exotica, mainly for their aesthetic and economic value;

2) iconographic themes with a strong religious/symbolic meaning (such as Taweret or the

"sacred monkeys") that were chosen as particularity fitting in to the specific needs of the (evolving) traditional Minoan symbolism, and are soon reelaborated and transformed into something now definitely Minoan: the same process applies also to less explicitly symbolical "imports" such as stone vessel production technology, reworked Egyptian stone vessels and Minoan scarabs (Phillips, 2006);

3) other foreign objects of lower value (as for example Egyptian spheroid jars) imported in Crete and soon locally reproduced, with a much wider diffusion throughout the island with respect to luxury objects, reaching also peripheral centers as Kato Zakros (Phillips, 2006, 2008);

4) objects testifying a somehow "official" form of contact (i.e. that may be considered to be a sort of diplomatic gift/exchange) between Egyptian and Minoan élites, the evidence for which is (until now) limited to the Khyan lid (as the User statuette is more likely to be the evidence of trade – whether direct or by intermediaries).

It must be observed that each single imported Egyptian product on Crete may be assigned to more than one of these scenarios. It is also most important to point out that the role of the different local/regional élites is not clearly recognizable, although there must have been very significant local differences in the ways of contact/absorption of foreign cultural elements between the different regions/palatial centers in Crete (Carinci, 2000). Uncertainty stems also from the peculiar overall nature of Minoan adoption of foreign influence: with regard to Egyptian influence on Minoan Protopalatial culture, it has been observed that if the local élites show distinct interest for some specifically Egyptian objects, raw materials and iconographic themes, the reception of these is always explicitly Minoan, making the definition of "foreign (Egyptian) influence" very ambiguous.

During MM I-II, the circulation of Egyptian elements such as exotica seems to be fundamentally concentrated around the Knossian area, where they become gradually "Minoanised" and subsequently circulated to peripheral centers such as Mallia and Phaistos. The latter, in particular, was most probably also involved (even if it is hard to determine whether directly or indirectly) in the process of exchange with Egypt as early as MM IB, since the majority of Kamares wares found along the Nile valley have been attributed to the Phaistian

production both on stylistic ground and by NAA (Kemp and Merrillees, 1980; MacGillivray, 1995, 1998). The process of exchange leading to this distribution of imported objects and technical/artistic influences in both countries (Crete and Egypt) was probably operated by middle-class specialists (Watrous, 1998), whether directly or indirectly involved in "direct" contact with their foreign counterparts, and reflect the development of a wider, multinational Mediterranean trading network and commercial economy, enhanced also by contemporary innovations in sailing techniques (Cline, 1994; Watrous, 1998).

Findings such as the Khyan lid (in the same palace also the fragments of at least 20 Canaanite jars were found that find close parallels with imported ware found at Poros[4]), the only royal inscribed object found so far in Neopalatial contexts on Crete, may be however a good hint at this regard, as Khyan was known as one of the most active Hyksos kings in foreign politics, and it is during his reign (dated to about 1640-1600 BC) that the exported objects of Hyksos origin reach their widest distribution in the Mediterranean (Bietak, 2000; Eriksson, 2001, 2003), and it would be rather tempting to hypothesize an actual form of "diplomatic" contact. The process of adoption and adaptation of Egyptian themes in Minoan tradition follows on during the Neopalatial period (MM III – LM I A), when elements such as the iconography of the Pothnia Theron and the "Blue Monkeys", as well as some Minoan hieroglyphs of most likely Egyptian inspiration spread in several palatial centers and peak sanctuaries, always showing the same conscious choice of some specific and very precise symbolism. This would be hardly fitting into the "classic" picture of a religious/economic élite importing exotica as status-symbol elements of distinction from the lower classes, as appears to be the case for many other centers relating with the Egyptian court, as for example the town of Byblos during Old Kingdom (where Egyptian royal iconography – completely absent in Crete – was adopted by the local ruling élites, Vercoutter, 1954, 1956; Watrous, 1998; Feldman, 2006).

To sum up, during the whole Middle Bronze Age it seems hard to imagine a "real" Egyptian influence (in the classic sense) on Minoan culture through a specific, direct channel of communication/exchange, while it seems very much more likely that a wide and multi-level network of international exchange, involving an imprecise number of intermediaries from different countries, was already well established by the Protopalatial period and the Middle Kingdom in Egypt, and gradually enhanced the circulation of goods, ideas, themes and

[4] McGillivray, pers. Comm. 2013, for which I am most grateful.

techniques that would culminate in the Late Bronze Age artistic koiné (Kantor, 1947; Feldman, 2006). Interrelations between Crete and Egypt were most probably indirect for a significant part, and took place through Levantine trading ports at least until the Neopalatial period, while "official" diplomatic relations become certainly attested only with the XVIII Dynasty.

However, long-range exchanges, absorption and re-elaboration of external ideas and symbolism do certainly have a significant role in the growing complexity and social articulation of Minoan culture already by Protopalatial times, but this influence is never really explicit and seems always to fit into a specific Minoan conception: its nature and forms tend to evolve uninterruptedly from Protopalatial to Postpalatial times in correspondence with the different phases of growth and demise of Minoan – on the one side, and on the other – Egyptian political, economic and social situation, and their respective cultural and commercial international networks from the Middle to the Late Bronze Age. It is however understood that the actual proportion of the contacts between Crete and Egypt must be somehow "masked" by our state of knowledge: a hint in this regard can be found in documents such as the London Medical Text and the Ebers papyrus (Haider, 2001), both texts implying a much deeper knowledge by the Egyptian élites of the "Keftian" culture and beliefs (as deep as to quote Minoan illnesses and divinities, and to make scribes practice on the spelling of Minoan personal names), as well as in the abovementioned choice, adoption and transformation of Egyptian into Minoan symbolism, as the transformation of Taweret into the Minoan Genius. After all, Egypt lies only 800 km to the south of Crete (a distance that may be reduced to 550 km of open sea, sailing to the Libyan coast and then to the Delta following the coast), a journey that may be enhanced by summer blowing ethesian winds, and that may be done the other way round through the Levantine coast, Cyprus and Rhodes (two islands that do start to play an extremely significant role in the Minoan – Levantine – Egyptian trading networks already by the final Middle Bronze Age, cfr. Helck, 1983).

It seems very likely that many other "contacts" between Crete and Egypt may have taken place from the III millennium BC on, but materials may have disappeared since then, or not have been found yet. Only after the fall of the Hyksos kings (by 1570-1530 BC), when taking over their international trading network and foreign political influence had a very strong political reflection on the XVIII Dynasty Kings and when receiving an "embassy" from the Aegean becomes an highly appreciated honor for the Thutmoside viziers and dignitaries who wanted such episodes to be depicted in their Theban tombs, official relations between Egypt and Minoan Crete are explicitly attested, and Minoan people (including the artisans who

reached Tell el Dab'a and other Levantine centers to paint their frescoes in the royal palaces) reach Egypt with their ideas, styles and techniques now being adopted, and "Egyptianised" in turn, configurating an actual "Minoan fashion" (Kantor, 1947; Vercoutter, 1954, 1956; Wiener, 1984; Wachsmann, 1987; Crowley, 1998; Morgan, 2010a, 2010b; Marinatos and Morgan, 2010).

II.2 New Kingdom Egypt and Late Bronze Age Crete

The early New Kingdom in Egypt witnesses a significant growth of interest by Egyptian élites for foreign "exotic" lands in general, including Minoan Crete. The interest for the Aegean in particular reached its apex during the Thutmoside age with the representation of Keftiw delegations to be met by Egyptian viziers and dignitaries (Vercoutter, 1956; Wachsmann, 1987), when Minoan paintings are realized in palatial contexts, the influence of Minoan themes on Egyptian art becomes much more explicit (Vercoutter, 1956; Crowley, 1998), "Keftiw ships" are said to be allested in royal docks at Peru Nefer-Tell el Dab'a (Glanville, 1931, 1932; Gundacker, 2010, 2017), Minoan "embassies" are depicted in the high officers Theban tombs and Minoan divinities and names are spelled in scribal exercise texts. Minoan and Helladic wares are attested from Tell el Dab'a-Avaris and Saqqara to the north to as far south as Aniba (Kemp and Merrillees, 1980).

All of this elements have lead some scholars to speak of an actual "Minoan (or Aegean) fashion" (Vercoutter, 1954, 1956; Wiener, 1984; Crowley, 1998), of the presence of resident Aegean natives in Thutmoside Egypt (Petrie, 1892; Breasted, 1948; Vercoutter, 1954, 1956; Kemp and Merrillees, 1980; Wachsmann, 1987; Bietak, 1999, 2005, 2007), and, possibly, of an actual Minoan "colony" in northern Egypt, whose specific location would be still to be identified (Bietak, 1999, 2018; Duhoux, 2003). Even if archaeologically attested interrelations follow on all through the Late Bronze Age, this "Minoan fashion" is typical only of the Thutmoside age and the early XVIII Dynasty, and seems to cease quite abruptly between the reign of Amenhotep II and the reign of Amenhotep III, when "Keftiw" people are no longer

depicted in the Egyptian tombs, if not much less well understood and mistaken as general "foreigners" with no more Aegean traits (as in Horemheb's tomb). This sudden loss of interest for Minoan Crete by Egyptian élites has been variously linked to the Mycenaean conquest of the island by Late Minoan II/III A1 (cfr. Vercoutter, 1954, 1956; Wachsmann, 1987; Rehak, 1998).

Apart from the hypothetical presence of a Minoan "colony" in the Delta (Duhoux, 2003), it seems very likely that this "Minoan fashion" was a peculiar characteristic of the élites' social display during the (late) Thutmoside age, in particular during Hatshespsut and Thutmosis III's reigns. It may be quite interesting at this regard to remind a passage by W.M. Flinders-Petrie (1892), who claims to have found at Ghurob

> [clear] traces of foreign occupation […] in a town occupied by people from the Aegean and Asia Minor [sic].

For the sake of history of the subject, Petrie claims to have found traces of a peculiar burial practice, involving the preservation of the inhumated body accompanied with the ritual pyre of the funeral assemblage, a practice that Petrie interpreted as a combination of Aegean and Egyptian traditions. The "exotic" interests of Thutmosis III are well known from Egyptian literature and fit perfectly into his "imperial" foreign policy and self-representation. Findings and documents such as the Minoan paintings of Tell el Dab'a (dated to his reign), the exotic plants in the botanical garden at Karnak, the Annals and other texts reporting the king's interest in "exotic" knowledge (Grimal, 1988) do fit perfectly into this picture. The followers of Thutmosis III seem not to have shared the same "exotic" interest, at least for what concerns the Aegean: from the reigns of Amenhotep II and Thutmosis IV very few hints of contact with the Aegean are attested so far (Cline, 1994; Phillips, 2008), and when Egyptian interest for the northern shore of the Mediterranean seems to be resumed under Amenhotep III, the whole Aegean had already fallen under Mycenaean influence. The renewed interest for trans Mediterranean travels by this king (explicitly testified by the E_n list at Kom el Hetan and by materials as the plaques bearing his cartouche found in LM III A1 contexts in several Aegean sites, possibly implying a diplomatic embassy) was probably mainly commercial, and in fact Helladic wares start to be attested in large quantities in Egypt from contexts dated to his reign, and to the reign of his successor Amenhotep IV/Akhenaton, and Aegean or Aegeanising

paintings are once again being realized in the royal palaces of Malkata and Amarna (Kemp, 2000; Duhoux, 2003; Bietak, 2007).

Another interesting argument – if the name "Keftiw" is to be effectively associated to Crete at least at this later stage (for a contrary opinion, see Vandersleyen, 1999, 2018; Tiradritti, 2018) – could be the mention, in the Annals at Karnak, of "Keftiw" shipbuilding activity at the port of Peru-Nefer: it is difficult to point out whether these ships were actually built by Keftiw, to go to Keftiw, or even in the technique of Keftiw (Bietak, 1999, 2005, 2018). By regnal year 42, the Annals report Thutmosis III receiving an embassy from Tanaya, bringing Keftiw objects as a tribute to the king, and the two lands of Keftiw and the Isles in Midst of the Great Green are mentioned (in two separate lines) in the Triumphal Stela (Lichtheim, 1976; Duhoux, 2003), as well as amongst northern lands submitted to the authority of governor Thutiy (Breasted, 1948).

By far the most safely interpretable argument testifying to an official relationship between the Egyptian court and the Aegean élites, the depictions of Aegean natives in the Theban tombs show an explicit evolution of the Egyptian "formal" conception of the Aegean and its inhabitants, culminating in the remaking of the Keftiw in Rekhmira's tomb by the beginning of Amenhotep II's reign (with the above *caveat*). The only Aegean object found in contexts certainly datable to the following reign of Thutmosis IV consists of a jar containing an organic paste defined as "Keftiw drug" from this king's tomb (Merrillees, 1998) which, together with the mention of "Keftiw illness" and divinities in the London Medical Text (Haider, 2001), lead some authors to hypothesize the presence of Minoan healers/priests in Egypt, and is thought to reflect the Egyptian interest for Minoan "healing cults" (Merrillees, 1998; Kyriakidis, 2002).

On the other hand, the corpus of Minoan objects from Egyptian XVIII Dynasty contexts consists mainly in a few high-quality ceramic vessels (cfr. Kemp and Merrillees, 1980). They include: a fragment (defined as Aegean by Kemp and Merrillees, 1980, and as Egyptian in fabric by Hankey and Leonard, 1998) imitating Aegean productions comparable to LM I types that has been found at Kerma in a context preceding Ahmose's year 15, a local imitation of LM I B wares with parallels in Mallia found in Tomb SA17 in the Thutmoside age necropolis at Aniba, LM I B-LH II A sherds that were found in Tombs T.238 and T.631 at Abydos, a LM I B alabastron found at Saqqara, Tomb NE1, a LM I B alabastron from Kom el Rabi'a, a chévron decorated alabastron, a number of out of contexts sherds from Sidmant, and a LM IB – LH II A alabastron from Tomb 245 at Medinet al Ghurob, all probably datable to in-between the early

XVIII Dynasty and the reign of Thutmosis III. The small number of Minoan imports found in early XVIII Dynasty contexts seems quite striking, and particularly so if compared to the later distribution of Helladic wares. As early as LH II A Mycenaean wares start to be attested in Egypt (Kemp and Merrillees, 1980): a LH II A cup was found together with a LM I B alabastron at Saqqara, Tomb NE1, in a context dated to the middle XVIII Dynasty, a LH II A pithoid jar comes from a context dated to the reigns of Hatshepsut and Thutmosis III at Dra Abu el Naga, and another LH II A-B jar was found in Maket's Tomb, coffin 9, at Kahun (Cultraro, 2006), together with some LH II B sherds. Mycenean imports in Egypt during the following reign of Amenhotep III are still not abundant but, on the contrary, Aegyptiaca datable to his reign become widely attested in the Aegean (Phillips, 2008): 53 imports found in LM III A1 are known only from Crete (20 of them from Mochlos, Watrous, 1998). Some of the Egyptian imported objects from LM/LH III A1 sites do now testify contacts at the highest level, as for example 14 faience plaques bearing the cartouches of Amenhotep III and Queen Tiye found at Mycenae and at several other Aegean sites. One royal inscribed scarab of this king was found at Zapher Papoura, and the list goes on with the above-mentioned inscribed alabastron found at Katsamba and the rich funerary assemblage from the Royal Tomb at Isopata, that included at least 10 XVII/XVIII Dynasty alabastra, an Old Kingdom diorite cup and 2 Egyptian lapislazuli monkey statuettes (Phillips, 2008). By LH II B the number of Mycenaean imports in Egypt increases significantly: more than 2000 fragments of Helladic wares were found at Amarna and Sesebi (Merrillees, 1998), and Mycenaean imports continue to be attested to at least as late as the final XIX/early XX Dynasties (Cultraro, 2006). If the majority of Aegyptiaca in the Aegean appear to be linkable to the reign of Amenhotep III, on the other hand there seems to be very little to no evidence of contact during the reign of his successor Amenhotep IV/Akhenaton, of whom no inscribed object or direct link has ever been found in the Aegean (apart from the scarab inscribed with Queen Nefertiti's cartouche from the Uluburun Shipwreck, Bass, 1986; Pulak, 2005) and this may seem rather surprising, given the above-mentioned huge quantity of LH III wares found, for example, at Amarna (Kemp and Merrillees, 1980).

LH III A2 – B Aegean/Cypriot wares are attested also from Deir el Medina (Kemp and Merrillees, 1980), probably testifying the process of mixed direct/indirect artistic exchange and circulation of productions and themes typical of the Late Bronze Age koiné, and LM/LH III B wares findings follow on through the XIX Dynasty. Argolid wares have been found at Pi-Ramesse while Minoan wares do certainly start to reach Egypt once again, and particularly the

port sites of the western Egyptian-Libyan coast as Bates Island (Cultraro, 2006; Bietak, 2015). It has been observed (Watrous, 1998; Merrillees, 1998) that the LM III A2 period preferential trading routes from Crete show a "shift of interest" (Watrous, 1998) from an east-southward to a westward direction, leading to the central Mediterranean, where LM III have been found from several sites from Tunisia to Sardinia and Spain (cfr. Cultraro, 2006).

The site of Bates Island near Marsa Matruh, which was possibly a pirate harbour (Bietak, 2015), has revealed traces of an intense frequentation by Cretan "traders" all through the LM/LH III B period, and did probably play an extremely significant role as trading port in the route leading from Crete and the Eastern Mediterranean to the central-western Mediterranean, following a route that will be lately resumed by Phoenician prospectors. Late Minoan/Late Helladic III B wares have in fact been found as far south-west as Cyrenae and Carthage (cfr. Cultraro, 2006), and the important role played by Libyan ports such as Marsa Matruh in this trading route at least from the Late Bronze Age is testified also by findings as the Minoan amphorae found at the Ramesside fortress of Zawyiet Umm el Rakham, 25 km to the west of Marsa Matruh (cfr. Cultraro, 2006). By the end of the XIX/early XX Dynasty, however, Aegean contacts with Egypt seem to have definitely declined: Keftiw is no longer mentioned in official sources, while, by Ramesse III's reign, the Isles in the Midst of the Great Green are mentioned amongst the homelands of the Sea People at Medinet Habu, revealing a now completely different perception of the Aegean by Egyptian élites, in comparison with the rich, exotic lands which contributed to the maintenance of the pharaonic "cosmic order", bringing their tributes to the imperial XVIII Dynasty kings as Thutmosis III.

II.3 Aegean Natives in Theban tomb paintings

During the early XVIII Dynasty Aegean envoys/"ambassadors" (Vercoutter, 1954, 1956; Wachsmann, 1987; Matthäus, 1995; Vandersleyen, 1999; Duhoux, 2003) are depicted in several high officers' tombs at Thebes, which cover a span of about 2-3 generations (Vercoutter, 1954). Six amongst these "Aegean" paintings have been considered to be the most significant (Vercoutter, 1954, 1956; Wachsmann, 1987; Duhoux, 2003). These are (in chronological order) the tombs of User, Senmut, Useramon, Antef, Menkheperrasoneb, Rekhmira, ranging from the early Thutmoside age all through the reigns of Queen Hatshepsut and Thutmosi III (excluding the later tomb of Puymra), which implies a period of more than half a century. These paintings are held as the most significant for the archeology of contacts between the two cultures at this stage due to their explicit and carefully detailed iconographic precision (Vercoutter, 1954, 1956), and became the "archetypes" for the later depictions of Aegeans in more recent contexts such as the tombs of Amenmose and that of Horemheb (Vercoutter, 1956). The earliest depiction to explicitly name Keftiw with relation to Minoan Crete is that of Rekhmira (late Thutmosis III/early Amenhotep II), while in the older tombs of Useramon and Senenmut the people from the Aegean are only defined as "inhabitants of the Isles in the Midst of the Great Green (Vercoutter, 1954, 1956; Wachsmann, 1987; Duhoux, 2003). The "tribute bearers" in these Aegean "tribute scenes" show some fundamental common traits: all of the Aegean natives depicted (cfr. Vercoutter, 1954, 1956; Wachsmann, 1987; Rehak, 1998; Duhoux, 2003) are represented with a particularly narrow waist, reddish-brown skin, long curly black hair flowing down their back and curling on their foreheads, and no signs of beard or mustaches. The Aegean tribute bearers wear brightly colored garments, as well as shoes of a type that have significant parallels on Crete (Rehak, 1998), and are depicted as bringing offerings such as luxury objects, vessels and raw goods that do reproduce (at least partially) the actual evidence of Minoan productions and foreign exports/commerce by Neopalatial times (Cline, 1994; Rehak, 1998).

In all of the earlier paintings, the Aegean natives are depicted wearing the Minoan kilt (Vercoutter, 1954, 1956; Wachsmann, 1987; Rehak, 1998; Duhoux, 2003), and the same garment is worn by the "Keftiw" in the earliest depiction of the tribute in Rekhmira's tomb. In this context (TT 100), a scene of Aegean tribute was first painted during the reign of Thutmosis

III, but was subsequently obliterated and covered by a new painting of the Keftiw, wearing different clothes, by the time of the accession of Amenhotep II. The second version of the painting shows the Keftiw wearing a different garment that has been compared to the Mycenaean kilt worn, for example, by the "rython bearer" or the "captain of the blacks" in Knossian paintings (Rehak, 1998). The objects brought as offerings are now of more distinct Aegean origin: 15 out of 38 types of vessels depicted are certainly reproducing Aegean types, 13 show mixed Aegean and Levantine features and 10 are probably reproducing Syrian types (Vercoutter, 1954, 1956). For what concerns decorative schemes reproduced, 21 out of 22 have been placed in the list of Aegean motifs by Furumark. The offers brought by the Keftiw also include swords (the sword of the sixth bearer is shown unlimbered, something rather unusual in such kind of representations), daggers, pearls, lapislazuli, copper and silver ingots, and elephant ivory (but in other tomb paintings, such as that of Menkheperrasoneb, the Keftiw tribute also includes oil jars and agrimi horns, Warren, 1995). This assemblage has often been compared to the LM III Uluburun shipwreck (Bass, 1998). The tribute scene in Rekhmira's tomb is introduced by a general intitulation, and each register is accompanied by a specific description. The intitulation of the Aegean tribute (Obsomer, 2002):

> Receiving the tribute of Keftiw and of the Islands in the Midst of the Great Green

introduces the tribute scene accompanied by the specific description:

> Coming in peace of the Lords of the lands of Keftiw and the Isles in the Midst of the Great Green, bending and kneeling, for the power of his majesty Menkheperra (Thutmosis III). Because they have heard of his victory in all foreign lands. Bringing their gift on their back, to obtain the breath of life, willing to walk on the waters of his majesty, to be protected by his power.

This text does explicitly mention the lords (*Wrw*) of Keftiw and of the Islands in the middle of the Great Green (no more the "simple inhabitants" of the earliest Aegean tribute paintings, Vercoutter, 1954, 1956) bringing their tribute to the Egyptian king (through the person of the vizier) but the peculiar formulae seem to have a rather specific meaning, distinguishing the

Aegeans from the other foreign tribute bearers depicted in the painting (Punt, the Southern Lands and Retenu): the Aegeans (as well as Retenu) are said to be willing to «walk on the waters of his majesty», something that implies a sort of official alliance (Vandersleyen, 1999; Duhoux, 2003), but while Retenu are said to be "terrified in their hearts by his power" (Obsomer, 2002), the inscription referring to Keftiw and the Islands in the Midst of the Great Green reports them simply having «heard of his victory in all foreign lands».

Moreover, the Aegeans are the only "ambassadors" to be said to ask for the king's "protection" (something that may eventually mask a sort of commercial alliance, given the distance between the two countries). These arguments have been used to hypothesize the presence of an "official" Minoan colony in the Delta with its own political "status" and organization (cfr. above, Vercoutter, 1954, 1956; Duhoux, 2003), in a similar way to the later Greek colony at Naucratis, but the archaeological record of northeastern Lower Egypt is still inconclusive in this regard.

It is quite likely that this later version of the Keftiw in Rekhmira's tomb shows the most reliable and precise representation of Minoans/Mycenaeans in Egypt, while the depictions of Aegean tributes in later tombs seem much more stereotyped (and even misunderstood): in Menkheperrasoneb's tomb the "Lord of Keftiw" is represented with typical northern Syrian features, in Qenamon's tomb a Kefti is represented as a Nubian, and in Ineni's tomb the "Kefti" is even represented as an Hittite (Vercoutter, 1954, 1956; Wachsmann, 1987). The overall lack of precision of the foreign tribute scenes in those later tombs does not affect the depiction of Aegeans only: in Menkheperrasoneb's tomb the "Lord of Hatti" is represented as a Syrian, in Qenamon's a Libyan is depicted as a Syrian, and in Ineni's tomb an Asiatic Mentu is represented with typical African traits (Vercoutter, 1954, 1956). The painting of the Keftiw in Rekhmira's tomb second version is not only the most accurate and detailed representation of Aegeans in XVIII Dynasty Egypt, it also shows the deliberate and conscious choice to "update" what Egyptian élites perceived as really "Aegean", something that was felt to be as important as to justify the huge expenses to obliterate and re-paint the scene in a "more appropriate" way, and this must stem from an actual change in the Egyptian perception and knowledge of Keftiw and the Aegean.

This change has been variously linked to the Mycenaean conquest of Minoan Crete (cfr. f. e. Vercoutter, 1954, 1956; Rehak, 1998), or at least to the establishment of a mixed Mycenaean-Minoan élite power at Knossos by LM II/III, but it is not safely determinable whether the

changes in the garments of Keftiw in Rekhmira's tomb may effectively represent valid indicators of ethnicity (Rehak, 1998). Rehak observed that the Minoan kilt seems to appear on Crete by MM II (as for example on peak sanctuaries as Petsofa, Rutkowski, 1991, or on the "harvester vase"): it might have had a ritual significance all through the Neopalatial period, particularly in taureador scenes (as at Knossos, but also at Tell el Dab'a) and kept in use at least until LM III (Rehak, 1998). The Mycenaean "kilt" does however seem to appear at Minoan sites well before the fall of the New Palaces, being attested at Akrotiri by LM I A but also at Mallia as early as MM II (Barber, 1991; Rehak, 1998). The use of this garment as a specific indicator of Mycenaean ethnicity may thus be misleading or rather unsafe, as the use of Mycenaean "kilt" might as well represent social difference of some kind (age, status, role...) and the change of the Aegean clothes in Rekhmira's tomb painting may effectively represent a difference in the composition of the "embassy", possibly involving people from different Minoan/Aegean centers. Matthäus (1995) linked the changes in the ceramic assemblages represented to the the LM I B – LM II transition on Crete.

Considering all these potential sources of uncertainty, it is very hard to conclusively link the shift from the earlier "Theban" Aegeans to those of Rekhmira's second version to the transition from Minoan Crete to the Mycenaean conquest, but it seems however very likely that the older depictions of Keftiw in Senmut and Useramon's tombs represent an earlier episode, possibly a Minoan "embassy" to Thutmosis I (already suggested in Vercoutter, 1954, 1956), while it is almost certain that people of Minoan/Aegean origin were living in Egypt during the reigns of Hatshepsut/Thutmosis III. This presence, as well as the textual and iconographic sources about Aegeans in Egypt during the Thutmoside age, fits well in the new trends in Egyptian foreign policy, perception and use of the exotic by Thutmosis III in which the "Minoan fashion" is to be set, but it also testifies to the high level of official contact between the two countries by this time. Given the peculiar political situation of the early-middle XV century BC, it would not be surprising at all to find Minoan trading élites seeking commercial agreements with imperial Egypt, whose influence reaches a great part of the Levantine coast by this age. A commercial/political agreement would have at least guaranteed a good base for Minoan trade on the Levantine coast apart from local political changes, and findings such as the Minoan paintings in the Levantine and northern Egyptian palatial sites may be a part of this process. Finally, it has to be observed that in the Theban tomb paintings the Keftiw are never isolated: their hommages are always set in a general tribute scene involving many other

countries and ethnicities. In Rekhmira's tomb in particular the Keftiw bring their tribute separately in their own register, but this is set in a whole of tribute scenes from foreign lands including Punt, Syria and Nubia. Since the renewal of this painting is to be dated to soon after the death of Thutmosis III, it seems not unlikely that it actually may represent a diplomatic Minoan/Mycenaean mission for the coronation of Amenhotep II (Vercoutter, 1956; Duhoux, 2003).

II.4 Minoan (and/or "minoanising") paintings in Egypt and the Levant

Since the second half of the 20th century wall paintings on plaster of supposed Minoan origin have come to light in several palatial sites in the Levant and in Egypt. A significant part of these findings has been considered to be of truly Minoan origin, and to has been realized by itinerant Minoan artisans who spread in the Eastern Mediterranean in the Middle and Late Bronze Age (cfr. Niemeier, 1991; Shaw, 1995). However, the chronological relationship between the different contexts from which the paintings come from has shown to be problematic (Niemeier and Niemeier, 1991; Bietak, 1992; Shaw, 1995; Manning, 1999, 2006b; Bietak, 1999, 2004, 2007, Morgan, 2004, 2006, 2010a). Basically, the first reconstruction proposed by Niemeier and Niemeier (1991) would group the "Minoan" paintings in a single macro-phase corresponding to an advanced MB II period, at the apex of the Hyksos-Canaanite commercial network influence. In Niemeier and Niemeier's reconstruction, the diffusion this kind of "prestige" artifacts – that requires importing artisans themselves, and not only their finished product – is seen as the result of an "Aegeanizing" fashion that was part of the status display of royal courts at the time – the "Versailles effect" initially suggested by Malcolm Wiener (1984). Niemeier and Niemeier quote the Ugaritic version of myth of Anat, who was sent to *Kptr* (Crete) to search for the artisan-god Kothar Wa Khasis as an echo of this circulation. However, the actual chronological span of this "Minoan fashion" is all but straightforward: their periodisation seems in fact to have been "adjusted" around the (at the time) expectations of the Aegean High Chronology (AHC – Manning, 1999; Manning et al., 2006). This interlinkage is fundamentally based on the hypothetical contemporaneity between some of the Levantine and Egyptian Minoan paintings and those of Akrotiri on Thera, and on their attribution to the LM I A period, that in the AHC would span c. 1700 to c. 1600 BC. This reconstruction has however been questioned by the reanalysis of the relative and absolute chronologies of the different contexts that yielded the fragmentary Minoan paintings, showing that:

1) the paintings do not belong to a single chronological phase;

2) the paintings are the results of different workshops (and traditions).

The Alalakh VII paintings were executed some years before the fall of the city under Hattushili I (1628 or 1575/74 BC, depending on "Middle" or "Low" chronology), while the Tell el Dab'a specimens were executed some 60 to 150 years later. Fragments of Minoan paintings were also found at Alalakh IV, a phase that was probably contemporary with the reign of Thtumosi III in Egypt, in association with Cypriot RLWM, WP VI, WS I, WS II, BR I and BR II wares, typical of Cypriot LC I A2/II periods (Bergoffen, 2003).

This periodisation is however hardly supported by evidence (Bietak, 2007), but allows the authors to establish a relation between this group of findings and those of Alalakh VII, (formerly) used to argument in favor of the AHC (Manning, 1999, 2006b, 2007; Manning and Bronk-Ramsey, 2003; Manning et al., 2005). This is however a sort of circular argument: Niemeier and Niemeier don't report any proof for his periodisation for the destruction of the palace at around 1600BC, apart from the similarities between the local Minoan paintings and those from Akrotiri, that would find a *terminus ante quem* in the mature LM I A eruption at Thera, dated to 1628-1600BC in the AHC. On the other hand, the presence of Chocolate on White (CoW) Cypriot wares in the throne room at Kabri seems to show that the destruction of the palace must have taken place somewhere around the Middle-Late Bronze Age transition. The presence, in the same room, of Bichrome Wheel Made ware, recognized only at a later stage, may offer another suggestion about the periodisation originally suggested by the authors being too high (Bietak, 2007), and this impression is confirmed by the presence of WP VI, WS I and BR I wares from a rich tomb, showing that the Minoan paintings at Kabri may have been executed some 100years later than the date suggested by Kempinski (2002) and Niemeier and Niemeier (2002). More wall paintings on plaster came to light also at Mari (Parrot, 1958), Ebla (Matthiae, 1995), Qatna (Von Rüden, 2006), Tell Sakka (Taraqji, 1999), and Malkata (Kemp, 2000), all of them being found in palatial contexts. The specimens from Qatna were found in the palace destruction level dated at about 1340 BC (Novak and Pfaelzner, 2001; Von Rüden, 2006), and are probably the latest ones, together with the "Minoanising" paintings from Malkata (Kemp, 2000). The Ebla paintings come from a definitely older context (MB I-II) and represent a local tradition that had originated at least as early as EB IV, and are thus not to be considered "Minoan" (Bietak, 2007). The next group comes from the MB II second palace at Tell Sakka, near Damascus (Taraqji, 1999). These fragments were initially dated to the XVIII Century BC, but

then subsequently shifted to 1650-1600 BC on the basis of associated findings that included Egyptian Tell el Yahudiyah ware (Bietak, 2007). The Mari paintings (Margueron, 2004) are dated to a more or less contemporaneous period, as inferred from the correspondence in the archive that refer to the post MB II AB transition Hazor (Ben-Tor, 2004).

On present evidence, it seems undeniable that the spread of "Minoan" paintings and traveling artisans is no longer to be considered a contemporaneous and homogeneous phenomenon: the Qatna and Malkata paintings are about a century later than those from Tell el Dab'a and Alalakh IV, that are in turn much later that those of Alalakh VII. Both at Alalakh VII and at Kabri, the Minoan paintings do appear in a phase that precedes the earliest findings of RLWM, WS I and BR I wares in local contexts, while at Tell el Dab'a the paintings are attributed to a phase when all of these productions are already well attested, and that may be linked to LC I A2-B in Cyprus (and to LM I A-B in turn). The diffusion of WS I specimens at Tell el Dab'a and the Levant seems to confirm this chronological distribution, just as the (now lost) WS I specimen from Akrotiri (Merrillees, 2001; see dedicated chapter below) epitomizes the problems of the on-going chronological debate. It must be observed that the Mari and Tell Sakka paintings look very different from those from Alalakh, Kabri or Tell el Dab'a: their execution might be dated to a moment somewhere in-between 1700 and 1600 BC, and, together with the earlier specimens from Ebla, do testify to the presence of a local Syrian tradition of wall paintings on plaster, that precedes – and differs from in many technical aspects – the truly Minoan *a fresco* tradition. However, even excluding these "older" paintings from the sequence – and taking in consideration only truly Minoan or Minoanising paintings – the contexts attested so far spread across an at least 150 years-long time span (Bietak, 2007).

In conclusion, all the above may be summarized as follows:

1) Mari and Tell Sakka:

The wall paintings on plaster found at Mari and at Tell Sakka are the product of a local tradition which has probably no link at all with Minoan wall painting tradition, although at Mari some of the decorative patterns do seem to show some possible Minoan influence, particularly shown in the "marmorised" surfaces (for which there are parallels both at Phaistos – Levi, 1957 – and at Mallia – Daux, 1965), fragments of "ashlar masonry" buildings, running spirals (Niemeier and Niemeier, 1998, 2002). The correspondence found in the archive at Mari does however report of contacts between Crete and the city at that age, probably through the Palestinian coast, but times and processes of reciprocal exchange

and circulation of artistic influences and techniques is very difficult to reconstruct, and it is very hard to understand what originated and where. The Mari paintings, however, are certainly the product of a local tradition, where some Aegean influence is recognizable only on decorative fillings while the general iconographic programme is not Minoan at all.

2) Qatna:

The wall paintings found at Qatna seem to reflect a very different situation. Significant parallels with Late Minoan I are here clearly identifiable, both in techniques and decorative themes: spirals and palmettes, wavy horizons, and the overall decorative syntax as well as the surface treatment, clearly comparable to Minoan and Mycenaean paintings (Von Rüden, 2006). It is still uncertain whether these paintings where effectively executed following the Minoan *buon fresco* technique (Von Rüden, 2006). However, the "Minoan" paintings found at Qatna give the strong impression of being the result of an at least Minoan-inspired tradition, if not properly Minoan (Bietak, 2007), although the technique, symbolism and decorative syntax seem not as precisely Minoan (or Knossian) as in Tell el Dab'a, making it hard to attribute these findings to a truly Minoan (or Mycenaean, given the periodisation of the paintings, dated to the late XV/early XIV century BC) workshop/traveling artisans. Taking in account the significant chronological gap (possibly spanning more than a century) between these specimens and the earlier "Minoan" paintings in the Levant and Egypt (Alalakh, Tell Kabri and Tell el Dab'a) it seems very likely that the paintings from Qatna may be the result of a later "Aegeanising" fashion re-elaborated on local tradition, comparable to the "Aegeanising" paintings executed at Malkata by the same time (Kemp, 2000).

3) Alalakh:

The earliest paintings from Alalakh were found in the main hall of Yarim-Lim Palace, dated to phase VII, and they were interpreted as Minoan by Sir Leonard Woolley (1955). Fragments of ashlar dado imitations, rocky landscapes and the notched-plumes of a griffin found precise parallels in the Knossian paintings (Bietak, 2007), and to this adds the interpretation of some fragments of horns as a buchrania frieze (Niemeier, 1998). The very fragmentary state of the findings does not allow to reconstruct the symbolic programme with fair certainty, but the affinity between these paintings and Minoan Neopalatial productions seems very clear.

On the present state of evidence, it is hard to think that Knossian élites may have taken over the island and the control of maritime trading routes only by LM II/III (Manning, 2007) since:

1) There are significant signs of an expansion of Knossian power through a significant part (if not all) of the island already by MM III/LM I A (Wiener, 1984; 2007);

2) Already by LM II the evidence for Aegean imports of objects of certain Cretan origin becomes very scarce if any (while, on the contrary, Helladic wares become very abundant), but Minoan ware starts to be attested by this time in the Central Mediterranean (reaching Sicily, Sardinia, and Spain through the Libyan coastal ports, Cultraro, 2006).

The presence of Knossian symbolism outside the palatial center is not very surprising: in fact, it is only Knossos to have revealed so far a real "palatial symbolism" on wall paintings as early as MM III/LM I A, and it is quite obvious that it would be from this center that the Minoan "symbolism of power" would spread to other peripheral and later foreign centers, from Akrotiri to Tell al Dab'a[5].

4) Tell Kabri:

Fragments of Minoan paintings were found at Tell Kabri inside room 611 in the MB II C palace (Niemeier and Niemeier, 2002). The hall measured 8.80 by 9.30 meters, and featured three doorways and niches on three out of four walls. The fourth wall was very likely used as the background of the throne (Kempinsky, 2002). A fragmentary *a fresco* painting imitating a typical marmorized pavement and iris flowers in blue and red embellished the throne room's floor (Niemeier and Niemeier, 2002; Bietak, 2007), and more fragments of Minoan *frescoes* were found also under the threshold of room 698, and in the debris of plaster fallen from the walls. All of the paintings show clear Minoan features: the *a fresco* technique, the combination of compressed and stone polished plaster, the cord impressions to prepare the surface for patterns and the iconographic themes reconstructed by the Niemeiers give a sound base to this identification (Bietak, 2007). The LM I A paintings from the West House room 5 at Akrotiri seem to offer the closest parallels for the fragments of notched plumes, swallows, coastal landscapes, ashlar masonry façades, and round beams

[5] Wiener, pers. Comm, 22/04/2010.

recognized by the excavators amongst the fragments from Kabri (Niemeier and Niemeier, 2002), but no trace has been found so far of typical Knossian symbolism as the taureadors, the horns of consecration and the half rosettes found at Tell el Dab'a (Bietak, 2007).

5) Tell el Dab'a:

Similarly to Alalakh and Tell Kabri, here also fragments of Minoan paintings came to light from a royal palatial context (phase C/2), but the Tell el Dab'a specimens seem to be quite different from the other Minoan paintings found in the Levant so far for both their careful adherence to specific Minoan/Knossian "symbolism of power" and for their context in the general iconography of the Palace, which has revealed so far no hint of the traditional Egyptian royal symbolism (Bietak, 1999, 2005, 2007; Mairnatos and Morgan, 2005; Bietak et al., 2007; Morgan, 2006, 2010b; Marinatos, 2010). The stratigraphic reconstruction of the site is extremely complex (see detailed chapters below): after the earliest II millennium phases the site becomes the center of the Hyksos capital of Avaris (phases E/3 to D/2). The town of Avaris was conquered and destroyed by the Theban King Ahmose, founder of the XVIII Dynasty by 1550/1530 (phase D/1.2) and subsequently hosted military barracks (phase D/1.1). By the Thutmoside age (phases C/3-2) a royal palatial quarter is again established at Tell el Dab'a, and is probably identifiable as the port of Peru-Nefer mentioned in coeval Egyptian fonts (Daressy, 1929; Glanville, 1931, 1932; Bietak, 1999, 2005, 2018). The site maintains his economic and political importance all through the XVIII and XIX Dynasties probably also due to his position and maritime vocation, making it an interface between Egypt, the Levant and the Mediterranean (Bietak, 1999, 2005, 2018). The fragments of Minoan paintings were found in the Thutmoside palatial area at 'Ezbet Helmy, that consists of a large precinct including an artificial lake, several courts and gardens, and three palaces (G, F and J), built on a 7-meter-high platform (Bietak, 1992, 1999, 2005, 2007, 2018; Bietak et al., 2007). The majority of the fragments come from palace F, that was interpreted as having purely ceremonial functions due to the lack of typical private quarters (Bietak, 1992, 1999, 2005, 2018; Bietak et al., 2007), while a second scatter of fragments was found amongst the debris on a monumental threshold and partially still (partially) in situ alongside the road leading to palace G (Bietak, 1992, 1999, 2018; Bietak et al., 2007). These fragments were considered of purely Minoan origin (Bietak and Marinatos, 2000) due to the *a fresco* technique, the combination of compressed and stone polished plaster, the cord impressions, the use of crushed murex shells in the plaster – but also and most

importantly for the iconographic themes: typical LM I A artistic conventions are applied at Tell el Dab'a in a much more precise and careful way than in at any other site where Minoan paintings outside of Crete have been found so far: feline hunters, notched-plumes, half rosettes, maze patterns, paintings of acrobats teasing bulls, the horns, the rendering of the bull's coat, the dresses of the acrobats, the rocky and undulated landscapes and the overall compositive syntax are so strictly adherent to the LM I A-B wall painting tradition that they may only be considered the direct work of Minoan artisans living at Tell el Dab'a (Bietak, 1999; Bietak and Marinatos, 2000; Morgan, 2004, 2006; Bietak et al., 2007). The presence of specific themes of Knossian power in palace F (such as the taureador scenes, the half rosettes, the griffins and the maze pattern) seems very striking if compared to the absence of any reference to Egyptian power in the palace (Bietak, 1999, 2005, 2007), and the taureador theme in particular does not appear outside Knossos (with the exception of Tell el Dab'a, Bietak and Marinatos, 2000).

Furthermore, following Bietak's reconstruction, the throne room was embellished with a wall frieze including griffins flanking the throne identical to that of the throne room at Knossos (Bietak and Marinatos, 2000; Bietak, 2005, 2007; Bietak et al., 2007). The peculiar context of the paintings and their close Knossian parallels seem to show the reflection of a specific link between Knossos and the "Minoan" palace at Tell el Dab'a between c. 1500 BC and c. 1425 BC.

Their context and meanings seem different from the other sites as Alalakh and Tell Kabri (although the fragmentary nature of the paintings in these sites may be somehow misleading), for three main reasons:

1) The contemporaneity of the three sites that have yielded truly Minoan paintings is not absolutely certain: on the contrary it seems almost certain that the paintings from Alalakh VII should be 50 to 100 years older than those from Tell el Dab'a;

2) Even if the techniques employed at Alalakh, Tell Kabri and Tell el Dab'a are very similar, and probably all reflect the direct work of Minoan artisans, the iconographic themes and symbolic meanings reconstructed so far are quite different;

3) While the paintings from Alalakh and Tell Kabri seem to be part of iconographic programmes referring to local power, and may have had a mainly decorative function, at Tell el Dab'a the Minoan paintings show a deliberate choice of Neopalatial symbols of power and are inserted in a context completely lacking reference to local power.

A possible consequence of these observations is that the evidence of Knossian palatial symbolism found at Tell el Dab'a may be linked to a direct "official" contact between the Thutmoside port town and Late Minoan Crete, as testified by textual evidence in the Annals at Karnak and in the depictions of Minoan delegations in the Theban tombs of high officers of that age. This particular link has been variously interpreted, from the possible presence of an actual Minoan colony in the Delta (Vercoutter, 1956; Duhoux, 2003) to the hypothesis of an interdynastic marriage (Bietak, 1999, 2005, 2007, 2018), a practice that was very common at the Thutmoside court. The contemporaneity of these paintings with the abovementioned Aegean "tributes" in Theban tombs does highlight the possible identification of the site with Peru-Nefer, where "Keftiw ships" are reported to be constructed or repaitred in papyrus BM 10056 (Bietak, 2007, 2018).

To sum up, the so called "Minoan" wall and floor paintings found in the Eastern Mediterranean and Egypt during the last five decades cover a very significant time span and can neither be grouped into a single general phenomenon, nor attributed to a single cultural tradition as recent reanalysis of their chronological and symbolic contexts has shown that:

1. There has been a local Syrian wall painting tradition as early as Early Bronze Age IV at Ebla, and, slightly later, at Mari and Tell Sakka. All of these paintings employed the *a tempera* technique;

2. The paintings from Alalakh, Tell Kabri, Qatna, Malkata and Tell el Dab'a do on the other hand show different grades of Minoan influence, some of them being probably directly executed by Minoan artists;

3. There is a significant chronological difference between the mentioned contexts: the paintings from Qatna are much more recent and show the adoption of Minoanising themes by the local traditions. The earliest paintings of Alalakh and Tell Kabri are much more "Minoan", but seem to have had a primarily decorative function inside the local iconographic programmes in a sort of "Versailles effect" (Wiener, 1987; Niemeier, 1998);

4. The paintings from Tell el Dab'a, with their very precise reference to Minoan "symbolism of power" and particularly to Knossian palatial paintings, together with the textual evidence speaking of a relationship with Crete at the time, testify to the reality of direct and official contact between Thutmoside Egypt and late Neopalatial Crete, although the effective range and forms of this contact are still hard to reconstruct in detail.

Chapter III

LM I A absolute chronology and Archaeological arguments for the date of the Minoan eruption in its Mediterranean context

III.1 LM I A absolute chronology: a five decades long debate

All of these textual-archaeological synchronisms between Egypt and Late Minoan Crete have been used by the supporters of the so-called "traditional/Low" chronology to build a hypothetically coherent and reliable interrelated chronological framework (cfr. Warren and Hankey, 1989; Bietak, 2000, 2004, 2007; Wiener, 2001, 2003, 2006, 2007; Warren, 2006; see discussion below). As a result, the key question of the absolute date of the mature LM I A Theran eruption, offering both a *terminus ante quem* for the end of the Middle Bronze Age and a *terminus post quem* for the LM I A/B transition, has been variously attributed to the period in-between 1540 and 1500, or even 1480-1450 BC in the "Ultra-Low" chronology. Even if the latter hypothesis seems not likely at the present state of the debate (since it would require to "pack" the whole LM IB and LM II to a period of no more than 70 years, given the later synchronisms between LM III A1 and the reign of Amenhotep III), since the late 70's the whole "traditional" reconstruction of archaeologically attested synchronism has been seriously questioned by the radiocarbon measurements collected from a few key-sites in the Aegean, implying a shift of some 100-120 calendar years in the LM I A-B chronology (cfr. Kemp and Merrillees, 1980; Manning, 1999, 2005, 2007, 2009; Manning and Bronk-Ramsey, 2003;

Manning et al., 2006).

During the 90's, this chronological hypothesis seemed to be confirmed by the use of proxy data, mainly volcanic horizons comparable to the Theran eruption in Greenland ice-cores GRIP, NGRIP and DYE-3 (Zielinsky, 1994; Manning, 1999; Zielinsky et al., 2001; Hammer et al., 2003; Vinther et al., 2005) and years of anomalous tree-ring growth in the Belfast, Bristlecone, Hohenheim and Anatolian dendrochronological sequences (Manning, 1999; Kuniholm et al., 2001; Manning et al., 2002, 2006; Manning and Ramsey, 2004). The value of this proxy data in reconstructing the date of the Theran eruption was subsequently dismissed (Wiener, 2003, 2004, 2006; Pearce et al., 2007) and the absolute date of the mature LM I A Theran eruption was variously dated by supporters of the AHC to 1647-45 at a first stage, and then, finally, to 1627-1600 BC (Manning, 1999, 2014; Manning et al., 2006, 2014; Friedrich et al., 2006, 2014; Friedrich and Heinemeier, 2009).

Volcanic horizons in DYE-3 and other Greenland ice cores Contemporary volcanic horizons reflecting a major volcanic episode comparable to the Theran eruption have been identified in layers dated to c. 1645 BC in Greenland ice-cores GRIP, NGRIP and DYE-3. At a first stage, Rare Earth Elements analysis on 1645 BC volcanic horizon (Zielinsky et al., 1994; Manning, 1999; Hammer et al., 2003) seemed to confirm its attribution to the Minoan eruption on Thera, but this identification was subsequently dismissed because of the difference in Europium, Barium and Strontium content between the DYE-3 1645 BC volcanic horizon and the Theran tephra composition (cfr. Keenan, 2002, Pearce et al., 2007) and the 1645 BC horizon was subsequently attributed to the Late Holocene Aniakchak eruption in Alaska (Pearce et al., 2007). Another major horizon that would be compatible with the "High" chronology was identified at 1627 BC, but at least 10 major volcanic episodes have been recognized in the Greenland ice cores record from the XIX to the XIV centuries BC, including possible candidates that would be compatible with the "Low" chronology (Wiener, 2006; Fantuzzi, 2007). These include the volcanic episodes at 1524 BC in DYE-3, 1569 and 1564 BC in GRIP and other "minor" horizons in the XVI century in the GISP2 sequence (Zielinsky, 1994; Clausen et al., 1997; Southon, 2004; Vinther et al., 2005) and even horizons possibly compatible with the Ultra-Low chronology (1463 BC in DYE-3).

With regard to tree-ring growth anomalies in dendrochronological sequences, one major episode of annual tree ring low growth occurring at 1628 BC was identified in the Bristlecone dendrochronological sequences (La Marche and Hirschboek, 1984: but see discussion below after Pearson et al., 2018), and subsequently linked to other low-growth episode for the same

year identified in the Irish, English and Anatolian tree ring sequences (Manning, 1999). Its occurrence in the Anatolian Dendrochronological Sequence allowed some authors to link it to the Theran eruption (Manning, 1999; Manning et al., 2001, 2002), as episodes of low growth in dendritic sequences may reflect the altering of climate by the ejecta of a volcanic eruption blocking sunlight and causing particularly cold weather (La Marche and Hirschboek, 1984).

However, this identification was subsequently dismissed (Manning, 2005) as:

1) The Anatolian "floating sequence" turned out to be chronologically misplaced by 18-22 years (Manning et al., 2001);

2) The Bristlecone sequence, where the low growth episode was firstly linked to the Theran eruption, shows other comparable signals at both 1571-1570 and 1525-24 BC that could be linked to volcanic horizons in Greenland ice cores (Wiener, 2006);

3) There is no way, at the present state of our knowledge, to trace any particular tree-ring growth anomaly to a specific eruption (Pearce et al., 2007; Wiener, 2009).

III.2 Egyptian/egyptianising stone vases from Mycenae Shaft Graves and Akrotiri

Perhaps the most important (archaeological) argument for the supporters of the "Low" chronology (but also for the so-called "compromise Low"[6]) lies in three aegyptiaca from LM I A/LH I contexts, from Akrotiri (Akr*1800) and Mycenae Shaft Graves IV (NM829) and V (NM592)[7].

III.2.1 Akrotiri 1800 (strap handled rhyton, Akrotiri)

The first item consists in an Amphoriskos, 17,2 cm in height, with two parallel strap handles, made of typical "Egyptian alabaster" (calcite), reworked and drilled on the bottom to trasform it into a Minoan rhyton (Warren, 2006). The bottom of the vase has been badly damaged in antiquity and repaired with a patch of (apparently) the same material (Warren, 2006). The specimen was found at Akrotiri, Delta Room 18a (Doumas, 1992). The shape was originally thought to be a minoan production on egyptian raw imported material (Warren, 2000), but then recognised as an egyptian production reworked in the Aegean, most probably on Crete (Warren, 2006, 2009). The thin and vertically ribbed strap handles seem to indicate that the type was probably a stone version of single-handled metal production, to which a second parallel handle was added to support the weight of the stone product (Warren, 2006 with parallels[8]).

Although the shape is somewhat shorter and different (f. e. it lacks a base ring, although it

[6] A somewhat unfortunate term which indicates the possibility of a date for the Minoan eruption at Thera as early as 1570-30 BC without undermining the (basic) archaeological-based chronology.

[7] See figures 1-7, Appendix II.

[8] Petrie, 1937, pl. XXXIX 16.

may have been present before the bottom was broken and pierced[9]) if compared with other known XVIII dynasty types, all the available parallels (e.g. the rather straight sided cylindric neck, and the everted rim) plus the material (calcite vs gypsum) strongly links this piece to the early NK or, at the earliest, late/final SIP production and no earlier parallel could be found by the present author in the bibliography.

III.2.2 NM 592 (strap handled jar, Shaft Grave IV, Mycenae)

A 28,3 cm high, single strap-handled jug of Egyptian alabaster (calcite) was found in a LH I context (Dietz, 1991) in Shaft Grave IV at Mycenae. The shape is a stone imitation of Cypriot Red Lustrous Wheel Made, which is dated to Late Cypriot I A 2 (Eriksson, 1993, 2007). All the available parallels would place the shape after the beginning of the XVIII Dynasty (in particular the wide-spreading rim, Warren, 2006), and after the reign of Amenhotep I (Eriksson, 1993, 2007; Hein, 2007; 2018).

III.2.3 NM 829 (baggy alabastron converted into a bridge-spouted jar, Shaft Grave V, Mycenae)

This bridge-spouted jar (14,5 cm high, diam. 12,3 cm) was originally an Egyptian baggy alabastron that has been inverted, topped with a gold-leaf bronze rim. Two gold-leaf covered wooden handles were added to the shoulder, and a bridge-spout was added with four bronze pins (Warren, 2006).

The shape of the original alabastron, with a low, baggy profile and a flat base has strong parallels in the early XVIII Dynasty, but the non-everted rim finds its closest parallel in an alabastron from Alalakh VII (Lilyquist, 1995; Warren, 2006). Warren (2006) notes however

[9] Bietak, pers. Comm., 13/06/2018.

that the original rim may have been trimmed in Crete in the process of conversion of the vessel into a Minoan specimen.

III.2.4 Chronological discussion

All of the above elements seem to indicate that the eruption of Thera (which occurred after the above LH I contexts, Dietz, 1991; Warren, 2006, 2009, 2014) should be dated to the final SIP-NK transition at the earliest (Warren, 2006; Wiener, 2010).

Recently (Manning, 2014), it has been argued that the aforementioned vessels are to be dated to a much earlier period, perhaps up to the middle of the XVII century BC. However, this position relies on a rather inaccurate reading of the bibliography. Manning (2014:37) cites three arguments:

1) That NM 829 is defined as "late SIP" by Warren (2006), but as merely SIP by Lilyquist as reported in Wiener (2010:380). This statement is both imprecise – Warren (2006) doesn't date the vessel to the late SIP, but rather to the early XVIII Dynasty (or, more accurately, to a period between the Alalakh VII alabastron and the Thutmoside types) – and irrelevant to the debate: even if a production date as early as 1600 BC was suggested for the piece – and still taking in account Merrillees (2009) "Ultra" High cypriot chronology, then a date as high as 1630-1610 BC for the eruption would still be clearly infeasible (see below);

2) That the chronological value of the aforementioned vessels would be unreliable, as (a) they may be of Levantine production, and (b) the fragmentary nature of our knowledge of SIP stone vessel production is insufficient. As to (a), this argument relies on the position of Christine Lilyquist (1995, 1997) that Manning reports as cited in Wiener (2010). However, this argument is irrelevant to the chronological debate as Lilyquist does not suggest a date for these specific vessels as early as that required by the Aegean High Chronology (cfr. Lilyquist, 1995, 1997).

As to (b), Manning goes on by quoting Höflmayer (2012:444):

> Given the unsatisfactory state of research in the field of Egyptian stone vessels of the Second Intermediate Period and the early New Kingdom, it does not seem impossible that the two Egyptian stone vessels from the Mycenean shaft-graves could have been produced 1 or 2 generations earlier than previously suggested (i.e. in the Second Intermediate Period). A new critical re-evaluation of the development of Egyptian stone vessels from the Second Intermediate Period to the New Kingdom might be desirable in order to check for a possible earlier dating of the crucial synchronisms.

Again, this point is irrelevant for the debate on the chronology of the Minoan eruption, as «1 or 2 generations earlier» would still set the production of these vessels to 1620/1600 BC at the earliest, a date which would still not be compatible with the Aegean High Chronology (see below). Moreover, in the dedicated paragraph of the same paper, Höflmayer (2012:440) says:

> Warren dated this vase [NM 829] to the early 18th dynasty or a little bit earlier, to the latest Second Intermediate Period (Warren, 2006, 2009). He based his date on a comparison with drawings of stone vessels that are linked with certain kings (Lilyquist, 1995) […] originally published by Howard Carter (1916) regarding his work on tomb AN B in western Thebes […]. The forms depicted in Carter's report do not represent actual vessels, only "debris" of stone vessels was found […].

The observation that Warren would have based his dating only on the drawings by Carter is incorrect. In fact, if Warren cites Carter's types (after Lilyquist, 1995) for comparison, the main parallels cited (above) are the Alalakh VII alabastron and several Thutmoside baggy alabastra (f.e. Lilyquist, 1995, fig. 31).

Moreover, Höflmayer (2012:440-441) goes on by stating that:

> Also, the dates offered for these forms in Lilyquist's publication are based on fragmentary material; therefore, the similarity between the actual vessel and the depicted forms should not be used as an argument for dating, and instead one should seek for existing fully preserved vessels for parallels […].

> If we tentatively accept an early 18th Dynasty date for these 2 vessels, we have to conclude that the Minoan Santorini eruption took place after the start of the Egyptian New Kingdom […].

It has to be said that in a subsequent paper, Höflmayer (2018) changes his position as to the dating of the above mentioned vessels, but doesn't cite any putative earlier parallel or argument for an earlier dating, albeit repeating the above observations.

The critic to the chronological value of the mentioned vessels for the Aegean LM/LH I chronology seems rather unsubstantiated. Of course there may be changes in the chronological parallels if new specimens from SIP (and/or Levantine MBA) contexts will come to light, but – given the time that must be allowed for an Egyptian (and/or Levantine) alabastron to be traded to Crete/the Cyclades, be reworked and transformed into a Minoan product, be exported to the Greek mainland, and then become part of a funerary assemblage, it seems very unlikely that the contexts where this vessels have been found would turn out to be much earlier than previously thought, at least not as much as to fit a 1630/1610 BC date.

III.3 Minoan Eruption Pumice in the Levant and Egypt

The second argument for the "traditional" chronology lies in the chronological distribution of lumps of Minoan pumice (ejecta of the eruption) from Levantine and Egyptian sites, where it was stored (even for long periods) for several uses, and particularly as a tool for stone and metalworking (Wiener and Allen, 1998:26). Faure (1971, cited in Wiener and Allen, 1998:26) notes:

> fourteen separate uses of pumice recorded in classical antiquity: as an abrasive for stoneworking; in polishing marble, bone and metal; in the preparation/tanning of skins/parchments; for cleaning potting clay; as a component of concrete or an additive to certain paints; as an agent to retard fermentation; in cleaning the skin; as a medicine or as a depilatory; as a counteragent for inebriation; and as a toothpaste.

Pumice was certainly obtained through trade (particularly in the later periods), but was also waterborne and probably directly collected on the seashore in many cases, including some of the samples found at Tell el Dab'a (Wiener, 2010:374, n. 59, with references). In general terms it is clear that Theran Minoan pumice (as opposed to other sources, including the preceding Theran Cape Riva pumice, Bichler et al., 2003; Foster et al., 2009; Sterba et al., 2009) never appears in any context earlier than the SIP-NK transition or early LBA in the Levant.

At least 415 samples of Pumice from stratified contexts in Egypt, the Sinai, the Levant and the Aegean have been investigated so far (Bichler et al., 2003; Foster et al., 2009; Wiener, 2010:374) of which 154 came from Tell el Dab'a (Bichler et al., 2003; Wiener, 2010, n. 65). Of these, 32 have been analysed by NAA (all from contexts dated to late Thutmose III to Amenhotep II). 29 turned out to be from the Minoan eruption (the others being one from Nisyros and the other two from Kos; Foster et al., 2009) and some show traces of being waterborne and are therefore unlikely to postdate the eruption by a (very) long time-span (Wiener, 2010).

The chronological value of this argument has been recently questioned by Höflmayer (2012, 2018) and by Manning (2014).

Höflmayer (2012:441-442) correctly observes:

a) That if we accept a date as low as post-1450 BC for the stratum C/2 (where the pumice lumps have been found at Tell el Dab'a), then this would be in conflict with the chronological correlation between the reign of Thutmose III and Aegean LM I B/LH II A (the bibliography is immense, but see f.e. Warren, 2006; Manning, 2014);

b) That the number of available samples from the NK/LBA by far outreaches that of the samples available for the SIP/MBA. In fact this aspect is also admitted by Bietak (quoted in Wiener, 2010:374) noting that «However, and oddly enough, only 27 pumice lumps have been located of such older contexts».

It is undoubtedly true that much more data would be desirable (particularly from SIP/MB stratified pumice samples), and that this is an argument *ex silentio* – i.e. if samples of Minoan pumice will be identified from earlier contexts then the picture would change much. Minoan pumice is indeed more a *terminus ante quem* than a *terminus ad quem* (Höflmayer, 2018).

However, the coherent chronological distribution of the wide bulk of samples identified so far, plus the fact that at least part of them was waterborne, plus the absence of Minoan pumice from the (few) samples of predating contexts (f.e. Maiyana Tomb: Foster et al., 2009; Sterba et al., 2009) makes it rather unlikely that a 100-120 years' time span elapsed between the eruption and the pumice findings in Egypt and the Levant.

Höflmayer (2012:442; quoted also in Manning, 2014:31) further reports the author of a recent (at the time) publication on Minoan pumice (Sterba et al., 2009) as concluding that:

> since the number of excavated samples from later periods greatly exceeds the number of samples from the earlier period, the pumice data are still not conclusive.

Reading the original paper by Sterba et al. (2009), the quoted statement doesn't seem to be much of a conclusion (as it appears in the "introduction", on column 2 of the first page, Sterba et al., 2009:1738) but rather a (sound) *caveat*. In fact, the authors of that paper's conclusion is that:

> Pumice from the Minoan eruption of Santorini has not yet been found in pre-Eighteenth Dynasty contexts. Volcanic material from this eruption of Santorini is seen beginning just after Ahmose, or possibly in the last year or two of his reign. If the Egyptian chronology is used as reference frame, these findings contrast with the latest ^{14}C-dating of the Minoan eruption of 1627–1600 B.C.E. by Friedrich et al. (2006). Thus, various explanations are needed as to why masses of pumice from the Minoan eruption do not show up earlier – it lay uncollected on the shore; it was not favored for use; we have not yet excavated Hyksos-era workshops; and so forth. Or, this means that major upward adjustments are needed in the absolute chronology of Egypt and the Aegean, which thus far seem unwarranted from the egyptological point of view (Sterba et al., 2009:1743).

Höflmayer (2012:441) also contends that the first occurrence of Minoan pumice in Tell el-'Ajjul stratum H5 (Fischer, 2009), which he dates to env. 1525 BC, would imply a gap of at least a minimum of 75 years between the pumice from H5 and the samples from Tell el Dab'a stratum C/2. Höflmayer uses this as an argument against the eruption date at env. 1525 BC suggested by Wiener (2006, 2010). This argument is indeed of some relevance if a date for stratum C/2 at or later than 1470/50 BC is held as the only possibility.

However, (1) this date for C/2 is strongly questioned by Höflmayer himself (2018, following Kutschera et al., 2012 – see discussion below), and (2) the strong linkages given by the parallel sequence of imported Cypriot wares (as BR I, WS I, RLWM) in both Tell el Dab'a C/2 and Tell el-'Ajjul H5 makes it very unlikely that a significant time span separates the two phases (Bietak, 2013, with bibliography).

The scarcity of samples from contexts preceding the Thutmosid age can be a reflection of the fact that we lack evidence of metallurgic workshops from the age of Ahmose – of course the same argument may be applied (as Höflmayer, 2018, does) to the scarcity of pumice findings from SIP/MBA contexts. Moreover, it is also possible that, as already put forward by Malcolm Wiener (Wiener and Allen, 1998:27):

> (1) the Hyksos metal or other workshop area has not yet been uncovered in the excavated part of the enormous site of Dab'a, or (2) Hyksos metalworkers [and Levantine metalworkers too? AN] were accustomed to use other abrasives and so ignored the pumice

> floating in the Delta, perhaps because the existing methods of production of metal had social or symbolic significance resistant to change […].

Considering all the above (and the *caveat* that new samples from earlier contexts may overthrow the picture), it seems that pumice from the Minoan eruption from Egypt and the Levant does not offer a conclusive argument in favour of the "Low" chronology for the eruption (i.e. an eruption date not earlier than 1530/1500 BC), but still offers an (circumstantial) argument against an eruption date as early as 1630-10 BC.

III.4 Cypriot Pottery from Akrotiri, Egypt and the Levant

The third main argument for the archaeological chronology relies on a Cypriot White Slip I (henceforth WS I) fragmented vessel found in 1870 by H. Gorceix and H. Mamet almost certainly in the strata covered by ejecta of the eruption ("Volcanic Destruction Layer", henceforth VDL) at Akrotiri (Merrillees, 2001:91). This vessel, which got lost during World War I (Renaudin, 1922, quoted in Merrillees, 2001:90), consists in an open bowl, env. 11,7 cm in height, 22,8 cm in diameter, probably damaged and repaired in antiquity. It has been described in a number of publications, but the most accurate description is that of Merrillees (2001), based on a comparison of all available sources (Merrillees, 2001:93):

> Hemispherical bowl with round base and slides incurving to a plain rim […]; bifurcated handles set diagonally on the upper body, restored as a loop but probably originally in the shape of a wishbone. Painted decoration, consisting of a wavy line round the top of the body, below the rim; underneath a horizontal line band consisting of four parallel straight lines with diagonal hatching; descending from this band on either side of the body, two vertical bands, each of four parallel straight lines with diagonal hatching, either side of a vertical row of cross-hatched lozenges framed on each side by a vertical straight line; descending down the front of the body, two parallel vertical rows of cross-hatched lozenges, each linked to the horizontal band by a short wavy line and framed on the outer sides by a vertical row of dots and enclosed by a vertical band of four parallel vertical lines with diagonal hatching; descending from the horizontal band on either sides of the handle base, a vertical band of four parallel straight lines with diagonal hatching; between them and the next vertical band on the side of the body, a vertical row of dots or dashes. Brown clay pinkish-buff slip […].

The relative dating of this bowl in the Cypriot WS I sequence is variously placed between the LC I A1/2 transition and the LC IA/IB transition.

Merrillees (2001, 2009) dates the vase to the LC I A/B transition while, at the extremes,

Manning (1999, 2014) dates it to an earlier phase (LC I A1-A2 transition) stemming from the decoration "hangovers" form PWS (Manning, 1999:154-192), and Aström (1971, 1972) dates the piece to the LC IB1 period (i.e. 1525-1450 BC, Merrillees, 2009:248).

Since (1) the relative dating of the bowl in the LC I sequence is debated, and (2) the start of the LC I A period has been variously set from 1700 BC (Manning, 1999) to 1530 BC (cfr. Merrillees, 2009:248), after warning that:

> my preferred high chronology is a *terminus post quem*, for if it were found in due course to be seriously wanting, the date for the start of the Late Cypriot I would have to be lowered, not raised. (Merrillees, 2009:249)

Merrillees goes on formulating several possible chronological scenarios:

1) Taking in account the High Cypriot chronology, (a) within Manning's dating of the WS I bowl from Thera the vessel cannot have been produced prior to env. 1625 BC, giving a *terminus post quem* for the eruption that would already be in contrast with an eruption date of 1630-1610 BC (Merrillees, 2009:249); (b) within Merrilees (2001) classification of the bowl, the production date would be set to env.1600 BC, thus making an eruption date in the XVII century BC impossible; (c) within Aström's dating the eruption date would be even more incompatible with the AHC;

2) Taking in account a start date of 1600 BC for the LC I A period, (a) within Manning's classification the WS I bowl from Thera should have been produced no earlier than 1575 BC, thus ruling out any eruption date in the XVII century BC (but still allowing a date in the middle of the XVI century, see chronological discussion below); (b) within Merrillees' classification, the date of the bowl would be around 1550 BC, and the eruption date would have to be consequently later (see for example the 1525-1524 date proposed by Wiener, 2010); (c) within Aström's classification, the Theran Bowl would have to be dated from 1525 to 1450 BC, which would even rule out an eruption date at 1525-24 BC and barely possibly allow a date of 1500 BC;

3) Other scenarios proposed (as following the Cypriot Low Chronology as put forward by Eriksson (1992) would even rule out a possible date at 1500 BC, but this seems really too low even in the Low Aegean Chronology (see f.e. Warren, 2006; Wiener, 2010).

Furthermore, Merrillees (2009:249) observes that:

> the high chronology for the Late Cypriot period using Manning's classification for the Cypriot bowl is compatible with a date of around 1630, but only just, while the date of 1600 BC [and also 1625 BC, AN] for the start of the Late Bronze Age in Cyprus makes a synchronism with 1630 BC on Thera impossible. It also means that the Low Chronology for the Late Cypriot period, regardless of the classification used for the WS I bowl is completely incompatible with a Theran destruction at 1500 BC. This implies that for nearly all the specialists on Cyprus a date for the Minoan eruption of Santorini is too high at 1630 BC and too low at 1500 BC. Even if the range of possible choices were narrowed to between 1600 BC and 1530 BC, there would still be problems for the synchronism with Cyprus, unless, of course, a date for the destruction of the settlement on Thera were put at some time in between.

There is an apparent contradiction in the above statement that Manning's classification plus Cypriot High Chronology would barely allow an eruption date at 1630 BC, as in scenario 1 (a) above, Merrillees sets the production of the bowl to 1625 BC. This apparent contradiction may be solved if in fact, in the conclusions, Merrillees was referring to the (Ultra) High Cypriot Chronology which would set the beginning of LC I A to 1700-1670 BC (Manning, 1999). However, as Merrillees himself observes (see above), his own High Chronology – with the start of LC I A1 set at 1650 BC) is probably the highest possible scenario (Merrillees, 2009:249).

At this regard, Merrillees (2009:251) goes on observing that:

> Following the principle that the context should date the import, not the other way around, the beginning of Late Cypriot I should antedate 1630 BC by at least 25 years or more, if we follow the upper range indicated by scientific findings. While this may not be incompatible with the high chronology, it represents the top end of a very long range of possibilities and to my way of thinking unduly stretches the evidence and strains credibility.

However, it must be also noted that Merrillees (2009:251) concludes that:

> no-one is going to accept the presence of one stray White Slip I bowl in a destruction layer at the end of Late Minoan I A as a compelling argument for raising the date of the opening of the Late Cypriot IA beyond, let us say, 1600 BC. Still less would we advocate lowering the date of the Theran catastrophe to accomodate the indipendently established chronologies for the Late Bronze Age in Cyprus. I do note, however, some give in the scientific dating of the Minoan eruption of Santorini close to the end of the 17th century BC would fit the high chronology more comfortably as well as satisfy me.

The chronological value of the WS I ware to which the Theran specimen belongs comes from two facts:

1) That this specific class of ware was exported to all the Eastern Mediterranean, from the Aegean (f.e. apart from Akrotiri, on Rhodes and Melos, Merrillees, 2001) to a number of sites in Anatolia, the Levant and Egypt, and – much more importantly –

2) That the parallel relative chronological sequences of other classes of imported Cypriot wares in sites such as Tell el Dab'a and 'Ezbet Helmi, Tell el-'Ajjul, Tell Abu al Kharaz, Ashkelon, Lachish, Alalakh – most notably White Painted III, IV, V and VI (WP III/IV/V/VI), Proto-Base Ring (PBR) and Base Ring I (BR I), Red Lustrous Wheel Made (RLWM), and, of course, Proto-White Slip (PWS) and WS I – always reflect the same relative sequence observable in Cyprus from MC III to LC I A2/B (cfr. Bietak and Hein, 2001; Oren, 2001; Bergoffen, 2001; Fischer, 2001; Yon, 2001; Wiener 2001; Bietak, 2013).

As Malcolm Wiener notes, it must also be emphasized that «the WSI bowl from Akrotiri was shipped from Cyprus to Akrotiri, in all likelihood via Crete, used in antiquity, broken, repaired, and reused before the eruption, all of which must have taken some time» (Wiener, 2001, 2010[10]).

[10] Also Wiener, pers. Comm., June 2018.

A detailed chronological seriation of PWS – WS I was attempted by Kathryn Eriksson (2001) by comparing the assemblages from 19 different contexts (most notably from Toumba tou Skourou and Pendayia-Mandres). Eriksson subdivides the development of PWS (the ceramic class dated between the MC III-LC I A1 and the LC I A1-A2 transitions recognised by Popham, 1962, as the prototype of the subsequent White Slip wares) into three distinct sub-phases (PWS 1, PWS 2 and Transitional PWS-WS, Eriksson, 2001:53-57):

1) Phase 1 PWS is still linked to the preceding White Painted tradition of Middle Cypriot III, particularly for the lower body shape and decoration (Eriksson, 2001:53). A bowl of this style was in fact found in Pendayia-Mandres Tomb 1 in the lower layer and nine more vessels were found in the upper layer, in both cases in association with MC III wares and no examples of the following PBR or WS. Examples of this Phase 1 PWS were also found at Pendayia-Mandres Tomb 2, this time in association with later Phase 2 and Transitional PWS showing the very typical "rope lattice" decoration (see below), at Myrtou-Stephania Tomb 14A and at Toumba tou Skourou Tomb I, this time together with PBR. However, the latter two contexts were mixed and had been in use for a very long period (Eriksson, 2001:55).

2) Phase 2 PWS represents a distinctly evolved form of PWS. Typical of this phase are the hemispherical cups and rope lattice decoration (as opposed to the lower body and base metope decoration of the preceding phase) and the appearance of the framed lozenge decoration (that will be typical of the following WS I decoration). Apart from the abovementioned examples from Pendayia-Mandres Tomb 1 (Upper) and Tomb 2, bowls of these phase have been found in Pendayia-Mandres Tomb 3 and, most notably, at Toumba tou Skourou.

   In the latter site, sherds of phase 2 PWS were found in both square C 12, together with PBR, and in square D 12, in association with WP V ware (Vermeule and Wolsky, 1990:30-31), but most importantly in Tomb III, where no WS I or BR I was found, therefore indicating a chronological precedence of PWS 2 and Transitional PWS/WS over typical LC I A2 wares (Eriksson, 2001:55). Interestingly, also sherds of a Late Minoan I A vase were found in the Tomb niche that could show that LM I A had already started before the onset of LC I A2, but unfortunately the contextual relationship is unclear (Eriksson 2001:55).

Phase 2 PWS was also found at Enkomi phase Ia already in association with LC I A2 wares as BR I and WS I (but see discussion in Eriksson, 2001:56) and at Akhera-Paradisi Tomb 1, where BR I is attested, but not WS I.

3) Transitional PWS/WS is characterized by the progressive substitution of the rope lattice decoration (found also on the Theran specimen, and advocated by Manning, 1999, to support a production date for the bowl at the LC I A1/A2 transition or earlier) with the ladder lattice typical of the subsequent WS I style. Bowls or sherds of this class have been found in Pendayia-Mandres Tomb 2 (see above) as well as at Toumba tou Skourou Tomb I, chamber 2 (nine vessels, in association with WS I vessels including the classical framed-lozenge style comparable to a specimen from Tell el Dab'a; Eriksson, 2001:56). A PWS tankard with rope lattice decoration and pendent lines framing a double row of dot-framed lozenges was found in Tomb II, chamber 1 in association with PBR and BR I but without traces of WS I.

Since (1) the subsequent WS I and chronologically associated BR I and RLWM are very clearly distinguishable, and (2) their relative chronological sequence is almost identically repeated in the imports from the foreign contexts cited above, this development allows to construct a sound synchronism via Cyprus between Egypt, the Levant and the Aegean. Although it is undoubtedly true that imported wares offer more a *terminus ante quem* than a *terminus ad quem* (cfr. Maguire, 2009), if we hold to the principle that a context should be dating the import and not *vice versa* (Merrillees, 2009, above), with all the problematic implications for dating the Theran eruption, we nonetheless have a solid network of synchronisms, at least on the relative chronology-scale (see Wiener, 2001, 2010; Bietak, 2013).

Cypriot imports in Tell el Dab'a are attested since the late Middle Kingdom, and the links become «strong and constant» particularly from stratum E/1, dated to the transition between the XVII and the XVI centuries BC (Bietak, in Bietak and Hein, 2001:171). Several examples of typical MC III WP III-IV and Red on Black wares have been found in the strata belonging to phases G to D/3, from domestic/settlement contexts as well as from tombs (stratum E/1). WP V (MC III to LC I A1) is attested from phase E/1 (Bietak, 2013:fig. 8.3) and becomes very abundant in stratum D/2 (Bietak, in Bietak and Hein, 2001:171). The increase of Cypriot imports toward the (late) SIP is most probably linked to the increased exploitation of the island's

resources, most notably copper (Stos-Gale, 2001; Eriksson, 2001; Bietak, in Bietak and Hein, 2001) within the Hyksos/Canaanite trading network. Tell el-Yahudiyeh ware of Egyptian production has in fact been found in several MC III-LC I A1 contexts in Cyprus (cfr. Bietak, 2013:89). Examples of piriform jars, typical of MB II B (Tell el Dab'a phase E/3) and biconical jars (Tell el Dab'a E/1 to D/2) have been found at Toumba tou Skourou (in Tomb V, Vermeule and Wolsky, 1990), at Arpera, and at Kalopsidha (Tomb 11) in contexts safely dated from MC III to LC I A1, establishing a link between the start of the LBA on Cyprus and the (late) SIP (cfr. Bietak, 2013; *contra* Manning, 1999).

PWS appears at the site only from phase D/2 (late SIP) to phase C (perhaps residual), while WS I, BR I and RLWM are attested only with phase C/2-3 (Thutmoside age, Bietak in Bietak and Hein, 2001:172; Bietak, 2013:fig. 8.3), setting both a *terminus post quem* (phase D/2) and a *terminus ante quem* (phase C/3) for the indirect dating of the LC I A1/A2 transition.

The chronological reliability of this interrelation has been recently questioned (Höflmayer, 2012:442-443, 2018; Manning, 2014:40). Höflmayer (2018) states that:

> even *if* the absolute date of Str. C/3 would be beyond doubt, White Slip I material as only found in fragmentary condition in secondary or tertiary contexts, no complete vessels have been found in situ. The first appearance is thus based on residual material and in fact only a few fragments: Bietak and Hein only mention six pieces deriving from Str. C/2-3 altogether and in fact for two fragments even a date in Str. D/2 (dated by the excavator to the late Hyksos period, but most likely earlier based on radiocarbon evidence) cannot be ruled out.

This statement seems both misleading and incorrect to some extent, as:

3) The chronological relevance of the Cypriot imports in Tell el Dab'a doesn't stem from WS I only, but rather lies in the whole sequence of different ceramic classes from MC III to LC I A2/B (as WP III-IV, WP V, PWS, WS I, BR I, RLWM);

4) Not *all* of the samples from Tell el Dab'a are from secondary or tertiary contexts.

In fact, the original publication to which Höflmayer refers (Bietak and Hein, 2001:174-180)

reports a total of 32 PWS to WS II specimens, from areas A/II, A/N, A/IV, A/V at Tell el Dab'a and H/I-H/V at 'Ezbet Helmi. Of these, 10 were certainly identified as PWS, 10 as WS I, 4 as WS II. The remaining 8 sherds lack specific diagnostic feature and were considered «indeterminate» WS (Hein, in Bietak and Hein, 2001:174-180).

Bietak (in Bietak and Hein, 2001:172) reports:

> six PWS occurrences in stratum D/2 (late Hyksos period), one of them, a complete bowl, found in the tomb of an infant together with an early bichrome vessel […] the other sherds come from settlement refuse. One more PWS sherd came from the fill of a New Kingdom casemate construction which, however, contained only Second Intermediate Period material. Moreover, there are five WS I occurrences in contexts of the early 18th Dynasty […] together with other Late Cypriote pottery comprising Bichrome ware, White Painted V and VI ware and Base Ring I.

The contexts of these (and the other unstratified or unclear sherds) are discussed in detail by Irmgard Hein in the subsequent chapter (Bietak and Hein, 2001:174-180), who concludes that:

> Due to the intense examination of the WS sherds and their contexts it becomes clear that PWS ware already definitely appeared in str. D/2, as the evidence from areas A/II, H/I and H/V demonstrates. Some PWS fragments occurred in later levels, often fill, debris layer, or other secondary positions. The second conclusion that emerges from this study is that WS I occurred in str. C, from the early 18th Dynasty onwards. There is only a slight possibility that it may already have been present in str. D/2 (see the discussion of the context of no.7057 C above; cf. Bietak supra) but it is very unlikely. (Hein, in Bietak and Hein, 2001:180)

As to the WS (ind.) fragment (7057 C) possibly coming from a context dated to phase D/2 Bietak (Bietak and Hein, 2001:172) notes that:

> [it] was found in the chamber of a tomb from str. D/2 and a case could, perhaps, be made for an appearance of WS I already in this stratum. However, the vault of the chamber had

> collapsed and the tomb had subsequently been completely plundered in the early New Kingdom and was used as a waste pit during str. C. […] In short, we cannot exclude the possibility that WS I already appeared in str. D/2 during the late Hyksos period, but there is no proof of this.

As observed above, the chronological relevance of this sequence of Cypriot imports in Tell el Dab'a and 'Ezbet Helmi is strongly endorsed by the fact that the same (or closely comparable) relative sequence of Cypriot imports is observed also in several sites in the Levant, that are chronologically linked to Tell el Dab'a through a huge number of safely-sequenced artefacts (cfr. Bietak, 2013; fig. 6 below).

Oren (2001) notes that (at the time), more than 1200 specimens of PWS to WS II had been found in Canaan, of which at least 250 were recognised as «early WS» (PWS and WS I, Oren, 2001:127), in particular:

1) Achziv: a rim fragment of a PWS bowl from a final MB III context in association with WP III-IV and RoB;

2) Akko: two WS I sherds from MB III/LB I tombs and fill deposits;

3) Tell Abu Hawam: more than 200 Cypriot imports of which only 4/5 have been identified as WS I and none as PWS, from LB Ib-IIa phases in association with RoB, WS II, BR I-II;

4) Tell Shiqmona: one framed-wavy line WS I sherd from a mixed LBA – Iron Age context;

5) Dor: one WS I framed-wavy line from an Iron Age context;

6) Tel Mevorakh: WP V and RoB in MB II B strata, and fragments of two/three WS I framed wavy lines bowls in a mixed conext in association with WS II and BR wares;

7) Megiddo: a section of a PWS rope lattice bowl from Stratum X, area AA, in association with MB III dipper juglets, Bichrome and WP III-IV ware. WP V-VI and early

Monochrome ware appear in the subsequent phase (Megiddo IX), but typical LC I A2 productions as WS I and BR I only appear from stratum VIII (dated to the Thutmoside age);

8) Hazor: two PWS rope lattice sherds, one from stratum 2 of Area H (LB IB), and the second from a mixed MB II-LBII context (locus P16), which also yielded a «late» WS I fragment and «a Myc. III B alabastron (sic!)» (Oren, 2001:132), plus two stratified WS I sherds from stratum 2 (LB IB) and stratum 1a (LB IIA);

9) Sippori: one WS I sherd from stratum VI, in association with Chocolate on White and Black Lustrous Wheel Made (LB I).

10) Tel Michal: several WP V and RoB sherds in Late Bronze fill deposits; «a few» WS I sherds from mixed LB II B contexts;

11) Jaffa: Oren (2001:132) mentions just «a few WS I sherds in an undetermined context»;

12) Ashkelon: more than 550 sherds from the MC to the LC period were found at the site. In particular, a PWS rope lattice rim sherd from level IV (MB III-LB I A) in association with typical MC III-LC I A1 wares (as WP V-VI) but with no traces of LC I A2 wares. A fragment of WS I ware was found in an Iron Age context;

13) Tel Batash: one WS I bowl from stratum X (MB II – LB I transition), in an assemblage dating to LB I A (Oren, 2001:132);

14) Lachish: one PWS rim sherd from the Fosse Temple area, attributed to Structure I, one WS I probably belonging to the the same assemblage, plus «Additional Cypriote imports […] RoB, wheelmade Bichrome, BR I, Monochrome and WS II categories» (Oren, 2001:133, with references);

15) Tel Sera: one WS I framed wavy line rim sherd together with a BR I juglet from Stratum XII:2 (LB I B);

16) Tell Far'a: «numerous Cypriote ceramics [from Petrie's excavations] including WP, RoB/B, WS and BR wares» (Oren, 2001:133 with references), five WS I sherds from the upper floor levels of the city gate complex (MBA-LB II, the two specifics contexts of the WS I sherds being dated by elevation to LB I-II, Oren, 2001:133).

17) Tel Ridan: typical MC wares including WP IV-V were found in settlement floors plus a fragment of PWS from a secondary context, no traces of LC I A2 wares;

18) Tel Dan: Oren (2001:143) mentions «only a handful of Cypriote imports» including WP III-IV and PWS from Stratum IX (MBA) to Str. VIII, and 2 WS I fragments from Stratum VIII (LB I);

19) Tell Heboua: several WP V-VI, BLWM, PWS «as well as a few WS I sherds» have been found in Stratum II, dated from the final SIP to the early XVIII Dynasty period (contemporaneous with Tell el Dab'a D/2-D/1 phases, Oren, 2001:140);

20) Tell el-'Ajjul: the site yielded the largest amount of imported Cypriot wares found so far in the Levant and Egypt. More than 1100 specimens were collected during Petrie's excavations (Oren, 2001:133) and have been systematically catalogued by Celia Bergoffen (1989). About 200 were recognised as MC (including RoB/R and WP IV-VI), at least 25 as PWS and no less than 200 as WS I. The site yielded also «a sizeable assemblage of Cypriote and Palestinian Bichrome vessels along with delicate Chocolate-on-White ware and numerous imported Egyptian ceramics» (Oren, 2001:133).

More in detail, WP V appears in settlement as well as in funerary contexts by City III phase dated to MB III (partially destroyed around 1600-1590 BC following Oren, 2001:135), and WP VI in City IIb and IIa. dated to the final MBA (from 1590 to Ahmose's campaign – corresponding to Tell el Dab'a phase D/2, Oren, 2001:135).

With regard to PWS, one complete wavy line and rope pattern PWS bowl was found in intramural Tomb 1463, dated to City IIb; one body sherd was found in a (open) context linked to the destruction horizon between Cities III and IIb; a total of 9 specimens (including a half-preserved bowl) were found in stratified contexts in Block AM, 3 of which were dated to City

IIb phase, 2 from City IIb/IIa horizon, 2 from City II a (LB IA, Oren, 2001:35) contexts and 2 from City I horizon (LB IB, Oren, 2001: 137-139). The majority of the subsequent WS I specimens were unfortunately found in disturbed deposits, and Oren cites only 7 safe contexts for the first appearance of this class, 5 of them dated to City IIa and 2 from City I, but none from late MBA City IIb (Oren, 2001:139).

Oren (2001:142-143) concludes that:

> PWS certainly appeared first in Canaan before WS I, or indeed, before any diagnostic LC ware (PBR, BR I, Monochrome, etc.). The chronological priority of PWS over WS I has been also observed in the Delta at Tell el-Dab'a and 'Ezbet Helmi […] WS I is reported in Canaanite LB IA contexts ca. 1550-1470 BCE at the earliest and is usually associated with diagnostic Late Cypriote ceramic, in agreement with the evidence from Egypt. The testimony of the archaeological record from both Canaan and Egypt concerning the first appearance of WS I pottery outside the island not before the 18th Dynasty must have a bearing on the controversial date of the eruption of Thera during LM I A (if indeed the famous WS I bowl came from its debris) and, with due reservation, on the dating of the Late Cypriote IA assemblages in Cyprus proper […]. The stratified contexts reviewed above reiterate our conclusion 30 years ago that diagnostic Late Cypriote pottery classes such as Base-ring, White Slip, Monochrome, White Shaved and others were not introduced to the markets of Canaan or Egypt before the LB IA or the beginning of the New Kingdom, ca. 1540/30 BCE […].

The renewed extensive excavations at Tell el-'Ajjul (Fischer, 2009) have produced a minimum of 830 imported Cypriote vessels, from horizon H/7 (MBA) to H/1 (LBA and later colluvium). In particular (Fischer, 2009:Table 1):

1) H/7: one Monochrome and one RoR specimen;

2) H/6: 8 Bichrome Wheel Made, 2 Black Slip, 7 Monochrome, 13 Red Slip, 1 RoB, 2 RoR, 1 WP V-VI;

3) H/5: 2 (possible) BR I, 35 Bichrome Wheel Made, 5 Black Slip, 96 Monochrome, 2

RLWM, 3 RoB, 2 RoR, 5 WP V-VI, 4 White Shaved, and 23 «early» WS I (a part of which is probably Transitional PWS/WS I, see above).

Here, again, typical MC/LC I A1 classes (as WP V-VI, RoB, RoR) appear in the MBA and follow through the transition to LBA, while LC I A2 diagnostic wares (such as RLWM, BR I and WS I) only appear at or after the beginning of the LBA – New Kingdom.

Fischer (2009:263-264, fig. 4) dates horizon H/5 to the half/late XVI century BC in a period contemporaneous to Tell el Dab'a phase D/2, but this opinion has been rejected by Manfred Bietak from the parallels with the imported Egyptian materials found in H/5 (Bietak, 2013:94, 2015:334; fig. 6 below).

III.5 Conclusions

To sum up, there are only a very few cases in the archaeological record that do not completely support the above chronological reconstruction, they are namely:

1) Tell el Dab'a: a single specimen, 7057C, from Tell el Dab'a (Bietak and Hein, 2001:172, see discussion above);

2) Tell el-'Ajjul: one BR I juglet reported by Petrie from a disturbed context at Tell el-'Ajjul «below […] City III (sic!)» (Oren, 2001:139, with references);

3) Tell el-'Ajjul: forty sherds of WS I reported by Petrie from levels that he ascribed to Palace I, which is MBA in age, but was destroyed most probably during Ahmose's campaign (Bergoffen, 2001:145).

One could possibly add to the above one more WS I bichrome bowl from Tell Abu al-Kharaz, which was found «in a fill in Area I close to the city wall» (Fischer, 2001:163), but the context is MB IIC to LB IA and was dated by Fischer (2001:164) to 1530±25 BC, a date which offers no support for an eruption date in the XVII century BC. Taking in account all the above, it is sound to maintain that (at the present state of the archaeological record), even over-stretching the evidence to the "highest" point, the Minoan eruption of Thera must have happened not earlier than the final SIP (i.e. 1580-1540 BC).

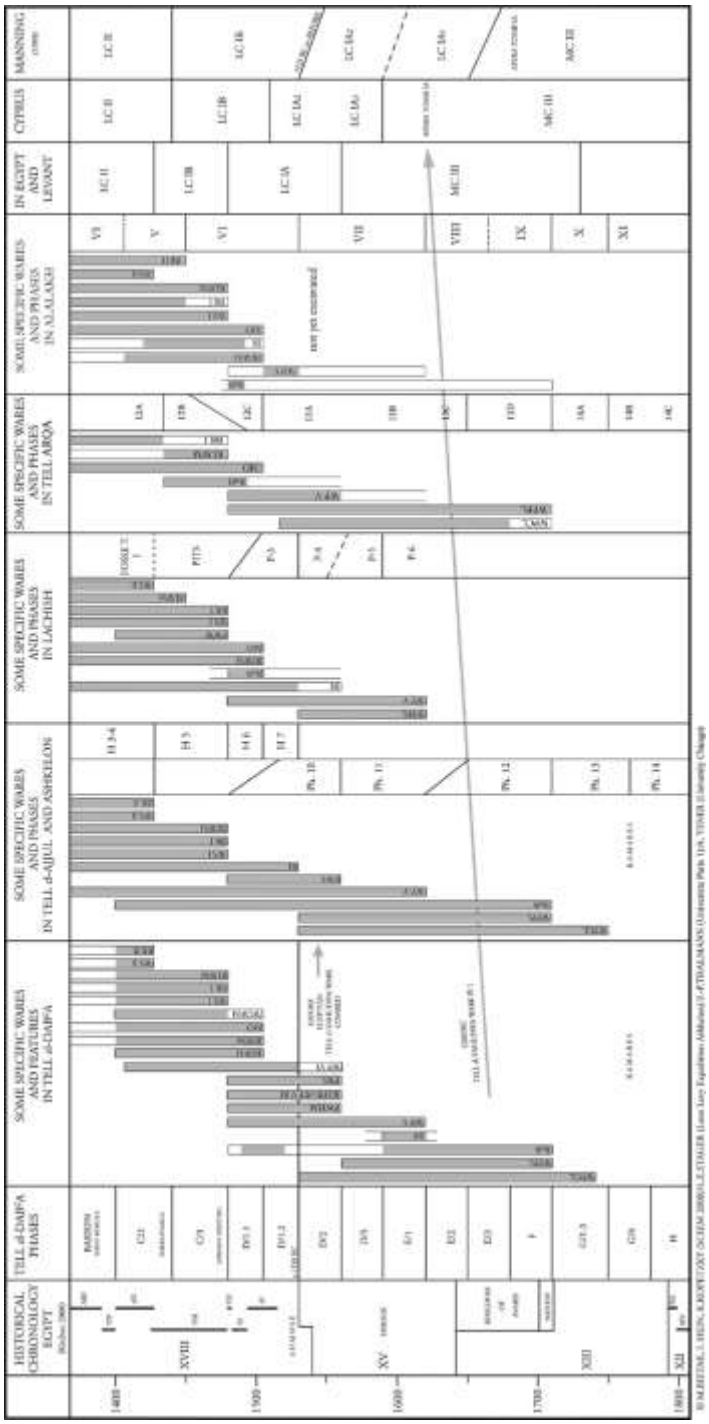

Fig. 6 The sequences of Cypriot imports in Tell el Dab'a and selected sites in the Levant (courtesy of Manfred Bietak)

Chapter IV

The chronologies of Tell el Dab'a

Tell el Dab'a is a huge multi-stratiphied tell-site where the remains of an important harbour town were found, which lasted from the Middle Kingdom to the SIP, when it became the Hyksos Capital Avaris and, subsequently, the royal port of Peru-Nefer during the XVIII Dynasty. After a gap, the site was reoccupied in the Ramesside age, when it became the southern part of the city of Pi-Ramesse, and was still recorded as "the Port of Avaris" in XX Dynasty texts (Bietak, 2018:31).

Chronologically overlapping stratigraphies from different excavated areas are in chronological order: F/I (MB I or possibly late EB IV to MB III), R/I (MB I to MB III), A/I-IV (MB I to MB III), A/V (MB II – MB III) and H/I-VI (MB III to LB II). The general stratigraphy of the site has been assessed by inter-linking these sequences on the base of (Bietak, 2013:78):

> pottery seriation and by recurring architectural features such as building material, house types, tomb types […]. Substantial studies on the statistical evaluation of the ceramics have been published (Bader, 2009; Kopetzky, 2004, 2010; Mueller, 2008), as the evaluation of tombs and offering deposits from stratigraphic contexts (Kopetzky, 1993; Forstner-Mueller 2008; Mueller, 2008; Schiestl, 2010) and typological corpus studies (Aston, 2004).

Bietak (2013:78) also notes that:

> There is no other site in the Near East where similar quantitative evaluations have been undertaken and published. […] statistical evaluation of the pottery collected from settlement layers shows that the percentage of ceramic classes and types has a repetitive

pattern in each phase of the settlement of Tell el- Dab'a which reflects the market situation at the relevant time. […] The ceramic dating was obtained by thorough study of the material culture of the Middle Kingdom, the Second Intermediate Period and the New Kingdom not only at Tell el-Dab'a but also at other sites in Egypt. Combinations of shapes which appear also at other well-dated sites, such as the royal complexes at Dahshur (Arnold 1977, 1982) or Memphis (Bader, 2009), were usable for cross-dating.

The result of this collation is a general stratigraphy subdivided in 19 phases (N/2-3 to C/2), covering a time span of about 600 years, from env. 2000/1980 BC to env. 1410 BC (Fig. 7; Bietak and Höflmayer, 2007; Bietak, 2013:Fig. 8.1).

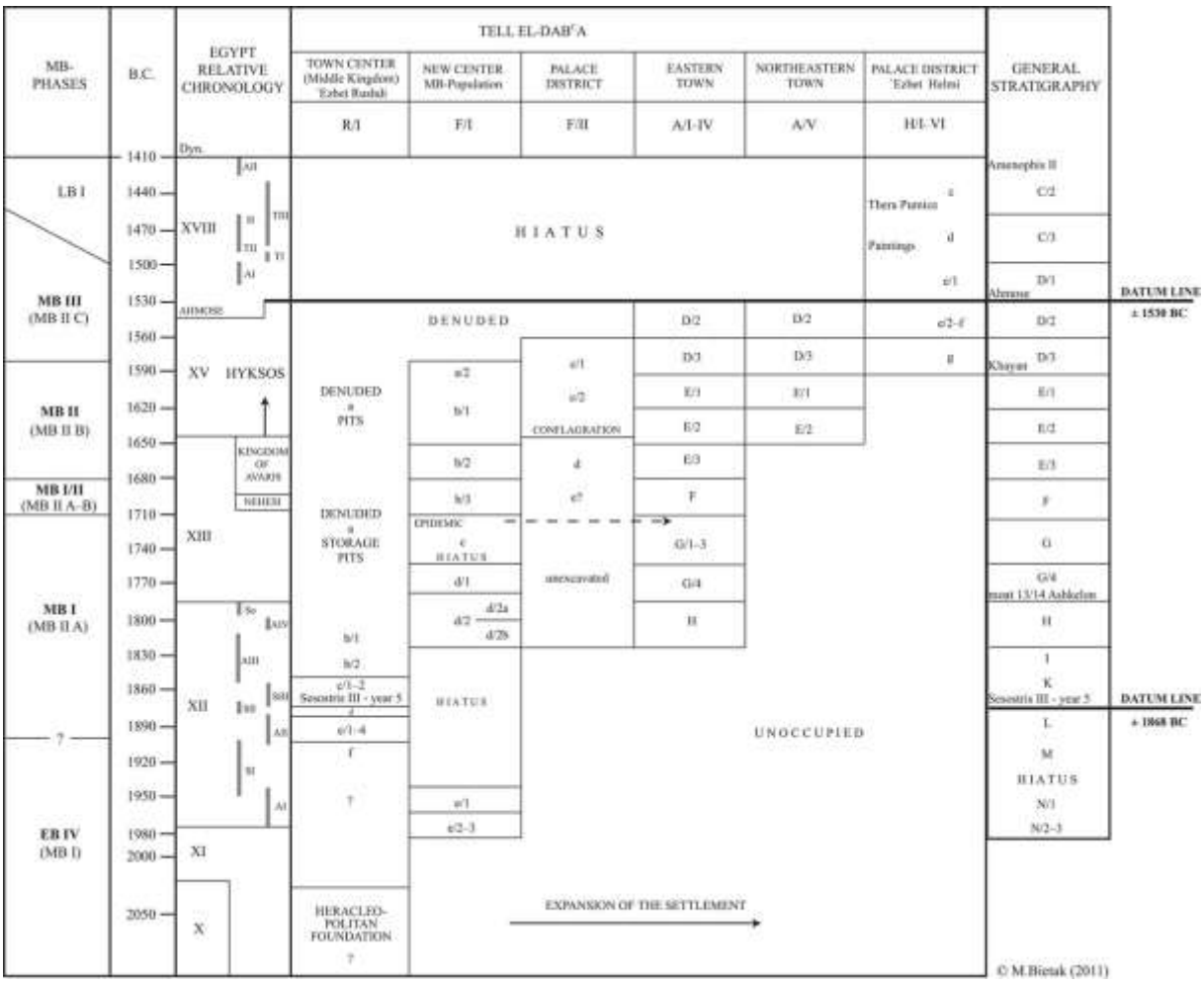

Fig. 7 The stratigraphies of Tell el Dab'a (after Bietak, 2013:Fig. 8.1)

This overall phasing has been linked to the Egyptian historical chronology by two *datum-*

lines (Bietak, 1998, 2013, 2015, 2018; Bietak and Hein, 2001; Bietak and Höflmayer, 2007; Kutschera et al., 2012):

1) A stela reporting a (re) foundation of the Temple in 'Ezbet Rushdi (Stratum K) in the year 5th of Sesostris III, dated to 1879-1868 BC;

2) The hiatus in occupation corresponding to phases D/1.1-2 that has been dated, on the base of the comparison between the typical ceramic assemblages of the preceding (D/2) and subsequent (C/3) phases, to the period between the fall of the Hyksos rule and the establishment of the New Kingdom and early XVIII Dynasty, i.e. from 1570-1520 BC on.

These *datum-lines* have been recently questioned (Manning, 2014; Höflmayer, 2012, 2018). With regard to 1), Höflmayer (2018:25-26, with references) observes that:

> There are several serious problems with this datum line. First, the planned settlement of Area F/I (local Str. e) which is dated to Amenemhet I and Senwosret I and which is supposed to be earlier than the settlement beneath the Middle Kingdom temple of Area R/I is devoid of any epigraphic dating evidence […]. Also pottery seriation was not possible for Area F/I Str. e because the stratum sits on virgin soil and is followed by a hiatus in occupation afterwards […]. The ultimate basis for the Amenemhet I – Senwosret I date for Area F/I Str. e are pottery comparisons with Seidlmayer's "Stufensystem" – a typological approach based on tomb repertoires, most of it excavated in the early days of Egyptology and in itself only a relative chronological assessment with very limited possibilities for linking it to the Egyptian historical chronology […]. Thus, dating evidence for Str. e of Area F/I seems to be rather imprecise and therefore any assumed date for Str. e/1-4 beneath the temple of 'Ezbet Rushdi remains rather vague as well.
>
> […]
>
> Also Bietak's interpretation of the stela is problematic. Although the text mentions land that obviously belongs to the temple, it remains unclear whether the 2600 square cubits refer to the original lot or to an enlargement or to additional land that was granted to the temple. Also Ernst Czerny recently expressed some skepticism about using the stela as a datum line: «It remains unclear, whether the stele relates to the original establishment of

> the temple or to an enlargement only. Even that it is unrelated to this particular temple, but was brought here from a proximate structure cannot be excluded. A few particularities of the stele, including the fact that the king's name is not enclosed into a cartouche, could possibly imply that it is not a contemporary document, but rather stems from the SIP».

Höflmayer suggests that the stela may in fact refer not to the foundation of the Temple in phase K, but rather to a subsequent enlargment and concludes that (Höflmayer, 2018:26):

> A firm link between the 5th year of Senwosret III mentioned on the stela and the construction of the temple in Str. K, however, cannot be established. This datum line should therefore be disregarded.

Again, this conclusion seems rather unsubstantiated, as, with regard to 1):

a) Even if it's true that date of the foundation of the first settlement in Area F/I is still unsettled, these layers are older than the context of the Stela from the Middle Kingdom temple by some 100-120 years (Bietak, 2013; Hein, 2018: Fig. 3), therefore a foundation date during the reign of Amenemhat I (es. in Bietak, 2013) or earlier, i.e. during the late XI Dynasty, doesn't necessarily reflect on the dating of phase K to which the Stela belongs (Bietak et al., 1998; Bietak, 2013);

b) The text of the stela names the temple, and provides the measurement of the plot of the phase K temple: «year 5, month 2, shemu season, under the Majesty (Namen von Sesostris III.) the land (cubits) belonging to the Estate of Amenemhet, justified, belonging to R3-w3ty, which are on the waters of this town, and wich are north of the Estate of Htty in R3-w3ty: 26 cubits» (Fischer, 1985, quoted in Bietak et al., 1998:18).

Taken as a linear measure, 26 cubits do not correspond to any of the plots in the temple area. However, the term reported in the stele (*mḥ*), can also refer to measures of areas with at least one side of 100cubits (i.e. 100 square cubits, defined «auroura», Gardiner, 1957:200).

If *mḥ* is to be read as 100 square cubits, then the area reported in the stele would be of 2600 square cubits (51x51).

To overcome this impasse, Bietak (1998:18) has convincingly suggested that the plot mentioned in the stele would include an additional stripe of 3 cubits on each side, leaving a passage area around the walls, thus summing up to 2601 square cubits. This measure is almost identical to the 2600 square cubits area mentioned in the text. Most importantly, none of the other plots of the temple would in any case offer a better approximation.

Moreover, the phase has been linked to the age of Sesostri III on safe ceramic parallels, which make the attribution even more sound (Bietak et al., 1998; Bietak, 2013).

As to 2), Höflmayer observes that the attribution of phase D/1 to the conquest of Avaris by Ahmose would rely only on the interpretation of:

a) the hiatus in occupation in area A;

b) the abandonment of the Hyksos fortress and the construction of siloi as storage facility for troops in area H, but that no sign of violent destruction has been found at the site(s).

Therefore, Höflmayer (2018:27) concludes that:

> This is, however, an *interpretation* [emphasis in the original]. There is no hard evidence to link the end of the Second Intermediate Period to the transition from Str. D/2 to D/1. An abandonment of a part of a site or a change in use of a certain area without any epigraphic evidence can hardly be used as a secure datum line for chronological purposes.

However, phase C/2 has been dated by 1) interlinked ceramic sequences, and 2) by the presence of scarabs from Ahmose to Amenhotep II, the latter offering the *terminus post quem* for the end of the phase. Since the scarabs were found in a phase C/2 workshop which abutts the weathered wall of a phase C/3 palace ramp, it has been observed that the preceding phases (C/3 and D/1) could be significantly earlier than the Thutmoside age workshops (Warburton, 2009; Manning, 2014, Höflmayer, 2018; see discussion below) but this hypothesis seems to be disconfirmed by the strong similarity in the Egyptian assemblages from phases C/3 and C/2, which sets them both to the Thutmoside age or the early XVIII Dynasty at earliest (phases D/1-C/3, Bietak, 2013, 2016:3).

It is true that no destruction horizon has been recognised so far in Tell el Dab'a and 'Ezbet Helmi, but it's hard to see why this should be taken as an argument in favour of an earlier date. In fact, the marked difference between the ceramic assemblages from the preceding (D/2) and the following (C/3) phases clearly shows a shift from (late) MBA to the Thutmoside age. This difference is clear in both Egyptian wares (most importantly Black Rim Ware, Hein, 2018:137-138) and imported Levantine and Cypriot wares (see above).

Moreover, as Manfred Bietak notes[11]:

> The fact that there is no destruction visible is not a serious argument and it would be even in accord with the Manethonian tradition after Flavius Josephus, namely that the Egyptians were already in despair of not being able to take the town. But a treaty was finally concluded allowing the inhabitants to retreat freely to the southern Levant. Of course this is not a historical record, but many cities finally surrender when besieged for a long time. In this case no destructions can be observed. As the defence walls have only been excavated at the river side in a restricted area one cannot claim records on a siege. Besides the town was looted. All tombs except one were completely plundered and the inhumations largely damaged.

Another key argument for the chronology of Tell el Dab'a is the dating of Khayan. Area F/II has shown the evidence of a Hyksos palace that underwent at least two major phases of use. The foundation date of the palace is still unsettled, but the first phase (c.2) ends with a fire destruction horizon at the transition between phases E/3 and E/2. The subsequent refoundation in str. c.1 (phases E/1-D/3) has been dated to sometime before the reign of Khayan, during which the palace was still in use stemming from a series of seal impressions bearing the names of that king found in fireplaces and offering pits (contexts L81 and L803), but not considered by the excavators to represent properly a third *datum line* (Bietak, 2016:3; Höflmayer, 2018:7).

The transition between phases E/1 and D/3 is dated by the excavators to 1600-1590 BC (Bietak, 2013, 2016), and fits with the "historical" date for the reign of Khayan. This date is based on the Turin Canon and on a note on the Rhind mathematical papyrus and placed between the end of the XVII and the beginning of the XVI century BC, 2-3 generations before the

[11] Bietak, pers. Comm., 5/7/2018.

conquest of Avaris (Von Beckerath, 1997; Hornung et al., 2006).

It has been recently suggested (Manning, 2014; Höflmayer, 2018) that the absolute date for this king should be backshifted by as much as 120 years, setting it to the (second) half of the XVIII century BC, and in (partial) contemporaneity with the XIII Dynasty (from Neferhotep I to Sobekhotep IV). This hypothesis relies mainly on two arguments: (1) the results of Bayesian radiocarbon chronology from Tell el Dab'a, which will be discussed in some detail below, and (2) 41 seal impressions bearing the name of Khayan from a context dated to the XIII-XVII Dynasty at Tell Edfu in association with 9 sealings of Sobekhotep IV (Möller and Marouard, 2011:fig. 11).

This hypothesis, at least at the present state of evidence, is rejectable on the base of two arguments, summarised by Bietak (2016:3):

1) Among the only four pottery items presented for the abandonment horizon is a modelled rim jar of Marl A3, dating to the 17th Dynasty (Möller et al., Egypt and the Levant 21, fig. 16/ED2654.3/1; Ilin-Tomich, JEH 7, 150) with a seal impression belonging to the Late Palestinian Group that doesn't date before the Hyksos Period and is absent from 13th Dynasty contexts (Ben-Tor, Ms Khayan Conference, Vienna 2014).

2) There is no evidence from the northern part of Egypt that the 13th and the 15th Dynasty overlapped; ceramic development and seal typology are distinctly different. As Sebekhotep IV still maintained relations with Lebanon, like Neferhotep I, it is unlikely that was possible with the Hyksos ruling in Avaris. Thus, Khayan's position before Apophis within the Hyksos succession remains the same as previously assumed, with perhaps one king in between the two (Yanassy?). Manning seems to overlook that a 13th and 15th Dynasty overlap would shorten the SIP by about 50-80 years. This would enlarge the gap between historical and radiocarbon dates for this period considerably.

In general terms, the association of seal impressions of rulers of different Dynasties doesn't necessarily imply the contemporaneity between these rulers. As a matter of fact, seals (including royal seals) were often kept in use for a very long time (Bietak, 2004; Ben-Tor, 2018). For example, in one of the Thutmoside contexts at Tell el Dab'a, only 2 seal impressions were from the XVIII Dynasty, in association with others from the XII, XIII and XV Dynasties. including royal seals of the XII and XIII Dynasties (Bietak, 2004).

Taking all the above in consideration, the only argument which could still stand in favour of the High chronology relies on the interpretation of Bayesian models for combining radiocarbon dates, which will be the subject of the next chapter.

Chapter V

Radiocarbon dating for Tell el Dab'a and Akrotiri

V.1.1 The Bayesian radiocarbon chronology of Tell el Dab'a

A total of 66 radiocarbon dates on 47 samples (61 radiocarbon determinations – henceforth RDs – plus 5 weighted averages from samples subdivided between the VERA AMS facility in Vienna and the ORAU at Oxford) have been published by Kutschera et al. (2012). All the samples were short-lived materials (charred Poaceae seeds, mostly *Triticum, Hordeum, Lolium*) in order to avoid possible inbuilt age problems (f.i. old wood effect), although the use of charred seeds from loose contexts in large and multistratiphied sites may open the serious problem of floating/residual material from the preceding phases as a consequence of ancient re-excavation, mud brick decay and pit digging (cfr. Easton and Weninger, 2018). This aspect was in fact admitted by the authors (Kutschera et al., 2012:410) though it was subsequently considered not significant in several recent publications (Manning et al., 2014; Manning, 2014; Höflmayer, 2012, 2015, 2018).

Seven dated samples (AMS-17, AMS-15, AMS-47, AMS-44, AMS-06, AMS-01, and AMS-02) were excluded from the model due to contextual uncertainty (Kutschera et al., 2012:414) while 5 samples (AMS-48, AMS-39, AMS-30, AMS-40 and AMS-35) were subdivided between the two laboratories to check for possible counting error (Kutschera et al., 2012:411-13). The preliminary results of the study showed that after calibration against the IntCal09 curve the majority of results appeared to be older than the expected "historical/archaeological" chronology (fig. 8, after Kutschera et al., 2012:fig. 4):

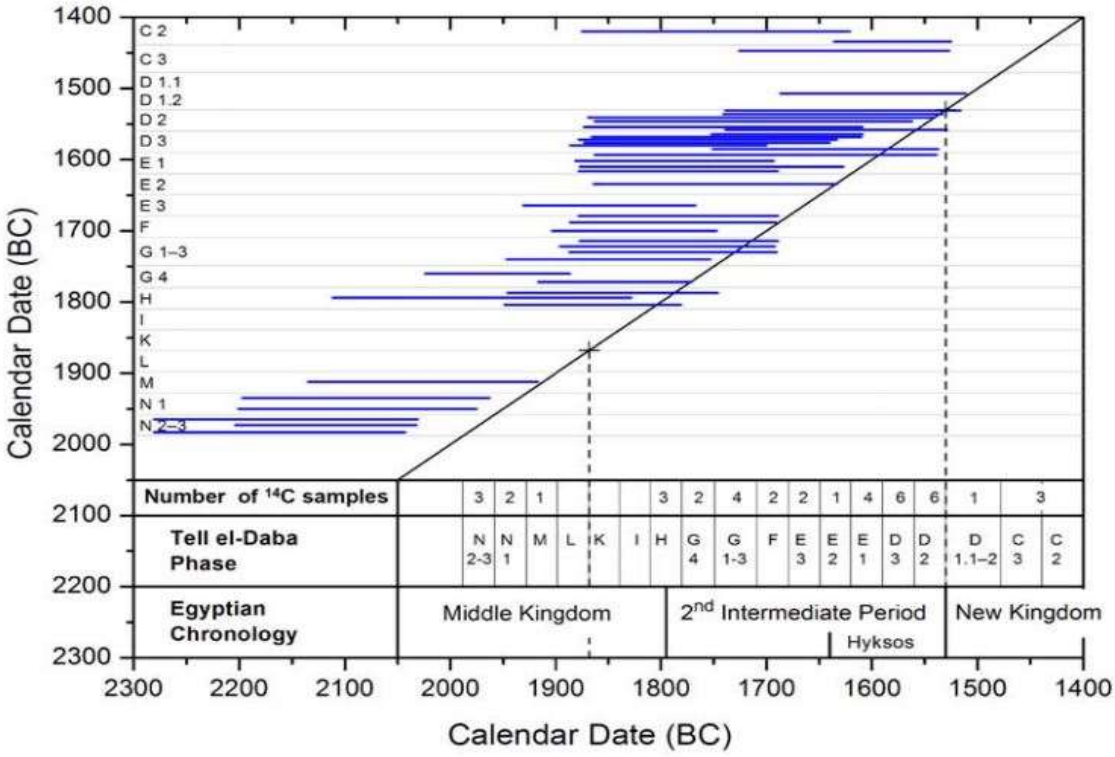

Fig. 8 The apparent offset of calibrated radiocarbon dates from Tell el Dab'a after Kutschera et al., 2012 – archaeological-historical chronological expectations are represented by the diagonal line, radiocarbon dates calibrated against IntCal09 are represented by blue lines.

In order to check for a possible constant offset which could explain this difference, Kutschera et al. (2012:415) go on stating that:

> Accepting that the phases are in the correct chronological order, and that the samples do belong to the respective phases, one can apply Bayesian sequencing (Bronk-Ramsey 2009a, b), which considerably reduces the uncertainties.

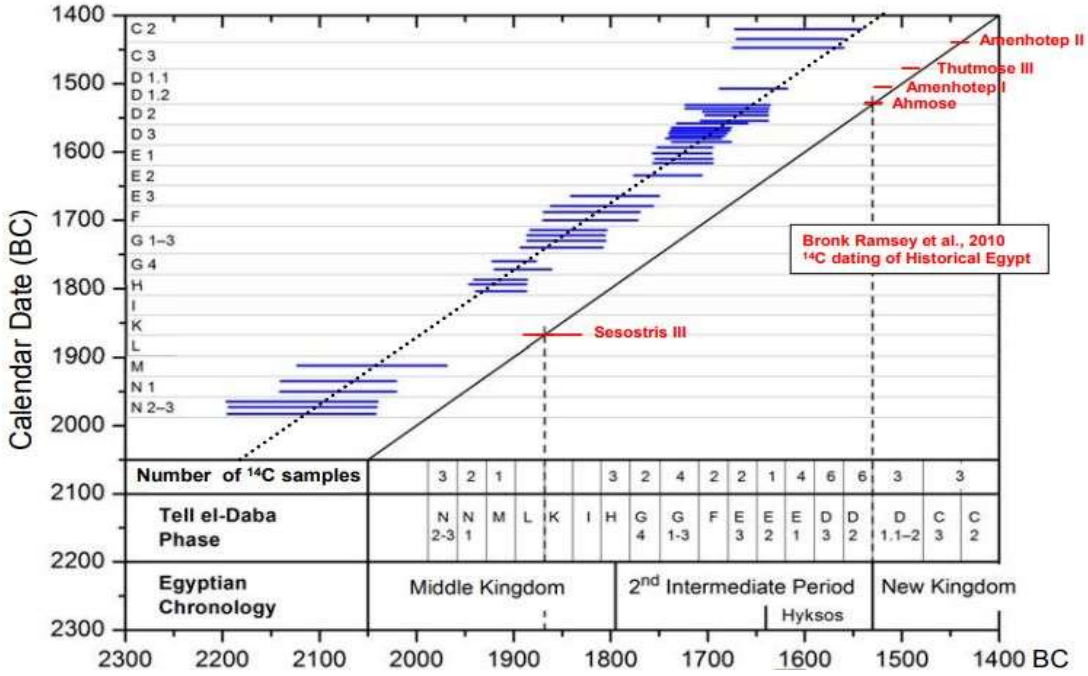

Fig. 9 Sequenced calibration results after Kutschera et al., 2012:418, fig. 7.

The results of the model are used to support a systematic/constant shift of 120 calendar years that is unreconcilable with the archaeological/historical chronology. Various interpretations have been suggested for this apparently constant offset, ranging from systemic problems in radiocarbon dating for the period and geographical area to the need of a complete revision of the archaeological dating of Tell el Dab'a and the interrelated sites.

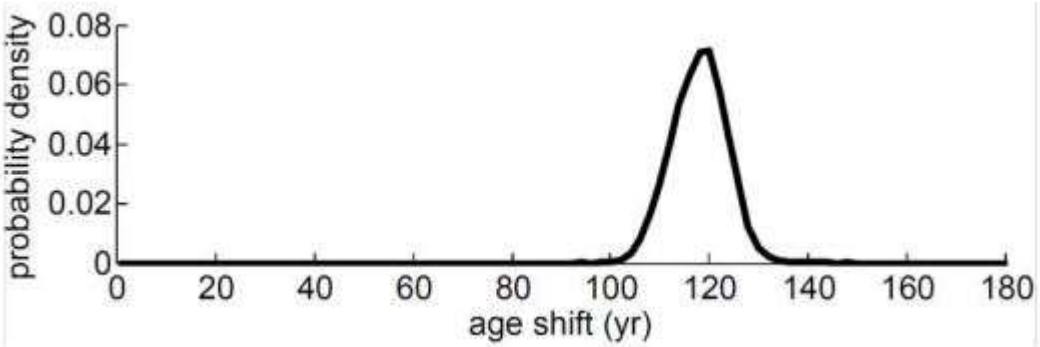

Fig. 10 Bayesian posterior probability distribution of the offset in the model by Kutschera et al., 2012:fig. 5.

The aim of this study is to show that this alleged "constant" offset is neither constant nor systematic, and probably only an artefact of the method, or – in more accurate words – a systemic (vs systematic) problem which is a function of priors/bayesian normalization/RDs error/curve error/curve shape (aka "wiggles" and "plateaus")/residual aut intrusive samples.

A Bayesian model for chronology estimates the probability that an event *X* occurred in a certain period *t* based on dating measurements RDs of related objects (posterior probability). This is done by combining the probability of finding measured RDs for objects belonging to *t* (likelihood) and a prior probability, i.e. information on the objects not derived from the measurement, and then calculate the only possible chronological interval where all the RDs fit the model's priors (Bronk-Ramsey, 2009). However, the accuracy of this radiocarbon-based chronological interpretation relies on (1) the nature of the prior information supplied (i.e. assuming *a priori* that the sample is strictly representative of the phase and not residual, that there is no reservoir effect or alteration in the samples, etc...), and (2) the accurate *interpretation* (vs the sometimes claimed "objectivity" of Bayesian chronology as opposed to archaeological chronology) of the results (and implications) of the testing. As Federico Antolini (in Fantuzzi and Antolini, 2018:248) observes:

> Hypothesis testing verifies the plausibility of an initial hypothesis (null hypothesis) in contrast with an alternative hypothesis. This consists in proving whether or not the null hypothesis is improbable and in quantifying its improbability. So, whichever testing technique is used, hypothesis testing is not meant to prove the null hypothesis. A typical application of hypothesis testing to archaeology is the comparison of age determinations, in which the null hypothesis is the contemporaneity of two or more samples. The result of the testing cannot provide an argument in favour of contemporaneity, but only against it. This should always be kept in mind as too often, and definitely not only in archaeology, the result of a test is misinterpreted as a neat and definite response between the null and the alternative hypothesis.

V.1.2 The radiocarbon dataset for Tell el Dab'a

In stratigraphical order, the published radiocarbon dates for Tell el Dab'a are as follows:

1) Phase C/2: one sample (AMS-25, *Lolium* type seeds) has been radiocarbon dated to 3414±35 BP (VERA-3031, $\delta^{13}C$ -21±1.4) which is almost certainly a residual/floating sample (giving a calibrated date of 1875-1621 BC, Kutschera, 2012:412), but was nonetheless included in the original model (above);

2) Phase C/2-3: two samples:
   1. AMS-48, *Lolium* type seeds, subdivided between Vienna (VERA-3724, 3320±29 BP, $\delta^{13}C$ -21.4±0.5) and Oxford (OxA-15959, 3296±31 BP, $\delta^{13}C$ -23.5±0.3; OxA-15957, 3322±31 BP, $\delta^{13}C$ -22.4±0.3). The RDs were considered as a whole and combined in a weighted mean (3313±17 BP) which was used in the model by Kutschera et al., 2012. In addition, one measurement on humic acids extracted from the sample was also performed (OxA-15958, 3287±33 BP, $\delta^{13}C$ -22.4±0.3) but not included in the model by Kutschera et al.;
   2. AMS-49, *Lolium* type seeds, (VERA-3725, 3336±29 BP, $\delta^{13}C$ -26.3±0.5);

3) Phase C/3: one sample (AMS-17, Poaceae seeds) was dated to 3424±31 BP (VERA-2632 BP, $\delta^{13}C$ -22.7±0.5) but excluded from the dataset due to contextual uncertainty;

4) Phase D/1: one sample (AMS-26, *Lolium* type seeds) dated at Vienna (VERA-3032, 3314±36 BP, $\delta^{13}C$ -22.9±1.2);

5) Phase D/2-D/1: two samples, both excluded from the dataset for contextual uncertainty (Kutschera et al., 2012:414, Tab. 1b):
   1. AMS-15, Poaceae seeds (VERA-2630, 3345±31 BP, $\delta^{13}C$ -22.7±0.6);
   2. AMS-47, *Lolium* type seeds (VERA-3623, 3356±23 BP, $\delta^{13}C$ -22.6±0.4);

6) Phase D/2: five samples:
   1. AMS-28, Poaceae seeds (VERA-3032, 3337±44 BP, $\delta^{13}C$ -24.5±0.6);
   2. AMS-13, *Triticum sp.* Poaceae seeds, (VERA-2628, 3359±34 BP, $\delta^{13}C$ -22.6±0.5);

3. AMS-12, *Lolium* type seeds (VERA-2627, 3390±34 BP, $\delta^{13}C$ -21.7±0.5);
4. AMS-46, Poaceae seeds (VERA-3622. 3394±36 BP, $\delta^{13}C$ -21.0±0.6);
5. AMS-39, *Lolium* type seeds, subdivided between Vienna (VERA-3621, 3354±26 BP, $\delta^{13}C$ -22.0±0.5) and Oxford (OxA-15953, 3354±26 BP, $\delta^{13}C$ -22.4±0.3; OxA-15901, 3479±33 BP, $\delta^{13}C$ -22.9±0.3), results combined in weighted mean (3399±37 BP) used in the Bayesian model by Kustschera et al., 2012. Two additional RDs from humic acid (OxA-15979, 3383±30 BP, $\delta^{13}C$ -22.9±0.3; OxA-15980, 3392±31 BP, $\delta^{13}C$ -22.6±0.3), also not included in the model;

7) Phase D/3-D/2: one sample, AMS-45, *Lolium* type seeds (VERA-3645, 3351±38 BP, $\delta^{13}C$ -21.8±0.6);

8) Phase D/3: six samples:
   1. AMS-37, *Lolium* type seeds (VERA-3620, 3377±33 BP, $\delta^{13}C$ -23.0±0.5);
   2. AMS-14, *Lolium* type seeds, Poaceae seeds (VERA-2629, 3384±30 BP, $\delta^{13}C$ -2.1±0.6);
   3. AMS-36, *Lolium* type seeds (VERA-3619, 3396±34 BP, $\delta^{13}C$ -22.9±0.5);
   4. AMS-18, *Lolium* type seeds (VERA-2895, 3426±26 BP, $\delta^{13}C$ -13.3±0.9);
   5. AMS-19, Poaceae seeds (VERA-2896, 3428±37 BP, $\delta^{13}C$ -21.0±0.7);
   6. AMS-27, Cerealia seed (VERA-3033, 3480±28 BP, $\delta^{13}C$ -22.0±1.9);

9) Phase E/1: 4 samples:
   1. AMS-11, *Lolium* type/*Bromus*/*Agropyron sp.* seed (VERA-2626, 3389±36 BP, $\delta^{13}C$ -22.8±0.5);
   2. AMS-29, Poaceae seeds (VERA-3617, 3422±35 BP, $\delta^{13}C$ -24.4±0.5);
   3. AMS-31, *Lolium* type seeds (VERA-3636, 3449±26 BP, $\delta^{13}C$ -25.0±0.6);
   4. AMS-30, Cerealia seeds, subdivided between Vienna (VERA-3618, 3436±35 BP, $\delta^{13}C$ -22.8±0.5) and Oxford (OxA-15949, 3437±30 BP, $\delta^{13}C$ -23.7±0.3; OxA-15948, 3511±32 BP, $\delta^{13}C$ -22.9±0.3), combined in a weighted mean (3462±25 BP) used in the model by Kutschera et al., 2012;

10) Phase E/2: one sample, AMS-33, *Lolium* type seeds (VERA-3637, 3415±26 BP, $\delta^{13}C$ -32.4±0.4);

11) Phase E/3: one sample, AMS-20, *Hordeum vulgare* seeds (VERA-2897, 3525±26 BP, $\delta^{13}C$ -17.0±0.8);

12) Phase F-E/3: one sample, AMS-43, Poaceae seeds (VERA-3643, 3450±26 BP, $\delta^{13}C$ -22.3±0.5);

13) Phase F: two samples:
    1. AMS-10, *Lolium sp.*/*Lolium* type/*Lolium*/*Bromus sp*. seeds (VERA-2625, 3467±35 BP, $\delta^{13}C$ -21.3±0.5);
    2. AMS-21, *Lolium* type/*Phalaris*/*Cynodon sp*. seeds (VERA-2898, 3505±27 BP, $\delta^{13}C$ -16.9±0.6);

14) Phases G/1-3: five samples, four included in the model by Kutschera et al., 2012:
    1. AMS-42, *Lolium* type, Poaceae seeds (VERA-3642, 3447±25 BP, $\delta^{13}C$ -21.3±0.4);
    2. AMS-08, *Triticum dicoccum* seeds (VERA-2623, 3466±39 BP, $\delta^{13}C$ -19.6±0.5);
    3. AMS-07, *Lolium* type, Poaceae seeds (VERA-2622, 3481±36 BP, $\delta^{13}C$ -21.6±0.5);
    4. AMS-09, *Hordeum vulgare*, *Lolium* type seeds (VERA-2624, 3530±34 BP, $\delta^{13}C$ -19.9±0.4);
    5. AMS-44, *Lolium* type seeds (VERA-3644, 3641±36 BP, $\delta^{13}C$ -23.9±0.5), excluded from the model due to contextual uncertainty (Kutschera et al., 2012:414, Tab. 1b);

15) Phase G/4, two samples:
    1. AMS-40, *Lolium* type seeds, subdivided between Vienna (VERA-3640, 3530±38 BP, $\delta^{13}C$ -23.8±0.5) and Oxford (OxA-15956, 3504±32 BP, $\delta^{13}C$ -23.3±0.3; OxA-15954, 3532±34 BP, $\delta^{13}C$ -23.1±0.3), weighted mean in the model 3521±20 BP. Two additional RDs on humic acids (OxA-15981, 3570±30 BP, $\delta^{13}C$ -23.3±0.3; OxA-15955, 3530±32 BP, $\delta^{13}C$ -22.7±0.3) not included in the model by Kutschera et al., 2012;
    2. AMS-22, Poaceae seeds (VERA-2899, 3591±26 BP, $\delta^{13}C$ -20.4±1.0);

16) Phase H: three samples:
    1. AMS-34, Poaceae seeds (VERA-3638, 3522±37 BP, $\delta^{13}C$ -23.7±0.5);

2. AMS-35, *Lolium* type seeds, subdivided between Vienna (VERA-3639, 3553±23 BP, $\delta^{13}C$ -22.7±0.4) and Oxford (OxA-15951, 3522±32 BP, $\delta^{13}C$ -24.0±0.3; OxA-15952, 3577±32 BP, $\delta^{13}C$ -22.8±0.3), weighted mean: 3551±17 BP. Two additional RDs on humic acids (OxA-15950, 3490±32 BP, $\delta^{13}C$ -22.2±0.3; OxA-15978, 3589±32 BP, $\delta^{13}C$ -23.3±0.3);
3. AMS-03, *Lolium* type seed (VERA-2618, 3593±34 BP, $\delta^{13}C$ -21.0±0.4);

17) Phase H (?): one sample, AMS-06, *Triticum sp./Lolium* type seed (VERA-2621, 3493±34 BP, $\delta^{13}C$ -22.3±0.5), excluded from the dataset due to contextual uncertainty;

18) Phase H or N1: one sample, AMS-01, Poaceae seed (VERA-2616, 3610±37 BP, $\delta^{13}C$ -23.1±0.5), excluded from the dataset due to contextual uncertainty;

19) Phases I to L: no samples available;

20) Phase M: one sample, AMS-16, Cerealia, *Lolium* type seeds (VERA-2631, 3643±35 BP, $\delta^{13}C$ -23.7±0.6);

21) Phase N/1: two samples:
1. AMS-05, Poaecae, *Lolium* type seed (VERA-2620, 3688±36 BP, $\delta^{13}C$ -22.7±0.4);
2. AMS-04, Poaecae, *Lolium* type seed (VERA-2619, 3697±37 BP, $\delta^{13}C$ -22.8±0.4);

22) Phase N/1-3: one sample, AMS-02, Poaecae, *Lolium* type seed (VERA-2617, 3433±38 BP, $\delta^{13}C$ -19.7±0.5), excluded from the dataset due to contextual uncertainty;

23) Phase N/2-3: three samples:
1. AMS-23, Poaceae seeds (VERA-2901, 3725±30 BP, $\delta^{13}C$ -17.8±0.6);
2. AMS-41, *Lolium* type seeds (VERA-3641, 3739±38 BP, $\delta^{13}C$ -21.9±0.8);
3. AMS-23, *Lolium* type seeds (VERA-2900, 3755±26 BP, $\delta^{13}C$ -15.8±0.7).

V.1.3 Calibration of the Tell el Dab'a ^{14}C dataset

When RDs are grouped by phase and individually calibrated against IntCal13, the radiocarbon dataset for Tell el Dab'a appears as follows (Fig. 11).

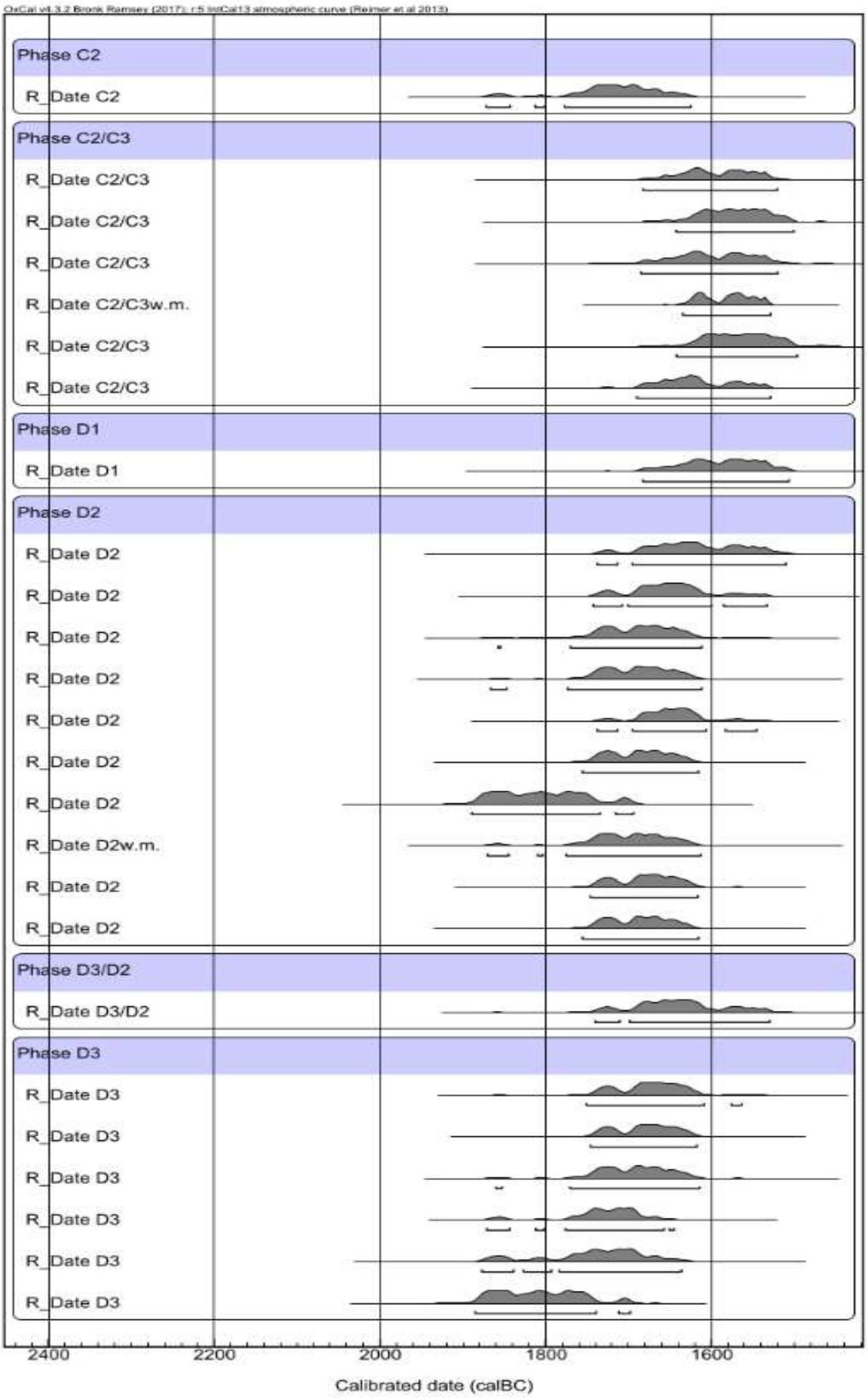
OxCal v4.3.2 Bronk Ramsey (2017); r:5 IntCal13 atmospheric curve (Reimer et al 2013)
Phase C2
R_Date C2
Phase C2/C3
R_Date C2/C3
R_Date C2/C3
R_Date C2/C3
R_Date C2/C3w.m.
R_Date C2/C3
R_Date C2/C3
Phase D1
R_Date D1
Phase D2
R_Date D2
R_Date D2
R_Date D2
R_Date D2
R_Date D2
R_Date D2
R_Date D2
R_Date D2w.m.
R_Date D2
R_Date D2
Phase D3/D2
R_Date D3/D2
Phase D3
R_Date D3
R_Date D3
R_Date D3
R_Date D3
R_Date D3
R_Date D3
2400
2200
2000
1800
1600
Calibrated date (calBC)

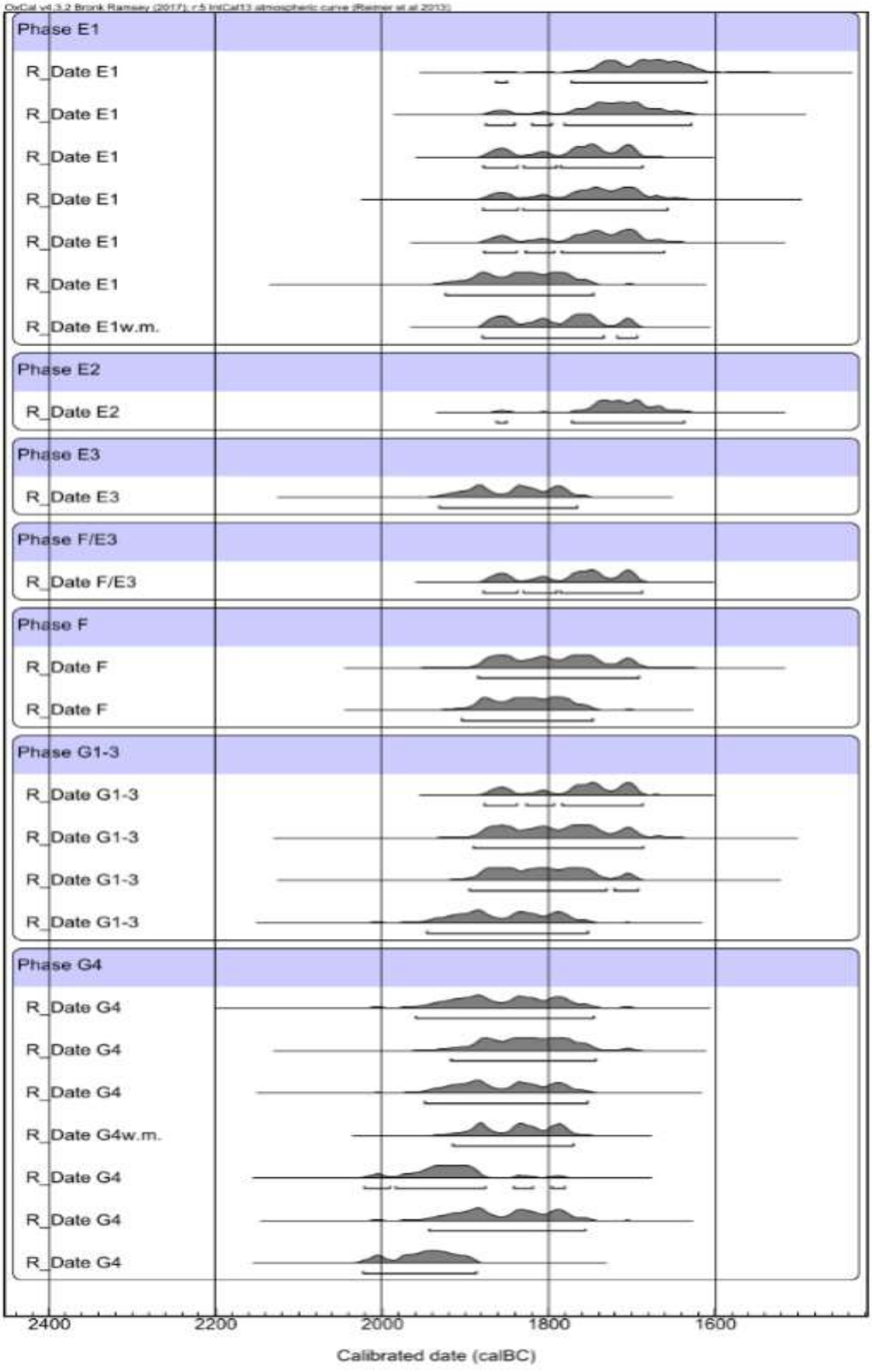
OxCal v4.3.2 Bronk Ramsey (2017); r:5 IntCal13 atmospheric curve (Reimer et al 2013)
Phase E1
R_Date E1
R_Date E1
R_Date E1
R_Date E1
R_Date E1
R_Date E1
R_Date E1w.m.
Phase E2
R_Date E2
Phase E3
R_Date E3
Phase F/E3
R_Date F/E3
Phase F
R_Date F
R_Date F
Phase G1-3
R_Date G1-3
R_Date G1-3
R_Date G1-3
R_Date G1-3
Phase G4
R_Date G4
R_Date G4
R_Date G4
R_Date G4w.m.
R_Date G4
R_Date G4
R_Date G4
2400
2200
2000
1800
1600
Calibrated date (calBC)

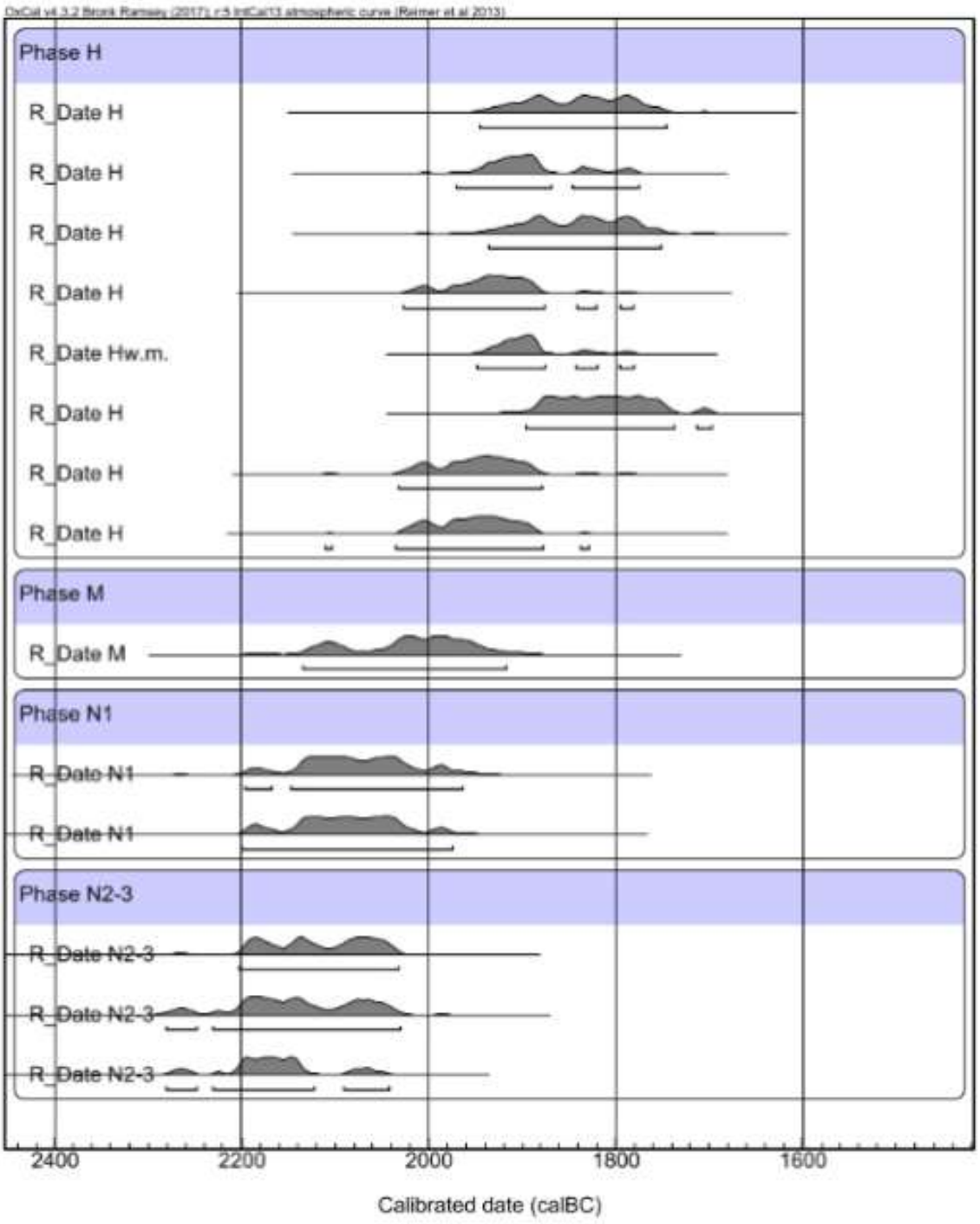

Fig. 11 Unsequenced calibration of the Tell el Dab'a dataset with OxCal 4.3.2 (Bronk-Ramsey 2017) against IntCal13 (Reimer et al., 2013). The "wiggles" (Z-shapes) in the distribution of dates show already by eye the presence of residual/older samples (Easton and Weninger, 2018). This aspect has been accounted for in the model by Kutschera et al. by applying Outlier Analysis (Bronk-Ramsey, 2009), see Fig. 10 above. However, the single-calibration distribution seems

to show that the alleged "offset" is not systematic but varies from phase to phase, with some of the phases mean age being apparently older than the earlier ones (Figs 12, 15 below).

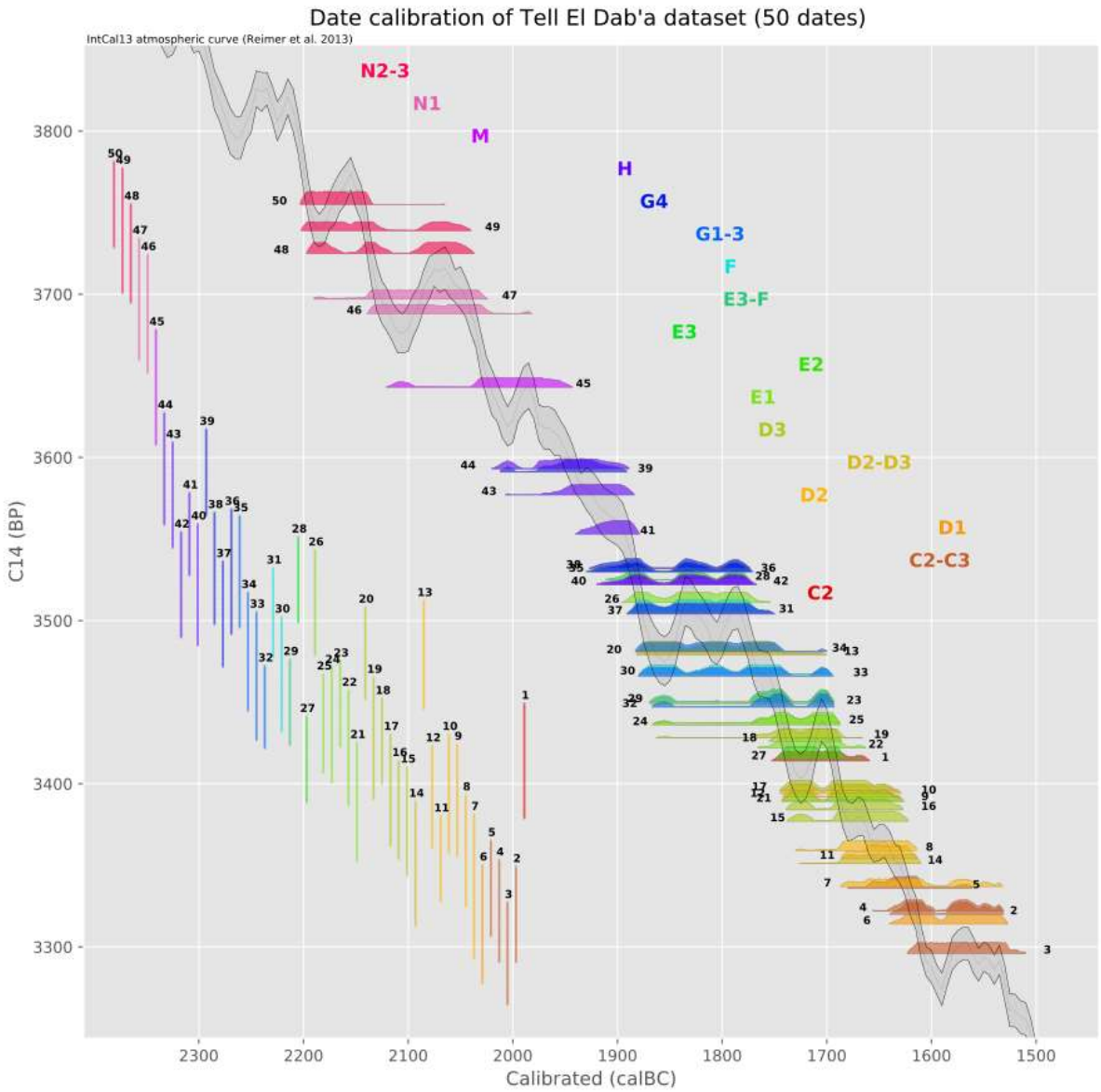

Fig. 12 Quantum/Contingency calibration (c14.bpinfo.org) of the Tell el Dab'a dataset plotted against the IntCal13 Calcurve.

In particular, the visual plot of Quantum-calibrated RDs on the curve shows:

1) That the gap corresponding to phases I-L is immediately apparent;

2) That the calibrated mean age of several phases is apparently earlier than the preceding phase (f.e. phases C/2, D/2, E/3, ...);

3) That the alleged offset of 120 cal years is not necessarily constant or systematic, but may be just a function of Priors/RDs error/Curve wiggles, and, most importantly, of the presence of older seeds from earlier strata due to ancient re-excavations (see Figs 13-14 below);

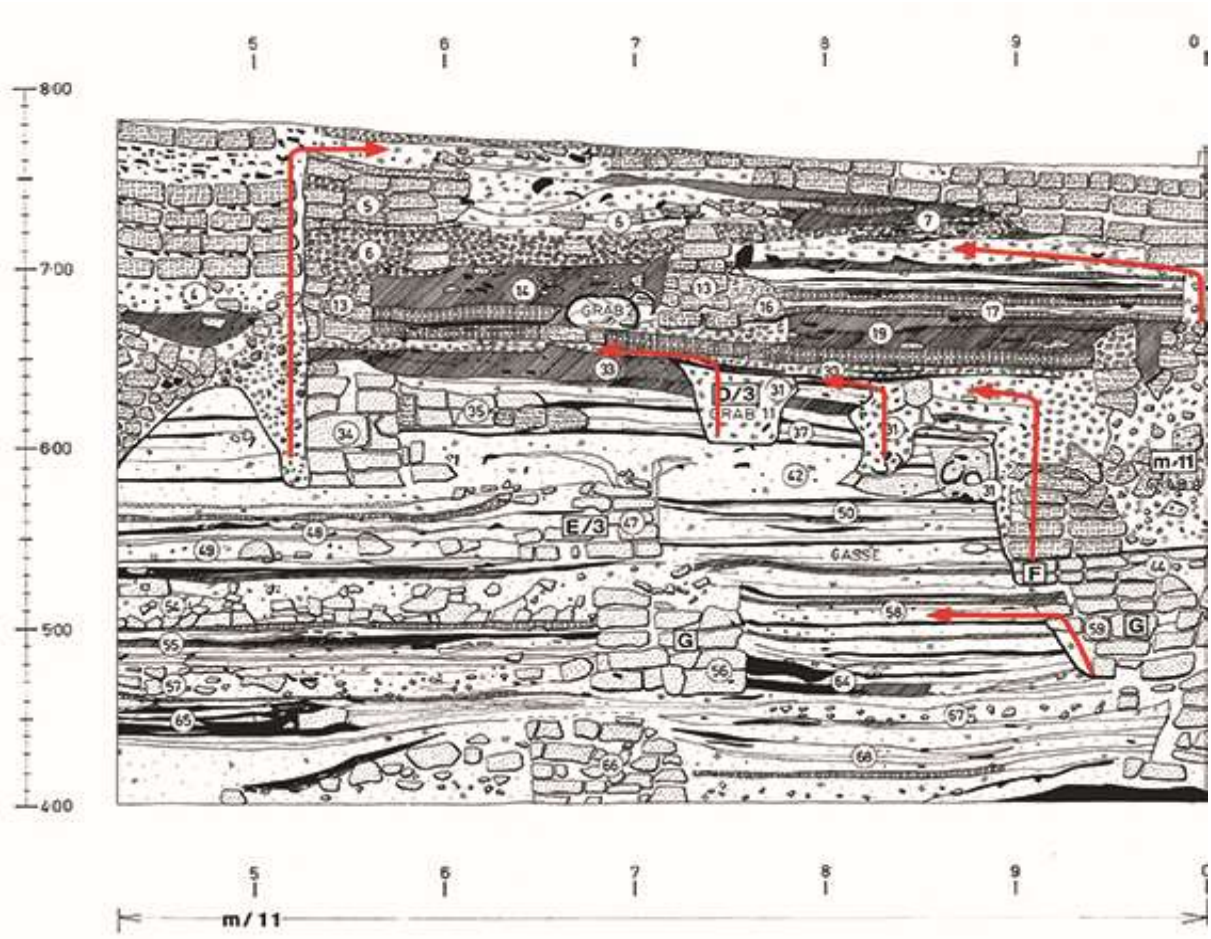

Fig. 13 Southern profile (m/11) from Area A II showing the dislocation of carbon materials from earlier strata (red arrows), on courtesy of Manfred Bietak.

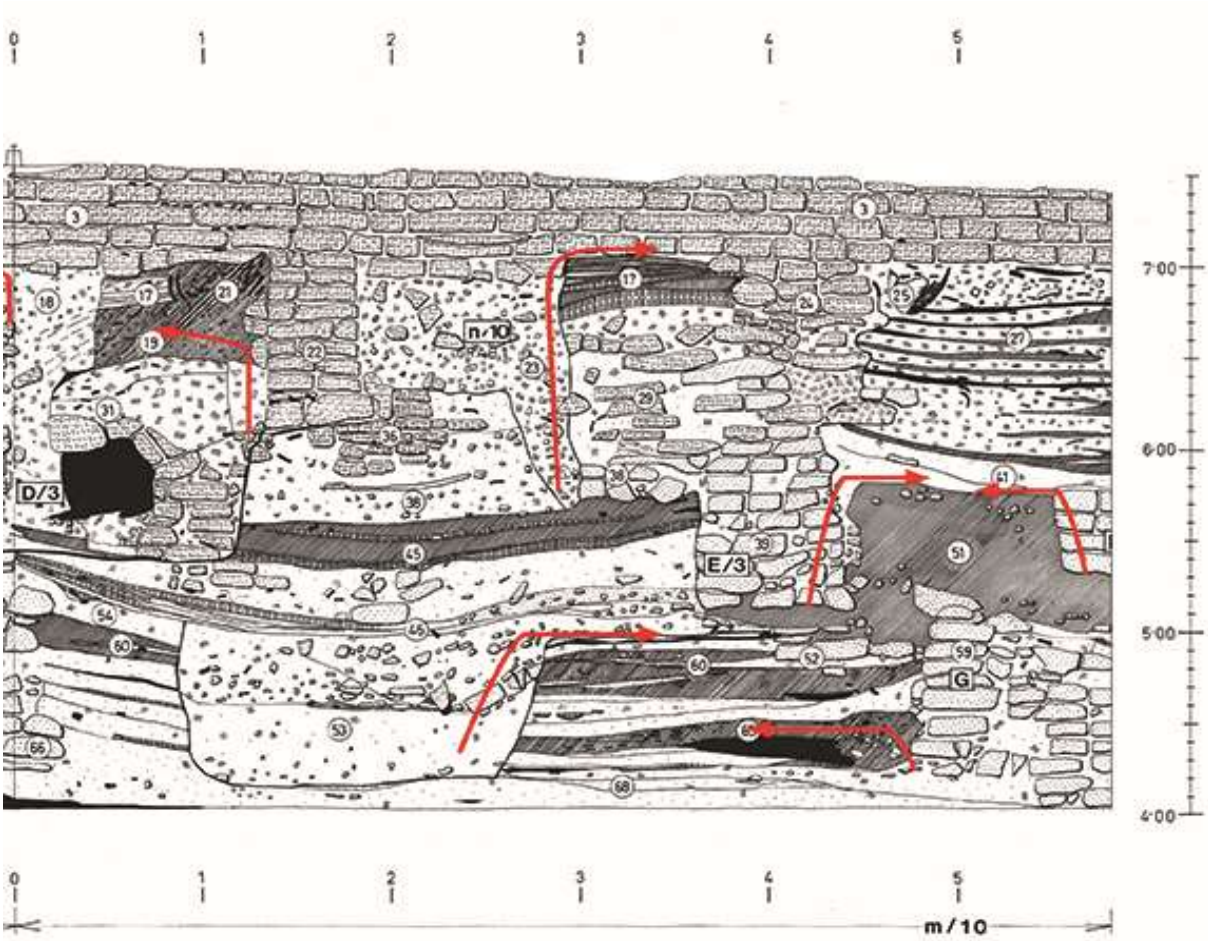

Fig. 14 Southern profile (m/10) from Area A II showing the dislocation of carbon materials from earlier strata (red arrows), on courtesy of Manfred Bietak.

To this one should add the recent discovery of significant offsets between the data for the period 1700-1500 BC in IntCal13 and the recent dendrochronological data from Arizona and Ireland (Pearson et al., 2018). The inclusion of those dataset in the next version of IntCal (Reimer et al., forthcoming) will most probably lower the calibrated results of phases D/2-3 to C/3 by 50-100 years (Fig. 15 below).

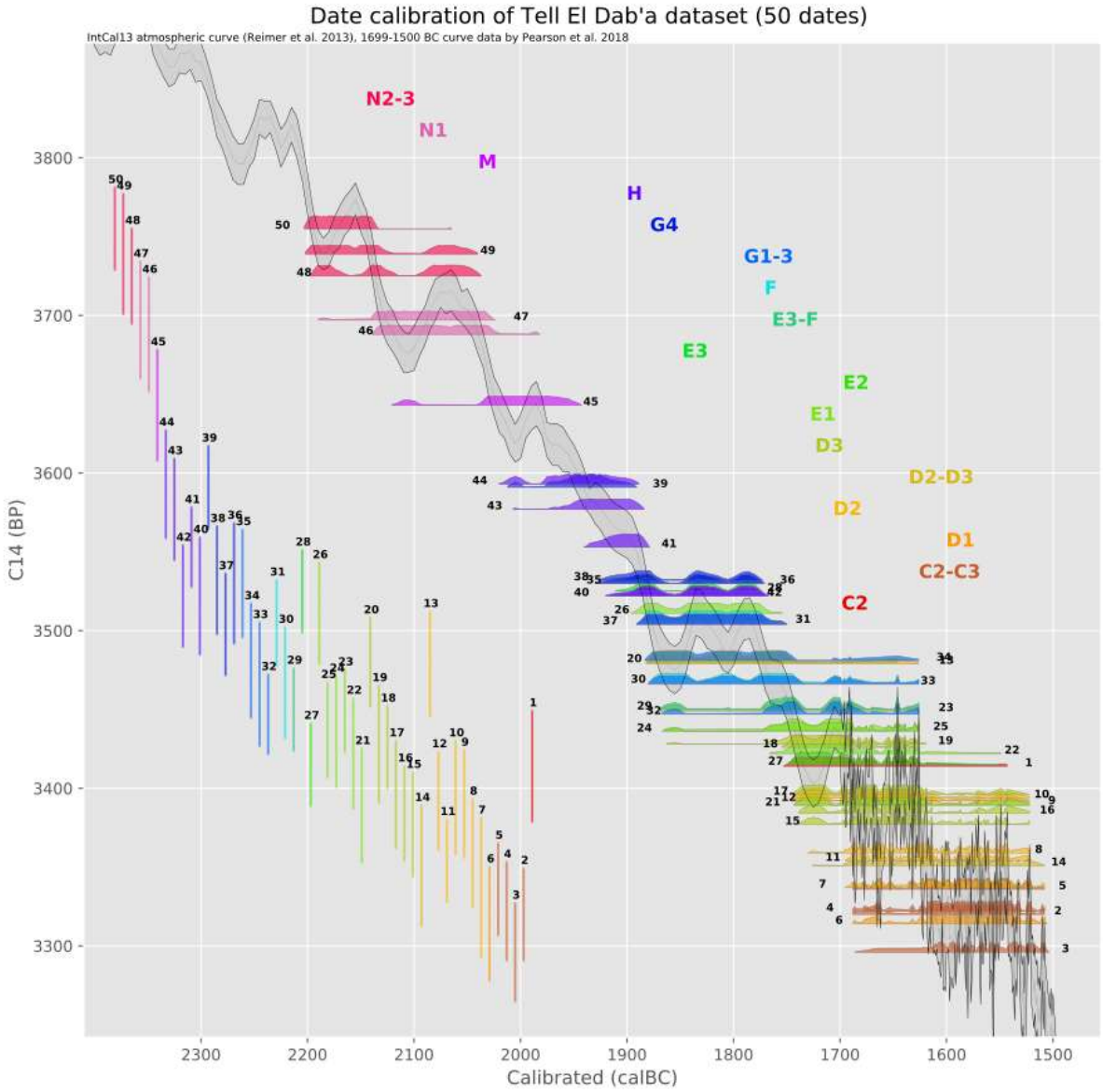

Fig. 15 Quantum/Contingency calibration (c14.bpinfo.org) of the Tell el Dab'a dataset plotted against the IntCal13 Calcurve plus the data from Pearson et al., 2018 (for the period 1700-1500 BC – pooled Pinus and Quercus data).

Since the relative sequence of those phases is one of the priors in the Bayesian model by Kutschera et al., 2012, this correction is likely to affect significantly the outcome of the model, as well as the radiocarbon dating from Levantine and Aegean MB to early LB sites, including Akrotiri.

A comparison between the unsequenced, modelled-sequenced, and Quantum/Contingency calibration vs expected historical/archaeological date would be as follows:

Phase	Lab. No	^{14}C age	Calibration (Unsequenced, 2sigma)	Modelled calibration 2sigma (after Kutschera et al., 2002)	Quantum-contingency calibration date[1]	Expected historical/archaeological date
C/2	VERA-3031	3414±35	1872-1625	1667-1537	Not included[1]	1480-1425
C/2-3	VERA-3724	3320±29	1683-1521	Weighted	1530-1480	1520-1425
C/2-3	OxA-15959	3296±31	1643-1501	Weighted	1530-1480	1520-1425
C/2-3	OxA-19597	3322±31	1686-1521	Weighted	1530-1480	1520-1425
C/2-3	- Weighted mean (AMS-48)	3313±17	1635-1529	1665-1543	Not included	1520-1425
C/2-3	OxA-15958*	3287±33	1643-1497	Not included	Not included	1520-1425
C/2-3	VERA-3725	3336±29	1691-1529	1668-1546	1530-1480	1520-1425
C/3	VERA-2632	3424±31	1875-1636	Not included	1530-1480	1520-1480
D/1	VERA-3032	3314±36	1684-1507	1688-1601	1560-1520	1550-1520
D/1-2	VERA-2630	3345±31	1736-1531	Not included	Not included	1580-1520
D/1-2	VERA-3623	3356±23	1736-1565	Not included	Not included	1580-1520
D/2	VERA-3616	3337±44	1738-1511	1723-1630	1600-1550	1580-1550
D/2	VERA-2628	3359±34	1743-1534	1698-1631	1600-1550	1580-1550
D/2	VERA-2627	3390±34	1858-1612	1722-1633	1600-1550	1580-1550
D/2	VERA-3622	3394±36	1867-1612	1722-1633	1600-1550	1580-1550
D/2	VERA-3621	3354±26	1738-1546	Weighted	1600-1550	1580-1550
D/2	OxA-15953	3392±31	1756-1616	Weighted	1600-1550	1580-1550
D/2	OxA-15901	3479±33	1890-1695	Weighted	Not included[1]	1580-1550
D/2	- Weighted mean (AMS-39)	3399±37	1871-1613	1708-1633	Not included	1580-1550
D/2	OxA-15979*	3383±30	1747-1617	Not included	Not included	1580-1550
D/2	OxA-15980*	3392±31	1756-1616	Not included	Not included	1580-1550
D/3-D/2	VERA-3645	3351±38	1741-1530	1731-1656	1635-1550	1610-1550
D/3	VERA-3620	3377±33	1751-1564	1738-1673	1635-1590	1610-1580

D/3	VERA-2629	3384±30	1747-1618	1738-1674	1635-1590	1610-1580
D/3	VERA-3619	3396±34	1861-1615	1739-1674	1635-1590	1610-1580
D/3	VERA-2895	3426±26	1872-1646	1741-1681	1635-1590	1610-1580
D/3	VERA-2896	3428±37	1878-1637	1741-1677	1635-1590	1610-1580
D/3	VERA-3033	3480±28	1886-1699	1745-1682	Not included[1]	1610-1580
E/1	VERA-2626	3389±36	1864-1611	1754-1693	1660-1620	1640-1600
E/1	VERA-3617	3422±35	1876-1629	1756-1694	1660-1620	1640-1600
E/1	VERA-3636	3449±26	1879-1688	1757-1694	1660-1620	1640-1600
E/1	VERA-3618	3436±35	1879-1658	Weighted	1660-1620	1640-1600
E/1	OxA-15949	3437±30	1878-1662	Weighted	1660-1620	1640-1600
E/1	OxA-15948	3511±32	1924-1747	Weighted	Not included[1]	1640-1600
E/1	- Weighted mean (AMS-30)	3462±25	1880-1694	1759-1694	Not included	1640-1600
E/2	VERA-3637	3415±26	1863-1638	1781-1702	1700-1650	1660-1630
E/3	VERA-2897	3525±26	1932-1766	1846-1747	Not included[1]	1700-1660
F-E/3	VERA-3643	3450±26	1879-1688	1863-1755	Not included	1740-1660
F	VERA-2625	3467±35	1885-1692	1870-1767	1750-1710	1740-1690
F	VERA-2898	3505±27	1905-1747	1871-1770	1750-1710	1740-1690
G/1-3	VERA-3642	3447±25	1878-1688	1884-1802	1790-1750	1780-1730
G/1-3	VERA-2623	3466±39	1891-1687	1886-1802	1790-1750	1780-1730
G/1-3	VERA-2622	3481±36	1896-1693	1887-1803	1790-1750	1780-1730
G/1-3	VERA-2624	3530±34	1947-1753	1894-1802	1790-1740	1780-1730
G/1-3	VERA-3644	3641±36	2135-1913	Not included	Not included	1780-1730
G/4	VERA-3640	3530±38	1960-1746	Weighted	1830-1790	1820-1770
G/4	OxA-15956	3504±32	1918-1744	Weighted	1830-1790	1820-1770
G/4	OxA-15954	3532±34	1949-1754	Weighted	1830-1790	1820-1770
G/4	- Weighted mean (AMS-40)	3521±20	1916-1771	1920-1832	Not included	1820-1770
G/4	OxA-15981*	3570±30	2022-1781	Not included	Not included	1820-1770
G/4	OxA-15955*	3530±32	1944-1757	Not included	Not included	1820-1770
G/4	VERA-2899	3591±26	2023-1887	1928-1867	Not included[1]	1820-1770
H	VERA-3638	3522±37	1946-1746	1942-1884	1855-1820	1850-1800
H	VERA-3639	3553±25	1971-1776	Weighted	Not included[1]	1850-1800

H	OxA-15951	3522±32	1936-1752	Weighted	1855-1820	1850-1800
H	OxA-15952	3577±32	2028-1782	Weighted	Not included[1]	1850-1800
H	- Weighted mean (AMS-35)	3551±17	1949-1781	1940-1886	Not included	1850-1800
H	OxA-15950*	3490±32	1897-1698	Not included	Not included	1850-1800
H	OxA-15978*	3589±32	2033-1879	Not included	Not included	1850-1800
H	VERA-2618	3593±34	2111-1829	1946-1886	Not included[1]	1850-1800
H(?)	VERA-2621	3493±34	1907-1698	Not included	Not included	1850-1800
H or N/1	VERA-2616	3610±37	2124-1884	Not included	Not included	1970-1800
M	VERA-2631	3643±35	2135-1918	2124-1972	1990-1940	1950-1900
N/1	VERA-2620	3688±36	2197-1964	2141-2021	2020-1980	1980-1930
N/1	VERA-2619	3697±37	2201-1975	2143-2022	2020-1980	1980-1930
N/1-3(?)	VERA-2617	3433±38	1879-1641	Not included	Not included	2020-1930
N/2-3	VERA-2901	3725±30	2203-2033	2197-2042	2090-2000	2020-1970
N/2-3	VERA-3641	3739±38	2281-2031	2198-2041	2090-2000	2020-1970
N/2-3	VERA-2900	3755±26	2281-2043	2198-2043	2090-2000	2020-1970

- [1]Subjective prior: phase length = min.25 max. 50 cal years; phases relative sequence is correct. Phase D/1 encompasses the 1550 BC decade;
- [1]Subjective prior: 9 Dates excluded as possible “floating” seeds from older phases: [1, 13, 20, 26, 28, 39, 41, 43, 44: see quantum/contingency calibration on curve Fig. 12 above, 50 dates dataset Ids];
- *dates on humic acids.

V.2.1 The bayesian radiocarbon chronology for Akrotiri

By now, it is generally accepted that the radiocarbon dates of the final phases of occupation at Akrotiri should imply a shift of some 50 to 120 years away from the traditional chronology,

an “offset” which is (apparently) identical to the one hypothesised for the Tell el Dab’a sequence. In fact, the vast majority of the RDs obtained from samples collected in contexts sealed within the volcanic destruction level (henceforth VDL) shows results that are consistent with an eruption date in the XVII cent. BC. However, when individually calibrated, 24 out of 28 results in the Akrotiri VDL dataset can also be consistent with a date in the XVI cent. BC at a confidence interval of 95.4% (Fig. 16 below).

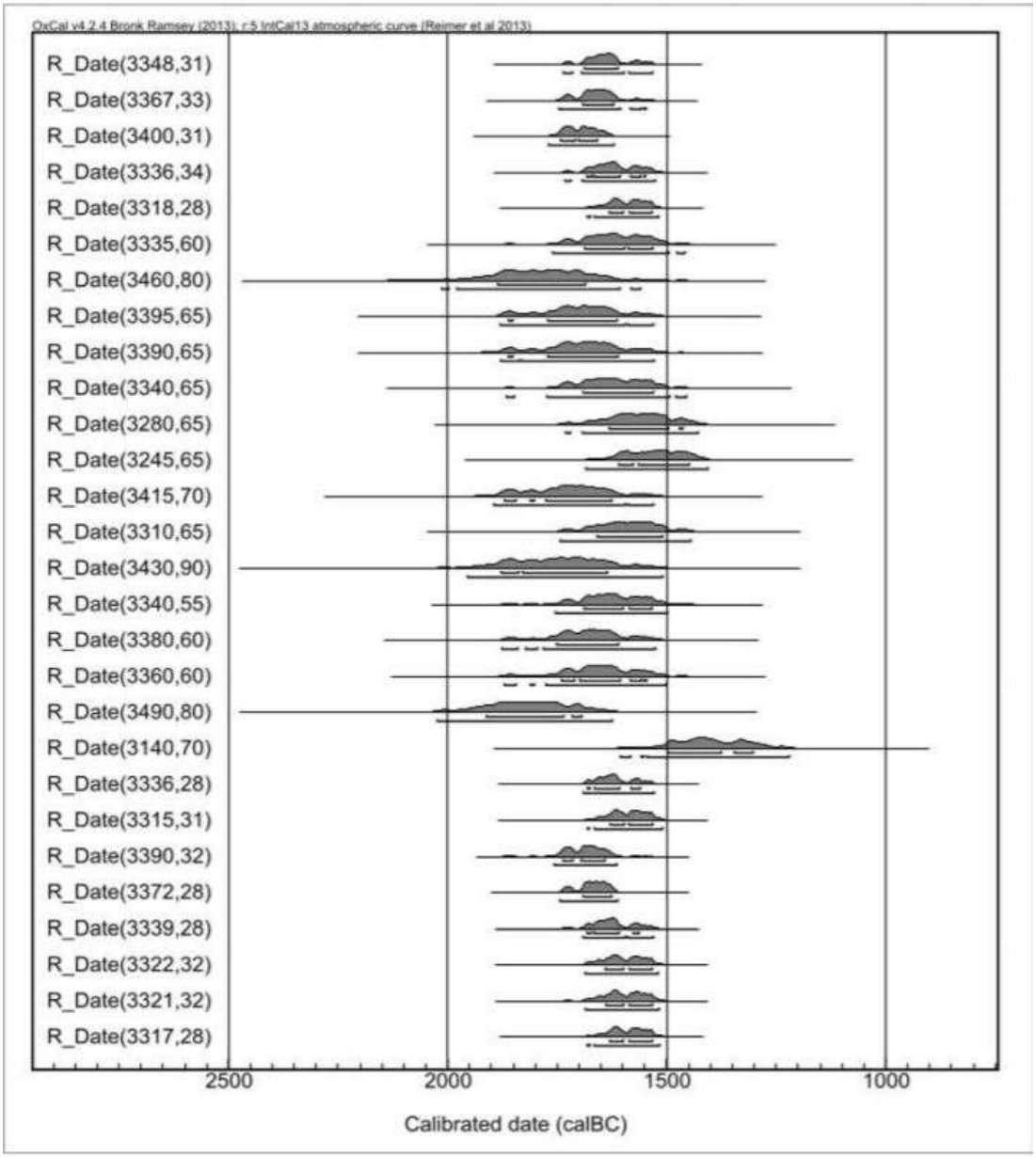

Fig. 16 Unsequenced calibration of the Akrotiri VDL dataset (after Manning et al., 2006) against IntCal13 (after Fantuzzi and Antolini, 2018).

To overcome this impasse, proponents of the high chronology have tried to combine the radiocarbon dates from Akrotiri (and other sites) with the use of Bayesian modelling programs, and in particular OxCal's R_Combine and Tau_Boundaries. A Bayesian model for chronology (see above) estimates the probability that an event *X* occurred in a certain period *t* based on dating measurements RDs of related objects (posterior probability). As observed above, this is done by combining the probability of finding measured RDs for objects belonging to *t* (likelihood) and a prior probability, i.e. information on the objects not derived from the measurement (cfr. above, Ward and Wilson, 1978; Bronk-Ramsey, 2009; Fantuzzi and Antolini, 2018, with references).

More specifically, R_Combine calculates the only possible chronological interval where all the RDs fit together, assuming that they all represent the radiocarbon date of the eruption event, i.e. that they are all contemporaneous, while Tau_Boundaries take into account the possibility that some of the dates may be earlier (Bronk-Ramsey, 2009). The absolute date of the eruption has been consequently suggested to be 3345±8 BP which, in calibrated terms, would date the eruption between 1643 and 1621 BC or between 1665 and 1614 BC (Fig. 17 below).

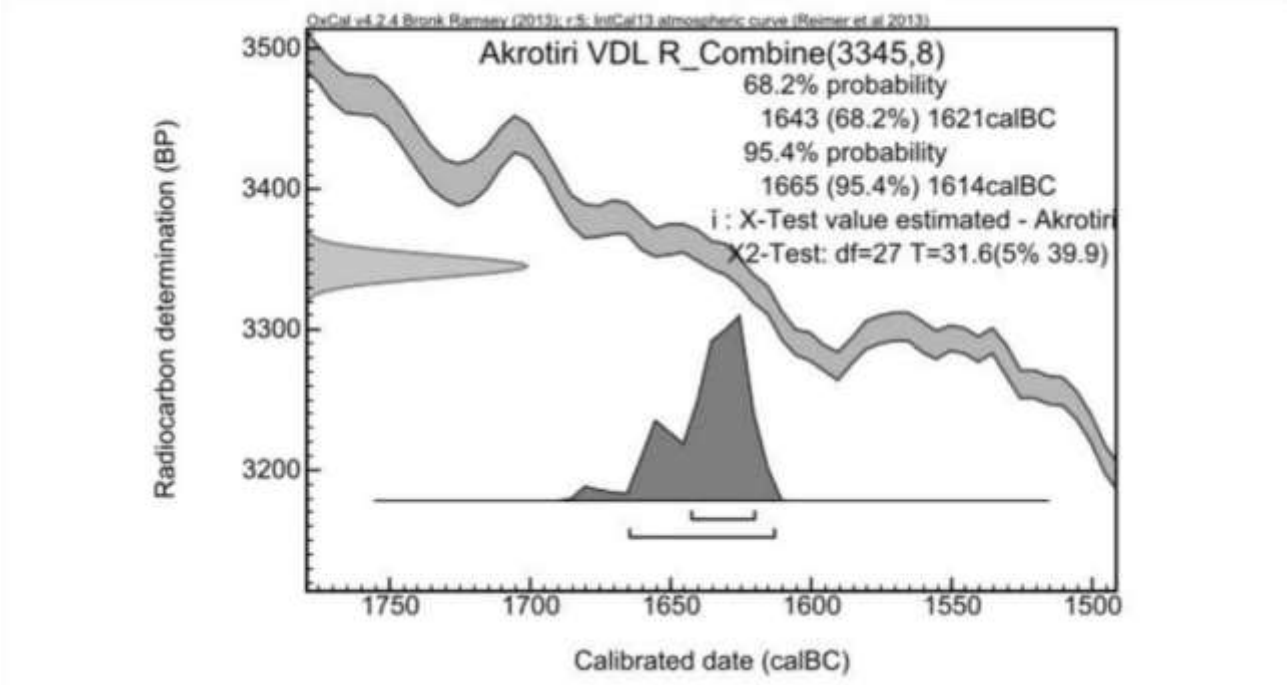

Fig. 17 R_Combine results of the Akrotiri VDL dataset (after Manning et al., 2006) against IntCal13 (after Fantuzzi and Antolini, 2018)

In the specific case, the use of R_Combine requires:

1) That all the sampled organisms are contemporaneous;
2) That they all died in a moment close to the final eruption;
3) That there is no intrusive material in the tested samples;
4) That no sample in the dataset presents alterations or reservoir effects.

The use of R_Combine requires that all these conditions are met *a priori*. Thus, it is not possible to use R_Combine to verify the reliability of those conditions without incurring a serious vicious circle. As for conditions 1) and 2), such programs can be useful to work out whether the radiocarbon determinations can represent the same event given their contemporaneity, but not to show if they represent a single event. As a consequence: 1) radiocarbon dates of different real ages may misleadingly be considered contemporaneous, and 2) the results in calibrated terms would be consequently altered (see f.e. Steier and Rom, 2000; Weninger et al., 2015; Fantuzzi and Antolini, 2018).

V.2.2 The radiocarbon dataset for Akrotiri

More in detail, the whole radiocarbon dataset for Akrotiri (early LM I A to VDL) presented by Manning et al. (2006) is as follows:

Lab no.	**Material**	**Taxon**	**^{14}C date**	**δ^{13}C**	**Context (after Manning et al., 2006)**	**Phase**
OxA-11250	Charcoal	*Olea europaea*	3550±45	-23.4	Secure	LM I A (early)
OxA-10312	Charcoal (bark)	*Tamarix sp.*	3293±27	-24	Secure	LM I A (late)
VERA-2748	"	"	3319±28	-24.6	"	"
OxA-10313	Charcoal	*Tamarix sp.*	3353±27	-24.1	Secure	LM I A (late)
VERA-2749	"	"	3335±33	-25	"	"

OxA-10314	Charcoal (pith)	*Tamarix sp.*	3330±27	-24.5	Secure	LM I A (late)
VERA-2650	"	"	3325±28	-25.7	"	"
OxA-10315	Charcoal (bark)	*Olea europaea*	3446±39	-24	Secure	LM I A (late)
VERA-2743	"	"	3413±28	-24.3	"	"
OxA-10316	Charcoal	*Olea europaea*	3342±38	-24.4	Secure	LM I A (late)
VERA-2744	"	"	3427±31	-20.4	"	"
OxA-10317	Charcoal (bark)	*Olea europaea*	3440±35	-24.1	Secure	LM I A (late)
VERA-2745	"	"	3386±28	-22.9	"	"
OxA-10318	Charcoal	*Olea europaea*	3355±40	-24.2	Secure	LM I A (late)
VERA-2746	"	"	3471±28	-18.1	"	"
OxA-10319	Charcoal	*Olea europaea*	3424±38	-24.4	Secure	LM I A (late)
VERA-2747	"	"	3386±30	-26.4	"	"
OxA-11817	Charred seeds	*Lathyrus sp. (?)*	3348±31	-22.9	Secure	VDL
OxA-11818	Charred seeds	*Hordeum sp.*	3367±33	-25.8	Secure	VDL
OxA-11820	Charred seeds	*Hordeum sp.*	3400±31	-25.2	Secure	VDL
OxA-11869	Charred seeds	*Horedum sp.*	3336±34	-22.8	Secure	VDL
OxA-12170	Charred seeds	*Lathyrus sp. (?)*	3336±28	-22.9	Secure	VDL
VERA-2757	"	"	3315±31	-24.1	"	"
-repetition	"	"	3390±32	-21.5	"	"
OxA-12171	Charred seeds	*Hordeum sp.*	3372±28	-25.7	Secure	VDL
VERA-2758	"	"	3339±28	-26.5	"	"
-repetition	"	"	3322±32	-24.7	"	"
OxA-12172	Charred seeds	*Hordeum sp.*	3321±32	-23.1	Secure	VDL
VERA-2756	"	"	3317±28	-21.6	“	“
OxA-12175	Charred seeds	*Hordeum sp.*	3318±28	-24.7	Secure	VDL
OxA-1548	Charred seeds	*Lathyrus sp.*	3335±60	-23	Secure	VDL
OxA-1549	Charred seeds	*Lathyrus sp.*	3460±80	-23	Secure	VDL
OxA-1550	Charred seeds	*Lathyrus sp.*	3395±65	-23	Secure	VDL
OxA-1552	Charred seeds	*Lathyrus sp.*	3390±65	-23	Secure	VDL
OxA-1553	Charred seeds	*Lathyrus sp.*	3340±65	-23	Secure	VDL
OxA-1554	Charred seeds	*Lathyrus sp.*	3280±65	-23	Secure	VDL
OxA-1555	Charred seeds	*Lathyrus sp.*	3245±65	-23	Secure	VDL
OxA-1556	Charred seeds	*Hordeum sp.*	3415±70	-23	Secure	VDL
K-5352	Pulses	-	3310±65	-22.5	Secure	VDL
K-5353	Pulses	-	3430±90	-20.5	Secure	VDL
K-3238	Pulses	-	3340±55	-20.6	Secure	VDL
K-4255	Charred twig	*Tamarix sp.*	3380±60	-23.8	Secure	VDL

Hd-7092-6795	peas	*peas*	3360±60	-	Secure	VDL
Hd-6058-5519	Grains	-	3490±80	-	Secure	VDL
Hd-6059-7967	Grains	-	3140±70	-	Secure	VDL

Hypothesis testing (which is the basis of all tests derived from Ward and Wilson, 1978, as is the case of OxCal's R_Combine, above) verifies the plausibility of an initial hypothesis (null hypothesis) in contrast with an alternative hypothesis. This consists in proving whether or not the null hypothesis is improbable and in quantifying its improbability. So, whichever testing technique is used, hypothesis testing is not meant to prove the null hypothesis (Ward and Wilson, 1978; Fantuzzi and Antolini, 2018:247-248, with references). Under this aspect, the R_Combine results from Akrotiri have been presented to the public in a very misleading way. The 5% confidence level chosen for the Chi-square test (see Fig. 17 above) does in fact only mean that the combination of RDs has *less than 95%* probability of being wrong. To address what the actual improbability of this combination is it is sufficient to run the Ward and Wilson test with a different confidence level (this function is already accessible online on http://c14.bpinfo.org). The VDL dataset still passes the test with a confidence of 77%, but it fails already at 75%. This means that the RDs in the dataset have at least a 75% of probability of *not* representing the same event (Figs 18a, b below).

a)

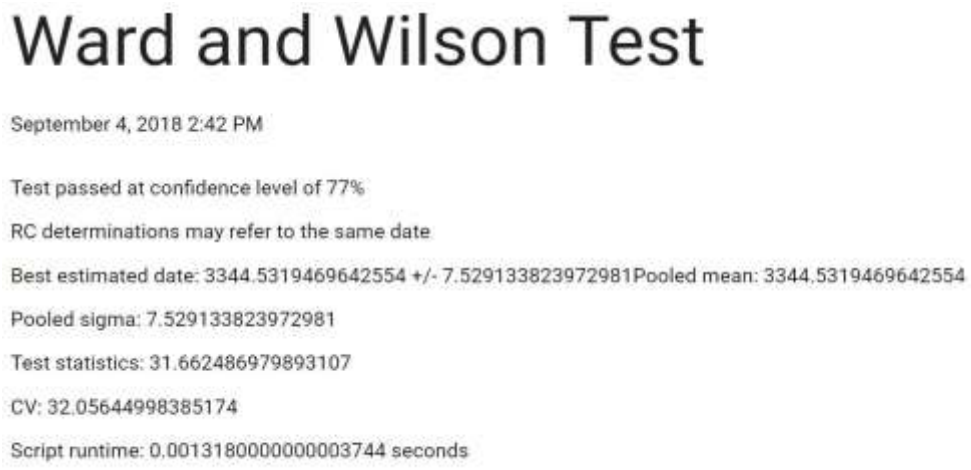

b)

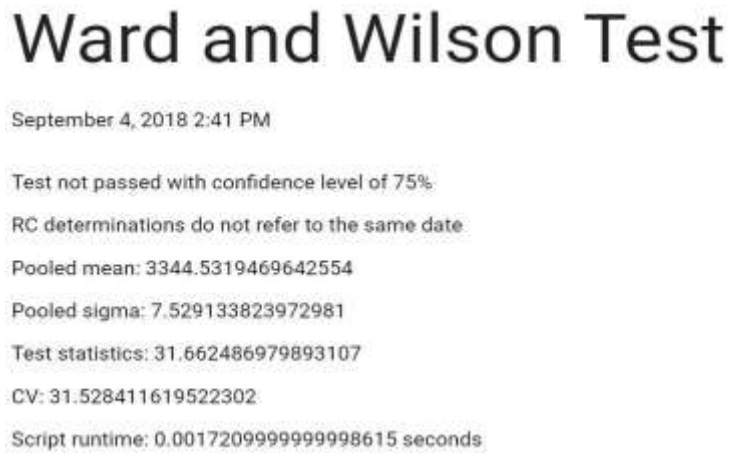

Figs 18a, 18b Results of Ward and Wilson test under different confidence intervals (c14.bpinfo.org). The results of the analysis show that the combination of RDs (null hypothesis) has an improbability up to 75%.

Moreover, even excluding *a priori* possible stratigraphic/contextual and treatment/counting errors by the laboratory, the variability in measured ^{14}C ages may be caused by a long series of effects:

1) The seasonal variability in ^{14}C absorption by plants, depending on the growing season, which may cause alterations from 8 to 32 radiocarbon years;

2) The local variability of the ^{14}C atmospheric content which is not recognized by the calibration curve (which is a smoothed, approximated band for the whole northern hemisphere);

3) Reservoir effects deriving mainly from:
   a) deep sea water upwelling and degassing;
   b) volcanic ventings, causing the absorption of old carbon from depauperated CO_2 by the sampled plants.

Most importantly at this regard, the presence of sources of volcanic CO_2 on Thera has been

proved beyond any doubt (McCoy and Heiken, 2000), although it is still unclear to what extent it might have affected the grains and olives found at Akrotiri. As opposite to the Tell el Dab'a record, the samples from Akrotiri were collected from closed contexts (as storage jars) therefore ruling out the possibility of residuals. However, from the mathematical point of view of (combined) calibration, the (hypothetical) presence of volcanic reservoir-affected samples would have a similar impact on the final outcome of the tests.

In any case the RDs for the Minoan eruption *as well as those from earlier (late) LM I A contexts* (Figs 19-20 and 21-22 below) fall into a part of the calibration curve where a difference of only 20 radiocarbon years would be enough to shift it from the low to the high chronology or vice versa.

This effect is much more enhanced when the RDs from Akrotiri are calibrated against the data from Pearson et al. (2018). Impressively, out of a total of 44 dates only 6 do not include the decade 1560-50 in their 1sigma (!) range (Figs 19, 21 below).

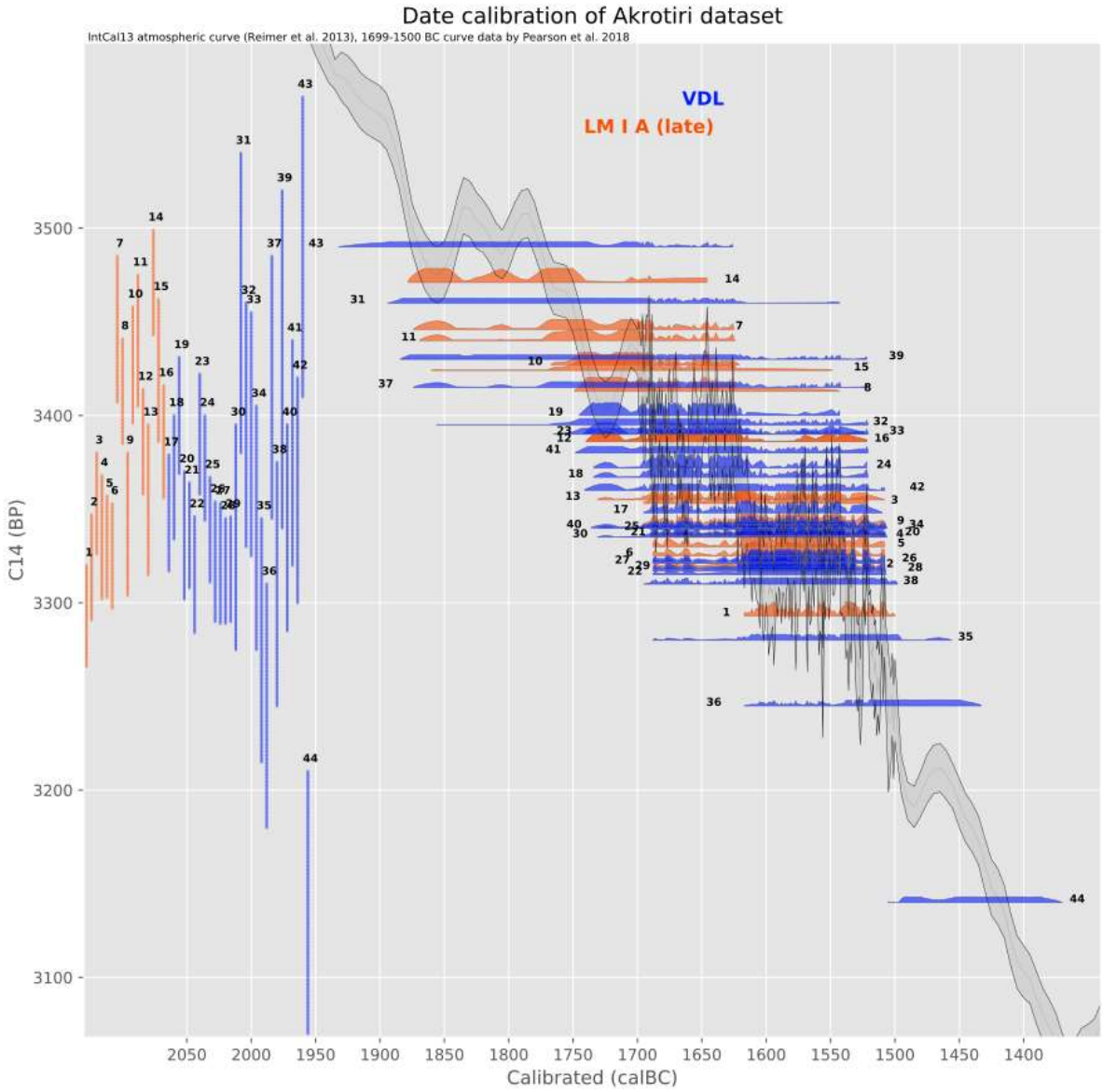

Fig. 19 Quantum calibration (1sigma) of the Akrotiri "late" LM I A (magenta) and VDL (blue) datasets. Out of a total of 44 RDs, only 6 [7, 10, 11, 14, 43, 44] do not include the year 1550 BC.

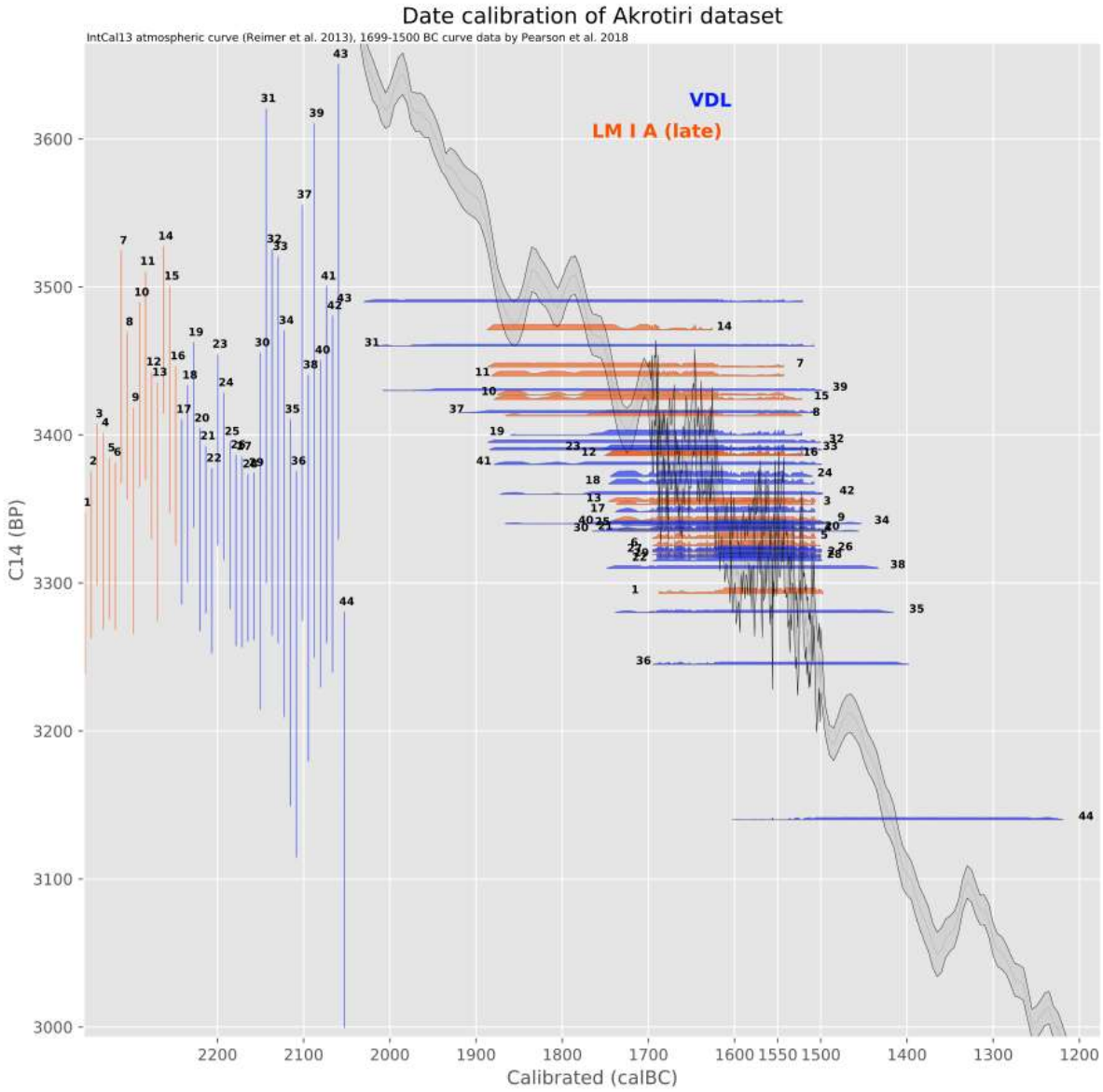

Fig. 20 Quantum calibration (2sigma) of the Akrotiri "late" LM I A (magenta) and VDL (blue) datasets. Out of a total of 44 RDs, only 1 [14] does not include the year 1550 BC.

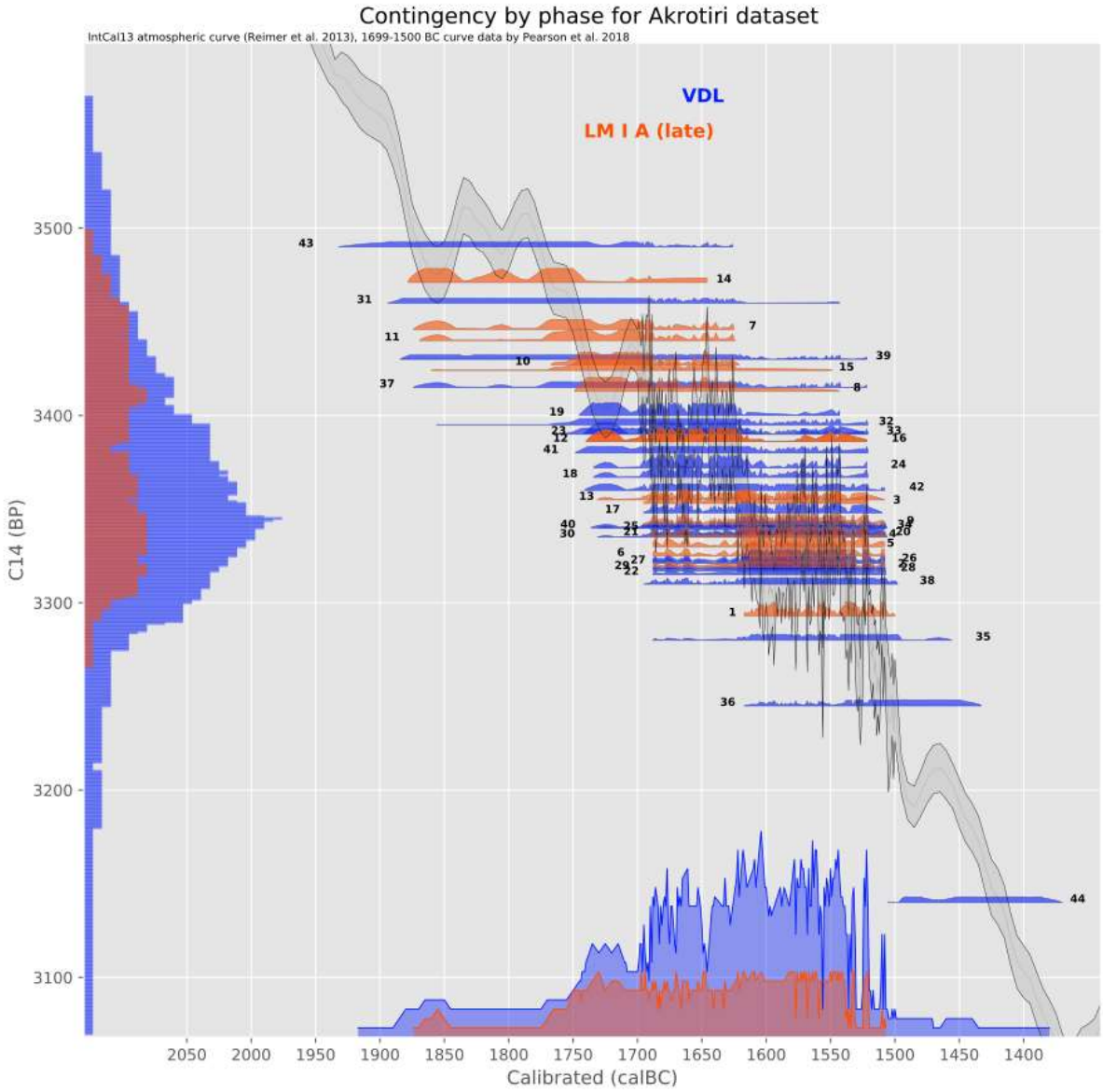

Fig. 21 Contingency curves (1sigma) built by phase from corresponding dates for Akrotiri "late" LM I A (magenta) and VDL (blue) clearly showing the overlapping between the two phases. Note that the height of the contingency curve is the result of the number of dates compatible with a certain year. Because more dates are in the VDL phase than in the LM I A late, the blue curve is higher. However, curve extent is more important. Since contingency curves occupy approximately the same range the calibrated results for the two phases are substantially indistinguishable.

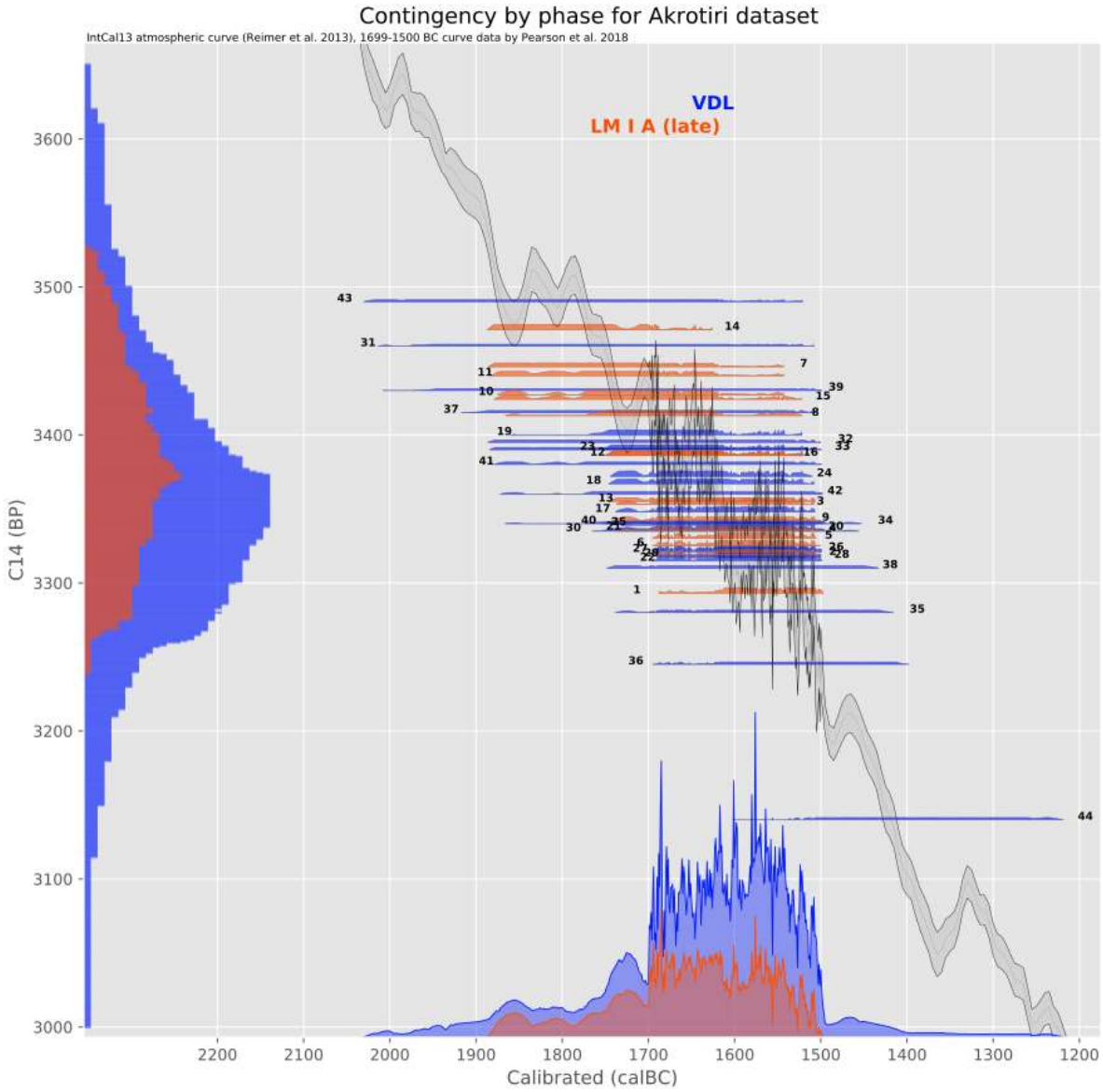

Fig. 22 Contingency curves (2sigma) built by phase from corresponding dates for Akrotiri "late" LM I A (magenta) and VDL (blue) clearly showing the overlapping between the two phases.

V.2.3 The radiocarbon dataset for the Theran olive tree-branch

The last argument in favour of the AHC consists in the analysis of radiocarbon dates from an olive tree branch which was buried by the ejecta of the eruption and believed to be alive at the time of the volcanic event (Friedrich et al., 2006). The authors have used x-ray tomography to try to identify the number of annual rings in the branch, which was subdivided in four sequences (rings 1 to 13, 14 to 37, 38 to 59, 60 to 72, all with an estimated uncertainty of ±3/5, Friedrich et al., 2006, Supporting materials: table S1).

In detail, the radiocarbon dates for the olive tree-rings sections are as follows:

Lab no.	**^{14}C age**	**Rings**	**Estimated counting error (after Friedrich et al. 2006)**
Hd-23599/24426	3383±11	1 to 13	±3
Hd-23587	3372±12	14 to 37	±5
Hd-23589	3349±12	38 to 59	±5
Hd-23588/24402	3331±10	60 to 72	±3

Since then, the reliability of this counting (and of ring counting in olives in general) has been seriously questioned (e.g. Wiener, 2009, 2010; Cherubini et al., 2013; Ehrlich et al., 2018; *contra* Friedrich and Heinemeier, 2009; Friedrich et al., 2014; Manning, 2014), and the 72 years-figure was subsequently dismissed (Friedrich et al., 2014).

Supporters of the AHC have consequently argumented that, even without the tree-ring counting, the calibrated intervals (against IntCal 04, 09 and 13) would allow only a date in the XVII century BC, or just slightly later (Friedrich et al., 2014). Following Manning (2014:74):

> However, this is in fact not a major issue, since we don't need any ring count to achieve a reasonably precise dating of the olive branch. A Sequence analysis simply using the direction of growth (and no tree-rings) on the olive branch sample allows a fairly precise dating while entirely circumventing any arguments [sic!] over whether or not Friedrich et al. were correct about being able to recognize annual growth increments in olive using X-ray tomography […]. Such an analysis places the centre of the last dated wood segment at 1637-1610 BC at 68.2% probability […].

After re-calibration of the four dates sequence for the Theran olive branch against the data from Pearson et al., 2018 (Figs 23-24 below), this picture is overturned. Not only would a date (or, more accurately, a *terminus post quem*) for the eruption event at 1525 BC (1sigma) or even 1510 BC (2sigma) be fitting into the radiocarbon data, but this would even remain valid also *if* one wants to accept (!) the tree-ring count by Friedrich et al. 2006 (as well as the 74 years figure suggested by Manning, 2014:76). Thus, the olive tree branch dating is no longer an argument for the "high" date of the eruption, but in contrast it may be even regarded to as a (circumstantial) proof for the "low" (i.e. Archaeology-based) chronology (Figs 23-24 below). Moreover, this may show that – at least for the time-span in question – we have definitely reached the precision limits of radiocarbon dating.

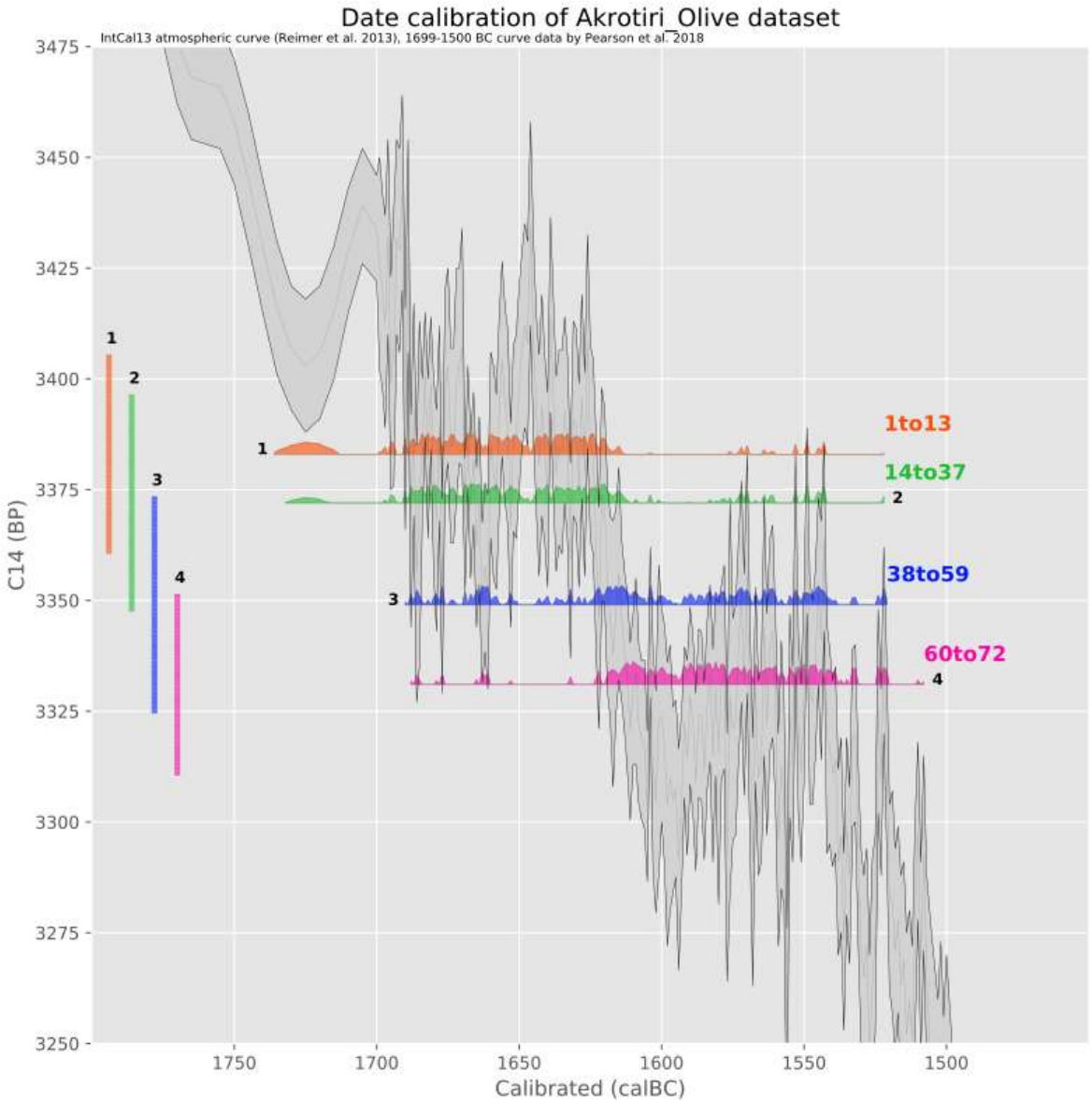

Fig. 23 Quantum/contingency calibration (1sigma) of the olive branch sections against IntCal 13 plus data from Pearson et al., 2018. The distribution and relative height of the peaks in the "mini-gaussians" (orange, green, blue and violet "bells") clearly show that an eruption date as late as 1525 BC is just as acceptable as a date in the late XVII century, and it would even fit with the much-discussed tree ring count by Friedrich et al., 2006.

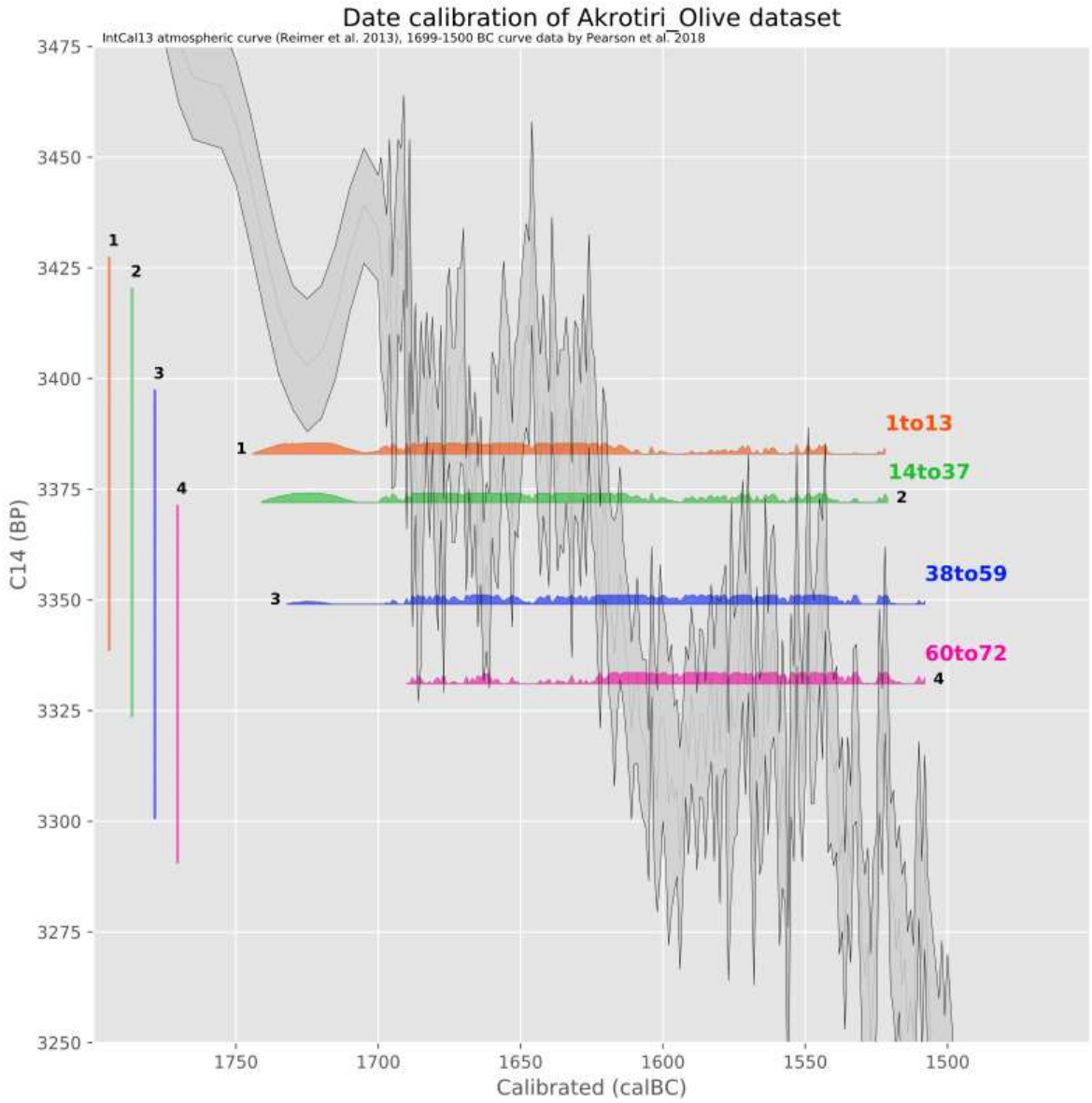

Fig. 24 Quantum/contingency calibration (2sigma) of the olive branch sections against Intcal 13 plus data from Pearson et al., 2018. The distribution and relative height of the peaks in the "mini-gaussians" (orange, green, blue and violet "bells") clearly show that 1) an eruption date as late as 1525 BC is just as acceptable as a date in the late XVII century, and that 2) even a date as "low" as 1510 BC would be acceptable and still fit with the much-discussed tree ring count by Friedrich et al., 2006.

Chapter VI

Conclusions

This dissertation examines two sources of evidence in order to decide the dating of the Theran volcanic eruption with all of its archaeological and historical consequences. Despite a significant part of the archaeological data not being precisely dated (for detailed discussion see Chapters II and III), we can make three major observations about the archaeological-based chronologies:

1) That almost all the archaeological arguments and hypothetical reconstructions put forward in support of the AHC rely either (or only) on *argumenta ex silentio* (i.e. by highlighting lacunae in the archaeological record/interpretations) or have in fact simply shown that a high chronology is not impossible (Chapters III, IV);

2) That the main argumentation in support of the AHC consisted in the Bayesian interpretation of radiocarbon data which has turned out to be seriously questionable, while the new re-analysis presented here shows that, based on a one-by-one analysis (i.e. without using any kind of statistical error-minimization), the large majority of radiocarbon results is actually consistent with the Low Chronology (Chapter V);

3) That the interrelations of archaeological evidence allows us, at the very least, to formulate a solid relative chronology, which in particular shows: a) that the LC I A2 period was more or less contemporaneous with the LM I A period (and the Theran eruption – Chapter III); b) that the LC I A1/2 transition period was more or less contemporaneous with phases D/2 to C/2 at Tell el Dab'a (Chapter IV), corresponding to the very end of the SIP and the re-organisation at the beginning of the XVIII Dynasty (therefore explaining the relative scarcity of "early" WS at the site as well as the presence of early-XVIII Dynasty reworked vessels in Myceanae Shaft Graves).

As to the radiocarbon dating for the two key-sites of Akrotiri and Tell el Dab'a, on the other end, it is possible to draw some firm conclusions. Summing up all the above evidence, we may observe:

1) That the apparent 120 years-offset in the calibrated results from Tell el Dab'a can simply be a consequence of the presence of residual seeds from stratigraphical reworking (Paragraphs V.1.1-3);

2) That the radiocarbon dataset for Akrotiri is insufficient to establish a precise absolute date for the Theran eruption, since a) the RDs for both the VDL and the earlier "late" LM I A contexts fall into a part of the calibration curve where a difference of only 20 radiocarbon years would be enough to shift the outcome of calibration from the low to the high chronology or *vice versa*; b) the probable presence of presently unquantified reservoir effects deriving from volcanic ventings makes it impossible to refine the precision of the suggested date, by whatever statistical method (Paragraphs V.2.1-3);

3) That statistical tools which artificially reduce the uncertainty in the results have been inaccurately applied to the datasets, with the results of enhancing the (previously underestimated) offset between the IntCal data and the annual tree-ring calibration data by Pearson et al., 2018 for the relevant time-span (Chapter V);

4) That a new approach which applies quantum-based calibration (Paragraph I.2.1-3; Chapters V, Appendix I) in combination with the recently published dendrochronological data by Pearson et al. (2018) provides evidence in favour of an eruption date in the XVI century BC. In particular, out of a total of 44 RDs for the "late" LM I A and for the VDL, only 6 do not include the 1560-1550 Cal BC decade in their 1sigma intervals (Paragraph V.2.2);

5) That even the much-discussed olive branch's radiocarbon sequence calibrated against the Pearson et al. data (Paragraph V.2.3) allows with an acceptable probability an eruption date as low as 1525 BC (1sigma), maybe even 1510 BC (2sigma).

One final, and methodologically most important, conclusion is that – in the specific case study – we have probably reached the precision limit of radiocarbon dating (at least in its present form), and have certainly reached the precision limit of present statitiscal tools for radiocarbon age refinement. Realistically, none of the above detailed arguments can offer a conclusive answer to the *vexata quaestio* of the date of the eruption (with all its implications).

A glimmer of hope may, however, come from the combination of pottery dating with radiocarbon, for example by means of Correspondence Analysis (cfr. Easton and Weninger, 2018) and the new calibration methods presented here (cfr. Paragraph I.2.3; Chapter V), which could not only refine the chronology, but also (perhaps) allow us to identify the "outliers" (as the stratigraphically reworked seeds at Tel el Dab'a, or, in the case of Akrotiri, the hypothetical volcanic reservoir-affected samples). Together such an approach might also support the quantification of these offsets.

Appendix I

Quantum/Contingency calibration in http://c14.bpinfo.org

The Python-program code used for this study is as follows (detailed description of each mathematical operation in the algorithms and methods developed for the present project and used to obtain the results above is reported under the "def" headers):

1) Contingency/quantum calibration:

"Contingency_calibration" function in http://c14.bpinfo.org. Quantum theory-based calibration derived from Weninger, 1986; Weninger et al., 2015.

```
# coding: utf-8

TITLE = "calibration_contingency_algorithm"


def read_intcal(filename):
    '''reads intcal13 file or other calibration curve as dataframe
    adds corresponding AD/BC year for each cal BP year
    defines corresponding C14 upper and lower curve'''
    whole_calcurve = pd.read_table(filename, sep=',')
    whole_calcurve['ADBC'] = 1950 - whole_calcurve['CAL BP']
    whole_calcurve['C14upper'] = whole_calcurve[' 14C age'] + whole_calcurve['Error']
    whole_calcurve['C14lower'] = whole_calcurve[' 14C age'] - whole_calcurve['Error']
```

```
    return whole_calcurve

def read_dates(dates_file):
    '''reads the input csv file with RC determinations and returns
    a list of means and a list of standard deviations'''

    datesDict = {}
    meanList = []
    stDevList = []
    phasesDict = {}

    infile = open(dates_file)
    line = infile.readline()
    count = 0
    ID_pos = None
    date_pos = None
    sigma_pos = None
    phase_pos = None
    phase_specified = True
    while line:
        lineList = line.split(',')
        lineList = [x.strip() for x in lineList]

        if count == 0:  # first line is header
            for el in enumerate(lineList):
                pos = el[0]
                val = el[1].strip().lower()

                if val == 'id':
                    ID_pos = pos
                elif val == 'date':
                    date_pos = pos
                elif val == 'sigma':
```

```
            sigma_pos = pos
        elif val == 'phase':
            phase_pos = pos

    if (ID_pos is None) or (date_pos is None) or (sigma_pos is None):
        infile.close()
        raise Exception('Unable to find either id, date or sigma csv headers')
    if phase_pos is None:
        phase_specified = False

else:
    dateID = int(lineList[ID_pos])
    date = lineList[date_pos]
    sigma = lineList[sigma_pos]
    phaseID = 1
    if phase_specified == True:
        phaseID = lineList[phase_pos]

    mean = int(date)
    meanList.append(mean)

    stDev = int(sigma)
    stDevList.append(stDev)

    datesDict[dateID] = (mean, stDev)

    if phaseID in phasesDict:
        phasesDict[phaseID].append(dateID)
    else:
        phasesDict[phaseID] = [dateID]

line = infile.readline()
count += 1
```

```
    infile.close()
    return datesDict, phasesDict

def get_phases_color_dict(phasesList):
    d = {}
    i = 0
    for p in phasesList:
        d[p] = (randint(0,100)/100.0, 0.99, 0.99)
    return d

def findUpperLower(alfa, meanDict, stDevDict):
    '''returns the extreme years of the overall interval covered by the dataset'''
    datesList = sorted(meanDict.keys())
    uppBound, lowBound = meanDict[datesList[0]], meanDict[datesList[0]]
    for date in datesList:
        up = meanDict[date] + alfa * stDevDict[date]
        low = meanDict[date] - alfa * stDevDict[date]
        if up > uppBound:
            uppBound = up
        if low < lowBound:
            lowBound = low
    return uppBound, lowBound


def calculateContingency(alfa, meanDict, stDevDict):
    '''returns the contingency interval, i.e. the largest interval of years common to all
    measurements of the dataset. If there is no common interval, there is no contingency
    and the result means a distance between the closest non-overlapping measurements
    Result is given as a tuple: (upper bound, lower bound, interval length)'''

    dateList = sorted(meanDict.keys())
    up = []
    low = []
```

```
    for date in dateList:
        up.append(meanDict[date] + alfa * stDevDict[date])
        low.append(meanDict[date] - alfa * stDevDict[date])
    return min(up), max(low), min(up) - max(low)


def calculateRelevance(contingency, alfa, meanDict, stDevDict):
    '''relevance of a measurement is the ratio between a measurement interval
    and the contingency interval and is given as a percentage. In other words
    it quantifies how well a measurement interval covers the contingency interval.
    Obviously, it is only significant when a contingency interval exists.'''

    dateList = sorted(meanDict.keys())
    if contingency < 0:
        return ("No contingency interval exists for this dataset\n")
    relev = {}
    up = []
    low = []
    for date in dateList:
        mean = meanDict[date]
        relev[date] = (mean, (100 * contingency / ((mean + alfa *
                                        stDevDict[date]) - (mean - alfa * stDevDict[date]))))
    return relev


def calculateDatasetRepresentativity(contingency, alfa, meanDict, stDevDict):
    '''Dataset representativity is the ratio, expressed as a percentage, between the
    lengths of the contingency interval and the total interval covered by the dataset.
    Obviously, it is only significant when a contingency interval exists.'''

    dateList = sorted(meanDict.keys())
    if contingency < 0:
        return ("No contingency interval exists for this dataset\n")
```

```
    up = []
    low = []
    for date in dateList:
        up.append(meanDict[date] + alfa * stDevDict[date])
        low.append(meanDict[date] - alfa * stDevDict[date])
    return (100 * (contingency / (max(up) - min(low))))


def buildDict10(alfa, meanDict, stDevDict, lowBound, uppBound, threshold):
    '''builds a dictionary with as many keys as years covered by the dataset.
    A value contains:
    0) a list of either 1 or 0, where 1 in poition j means that the year is covered
        by the j-th measurement of the dataset, 0 if it is not
    1) the sum of the numbers in the list in 0)
    2) ratio between sum in 1) and number of measurements (i.e. number of actual 1s and
        number of total possible 1s)
    3) signed difference between the ratio in 2) and a threshold'''

    dateList = sorted(meanDict.keys())
    dict10 = {}
    for i in range(lowBound, uppBound + 1):
        dict10[i] = [[], 0.0, 0.0, 0.0]
        for date in dateList:
            if (i >= meanDict[date] - alfa * stDevDict[date] and
                    i <= meanDict[date] + alfa * stDevDict[date]):
                dict10[i][0].append(1)
            else:
                dict10[i][0].append(0)
        dict10[i][1] = sum(dict10[i][0])
        dict10[i][2] = float(dict10[i][1]) / float(len(dateList))
        dict10[i][3] = dict10[i][2] - threshold
    return dict10
```

```
def build_count1perRC(dict10, meanDict):
    '''uses the result of buildDict10 to build 2 lists, which will be used in buildDictNorm,
    to take into account variances of single measurements.
    It counts the number of 1s for a measurement, i.e. the width of its interval, in the first
    list and the ratio 1-to-count in the second list.
    These lists have as many elements as measurements'''

    dateList = sorted(meanDict.keys())
    count1perRC = []
    for j in range(len(dateList)):
        count = 0
        for i in dict10:
            count += dict10[i][0][j]
        count1perRC.append(float(count))
    normCount1perRC = []
    for count in count1perRC:
        normCount1perRC.append(1.0 / count)
    return count1perRC, normCount1perRC


def buildDictNorm(count1perRC, meanDict, lowBound, uppBound, dict10,
normCount1perRC):
    '''builds a dictionary with as many keys as years covered by the dataset.
    A value contains:
    0) a list of positive floats <=1. Number in position j represents the weight
        of measurement j on that year
    1) the sum of the numbers in the above list
    2) distance of the sum in 1) and the maximum possible sum, which would occur
        when a year is covered by all measurements
    3) ratio between the sum in 1) and the maximum possible sum, given as %'''

    dateList = sorted(meanDict.keys())
```

```
    dictNorm = {}
    for i in range(lowBound, uppBound + 1):
        dictNorm[i] = [[], 0.0, 0.0, 0.0]
        for j in range(len(dateList)):
            val = float(dict10[i][0][j]) / count1perRC[j]
            dictNorm[i][0].append(val)
        dictNorm[i][1] = sum(dictNorm[i][0])
        dictNorm[i][2] = sum(normCount1perRC) - dictNorm[i][1]
        try:
            dictNorm[i][3] = 100 * dictNorm[i][1] / sum(normCount1perRC)
        except ZeroDivisionError:
            dictNorm[i][3] = 0.0
    return dictNorm


def phase_analysis(alfa, datesDict, phasesDict):
    threshold = stats.norm.cdf(alfa) - stats.norm.cdf(-1 * alfa)

    contingencyDict = {}
    transitionDict = {}
    dict10_byphase_dict = {}
    dictNorm_byphase_dict = {}

    bounds = {}
    phasesList = sorted(phasesDict.keys())
    for phaseID in phasesList:
        meanDict = {}
        stDevDict = {}
        for dateID in phasesDict[phaseID]:
            meanDict[dateID] = datesDict[dateID][0]
            stDevDict[dateID] = datesDict[dateID][1]

        uppBound, lowBound = findUpperLower(alfa, meanDict, stDevDict)
```

```
        bounds[phaseID] = (uppBound, lowBound)

        dict10 = buildDict10(alfa, meanDict, stDevDict,
                             lowBound, uppBound, threshold)
        dict10_byphase_dict[phaseID] = dict10

        count1perRC, normCount1perRC = build_count1perRC(dict10, meanDict)
        dictNorm = buildDictNorm(
            count1perRC, meanDict, lowBound, uppBound, dict10, normCount1perRC)
        dictNorm_byphase_dict[phaseID] = dictNorm

        contingency = calculateContingency(alfa, meanDict, stDevDict)
        contingencyDict[phaseID] = (contingency[0], contingency[1])

        relevance = calculateRelevance(
            float(contingency[2]), alfa, meanDict, stDevDict)

    for i in range(1, len(phasesList)):
        transition = bounds[phasesList[i]][0] - bounds[phasesList[i - 1]][1]
        transitionDict[i] = (bounds[phasesList[i]][0],
                             bounds[phasesList[i - 1]][1])

    return contingencyDict, transitionDict, dict10_byphase_dict, dictNorm_byphase_dict



def quickSort(thisList,low,high,propertyIndex):
    '''standard function to sort a list of numbers in ascending order'''
    i,j = low,high
    mid = int((high+low)/2)
    pivot = thisList[mid][propertyIndex]
    while (i <= j):
        while thisList[i][propertyIndex] < pivot :
            i+=1
```

```
        while thisList[j][propertyIndex] > pivot :
            j-=1
        if i < j :
            a = thisList[i]
            thisList[i] = thisList[j]
            thisList[j] = a
            i+=1
            j-=1
        elif i == j:
            i+=1
            j-=1
    if low < j:
        quickSort(thisList,low,j,propertyIndex)
    if i < high :
        quickSort(thisList,i,high,propertyIndex)


def sort_dates(datesList):
    '''date means are collected in a list and sorted
    returns a dictionary where key is dateID and value is sorted position'''
    sorted_dates = []
    for j in range(len(datesList)):
        sorted_dates.append([datesList[j], datesDict[datesList[j]][0]])
    quickSort(sorted_dates, 0, len(sorted_dates)-1, 1)
    sorted_dates_Dict = {}
    for j in range(len(sorted_dates)):
        sorted_dates_Dict[sorted_dates[j][0]] = j
    return sorted_dates_Dict


def set_calcurve(curve_filename, datesDict, alfa, y_min, y_max):
    '''read calibration curve and select part of interest, based on dataset'''
    whole_calcurve = read_intcal(curve_filename)
```

```
    lower_wider_margin = int((y_max - y_min)*0.02)
    upper_wider_margin = int((y_max - y_min)*0.02)
    intcal_upperbound = max(whole_calcurve.index[whole_calcurve[‘ 14C age’] ==
min(whole_calcurve[‘ 14C age’][whole_calcurve[‘ 14C age’] >= y_max])].tolist())-
upper_wider_margin
    intcal_lowerbound = min(whole_calcurve.index[whole_calcurve[‘ 14C age’] ==
max(whole_calcurve[‘ 14C age’][whole_calcurve[‘ 14C age’] <
y_min])].tolist())+lower_wider_margin
    intcal = whole_calcurve[intcal_upperbound:intcal_lowerbound]
    x = intcal[‘ADBC’]
    intcalcurve = intcal[‘ 14C age’]
    lowercurve = intcal[‘C14lower’]
    uppercurve = intcal[‘C14upper’]
    return intcal


def find_cal_extremes(intcal, y_min, y_max):
    ‘‘‘find left_index e right_index, i.e. intcal data frame row indices of extreme calibrated
dates for the dataset’’’
    for yC14 in (y_min,y_max+1):
        up_index_xleft = intcal.index[intcal[‘C14upper’] ==
min(intcal[‘C14upper’][intcal[‘C14upper’] >= yC14])].tolist()
        up_index_xright = intcal.index[intcal[‘C14upper’] ==
min(intcal[‘C14upper’][intcal[‘C14upper’] - yC14 <= -10])].tolist()
        low_index_xleft = intcal.index[intcal[‘C14lower’] ==
max(intcal[‘C14lower’][intcal[‘C14lower’] - yC14 <= 10])].tolist()
        low_index_xright = intcal.index[intcal[‘C14lower’] ==
max(intcal[‘C14lower’][intcal[‘C14lower’] < yC14])].tolist()
        if yC14 == y_min:
            right_index = up_index_xright[0]
            for index in (up_index_xright+low_index_xright):
                if intcal[‘ADBC’][index] > intcal[‘ADBC’][right_index]:
                    right_index = index
```

```
        else:
            left_index = up_index_xleft[0]
            for index in (up_index_xleft+low_index_xleft):
                if intcal['ADBC'][index] < intcal['ADBC'][left_index]:
                    left_index = index
    return left_index, right_index


def build_all_dates_df(intcal, left_index, right_index):
    '''calcurve is defined discretely and does not cover each year BP.
    For annual precision of calbration, all BP years (annual bins) are needed.
    The function interpolates for missing years and builds a version of calcurve in the interval
of interest
    where each row is a BP year.'''

    all_dates_Dict = {
        "CAL BP": [],
        "14C age": [],
        "ADBC": [],
        "Error": [],
        "C14upper": [],
        "C14lower": []}

    index_CE = left_index
    for xADBC in range(intcal['ADBC'][left_index], intcal['ADBC'][right_index] + 1):
        if xADBC in (intcal['ADBC'].tolist()):
            index_CE = intcal.index[intcal['ADBC'] == xADBC].tolist()[0]
            all_dates_Dict["CAL BP"].append(intcal["CAL BP"][index_CE])
            all_dates_Dict["14C age"].append(intcal[" 14C age"][index_CE])
            all_dates_Dict["Error"].append(intcal["Error"][index_CE])
            all_dates_Dict["ADBC"].append(xADBC)
            all_dates_Dict["C14upper"].append(intcal["C14upper"][index_CE])
            all_dates_Dict["C14lower"].append(intcal["C14lower"][index_CE])
```

```
        else:
            index_FL = index_CE + 1
            all_dates_Dict["CAL BP"].append(all_dates_Dict["CAL BP"][-1] - 1)
            y14C_CE = intcal[" 14C age"][index_CE]
            y14C_FL = intcal[" 14C age"][index_FL]
            xADBC_CE = intcal["ADBC"][index_CE]
            xADBC_FL = intcal["ADBC"][index_FL]
            y14C = y14C_CE - (xADBC_CE - xADBC) * (y14C_CE - y14C_FL) / (xADBC_CE
- xADBC_FL)
            all_dates_Dict["14C age"].append(y14C)
            all_dates_Dict["ADBC"].append(xADBC)
            error_CE = intcal["Error"][index_CE]
            error_FL = intcal["Error"][index_FL]
            error = error_CE - (xADBC_CE - xADBC) * (error_CE - error_FL) / (xADBC_CE -
xADBC_FL)
            all_dates_Dict["Error"].append(error)
            up_y14C_CE = intcal["C14upper"][index_CE]
            up_y14C_FL = intcal["C14upper"][index_FL]
            up_y14C = up_y14C_CE - (xADBC_CE - xADBC) * (up_y14C_CE - up_y14C_FL) /
(xADBC_CE - xADBC_FL)
            all_dates_Dict["C14upper"].append(up_y14C)
            low_y14C_CE = intcal["C14lower"][index_CE]
            low_y14C_FL = intcal["C14lower"][index_FL]
            low_y14C = low_y14C_CE - (xADBC_CE - xADBC) * (low_y14C_CE -
low_y14C_FL) / (xADBC_CE - xADBC_FL)
            all_dates_Dict["C14lower"].append(low_y14C)

    all_dates_df = pd.DataFrame(all_dates_Dict, index=all_dates_Dict["CAL BP"])
    return all_dates_df


def contingency_analysis():
    '''calculates all values related to contingency
```

```
    use just phase_analysis for contingency by phase'''

    threshold = stats.norm.cdf(alfa) - stats.norm.cdf(-1 * alfa)
    contingencyDict, transitionDict = None, None
    if len(phasesDict.keys()) > 1:
        contingencyDict, transitionDict, dict10_byphase_dict, dictNorm_byphase_dict =
phase_analysis(
            #output_folder,
            alfa, datesDict, phasesDict)

    meanDict = {}
    stDevDict = {}
    datesList = sorted(datesDict.keys())
    for dateID in datesList:
        meanDict[dateID] = datesDict[dateID][0]
        stDevDict[dateID] = datesDict[dateID][1]

    uppBound, lowBound = findUpperLower(alfa, meanDict, stDevDict)
    dict10 = buildDict10(alfa, meanDict, stDevDict,
                         lowBound, uppBound, threshold)
    count1perRC, normCount1perRC = build_count1perRC(dict10, meanDict)
    dictNorm = buildDictNorm(count1perRC, meanDict,
                         lowBound, uppBound, dict10, normCount1perRC)

    contingency = calculateContingency(alfa, meanDict, stDevDict)
    representativity = calculateDatasetRepresentativity(float(contingency[2]), alfa, meanDict,
stDevDict)
    relevance = calculateRelevance(float(contingency[2]), alfa, meanDict, stDevDict)

def calibrate_contingency_by_phase(phasesList, all_dates_df, dict10_byphase_dict,
dictNorm_byphase_dict):
    '''calibration of contingency by phase
    xBP is the annual bin on the x-axis
```

noIntcalError: calibrated contingency is contingency at y=calcurve(xBP)

IntcalError: calibrated contingency is the average contingency measured along the vertical thickness of calcurve at x=xBP’”

```
calibDict10_noIntcalError = {}
for phaseID in phasesList:
    calibDict10_noIntcalError[phaseID] = {}
    for xBP in (all_dates_df.index.tolist()):
        xADBC = all_dates_df["ADBC"][xBP]
        yC14 = all_dates_df["14C age"][xBP]
        try:
            cont10 = dict10_byphase_dict[phaseID][yC14][1]
        except:
            cont10 = 0
        calibDict10_noIntcalError[phaseID][xBP] = cont10
    all_dates_df["cont10_noIntcalError_"+str(phaseID)] =
pd.Series(calibDict10_noIntcalError[phaseID])

calibDictNorm_noIntcalError = {}
for phaseID in phasesList:
    calibDictNorm_noIntcalError[phaseID] = {}
    for xBP in (all_dates_df.index.tolist()):
        xADBC = all_dates_df["ADBC"][xBP]
        yC14 = all_dates_df["14C age"][xBP]
        try:
            contNorm = dictNorm_byphase_dict[phaseID][yC14][1]
        except:
            contNorm = 0
        calibDictNorm_noIntcalError[phaseID][xBP] = contNorm
    all_dates_df["contNorm_noIntcalError_"+str(phaseID)] =
pd.Series(calibDictNorm_noIntcalError[phaseID])
```

```
    calibDict10_IntcalError = {}
    for phaseID in phasesList:
        calibDict10_IntcalError[phaseID] = {}
        for xBP in (all_dates_df.index.tolist()):
            xADBC = all_dates_df["ADBC"][xBP]
            contList = []
            for yC14 in range(int(round(all_dates_df["C14lower"][xBP])),
int(round(all_dates_df["C14upper"][xBP]))+1):
                try:
                    cont10 = dict10_byphase_dict[phaseID][yC14][1]
                    contList.append(cont10)
                except:
                    contList.append(0)
            calibDict10_IntcalError[phaseID][xBP] = sum(contList)
        all_dates_df["cont10_IntcalError_"+str(phaseID)] =
pd.Series(calibDict10_IntcalError[phaseID])

    calibDictNorm_IntcalError = {}
    for phaseID in phasesList:
        calibDictNorm_IntcalError[phaseID] = {}
        for xBP in (all_dates_df.index.tolist()):
            xADBC = all_dates_df["ADBC"][xBP]
            contList = []
            for yC14 in range(int(round(all_dates_df["C14lower"][xBP])),
int(round(all_dates_df["C14upper"][xBP]))+1):
                try:
                    contNorm = dictNorm_byphase_dict[phaseID][yC14][1]
                    contList.append(contNorm)
                except:
                    contList.append(0)
            calibDictNorm_IntcalError[phaseID][xBP] = sum(contList)
        all_dates_df["contNorm_IntcalError_"+str(phaseID)] =
pd.Series(calibDictNorm_IntcalError[phaseID])
```

```
def set_pdf(datesCollection, pdf_type='uniform'):
    '''calculate probability distribution function (pdf, or line height) for each date
    only uniform distribution considered here'''
    prob = {}
    pdf = 0.0
    for dateID in datesCollection:
        prob[dateID] = {}
        mean, sigma = datesDict[dateID][0], datesDict[dateID][1]
        if pdf_type == 'uniform':
            y_min, y_max = mean-alfa*sigma, mean+alfa*sigma
            pdf = 1.0/(y_max - y_min)
            for i in range(y_min, y_max+1):
                prob[dateID][i] = pdf
        if pdf_type == 'normal':
            for i in range(mean-3*sigma, mean+3*sigma+1):
                pdf = stats.norm(i, mean, sigma)
                prob[dateID][i] = pdf
    return prob


def calibrate_pdf_single_date(phasesDict, all_dates_df, prob):
    '''calculate calibrated distribution function for each date (improperly known as "calibrated
mini-gaussian")'''
    calibDict_bydate = {}
    phasesList = sorted(phasesDict.keys())
    for phaseID in phasesList:
        calibDict_bydate[phaseID] = {}
        for dateID in phasesDict[phaseID]:
            calibDict_bydate[phaseID][dateID] = {}
            for xBP in (all_dates_df.index.tolist()):
                xADBC = all_dates_df["ADBC"][xBP]
```

```
            probList = []
            for yC14 in range(int(round(all_dates_df["C14lower"][xBP])),
                             int(round(all_dates_df["C14upper"][xBP])) + 1):
                try:
                    probList.append(prob[dateID][yC14])
                except:
                    continue
            if sum(probList) > 0:
                calibDict_bydate[phaseID][dateID][xADBC] = 0.5 * sum(probList) /
all_dates_df["Error"][xBP]

    xADBCs_calib_pdf = sorted(calibDict_bydate[phaseID][dateID].keys())
    xADBC_left = xADBCs_calib_pdf[0]
    xADBC_right = xADBCs_calib_pdf[-1]
    for xADBC in range(xADBC_left, xADBC_right + 1):
        if xADBC not in xADBCs_calib_pdf:
            calibDict_bydate[phaseID][dateID][xADBC] = 0

    return calibDict_bydate



def calibrate_pdf_combined_dates(phasesDict, all_dates_df, prob):
    '''calculate combined calibrated probability distribution function (prob column).
    At each x=xBP, it calculates the mean of all line heights (uncal pdf) taken along the vertical
thickness of calcurve'''
    calibDict = {}

    for xBP in (all_dates_df.index.tolist()):
        xADBC = all_dates_df["ADBC"][xBP]
        probList = []
        for dateID in datesDict:
            prob_one_date = []
            for yC14 in range(int(round(all_dates_df["C14lower"][xBP])),
```

```
int(round(all_dates_df["C14upper"][xBP]))+1):
            try:
                prob_one_date.append(prob[dateID][yC14])
            except:
                continue
        probList.append(0.5*sum(prob_one_date)/all_dates_df["Error"][xBP])
    calibDict[xBP] = sum(probList)
all_dates_df["prob"] = pd.Series(calibDict)



def plot_calibrated_dates():
    '''The function plots a graph of calibrated dates (aka minigaussians).
    Dates are not combined'''

    phasesList = sorted(phasesDict.keys())
    datesList = sorted(datesDict.keys())
    scaleminiga = 400
    scalefactory = 200 * alfa
    x = intcal['ADBC']
    intcalcurve = intcal[' 14C age']
    lowercurve = intcal['C14lower']
    uppercurve = intcal['C14upper']

    fig = plt.figure(figsize=(10, 10))
    gs = matplotlib.gridspec.GridSpec(1, 1, left=0.08, right=0.98, top=0.93, bottom=0.05)
    ax = fig.add_subplot(gs[:, :])
    ax.set_title("Date calibration of " + dataset_name + " dataset", size=14, ha='center')
    ax.set_xlabel("Calibrated (calBC)", size=12)
    ax.set_ylabel("C14 (BP)", size=12)
    ax.axis([min(x) - 60 - (100 * alfa), max(x) - 10, min(lowercurve) + 34 * alfa,
max(uppercurve) - 32 * alfa])
    ax.set_xticks(np.arange(-2050, -1350, step=50))
    ax.set_xticklabels([str(-i) for i in ax.get_xticks()])
```

```
    if alfa == 2:
        ax.set_xticks([-2200, -2100, -2000, -1900, -1800, -1700, -1600, -1500, -1400, -1300, -
1200])
        xticklabels = [str(-i) for i in ax.get_xticks()]
        ax.set_xticklabels(xticklabels)
    ax.text(ax.axis()[0] + 3, ax.axis()[3] + 1,
            "IntCal13 atmospheric curve (Reimer et al. 2013), 1699-1500 BC curve data by
Pearson et al. 2018",
            fontsize=7)
    ttl = ax.title
    ttl.set_position([.5, 1.01])

    # draw calibration curve
    ax.plot(x, intcalcurve, color='black', linewidth=0.3, alpha=0.2, gid="intcal")
    ax.plot(x, lowercurve, color='black', linewidth=0.3, gid="intcal")
    ax.plot(x, uppercurve, color='black', linewidth=0.3, gid="intcal")
    ax.fill_between(x, lowercurve, uppercurve, facecolor='lightgray', gid="intcal")

    color = iter(plt.cm.Set1(np.linspace(0.1, 0.9, len(phasesList))))
    colors = list(color)

    colors = get_phases_color_dict(phasesList)

    phases_avg_uncal = {}
    phases_top_uncal = {}
    for i in range(len(phasesList)):
        phaseID = phasesList[i]
        meanList = []
        for dateID in phasesDict[phaseID]:
            meanList.append(datesDict[dateID][0])
        phases_avg_uncal[phaseID] = np.mean(meanList)
        phases_top_uncal[phaseID] = np.max(meanList)
```

```
    k = 0
    sorted_dates_Dict = sort_dates(datesList)
    for i in range(len(phasesList)):
        phaseID = phasesList[i]
        color = mcolors.hsv_to_rgb(colors[phaseID])

        caliblim = [all_dates_df[all_dates_df["cont10_noIntcalError_" + str(phaseID)] >
0].ADBC.tolist()[0],
                    all_dates_df[all_dates_df["cont10_noIntcalError_" + str(phaseID)] >
0].ADBC.tolist()[-1]]

        ax.text(caliblim[0] + (caliblim[1] - caliblim[0]) / 2,
                phases_top_uncal[phaseID] + 10 + (50 * alfa) + np.random.random() * 10,
                "{}\n".format(phaseID), ha='center', fontsize='12', color=color, fontweight='bold',
gid=phaseID)

        # draw uncal date pdfs by phase on y-axis
        for j in range(len(phasesDict[phaseID])):
            dateID = phasesDict[phaseID][j]
            yC14s = sorted(prob[dateID].keys())
            values = [prob[dateID][yC14] for yC14 in yC14s]

            ax.hlines(yC14s, ax.axis()[0] + 1 + (1 + 3 * alfa) * k, ax.axis()[0] + 1 + (1 + 3 * alfa) *
k + (2 / alfa),
                      lw=2,
                      color=color, alpha=0.4, gid=phaseID)
            ax.text(ax.axis()[0] + 1 + (1 + 3 * alfa) * k + 2, 3 + max(yC14s),
                    "{}".format(dateID), ha='center', fontsize=7, color='k', fontweight='bold',
gid=phaseID)

            k += 1

        # draw calibrated mini-gaussian of single date onto the curve
```

```
        for j in range(len(phasesDict[phaseID])):
            dateID = phasesDict[phaseID][j]
            xADBCs = sorted(calibDict_bydate[phaseID][dateID].keys())
            ax.plot(xADBCs, datesDict[dateID][0] + scaleminiga *
pd.Series(calibDict_bydate[phaseID][dateID]),
                    color='gray', linewidth=0.2, gid=phaseID)
            ax.plot(xADBCs, datesDict[dateID][0] + 0 *
pd.Series(calibDict_bydate[phaseID][dateID]),
                    color='gray', linewidth=0.2, gid=phaseID)
            ax.fill_between(xADBCs, datesDict[dateID][0],
                            datesDict[dateID][0] + scaleminiga *
pd.Series(calibDict_bydate[phaseID][dateID]),
                            color=color, alpha=0.6, gid=phaseID)

            if sorted_dates_Dict[dateID] % 2 == 0:
                dateID_x = max(xADBCs) + np.random.random() * 20
            else:
                dateID_x = min(xADBCs) - 12 - np.random.random() * 20
            ax.text(dateID_x, datesDict[dateID][0],
                    "{}".format(dateID), fontsize=7, fontweight='bold', gid=phaseID)

    output_filename = "./calibration_" + shortDatasetName + "_cal_" + curve_shortname + "_"
+ str(
        alfa) + "sigma_" + str(versN) + ".svg"
    plt.savefig(output_filename, dpi=300)



def plot_calibrated_dates(output_folder):
    '''The function plots a graph of calibrated dates (aka minigaussians).
    Dates are not combined'''

    phasesList = sorted(phasesDict.keys())
```

```
datesList = sorted(datesDict.keys())
scaleminiga = 400
scalefactory = 400
x = intcal['ADBC']
intcalcurve = intcal[' 14C age']
lowercurve = intcal['C14lower']
uppercurve = intcal['C14upper']

fig = plt.figure(figsize = (10,10))
gs = matplotlib.gridspec.GridSpec(1, 1, left=0.08, right=0.98, top=0.93, bottom=0.05)
ax = fig.add_subplot(gs[:, :])

ax.set_title("Date calibration of " + dataset_name + " ", size=14, ha='center')
ax.set_xlabel("Calibrated (calBC)", size=12)
ax.set_ylabel("C14 (BP)", size=12)
ax.axis([min(x), max(x), min(lowercurve), max(uppercurve)])
ax.text(ax.axis()[0]+3, ax.axis()[3]+1, "IntCal13 atmospheric curve (Reimer et al. 2013)",
        fontsize=7)

#draw calibration curve
ax.plot(x, intcalcurve, color='black', linewidth=0.3, alpha=0.2, gid="intcal")
ax.plot(x, lowercurve, color='black', linewidth=0.3, gid="intcal")
ax.plot(x, uppercurve, color='black', linewidth=0.3, gid="intcal")
ax.fill_between(x, lowercurve, uppercurve, facecolor='lightgray', gid="intcal")

color=iter(plt.cm.Set2(np.linspace(0.1,0.9,len(phasesList))))
colors = list(color)

phases_avg_uncal = {}
for i in range(len(phasesList)):
    phaseID = phasesList[i]
    meanList =[]
    for dateID in phasesDict[phaseID]:
```

```
            meanList.append(datesDict[dateID][0])
        phases_avg_uncal[phaseID] = np.mean(meanList)


    sorted_dates_Dict = sort_dates(datesList)
    for i in range(len(phasesList)):
        color = colors[i]
        phaseID = phasesList[i]


caliblim=[all_dates_df[all_dates_df["cont10_noIntcalError_"+str(phaseID)]>0].ADBC.tolist()
[0],

all_dates_df[all_dates_df["cont10_noIntcalError_"+str(phaseID)]>0].ADBC.tolist()[-1]]

        ax.text(caliblim[0]+(caliblim[1]-caliblim[0])/2, phases_avg_uncal[phaseID]+100,
            "{}\n".format(phaseID), ha='center', fontsize='12', color=color, fontweight='bold',
gid=phaseID)

        #draw uncal date pdfs by phase on y-axis
        for j in range(len(phasesDict[phaseID])):
            dateID = phasesDict[phaseID][j]
            #draw C14 contingency by phase on y-axis
            yC14s = sorted(prob[dateID].keys())
            values = [prob[dateID][yC14] for yC14 in yC14s]
            ax.hlines(yC14s, ax.axis()[0]+15*j,
ax.axis()[0]+15*j+scalefactory*(pd.Series(values)), lw=2,
                    color=color, alpha=0.4, gid=phaseID)
            ax.text(ax.axis()[0]+15*j+4, 5+max(yC14s),
              "{}".format(dateID), ha='center', fontsize=9, color='k', fontweight='bold',
gid=phaseID)
```

```
        #draw calibrated mini-gaussian of single date onto the curve
        for j in range(len(phasesDict[phaseID])):
            dateID = phasesDict[phaseID][j]
            ax.plot(calibDict_bydate[phaseID][dateID].keys(),

datesDict[dateID][0]+scaleminiga*pd.Series(calibDict_bydate[phaseID][dateID]),
                    color='gray',linewidth=0.2, gid=phaseID)
            ax.plot(calibDict_bydate[phaseID][dateID].keys(),
                    datesDict[dateID][0]+0*pd.Series(calibDict_bydate[phaseID][dateID]),
                    color='gray',linewidth=0.2, gid=phaseID)
            ax.fill_between(calibDict_bydate[phaseID][dateID].keys(), datesDict[dateID][0],

datesDict[dateID][0]+scaleminiga*pd.Series(calibDict_bydate[phaseID][dateID]),
                    color=color,alpha=0.6, gid=phaseID)

            if sorted_dates_Dict[dateID] % 2 == 0:
                dateID_x = max(calibDict_bydate[phaseID][dateID].keys()) +
np.random.random()*20
            else:
                dateID_x = min(calibDict_bydate[phaseID][dateID].keys()) - 12 -
np.random.random()*20
            ax.text(dateID_x, datesDict[dateID][0],
                    "{}".format(dateID), fontsize=7, fontweight='bold', gid=phaseID)

    output_filename = output_folder + os.path.sep +
"calibration_"+shortDatasetName+"_"+str(alfa)+"sigma_"+str(versN)
    plt.savefig(output_filename + ".svg", dpi=300)
    plt.savefig(output_filename + ".png", dpi=300)


def plot_contingency_allTypes(byphase_contingency_dicts):
    '''The function sets up and launches plot_single_contingency
    Four graphs are produced, 1|0 and Norm versions of contingency, each with and without
```

```
calcurve error
    Contingency is calculated ONLY within a phase'''
    datesList = sorted(datesDict.keys())
    sorted_dates_Dict = sort_dates(datesList)

    versN = 2
    scalefactorsx = [[5, 0.10], [500, 10]]
    scalefactorsy = [[7, 8], [500 * alfa, 500 * alfa]]
    graphTypes = ["(1|0)", "(Norm)"]
    cal_columns = [["cont10_noIntcalError_", "cont10_IntcalError_", ],
                   ["contNorm_noIntcalError_", "contNorm_IntcalError_"]]
    versN = 1
    for i in range(2):
        plot_single_contingency(sorted_dates_Dict, scalefactorsx[i][0], scalefactorsy[i][0],
                                byphase_contingency_dicts[i], graphTypes[i], cal_columns[i][0])
        plot_single_contingency(sorted_dates_Dict, scalefactorsx[i][1], scalefactorsy[i][1],
                                byphase_contingency_dicts[i], graphTypes[i], cal_columns[i][1])


def plot_single_contingency(sorted_dates_Dict, scalefactorx, scalefactory,
                            byphase_contingency_dict, graphType, cal_column, versN=1):
    '''The function plots a graph of calibrated contingency.
    Contingency is calculated ONLY within a phase'''

    phasesList = sorted(phasesDict.keys())
    datesList = sorted(datesDict.keys())
    scaleminiga = 400
    x = intcal['ADBC']
    intcalcurve = intcal[' 14C age']
    lowercurve = intcal['C14lower']
    uppercurve = intcal['C14upper']

    fig = plt.figure(figsize=(10, 10))
```

```
    gs = matplotlib.gridspec.GridSpec(1, 1, left=0.08, right=0.98, top=0.93, bottom=0.05)
    ax = fig.add_subplot(gs[:, :])
    ax.set_title("Contingency by phase for " + dataset_name + " dataset ", size=14,
ha='center')
    ax.set_xlabel("Calibrated (calBC)", size=12)
    ax.set_ylabel("C14 (BP)", size=12)
    ax.axis([min(x) - 60 - (100 * alfa), max(x) - 10, min(lowercurve) + 34 * alfa,
max(uppercurve) - 32 * alfa])
    ax.set_xticks(np.arange(-2050, -1350, step=50))
    ax.set_xticklabels([str(-i) for i in ax.get_xticks()])
    if alfa == 2:
        ax.set_xticks([-2200, -2100, -2000, -1900, -1800, -1700, -1600, -1500, -1400, -1300, -
1200])
        xticklabels = [str(-i) for i in ax.get_xticks()]
        ax.set_xticklabels(xticklabels)
    ax.text(ax.axis()[0] + 3, ax.axis()[3] + 1,
            "IntCal13 atmospheric curve (Reimer et al. 2013), 1699-1500 BC curve data by
Pearson et al. 2018",
            fontsize=7)
    ttl = ax.title
    ttl.set_position([.5, 1.01])

    # draw calibration curve
    ax.plot(x, intcalcurve, color='black', linewidth=0.3, alpha=0.2, gid="intcal")
    ax.plot(x, lowercurve, color='black', linewidth=0.3, gid="intcal")
    ax.plot(x, uppercurve, color='black', linewidth=0.3, gid="intcal")
    ax.fill_between(x, lowercurve, uppercurve, facecolor='lightgray', gid="intcal")

    color = iter(plt.cm.Set2(np.linspace(0.1, 0.9, len(phasesList))))
    colors = list(color)

    colors = get_phases_color_dict(phasesList)
```

```
    phases_avg_uncal = {}
    phases_top_uncal = {}
    for i in range(len(phasesList)):
        phaseID = phasesList[i]
        meanList = []
        for dateID in phasesDict[phaseID]:
            meanList.append(datesDict[dateID][0])
        phases_avg_uncal[phaseID] = np.mean(meanList)
        phases_top_uncal[phaseID] = np.max(meanList)

    for i in range(len(phasesList) - 1, -1, -1):
        phaseID = phasesList[i]

        color = mcolors.hsv_to_rgb(colors[phaseID])

        caliblim = [all_dates_df[all_dates_df[cal_column + str(phaseID)] > 0].ADBC.tolist()[0],
                    all_dates_df[all_dates_df[cal_column + str(phaseID)] > 0].ADBC.tolist()[-1]]

        ax.text(caliblim[0] + (caliblim[1] - caliblim[0]) / 2,
                phases_top_uncal[phaseID] + 10 + (50 * alfa) + np.random.random() * 10,
                "{}\n".format(phaseID), ha='center', fontsize='12', color=color, fontweight='bold',
gid=phaseID)

        # draw C14 contingency by phase on y-axis
        yC14s = sorted(byphase_contingency_dict[phaseID].keys())
        values = [byphase_contingency_dict[phaseID][yC14][1] for yC14 in yC14s]
        ax.hlines(yC14s, ax.axis()[0], ax.axis()[0] + scalefactory * (pd.Series(values)), lw=2,
                  color=color, alpha=0.4, gid=phaseID)

        # draw calibrated mini-gaussian of single date onto the curve
        for j in range(len(phasesDict[phaseID])):
            dateID = phasesDict[phaseID][j]
            xADBCs = sorted(calibDict_bydate[phaseID][dateID].keys())
```

```
        ax.plot(xADBCs, datesDict[dateID][0] + scaleminiga *
pd.Series(calibDict_bydate[phaseID][dateID]),
                color='gray', linewidth=0.2, gid=phaseID)
        ax.plot(xADBCs, datesDict[dateID][0] + 0 *
pd.Series(calibDict_bydate[phaseID][dateID]),
                color='gray', linewidth=0.2, gid=phaseID)
        ax.fill_between(xADBCs, datesDict[dateID][0],
                    datesDict[dateID][0] + scaleminiga *
pd.Series(calibDict_bydate[phaseID][dateID]),
                    color=color, alpha=0.6, gid=phaseID)

        if sorted_dates_Dict[dateID] % 2 == 0:
            dateID_x = max(xADBCs) + np.random.random() * 20
        else:
            dateID_x = min(xADBCs) - 12 - np.random.random() * 20
        ax.text(dateID_x, datesDict[dateID][0],
                "{}".format(dateID), fontsize=7, fontweight='bold', gid=phaseID)

    # draw calibrated contingency by phase
    ax.plot(all_dates_df[all_dates_df[cal_column + str(phaseID)] > 0]['ADBC'],
            ax.axis()[2] + scalefactorx * all_dates_df[all_dates_df[cal_column +
str(phaseID)] > 0][
                cal_column + str(phaseID)],
            color=color, linewidth=0.7, gid=phaseID)
    ax.fill_between(all_dates_df[all_dates_df[cal_column + str(phaseID)] > 0]['ADBC'], 0,
                    ax.axis()[2] + scalefactorx * all_dates_df[all_dates_df[cal_column +
str(phaseID)] > 0][
                        cal_column + str(phaseID)],
                    facecolor=color, alpha=0.4, gid=phaseID)

  output_filename = "./contingency_" + shortDatasetName + "_" + curve_shortname + str(
    alfa) + "sigma_" + cal_column + str(versN) + ".svg"
  plt.savefig(output_filename, dpi=300)
```

```
def run(**kwargs):
    global dataset_name, shortDatasetName, curve_shortname, dataset_filename

    dataset_name = "Akrotiri"

    dataset_filename = kwargs.get('dataset_file_path')

    shortDatasetName = "dataset"

    curve_filename = kwargs.get('curve_file_path')

    curve_shortname = 'pooledpinusquercus'

    global alfa, versN
    versN = 1
    alfa = 2

    global datesDict, phasesDict, intcal
    datesDict, phasesDict = read_dates(dataset_filename)
    phasesList = sorted(phasesDict.keys())

    colors = get_phases_color_dict(phasesList)

    means, sigmas = [datesDict[i][0] for i in datesDict.keys()], [datesDict[i][1] for i in
datesDict.keys()]
    y_min = min([means[i] - alfa * sigmas[i] for i in range(len(means))])
    y_max = max([means[i] + alfa * sigmas[i] for i in range(len(means))])
    intcal = set_calcurve(curve_filename, datesDict, alfa, y_min, y_max)

    left_index, right_index = find_cal_extremes(intcal, y_min, y_max)
```

```
    global all_dates_df, prob, calibDict_bydate
    all_dates_df = build_all_dates_df(intcal, left_index, right_index)
    contingencyDict, transitionDict, dict10_byphase_dict, dictNorm_byphase_dict =
phase_analysis(
        alfa, datesDict, phasesDict)
    calibrate_contingency_by_phase(phasesList, all_dates_df, dict10_byphase_dict,
dictNorm_byphase_dict)
    prob = set_pdf(datesDict)
    calibDict_bydate = calibrate_pdf_single_date(phasesDict, all_dates_df, prob)
    byphase_contingency_dicts = [dict10_byphase_dict, dictNorm_byphase_dict]
    plot_contingency_allTypes(byphase_contingency_dicts)
```

2) Contingency Test

```
TITLE = 'contingency_test'

def findUpperLower(alfa, meanDict, stDevDict):
    '''returns the extreme years of the overall interval covered by the dataset'''
    datesList = sorted(meanDict.keys())
    uppBound, lowBound = meanDict[datesList[0]], meanDict[datesList[0]]
    for date in datesList:
        up = meanDict[date] + alfa * stDevDict[date]
        low = meanDict[date] - alfa * stDevDict[date]
        if up > uppBound:
            uppBound = up
        if low < lowBound:
            lowBound = low
    return uppBound, lowBound



def calculateContingency(alfa, meanDict, stDevDict):
    '''returns the contingency interval, i.e. the largest interval of years common to all
```

```
    measurements of the dataset. If there is no common interval, there is no contingency
    and the result means a distance between the closest non-overlapping measurements
    Result is given as a tuple: (upper bound, lower bound, interval length)'''

    dateList = sorted(meanDict.keys())
    up = []
    low = []
    for date in dateList:
        up.append(meanDict[date] + alfa * stDevDict[date])
        low.append(meanDict[date] - alfa * stDevDict[date])
    return min(up), max(low), min(up) - max(low)


def calculateRelevance(contingency, alfa, meanDict, stDevDict):
    '''relevance of a measurement is the ratio between a measurement interval
    and the contingency interval and is given as a percentage. In other words
    it quantifies how well a measurement interval covers the contingency interval.
    Obviously, it is only significant when a contingency interval exists.'''

    dateList = sorted(meanDict.keys())
    if contingency < 0:
        return ("No contingency interval exists for this dataset\n")
    relev = {}
    up = []
    low = []
    for date in dateList:
        mean = meanDict[date]
        relev[date] = (mean, (100 * contingency / ((mean + alfa *
                                        stDevDict[date]) - (mean - alfa * stDevDict[date]))))
    return relev


def calculateDatasetRepresentativity(contingency, alfa, meanDict, stDevDict):
```

```
    '''Dataset representativity is the ratio, expressed as a percentage, between the
    lengths of the contingency interval and the total interval covered by the dataset.
    Obviously, it is only significant when a contingency interval exists.'''

    dateList = sorted(meanDict.keys())
    if contingency < 0:
        return ("No contingency interval exists for this dataset\n")
    up = []
    low = []
    for date in dateList:
        up.append(meanDict[date] + alfa * stDevDict[date])
        low.append(meanDict[date] - alfa * stDevDict[date])
    return (100 * (contingency / (max(up) - min(low))))


def buildDict10(alfa, meanDict, stDevDict, lowBound, uppBound, threshold):
    '''builds a dictionary with as many keys as years covered by the dataset.
    A value contains:
    0) a list of either 1 or 0, where 1 in poition j means that the year is covered
        by the j-th measurement of the dataset, 0 if it is not
    1) the sum of the numbers in the list in 0)
    2) ratio between sum in 1) and number of measurements (i.e. number of actual 1s and
        number of total possible 1s)
    3) signed difference between the ratio in 2) and a threshold'''

    dateList = sorted(meanDict.keys())
    dict10 = {}
    for i in range(lowBound, uppBound + 1):
        dict10[i] = [[], 0.0, 0.0, 0.0]
        for date in dateList:
            if (i >= meanDict[date] - alfa * stDevDict[date] and
                    i <= meanDict[date] + alfa * stDevDict[date]):
                dict10[i][0].append(1)
```

```
            else:
                dict10[i][0].append(0)
        dict10[i][1] = sum(dict10[i][0])
        dict10[i][2] = float(dict10[i][1]) / float(len(dateList))
        dict10[i][3] = dict10[i][2] - threshold
    return dict10


def build_count1perRC(dict10, meanDict):
    '''uses the result of buildDict10 to build 2 lists, which will be used in buildDictNorm,
    to take into account variances of single measurements.
    It counts the number of 1s for a measurement, i.e. the width of its interval, in the first
    list and the ratio 1-to-count in the second list.
    These lists have as many elements as measurements'''

    dateList = sorted(meanDict.keys())
    count1perRC = []
    for j in range(len(dateList)):
        count = 0
        for i in dict10:
            count += dict10[i][0][j]
        count1perRC.append(float(count))
    normCount1perRC = []
    for count in count1perRC:
        normCount1perRC.append(1.0 / count)
    return count1perRC, normCount1perRC


def buildDictNorm(count1perRC, meanDict, lowBound, uppBound, dict10,
normCount1perRC):
    '''builds a dictionary with as many keys as years covered by the dataset.
    A value contains:
    0) a list of positive floats <=1. Number in position j represents the weight
```

```
    of measurement j on that year
    1) the sum of the numbers in the above list
    2) distance of the sum in 1) and the maximum possible sum, which would occur
    when a year is covered by all measurements
    3) ratio between the sum in 1) and the maximum possible sum, given as %'''

    dateList = sorted(meanDict.keys())
    dictNorm = {}
    for i in range(lowBound, uppBound + 1):
        dictNorm[i] = [[], 0.0, 0.0, 0.0]
        for j in range(len(dateList)):
            val = float(dict10[i][0][j]) / count1perRC[j]
            dictNorm[i][0].append(val)
        dictNorm[i][1] = sum(dictNorm[i][0])
        dictNorm[i][2] = sum(normCount1perRC) - dictNorm[i][1]
        try:
            dictNorm[i][3] = 100 * dictNorm[i][1] / sum(normCount1perRC)
        except ZeroDivisionError:
            dictNorm[i][3] = 0.0
    return dictNorm



def produceOutput10(output_folder, meanDict, lowBound, uppBound, dict10):
    '''saves a .txt file with the relevant values in dict10.
    Tab separators used'''

    outfile_path = os.path.join(output_folder, 'res10.txt')
    outfile = open(outfile_path, 'w')
    outfile.write("Date" + ',')
    dateList = sorted(meanDict.keys())
    for date in dateList:
        mean = meanDict[date]
        outfile.write(str(mean) + ',')
```

```
    outfile.write("SumOfHits" + ‘,’ + "PropOfHits" + ‘,’ + "ThreshDist" + ‘\n’)
    for i in range(lowBound, uppBound + 1):
        outfile.write(str(i) + ‘,’)
        for j in range(len(dict10[i][0])):
            outfile.write(str(dict10[i][0][j]) + ‘,’)
        outfile.write(str(dict10[i][1]) + ‘,’ +
                      str(dict10[i][2]) + ‘,’ + str(dict10[i][3]) + ‘\n’)
    outfile.close()


def produceOutputNorm(output_folder, meanDict, lowBound, uppBound, dictNorm):
    ‘‘‘saves a .txt file with the relevant values in dictNorm.
    Tab separators used’’’

    outfile_path = os.path.join(output_folder, ‘resNorm.txt’)
    outfile = open(outfile_path, ‘w’)
    outfile.write("Date" + ‘,’)
    dateList = sorted(meanDict.keys())
    for date in dateList:
        mean = meanDict[date]
        outfile.write(str(mean) + ‘,’)
    outfile.write("SumOfHits" + ‘,’ + "DistFromMaxHit" +
                  ‘,’ + "%ofMaxHit" + ‘\n’)
    for i in range(lowBound, uppBound + 1):
        outfile.write(str(i) + ‘,’)
        for j in range(len(dictNorm[i][0])):
            outfile.write(str(dictNorm[i][0][j]) + ‘,’)
        outfile.write(str(
            dictNorm[i][1]) + ‘,’ + str(dictNorm[i][2]) + ‘,’ + str(dictNorm[i][3]) + ‘\n’)
    outfile.close()


def plotDict10(output_folder, dict10, outputName=‘10_plots’,
```

```
        contingencyData=None, transitionData=None):
    '''plots the last 3 columns of the corresponding .txt file vs years in 3 different graphs.'''

    dates = sorted(dict10.keys())
    labels = ['Dict10SumOfHits', 'PropOfHits', 'ThreshDist']
    fig, ax = plt.subplots(3, 1, figsize=(8, 6), sharex='col', sharey='row')
    for i in range(len(ax.flat)):
        axi = ax.flat[i]
        color = np.random.random(3)
        values = [dict10[date][i + 1] for date in dates]
        axi.vlines(dates, [0], values, lw=1,
                   color='dimgray', alpha=0.4, label=labels[i])
        axi.set_title(labels[i] + ' Plot', size=14)
        if contingencyData:
            phaseList = sorted(contingencyData.keys())
            for phaseID in phaseList:
                x_min, x_max = contingencyData[phaseID][0], contingencyData[phaseID][1]
                axi.axvspan(xmin=x_min, xmax=x_max,
                            color='blue', alpha=0.5, lw=0)
        if transitionData:
            for i in transitionData:
                x_min, x_max = transitionData[i][0], transitionData[i][1]
                axi.axvspan(xmin=x_min, xmax=x_max,
                            color='red', alpha=0.5, lw=0)

    output_file = os.path.join(output_folder, outputName + '.png')
    plt.savefig(output_file, dpi=fig.dpi)


def plotDictNorm(output_folder, dictNorm, outputName='norm_plots',
                 contingencyData=None, transitionData=None):
    '''plots the last 3 columns of the corresponding .txt file vs years in 3 different graphs.'''
```

```
    dates = sorted(dictNorm.keys())
    labels = ['SumOfHits', 'DistFromMaxHit', '%ofMaxHit']
    fig, ax = plt.subplots(3, 1, figsize=(8, 6), sharex='col', sharey='row')
    for i in range(len(ax.flat)):
        axi = ax.flat[i]
        color = np.random.random(3)
        values = [dictNorm[date][i + 1] for date in dates]
        axi.vlines(dates, [0], values, lw=1,
                   color='dimgray', alpha=0.4, label=labels[i])
        axi.set_title(labels[i] + ' Plot', size=14)
        if contingencyData:
            phaseList = sorted(contingencyData.keys())
            for phaseID in phaseList:
                x_min, x_max = contingencyData[phaseID][0], contingencyData[phaseID][1]
                axi.axvspan(xmin=x_min, xmax=x_max,
                            color='blue', alpha=0.5, lw=0)
        if transitionData:
            for i in transitionData:
                x_min, x_max = transitionData[i][0], transitionData[i][1]
                axi.axvspan(xmin=x_min, xmax=x_max,
                            color='red', alpha=0.5, lw=0)

    output_file = os.path.join(output_folder, outputName + '.png')
    plt.savefig(output_file, dpi=fig.dpi)


def plot_coveredIntervals(output_folder, y_dates, datesDict, dict10,
outputName='covered_intervals',
                          contingencyData=None, transitionData=None):
    x_years = sorted(dict10.keys())
    minx, maxx = x_years[0], x_years[-1]
    miny, maxy = y_dates[0] - 1, y_dates[-1] + 1
    label = 'RC determinations as intervals'
```

```
matrix10 = []
for i in range(len(y_dates)):
    row = []
    for x_year in x_years:
        row.append(dict10[x_year][0][i])
    matrix10.append(row)

axis_bounds = [minx, maxx, miny, maxy]
fig = plt.figure()
gs = matplotlib.gridspec.GridSpec(1, 1)
ax = fig.add_subplot(gs[:, :])
ax.axis(axis_bounds)
ax.set_title(label, size=14)
for i in range(len(y_dates)):
    y = float(y_dates[i])
    row = matrix10[i]
    j = 0
    while row[j] == 0:
        j += 1
    x_min = float(x_years[j])
    while row[j] == 1 and j < len(row) - 1:
        j += 1
    x_max = float(x_years[j])

    ax.broken_barh([(x_min, x_max - x_min)], (y - 0.25, 0.5),
                facecolor='dimgray', alpha=1, lw=0)

if contingencyData:
    phaseList = sorted(contingencyData.keys())
    for phaseID in phaseList:
        x_min, x_max = contingencyData[phaseID][0], contingencyData[phaseID][1]
        ax.axvspan(xmin=x_min, xmax=x_max,
                color='lightgreen', alpha=0.4, lw=0)
```

```
    if transitionData:
        for i in transitionData:
            x_min, x_max = transitionData[i][0], transitionData[i][1]
            ax.axvspan(xmin=x_min, xmax=x_max,
                       color='lightcoral', alpha=0.4, lw=0)


    output_file = os.path.join(output_folder, outputName + '.png')
    plt.savefig(output_file, dpi=fig.dpi)


def phase_analysis(output_folder, alfa, datesDict, phasesDict):
    threshold = stats.norm.cdf(alfa) - stats.norm.cdf(-1 * alfa)

    contingencyDict = {}
    transitionDict = {}

    bounds = {}
    phasesList = sorted(phasesDict.keys())
    for phaseID in phasesList:
        print("phase {}".format(phaseID))
        meanDict = {}
        stDevDict = {}
        for dateID in phasesDict[phaseID]:
            meanDict[dateID] = datesDict[dateID][0]
            stDevDict[dateID] = datesDict[dateID][1]

        uppBound, lowBound = findUpperLower(alfa, meanDict, stDevDict)
        bounds[phaseID] = (uppBound, lowBound)
        print("uppBound = {}".format(uppBound) +
              ", lowBound = {}".format(lowBound))

        dict10 = buildDict10(alfa, meanDict, stDevDict,
```

```
                    lowBound, uppBound, threshold)
        count1perRC, normCount1perRC = build_count1perRC(dict10, meanDict)
        dictNorm = buildDictNorm(
            count1perRC, meanDict, lowBound, uppBound, dict10, normCount1perRC)

        contingency = calculateContingency(alfa, meanDict, stDevDict)
        contingencyDict[phaseID] = (contingency[0], contingency[1])
        print("the contingency for phase {} is {} years, from {} to {}".format(phaseID,
                                                    contingency[2],
                                                    contingency[0],
                                                    contingency[1]))
        relevance = calculateRelevance(
            float(contingency[2]), alfa, meanDict, stDevDict)
        print("relevance {}\n\n".format(relevance))

        plotDict10(output_folder, dict10, str(phaseID) + '_10_plots')
        plotDictNorm(output_folder, dictNorm, str(phaseID) + '_norm_plots')

        plot_coveredIntervals(output_folder, phasesDict[phaseID], datesDict, dict10, str(
            phaseID) + '_covered_intervals')

    for i in range(1, len(phasesList)):
        transition = bounds[phasesList[i]][0] - bounds[phasesList[i - 1]][1]
        transitionDict[i] = (bounds[phasesList[i]][0],
                             bounds[phasesList[i - 1]][1])
        print("the transition from phase {} to phase {} spans {} years from {} to
{}".format(phasesList[i - 1],
                                                        phasesList[i],
                                                        transition,
                                                        bounds[phasesList[i]][0],
                                                        bounds[phasesList[i - 1]][1]))
    return contingencyDict, transitionDict
```

```
def run(dataset_file, output_folder, alfa=1):
    '''runs analysis given sigma multiplicative factor, uses dataset.csv input file
    creates output folder containing the results'''

    # script starts here
    startTime = time.clock()

    # dataset_file is the csv file containing the dataset
    if not os.path.exists(dataset_file):
        raise Exception('Unable to find dataset.csv')

    # threshold is defined using a std norrmal distribution, only used in 1-0 method
    threshold = stats.norm.cdf(alfa) - stats.norm.cdf(-1 * alfa)

    datesDict, phasesDict = read_dates(dataset_file)
    contingencyDict, transitionDict = None, None
    if len(phasesDict.keys()) > 1:
        contingencyDict, transitionDict = phase_analysis(
            output_folder,
            alfa, datesDict, phasesDict)

    meanDict = {}
    stDevDict = {}
    datesList = sorted(datesDict.keys())
    for dateID in datesList:
        meanDict[dateID] = datesDict[dateID][0]
        stDevDict[dateID] = datesDict[dateID][1]
    uppBound, lowBound = findUpperLower(alfa, meanDict, stDevDict)
    dict10 = buildDict10(alfa, meanDict, stDevDict,
                         lowBound, uppBound, threshold)
    count1perRC, normCount1perRC = build_count1perRC(dict10, meanDict)
    dictNorm = buildDictNorm(count1perRC, meanDict,
```

```
                    lowBound, uppBound, dict10, normCount1perRC)

    produceOutput10(output_folder, meanDict, lowBound, uppBound, dict10)
    produceOutputNorm(output_folder, meanDict, lowBound, uppBound, dictNorm)

    contingency = calculateContingency(alfa, meanDict, stDevDict)

    # the following code explicitly returns contingency, relevance and representativity in literal
form
    std_out = "{} alfa:\n\n".format(alfa)
    std_out += "The contingency interval is {} - {} ({} years)\n".format(contingency[0],
                                                    contingency[1],
                                                    contingency[2])

    x_years = sorted(dict10.keys())
    minx, maxx = x_years[0], x_years[-1]

    std_out += "Total span: {} - {} \n\n".format(minx, maxx)

    representativity = calculateDatasetRepresentativity(
        float(contingency[2]), alfa, meanDict, stDevDict)
    if type(representativity) == type(str()):
        std_out += representativity
    else:
        std_out += "The contingency interval is representative of the {}% of the dataset
period\n".format(
            representativity)

    std_out += "\nRC determinations relevance:\n"
    relevance = calculateRelevance(
        float(contingency[2]), alfa, meanDict, stDevDict)
    if type(relevance) == type(dict()):
        for j in relevance:
```

```
        std_out += "{} : {}%\n".format(relevance[j][0], relevance[j][1])
    else:
       std_out += relevance
    std_out += '\n'

    # plots everything (to file)
    plotDict10(output_folder, dict10, 'all_dataset_' +
            '_10_plots', contingencyDict, transitionDict)
    plotDictNorm(output_folder, dictNorm, 'all_dataset_' +
             '_norm_plots', contingencyDict, transitionDict)
    datesList = sorted(datesDict.keys())
    plot_coveredIntervals(output_folder, datesList, datesDict, dict10, 'all_dataset_' +
                    '_covered_intervals', contingencyDict, transitionDict)

    endTime = time.clock()

    std_out += "Script runtime: " + str((endTime - startTime)) + " seconds"

    # saves std_out results
    save_std_out(output_folder, std_out)
```

3) Ward and Wilson Test

```
TITLE = 'ward_and_wilson'


def run(dataset_file, output_folder, confidence_level=0):
    '''reads the input csv file with RC determinations and prints
    the result of the test of Ward and Wilson'''


    # script starts here
    startTime = time.clock()
```

```
# dataset_file is the csv file containing the dataset
if not os.path.exists(dataset_file):
    raise Exception('Unable to find dataset.csv')


datesDict, phasesDict = read_dates(dataset_file)
meanDict = {}
stDevDict = {}
datesList = sorted(datesDict.keys())
for dateID in datesList:
    meanDict[dateID] = datesDict[dateID][0]
    stDevDict[dateID] = datesDict[dateID][1]
pm_num = sum([float(meanDict[dateID]) /
            float(stDevDict[dateID])**2 for dateID in datesList])
pm_den = sum([1 / float(stDevDict[dateID])**2 for dateID in datesList])
pooled_mean = pm_num / pm_den
pooled_var = 1 / pm_den
pooled_stDev = math.sqrt(pooled_var)


test_statistics = sum([((float(meanDict[dateID]) - pooled_mean)**2) /
                    float(stDevDict[dateID])**2 for dateID in datesList])
threshold = []
if confidence_level == 0:
    threshold = list(stats.chi2.ppf(
        [0.90, 0.95, 0.99], len(datesList) - 1))
```

```
    if test_statistics < threshold[0]:
        std_out = "Test passed at confidence level of 90%\nRC determinations may refer to
the same date\n\n"
        std_out += "Best estimated date: {} +/- {}\n".format(
            pooled_mean, pooled_stDev)
    elif test_statistics < threshold[1]:
        std_out = "Test passed at confidence level of 95%\nRC determinations may refer to
the same date\n\n"
        std_out += "Best estimated date: {} +/- {}\n".format(
            pooled_mean, pooled_stDev)
    elif test_statistics < threshold[2]:
        std_out = "Test passed at confidence level of 99%\nRC determinations may refer to
the same date\n\n"
        std_out += "Best estimated date: {} +/- {}\n".format(
            pooled_mean, pooled_stDev)
    else:
        std_out = "Test not passed with confidence level of 99%\nRC determinations do not
refer to the same date\n\n"

    std_out += 'Pooled mean: {}\n'.format(pooled_mean)
    std_out += 'Pooled sigma: {}\n'.format(pooled_stDev)
    std_out += 'Test statistics: {}\n\n'.format(test_statistics)
    std_out += 'CV1: {}\n'.format(threshold[0])
    std_out += 'CV2: {}\n'.format(threshold[1])
    std_out += 'CV3: {}\n'.format(threshold[2])
```

```
    elif confidence_level > 0 and confidence_level <= 100:
        threshold = list(stats.chi2.ppf(
            [float(confidence_level) / 100], len(datesList) - 1))
        if test_statistics < threshold[0]:
            std_out = ("Test passed at confidence level of {}%\nRC determinations may refer to
the same date\n\n"
                       .format(confidence_level))
            std_out += "Best estimated date: {} +/- {}".format(
                pooled_mean, pooled_stDev)
        else:
            std_out = ("Test not passed with confidence level of {}%\nRC determinations do not
refer to the same date\n\n"
                       .format(confidence_level))
        std_out += 'Pooled mean: {}\n'.format(pooled_mean)
        std_out += 'Pooled sigma: {}\n'.format(pooled_stDev)
        std_out += 'Test statistics: {}\n\n'.format(test_statistics)
        std_out += 'CV: {}\n'.format(threshold[0])

    else:
        raise Exception('Confidence level expressed in the wrong format')



    endTime = time.clock()
```

```
    std_out += "\nScript runtime: " + str((endTime - startTime)) + " seconds"


    save_std_out(output_folder, std_out)
```

4) Wiggle-matching Algorithm

```
TITLE = 'wiggle_matching_algorithm'


def read_intcal(filename):
    '''reads intcal13 file or other calibration curve as dataframe
    adds corresponding AD/BC year for each cal BP year
    defines corresponding C14 upper and lower curve'''
    whole_calcurve = pd.read_table(filename, sep=',')
    whole_calcurve['ADBC'] = 1950 - whole_calcurve['CAL BP']
    whole_calcurve['C14upper'] = whole_calcurve[' 14C age'] + whole_calcurve['Error']
    whole_calcurve['C14lower'] = whole_calcurve[' 14C age'] - whole_calcurve['Error']
    return whole_calcurve


def findUpperLower(alfa, meanDict, stDevDict):
    '''returns the extreme years of the overall interval covered by the dataset'''
    datesList = sorted(meanDict.keys())
    uppBound, lowBound = meanDict[datesList[0]], meanDict[datesList[0]]
    for date in datesList:
        up = meanDict[date] + alfa * stDevDict[date]
        low = meanDict[date] - alfa * stDevDict[date]
        if up > uppBound:
            uppBound = up
        if low < lowBound:
            lowBound = low
    return uppBound, lowBound
```

```
def calculateContingency(alfa, meanDict, stDevDict):
    '''returns the contingency interval, i.e. the largest interval of years common to all
    measurements of the dataset. If there is no common interval, there is no contingency
    and the result means a distance between the closest non-overlapping measurements
    Result is given as a tuple: (upper bound, lower bound, interval length)'''

    dateList = sorted(meanDict.keys())
    up = []
    low = []
    for date in dateList:
        up.append(meanDict[date] + alfa * stDevDict[date])
        low.append(meanDict[date] - alfa * stDevDict[date])
    return min(up), max(low), min(up) - max(low)


def calculateRelevance(contingency, alfa, meanDict, stDevDict):
    '''relevance of a measurement is the ratio between a measurement interval
    and the contingency interval and is given as a percentage. In other words
    it quantifies how well a measurement interval covers the contingency interval.
    Obviously, it is only significant when a contingency interval exists.'''

    dateList = sorted(meanDict.keys())
    if contingency < 0:
        return ("No contingency interval exists for this dataset\n")
    relev = {}
    up = []
    low = []
    for date in dateList:
        mean = meanDict[date]
        relev[date] = (mean, (100 * contingency / ((mean + alfa *
                                        stDevDict[date]) - (mean - alfa * stDevDict[date]))))
    return relev
```

```
def calculateDatasetRepresentativity(contingency, alfa, meanDict, stDevDict):
    '''Dataset representativity is the ratio, expressed as a percentage, between the
    lengths of the contingency interval and the total interval covered by the dataset.
    Obviously, it is only significant when a contingency interval exists.'''

    dateList = sorted(meanDict.keys())
    if contingency < 0:
        return ("No contingency interval exists for this dataset\n")
    up = []
    low = []
    for date in dateList:
        up.append(meanDict[date] + alfa * stDevDict[date])
        low.append(meanDict[date] - alfa * stDevDict[date])
    return (100 * (contingency / (max(up) - min(low))))


def buildDict10(alfa, meanDict, stDevDict, lowBound, uppBound, threshold):
    '''builds a dictionary with as many keys as years covered by the dataset.
    A value contains:
    0) a list of either 1 or 0, where 1 in poition j means that the year is covered
        by the j-th measurement of the dataset, 0 if it is not
    1) the sum of the numbers in the list in 0)
    2) ratio between sum in 1) and number of measurements (i.e. number of actual 1s and
        number of total possible 1s)
    3) signed difference between the ratio in 2) and a threshold'''

    dateList = sorted(meanDict.keys())
    dict10 = {}
    for i in range(lowBound, uppBound + 1):
        dict10[i] = [[], 0.0, 0.0, 0.0]
        for date in dateList:
            if (i >= meanDict[date] - alfa * stDevDict[date] and
```

```
                i <= meanDict[date] + alfa * stDevDict[date]):
            dict10[i][0].append(1)
        else:
            dict10[i][0].append(0)
    dict10[i][1] = sum(dict10[i][0])
    dict10[i][2] = float(dict10[i][1]) / float(len(dateList))
    dict10[i][3] = dict10[i][2] - threshold
return dict10


def build_count1perRC(dict10, meanDict):
    '''uses the result of buildDict10 to build 2 lists, which will be used in buildDictNorm,
    to take into account variances of single measurements.
    It counts the number of 1s for a measurement, i.e. the width of its interval, in the first
    list and the ratio 1-to-count in the second list.
    These lists have as many elements as measurements'''

    dateList = sorted(meanDict.keys())
    count1perRC = []
    for j in range(len(dateList)):
        count = 0
        for i in dict10:
            count += dict10[i][0][j]
        count1perRC.append(float(count))
    normCount1perRC = []
    for count in count1perRC:
        normCount1perRC.append(1.0 / count)
    return count1perRC, normCount1perRC


def buildDictNorm(count1perRC, meanDict, lowBound, uppBound, dict10,
normCount1perRC):
    '''builds a dictionary with as many keys as years covered by the dataset.
```

```
    A value contains:
    0) a list of positive floats <=1. Number in position j represents the weight
       of measurement j on that year
    1) the sum of the numbers in the above list
    2) distance of the sum in 1) and the maximum possible sum, which would occur
       when a year is covered by all measurements
    3) ratio between the sum in 1) and the maximum possible sum, given as %'''

    dateList = sorted(meanDict.keys())
    dictNorm = {}
    for i in range(lowBound, uppBound + 1):
        dictNorm[i] = [[], 0.0, 0.0, 0.0]
        for j in range(len(dateList)):
            val = float(dict10[i][0][j]) / count1perRC[j]
            dictNorm[i][0].append(val)
        dictNorm[i][1] = sum(dictNorm[i][0])
        dictNorm[i][2] = sum(normCount1perRC) - dictNorm[i][1]
        try:
            dictNorm[i][3] = 100 * dictNorm[i][1] / sum(normCount1perRC)
        except ZeroDivisionError:
            dictNorm[i][3] = 0.0
    return dictNorm


def phase_analysis(alfa, datesDict, phasesDict):
    threshold = stats.norm.cdf(alfa) - stats.norm.cdf(-1 * alfa)

    contingencyDict = {}
    transitionDict = {}
    dict10_byphase_dict = {}
    dictNorm_byphase_dict = {}

    bounds = {}
```

```
phasesList = sorted(phasesDict.keys())
for phaseID in phasesList:
    meanDict = {}
    stDevDict = {}
    for dateID in phasesDict[phaseID]:
        meanDict[dateID] = datesDict[dateID][0]
        stDevDict[dateID] = datesDict[dateID][1]

    uppBound, lowBound = findUpperLower(alfa, meanDict, stDevDict)
    bounds[phaseID] = (uppBound, lowBound)

    dict10 = buildDict10(alfa, meanDict, stDevDict,
                         lowBound, uppBound, threshold)
    dict10_byphase_dict[phaseID] = dict10

    count1perRC, normCount1perRC = build_count1perRC(dict10, meanDict)
    dictNorm = buildDictNorm(
        count1perRC, meanDict, lowBound, uppBound, dict10, normCount1perRC)
    dictNorm_byphase_dict[phaseID] = dictNorm

    contingency = calculateContingency(alfa, meanDict, stDevDict)
    contingencyDict[phaseID] = (contingency[0], contingency[1])

    relevance = calculateRelevance(
        float(contingency[2]), alfa, meanDict, stDevDict)

for i in range(1, len(phasesList)):
    transition = bounds[phasesList[i]][0] - bounds[phasesList[i - 1]][1]
    transitionDict[i] = (bounds[phasesList[i]][0],
                         bounds[phasesList[i - 1]][1])

return contingencyDict, transitionDict, dict10_byphase_dict, dictNorm_byphase_dict
```

```
def quickSort(thisList,low,high,propertyIndex):
    '''standard function to sort a list of numbers in ascending order'''
    i,j = low,high
    mid = int((high+low)/2)
    pivot = thisList[mid][propertyIndex]
    while (i <= j):
        while thisList[i][propertyIndex] < pivot :
            i+=1
        while thisList[j][propertyIndex] > pivot :
            j-=1
        if i < j :
            a = thisList[i]
            thisList[i] = thisList[j]
            thisList[j] = a
            i+=1
            j-=1
        elif i == j:
            i+=1
            j-=1
    if low < j:
        quickSort(thisList,low,j,propertyIndex)
    if i < high :
        quickSort(thisList,i,high,propertyIndex)

def sort_dates(datesList):
    '''date means are collected in a list and sorted
    returns a dictionary where key is dateID and value is sorted position'''
    sorted_dates = []
    for j in range(len(datesList)):
        sorted_dates.append([datesList[j], datesDict[datesList[j]][0]])
    quickSort(sorted_dates, 0, len(sorted_dates)-1, 1)
    sorted_dates_Dict = {}
```

```
    for j in range(len(sorted_dates)):
        sorted_dates_Dict[sorted_dates[j][0]] = j
    return sorted_dates_Dict


def set_calcurve(datesDict, alfa, y_min, y_max, filename):
    '''read calibration curve and select part of interest, based on dataset'''
    whole_calcurve = read_intcal(filename)

    wider_margin = int((y_max - y_min)*0.02)
    intcal_upperbound = max(whole_calcurve.index[whole_calcurve[' 14C age'] ==
min(whole_calcurve[' 14C age'][whole_calcurve[' 14C age'] >= y_max])].tolist())-
wider_margin
    intcal_lowerbound = min(whole_calcurve.index[whole_calcurve[' 14C age'] ==
max(whole_calcurve[' 14C age'][whole_calcurve[' 14C age'] <
y_min])].tolist())+wider_margin
    intcal = whole_calcurve[intcal_upperbound:intcal_lowerbound]

    return intcal


def find_cal_extremes(intcal, y_min, y_max):
    '''find left_index e right_index, i.e. intcal data frame row indices of extreme calibrated
dates for the dataset'''
    for yC14 in (y_min,y_max+1):
        up_index_xleft = intcal.index[intcal['C14upper'] ==
min(intcal['C14upper'][intcal['C14upper'] >= yC14])].tolist()
        up_index_xright = intcal.index[intcal['C14upper'] ==
max(intcal['C14upper'][intcal['C14upper'] < yC14])].tolist()
        low_index_xleft = intcal.index[intcal['C14lower'] ==
min(intcal['C14lower'][intcal['C14lower'] >= yC14])].tolist()
        low_index_xright = intcal.index[intcal['C14lower'] ==
max(intcal['C14lower'][intcal['C14lower'] < yC14])].tolist()
```

```
        if yC14 == y_min:
            right_index = up_index_xright[0]
            for index in (up_index_xright+low_index_xright):
                if intcal['ADBC'][index] > intcal['ADBC'][right_index]:
                    right_index = index
        else:
            left_index = up_index_xleft[0]
            for index in (up_index_xleft+low_index_xleft):
                if intcal['ADBC'][index] < intcal['ADBC'][left_index]:
                    left_index = index

    return left_index, right_index


def build_all_dates_df(intcal, left_index, right_index):
    '''calcurve is defined discretely and does not cover each year BP.
    For annual precision of calbration, all BP years (annual bins) are needed.
    The function interpolates for missing years and builds a version of calcurve in the interval
of interest
    where each row is a BP year.'''

    all_dates_Dict = {
        "CAL BP":[],
        "14C age":[],
        "ADBC":[],
        "Error":[],
        "C14upper":[],
        "C14lower":[]}

    index_CE = left_index
    for xADBC in range(intcal['ADBC'][left_index], intcal['ADBC'][right_index]+1):
        if xADBC in (intcal['ADBC'].tolist()):
            index_CE = intcal.index[intcal['ADBC'] == xADBC].tolist()[0]
```

```
            all_dates_Dict["CAL BP"].append(intcal["CAL BP"][index_CE])
            all_dates_Dict["14C age"].append(intcal[" 14C age"][index_CE])
            all_dates_Dict["Error"].append(intcal["Error"][index_CE])
            all_dates_Dict["ADBC"].append(xADBC)
            all_dates_Dict["C14upper"].append(intcal["C14upper"][index_CE])
            all_dates_Dict["C14lower"].append(intcal["C14lower"][index_CE])
        else:
            index_FL = index_CE+1
            all_dates_Dict["CAL BP"].append(all_dates_Dict["CAL BP"][-1]-1)
            y14C_CE = intcal[" 14C age"][index_CE]
            y14C_FL = intcal[" 14C age"][index_FL]
            xADBC_CE = intcal["ADBC"][index_CE]
            xADBC_FL = intcal["ADBC"][index_FL]
            y14C = y14C_CE - (xADBC_CE-xADBC)*(y14C_CE-y14C_FL)/(xADBC_CE-
xADBC_FL)
            all_dates_Dict["14C age"].append(y14C)
            all_dates_Dict["ADBC"].append(xADBC)
            error_CE = intcal["Error"][index_CE]
            error_FL = intcal["Error"][index_FL]
            error = error_CE - (xADBC_CE-xADBC)*(error_CE-error_FL)/(xADBC_CE-
xADBC_FL)
            all_dates_Dict["Error"].append(error)
            up_y14C_CE = intcal["C14upper"][index_CE]
            up_y14C_FL = intcal["C14upper"][index_FL]
            up_y14C = up_y14C_CE - (xADBC_CE-xADBC)*(up_y14C_CE-
up_y14C_FL)/(xADBC_CE-xADBC_FL)
            all_dates_Dict["C14upper"].append(up_y14C)
            low_y14C_CE = intcal["C14lower"][index_CE]
            low_y14C_FL = intcal["C14lower"][index_FL]
            low_y14C = low_y14C_CE - (xADBC_CE-xADBC)*(low_y14C_CE-
low_y14C_FL)/(xADBC_CE-xADBC_FL)
            all_dates_Dict["C14lower"].append(low_y14C)
```

```
    all_dates_df = pd.DataFrame(all_dates_Dict, index=all_dates_Dict["CAL BP"])

    return all_dates_df



def calibrate_contingency_by_phase(phasesDict, all_dates_df, dict10_byphase_dict,
dictNorm_byphase_dict):
    '''calibration of contingency by phase
    xBP is the annual bin on the x-axis
    noIntcalError: calibrated contingency is contingency at y=calcurve(xBP)
    IntcalError: calibrated contingency is the average contingency measured along the vertical
thickness of calcurve at x=xBP'''

    phasesList = sorted(phasesDict.keys())
    calibDict10_noIntcalError = {}
    for phaseID in phasesList:
        calibDict10_noIntcalError[phaseID] = {}
        for xBP in (all_dates_df.index.tolist()):
            xADBC = all_dates_df["ADBC"][xBP]
            yC14 = all_dates_df["14C age"][xBP]
            try:
                cont10 = dict10_byphase_dict[phaseID][yC14][1]
            except:
                cont10 = 0
            calibDict10_noIntcalError[phaseID][xBP] = cont10
        all_dates_df["cont10_noIntcalError_"+str(phaseID)] =
pd.Series(calibDict10_noIntcalError[phaseID])

    calibDictNorm_noIntcalError = {}
    for phaseID in phasesList:
        calibDictNorm_noIntcalError[phaseID] = {}
        for xBP in (all_dates_df.index.tolist()):
```

```
            xADBC = all_dates_df["ADBC"][xBP]
            yC14 = all_dates_df["14C age"][xBP]
            try:
                contNorm = dictNorm_byphase_dict[phaseID][yC14][1]
            except:
                contNorm = 0
            calibDictNorm_noIntcalError[phaseID][xBP] = contNorm
        all_dates_df["contNorm_noIntcalError_"+str(phaseID)] =
pd.Series(calibDictNorm_noIntcalError[phaseID])


    calibDict10_IntcalError = {}
    for phaseID in phasesList:
        calibDict10_IntcalError[phaseID] = {}
        for xBP in (all_dates_df.index.tolist()):
            xADBC = all_dates_df["ADBC"][xBP]
            contList = []
            for yC14 in range(int(round(all_dates_df["C14lower"][xBP])),
int(round(all_dates_df["C14upper"][xBP]))+1):
                try:
                    cont10 = dict10_byphase_dict[phaseID][yC14][1]
                    contList.append(cont10)
                except:
                    contList.append(0)
            calibDict10_IntcalError[phaseID][xBP] = sum(contList)
        all_dates_df["cont10_IntcalError_"+str(phaseID)] =
pd.Series(calibDict10_IntcalError[phaseID])

    calibDictNorm_IntcalError = {}
    for phaseID in phasesList:
        calibDictNorm_IntcalError[phaseID] = {}
        for xBP in (all_dates_df.index.tolist()):
            xADBC = all_dates_df["ADBC"][xBP]
```

```
            contList = []
            for yC14 in range(int(round(all_dates_df["C14lower"][xBP])),
int(round(all_dates_df["C14upper"][xBP]))+1):
                try:
                    contNorm = dictNorm_byphase_dict[phaseID][yC14][1]
                    contList.append(contNorm)
                except:
                    contList.append(0)
            calibDictNorm_IntcalError[phaseID][xBP] = sum(contList)
        all_dates_df["contNorm_IntcalError_"+str(phaseID)] =
pd.Series(calibDictNorm_IntcalError[phaseID])

def set_pdf(datesCollection, pdf_type='uniform'):
    '''calculate probability distribution function (pdf, or line height) for each date
    only uniform distribution considered here'''
    prob = {}
    pdf = 0
    for dateID in datesCollection:
        prob[dateID] = {}
        mean, sigma = datesDict[dateID][0], datesDict[dateID][1]
        if pdf_type == 'uniform':
            y_min, y_max = mean-alfa*sigma, mean+alfa*sigma
            pdf = 1/(y_max - y_min)
            for i in range(y_min, y_max+1):
                prob[dateID][i] = pdf
        if pdf_type == 'normal':
            for i in range(mean-3*sigma, mean+3*sigma+1):
                pdf = stats.norm(i, mean, sigma)
                prob[dateID][i] = pdf

    return prob

def calibrate_pdf_single_date(phasesDict, all_dates_df, prob):
```

```
    '''calculate calibrated distribution function for each date (improperly known as "calibrated mini-gaussian")'''
    calibDict_bydate = {}
    phasesList = sorted(phasesDict.keys())
    for phaseID in phasesList:
        calibDict_bydate[phaseID] = {}
        for dateID in phasesDict[phaseID]:
            calibDict_bydate[phaseID][dateID] = {}
            for xBP in (all_dates_df.index.tolist()):
                xADBC = all_dates_df["ADBC"][xBP]
                probList = []
                for yC14 in range(int(round(all_dates_df["C14lower"][xBP])), int(round(all_dates_df["C14upper"][xBP]))+1):
                    try:
                        probList.append(prob[dateID][yC14])
                    except:
                        continue
                if sum(probList) > 0:
                    calibDict_bydate[phaseID][dateID][xADBC] = 0.5*sum(probList)/all_dates_df["Error"][xBP]
    return calibDict_bydate

def calibrate_pdf_combined_dates(phasesDict, all_dates_df, prob):
    '''calculate combined calibrated probability distribution function (prob column).
    At each x=xBP, it calculates the mean of all line heights (uncal pdf) taken along the vertical thickness of calcurve'''
    calibDict = {}

    for xBP in (all_dates_df.index.tolist()):
        xADBC = all_dates_df["ADBC"][xBP]
        probList = []
        for dateID in datesDict:
            prob_one_date = []
```

```
        for yC14 in range(int(round(all_dates_df["C14lower"][xBP])),
int(round(all_dates_df["C14upper"][xBP]))+1):
            try:
                prob_one_date.append(prob[dateID][yC14])
            except:
                continue
        probList.append(0.5*sum(prob_one_date)/all_dates_df["Error"][xBP])
    calibDict[xBP] = sum(probList)
  all_dates_df["prob"] = pd.Series(calibDict)


def wiggleMatching(phasesDict, all_dates_df, phaseID, phaseStart, phaseEnd, prob=None):
  '''given a user-specified temporal window for the phase (in BP years),
  the function builds a dictionary which, for each date, assigns the average pdf along the
calcurve thickness to each xADBC.
  If the date pdf interval is completely outside of the calcurve domain (no-hit), the minimum
distance between the pdf interval
  and the calcurve, in the specified phase window, is assigned to the date'''
  wmDict_byDate = {}
  if prob == None:
    prob = set_pdf(phasesDict[phaseID])
  for dateID in phasesDict[phaseID]:
    mean, sigma = datesDict[dateID][0], datesDict[dateID][1]
    wmDict_byDate[dateID] = {}
    min_dist = 1000
    for xBP in range(phaseStart, phaseEnd+1):
      xADBC = all_dates_df["ADBC"][xBP]
      probList = []
      for yC14 in range(int(round(all_dates_df["C14lower"][xBP])),
int(round(all_dates_df["C14upper"][xBP]))+1):
        try:
          probList.append(prob[dateID][yC14])
        except:
```

```
                continue
            if sum(probList) > 0:
                wmDict_byDate[dateID][xADBC] = 0.5*sum(probList)/all_dates_df["Error"][xBP]
            else:
                dist_from_upper = (mean-alfa*sigma) - all_dates_df["C14upper"][xBP]
                dist_from_lower = all_dates_df["C14lower"][xBP] - (mean+alfa*sigma)
                dist = None
                if (dist_from_upper>0.0) & (dist_from_lower<0.0):
                    dist = dist_from_upper
                elif (dist_from_upper<0.0) & (dist_from_lower>0.0):
                    dist = dist_from_lower
                if (dist!=None):
                    if dist < min_dist:
                        min_dist = dist
        if len(wmDict_byDate[dateID].keys()) == 0:
            wmDict_byDate[dateID]["min_dist"] = min_dist

    return wmDict_byDate


def wiggleMatching_hypotheses(time_hp_dict, phasesDict, datesDict, all_dates_df):
    '''The user specifies a list of time windows for each phase.
    The function calculates a measure for the matching.
    The measure is the sum of the calibrated pdf areas for each date hitting calcurve in the specified window.
    If no-hit, the min distance from calcurve is subtracted from the above sum.
    The so-designed measure highly penalizes dates of the same phase when at least one of them shows a no-hit
    in the phase window hypothesized'''

    '''It has ABSOLUTELY nothing to do with wiggle-matching properly defined and established in literature.
    Needs to be substantially modified: right now it does not allow to isolate outliers, nor to
```

match a wiggle.

Need to make the assumption of fixed intervals between measures to shift measures left and right for actual wiggle matching’”

“‘Alternative approach: OPTIMIZATION, possibly with inclusion of stratigraphic knowledge (i.e. introduction of contraints)”’

```
wmHyp_dict = {}
for phaseID in time_hp_dict:
    max_area = 0
    hp_max_area = (0,0)
    wmHyp_dict[phaseID] = {}
    prob = set_pdf(phasesDict[phaseID])
    for hp in time_hp_dict[phaseID]:
        wmDict = wiggleMatching(phasesDict, all_dates_df, phaseID, hp[0], hp[1], prob)
        area = 0
        penalty = 0
        for dateID in wmDict:
            pdf_max = 0
            if list(wmDict[dateID].keys()) == [‘min_dist’]:
                penalty = -wmDict[dateID]["min_dist"]
                continue
            else:
                for xADBC in wmDict[dateID]:
                    if type(xADBC) == str:
                        continue
                    pdf = wmDict[dateID][xADBC]
                    if pdf > pdf_max:
                        pdf_max = pdf
                    area += pdf
            if area > max_area:
                max_area = area
                hp_max_area = hp
```

```
            wmHyp_dict[phaseID][hp[0] + 0.5*(hp[0]-hp[1])] = area + penalty

        return wmHyp_dict

def plot_wiggle_matching(time_hp_dict, phasesDict, datesDict, all_dates_df, versN,
shortDatasetName, dataset_name, output_folder):
    '''Plots the result of wiggleMatching_hypotheses.
    The matching measure for a time window is a line height in the central point of the window.
    Matching measures are plotted on the calcurve, at y=average(phase date means)'''
    ''' Positive matching in green, negative (unacceptable) matching in red'''
    wmHyp_dict = wiggleMatching_hypotheses(time_hp_dict, phasesDict, datesDict,
all_dates_df)
    phasesList = sorted(wmHyp_dict.keys())

    x = intcal['ADBC']
    intcalcurve = intcal[' 14C age']
    lowercurve = intcal['C14lower']
    uppercurve = intcal['C14upper']

    fig = plt.figure(figsize = (10,10))
    gs = matplotlib.gridspec.GridSpec(1, 1, left=0.08, right=0.98, top=0.93, bottom=0.05)
    ax = fig.add_subplot(gs[:, :])
    ax.set_title("Wiggle matching analysis of {}".format(dataset_name), size=14, ha='center')
    ax.set_xlabel("Calibrated (calBC)", size=12)
    ax.set_ylabel("C14 (BP)", size=12)
    ax.axis([min(x), max(x), min(lowercurve), max(uppercurve)])
    scalefactory = 500
    ax.text(ax.axis()[0]+3, ax.axis()[3]+1, "IntCal13 atmospheric curve (Reimer et al. 2013)",
            fontsize=7)

    #draw calibration curve
    ax.plot(x,intcalcurve, color='black', linewidth=0.3, alpha=0.2, gid="intcal")
    ax.plot(x,lowercurve, color='black', linewidth=0.3, gid="intcal")
```

```
    ax.plot(x,uppercurve, color='black', linewidth=0.3, gid="intcal")
    ax.fill_between(x, lowercurve, uppercurve, facecolor='lightgray', gid="intcal")

    color=iter(plt.cm.Set2(np.linspace(0.1,0.9,len(phasesList))))
    colors = list(color)

    for i in range(len(phasesList)):
        color = colors[i]
        phaseID = phasesList[i]
        prob = set_pdf(phasesDict[phaseID])

        meanList = []
        for j in range(len(phasesDict[phaseID])):
            dateID = phasesDict[phaseID][j]
            #draw C14 contingency by phase on y-axis
            yC14s = sorted(prob[dateID].keys())
            values = [prob[dateID][yC14] for yC14 in yC14s]
            ax.hlines(yC14s, ax.axis()[0]+15*j,
ax.axis()[0]+15*j+scalefactory*(pd.Series(values)), lw=2,
                      color=color, alpha=0.4, gid=phaseID)
            ax.text(ax.axis()[0]+15*j, 10+max(yC14s),
                "{}".format(dateID), ha='center', fontsize='10', color='k', fontweight='bold',
gid=phaseID)
            meanList.append(datesDict[dateID][0])
        mean_of_phase = np.mean(meanList)
        xBP_list = wmHyp_dict[phaseID].keys()
        xADBC_list = [1950 - xBP for xBP in xBP_list]
        matching_measure = pd.Series(wmHyp_dict[phaseID])
        ax.plot(xADBC_list,
              mean_of_phase+matching_measure,
              color='gray',linewidth=0.2, gid=phaseID)
        ax.plot(xADBC_list,
              mean_of_phase+0*matching_measure,
```

```
            color='gray',linewidth=0.2, gid=phaseID)
        ax.fill_between(xADBC_list, mean_of_phase,
            mean_of_phase+matching_measure, where=matching_measure > 0,
            color="lightgreen",alpha=0.6, gid=phaseID)
        ax.fill_between(xADBC_list, mean_of_phase,
            mean_of_phase+matching_measure, where=matching_measure <= 0,
            color="coral",alpha=0.6, gid=phaseID)
        ax.text(ax.axis()[1]-100, ax.axis()[3]-50-20*i,
            "Phase: {}".format(phaseID),
            ha='center', fontsize='16', color=color, fontweight='bold', gid=phaseID)

    output_filename = output_folder + os.path.sep + "wiggleMatching_" + shortDatasetName +
"_" + str(alfa) + "sigma_" + str(versN)
    plt.savefig(output_filename + ".svg", dpi=300)
    plt.savefig(output_filename + ".png", dpi=300)


def run(dataset_file, output_folder='.', **kwargs):
    dataset_name = "DATASET_NAME"
    shortDatasetName = "SHORT_DATASET_NAME"
    global alfa, versN
    versN = 1
    alfa = 1

    curve_filename = output_folder + os.path.sep + 'intcal13_curve.txt'

    global datesDict, phasesDict, intcal
    datesDict, phasesDict = read_dates(dataset_file)
    phasesList = sorted(phasesDict.keys())
    means, sigmas = [datesDict[i][0] for i in datesDict.keys()], [datesDict[i][1] for i in
datesDict.keys()]
    y_min = min([means[i]-alfa*sigmas[i] for i in range(len(means))])
    y_max = max([means[i]+alfa*sigmas[i] for i in range(len(means))])
```

```
    intcal = set_calcurve(datesDict, alfa, y_min, y_max, curve_filename)
    left_index, right_index = find_cal_extremes(intcal, y_min, y_max)
    all_dates_df = build_all_dates_df(intcal, left_index, right_index)
    contingencyDict, transitionDict, dict10_byphase_dict, dictNorm_byphase_dict =
phase_analysis(
            alfa, datesDict, phasesDict)
    calibrate_contingency_by_phase(phasesDict, all_dates_df, dict10_byphase_dict,
dictNorm_byphase_dict)
    prob = set_pdf(datesDict)
    calibDict_bydate = calibrate_pdf_single_date(phasesDict, all_dates_df, prob)

    # wiggle matching interval set
    time_hp_dict = {"E1":[(i,i+100) for i in range(3500,4115+1)]}
    plot_wiggle_matching(time_hp_dict, phasesDict, datesDict, all_dates_df, versN,
shortDatasetName, dataset_name, output_folder)
```

Appendix II

Following: Egyptian re-worked stone vessels and relative confronts mentioned in Chapter III.

*Fig. 1 Akr*1800*

Fig. 2 NM 592

Fig. 3 NM 829

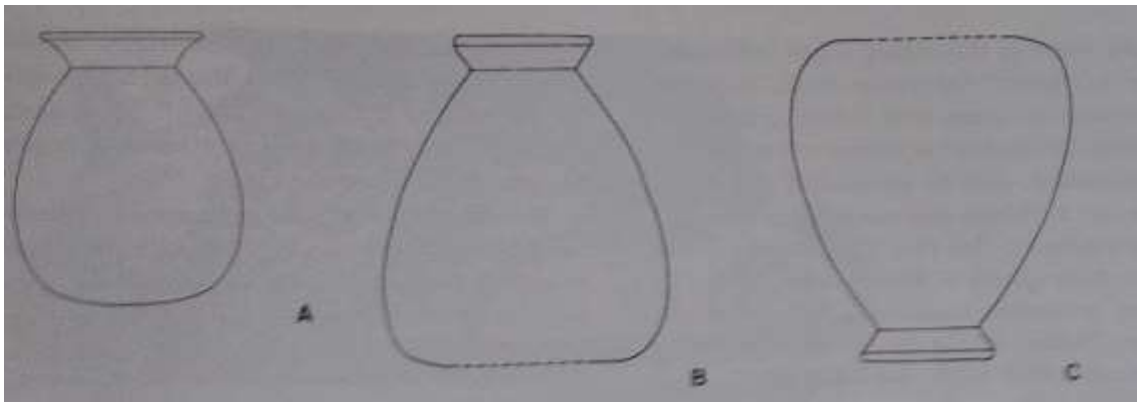

Fig. 4 Alabastron from Alalakh VII (A), Process of transformation of a baggy Egyptian alabastron into a Minoan jug (B-C, after Warren, 2006, fig.1B-C)

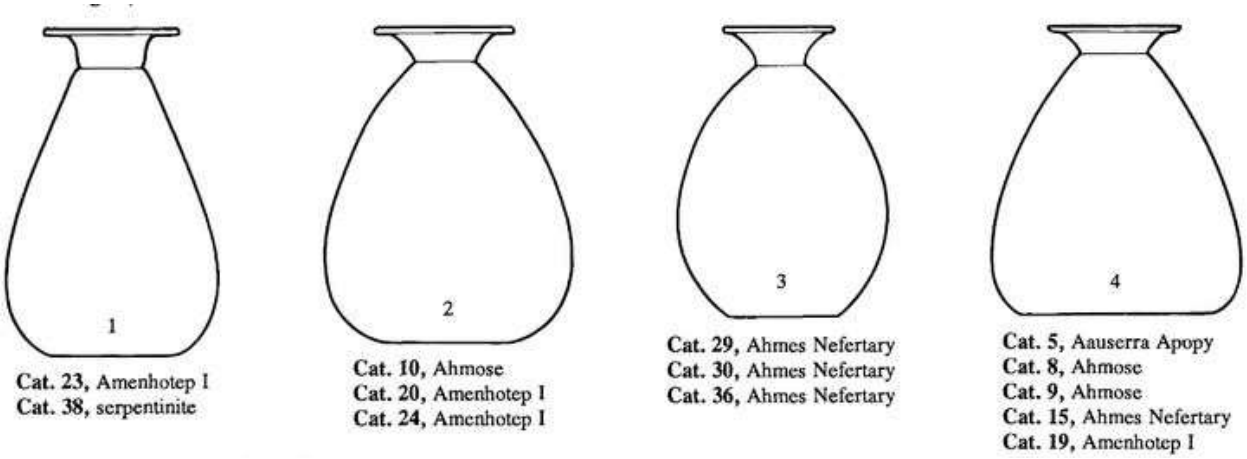

Fig. 5 Carter's shapes for the Early NK (after Lilyquist, 1995)

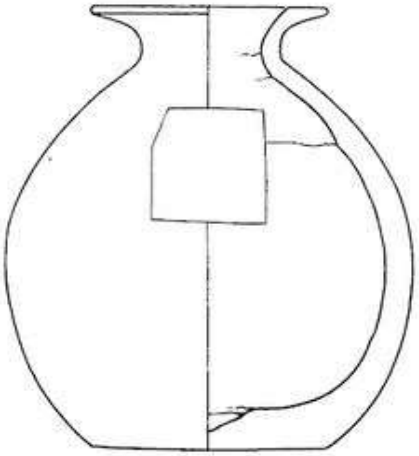

Fig. 31. **Cat. 29.** Ahmes Nefertary;
Carter shape 3; inscription, Fig. 35

Fig. 6 Securly dated Egyptian baggy alabastron (after Lilyquist, 1995, fig. 31)

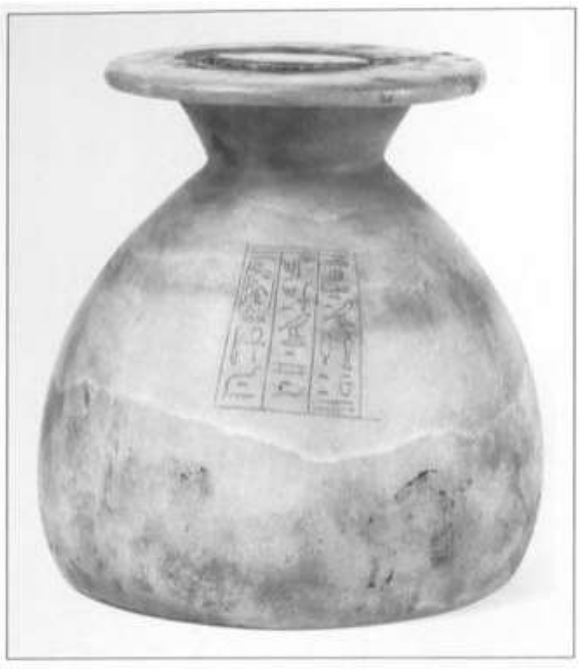

Fig. 66. **Cat. 56.** Tuthmosis II (Hatshepsut)

Fig. 67. *Left*, **Cat. 58.** Tuthmosis II (Hatshepsut);

Fig. 7 Typical baggy alabastra of Thutmoside age (after Lilyquist, 1995)

Bibliography

Aston, D.A., in collaboration with M. Bietak, with assistance of B. Bader, I. Forstner-Mueller and R. Schiestl, *Tell el Dab'a XII: A Corpus of Late Middle Kingdom and Second Intermediate Period Pottery* (vol I: Text, vol II: Plates). UZK, No. XXIII, OAW, Vienna, 2004.

Aström, P., Three Tell el Yahudiyeh juglets in the Thera Museum. In A. Kalogeropoulou (ed.), *Acta of the first scientific congress on the volcano of Thera*, Archaeological Services of Greece, Athens, 1971, pp. 415-21.

Aström, P., *The Swedish Cyprus Expedition*. Vol. IV, part 1B, Swedish Cyprus Expedition, Lund, 1992.

Bader, B., *Tell el Dab'a XIX, Auaris und Memphys in der Hyksoszeit, Vergleichsanalyse der materielles Kultur*. UZK, No. XXXI, OAW, Vienna, 2009.

Barber, C.J.W., *Prehistoric Textiles: The Development of Cloth in the Neolithic and Bronze Age with Special Reference to the Aegean*. Princeton University Press, Princeton, 1991.

Barrett, C.E., The Perceived Value of Minoan and Minoanizing Pottery in Egypt. *Journal of Mediterranean Archaeology*, No. 22.2, 2009, pp. 211-34.

Bass, G., A Bronze Age Shipwreck at Ulu Burun (Kas): 1984 Campaign. *American Journal of Archaeology*, Vol. 90, No. 3, 1986, pp. 269–96.

Bass, G., Sailing Between the Aegean and the Orient in the Second millennium BC. In E.H. Cline, D. Harris-Cline (eds.), *The Aegean and the Orient in the Second Millenium*. Proceedings of the 50th anniversary symposium *Aegaeum*, No. 18, Université de Liège, Liège, 1998, pp.

183-92.

Beckerath (Von), J., *Chronologie des pharaonischen Ägypten. Die Zeitbestimmung der ägyptischen Geschichte von der Vorzeit bis 332 v. Chr*. Münchner Ägyptologische Studien 46, Philipp von Zabern-Verlag, Mainz am Rhein, 1997.

Ben-Tor, D., Hazor and Chronology. *Aegypten und Levante/Egypt and the Levant*, Vol. XIV, 2004, pp. 45-67.

Ben-Tor, D., Evidence for Middle Bronze Age Chronology and Synchronisms in the Levant: A Response to Höflmayer et al. 2016. *Bulletin of the American Schools of Oriental Research*, No. 379, May 2018, pp. 43-54.

Bergoffen, C.J., *A Comparative Study of the Regional Distribution of Cypriote Pottery in Canaan and Egypt in the Late Bronze Age*. Ph.D. Dissertation, New York University, 1989.

Bergoffen, C.J., The Proto White Slip and White Slip I Pottery from Tell el-'Ajjul. In V. Karageorghis (ed.), *The White Slip Ware of Late Bronze Age Cyprus*. *Proceedings of an International Conference Organized by the Anastasios G. Leventis foundation, Nicosia, in Honour of Malcolm Wiener, Nicosia, 29th-30th October 1998*, OAW, Vienna, 2001, pp. 145-56.

Bergoffen, C.J., The Cypriote pottery from Alalakh: Chronological Considerations. In M.W. Bietak (ed.), *The synchronisation of Civilisations in the Eastern Mediterranean in the Second millennium BC. Proceedings of the SCIEM 2000-Euro Conference, Haindorf, 2-7 May 2001* (Contribution to the chronology of the Eastern Mediterranean 4). Vol. II, OAW, Vienna, 2003, pp. 395-410.

Bevan, A., Emerging Civilized Values? The Consumption and Imitation of Egyptian Stone Vessels in EMII-MMI Crete and its Wider Eastern Mediterranean Context. In J.C. Barrett, P. Halstead (eds.), *The Emergence of Civilisation Revisited*, Sheffield Studies in Aegean Archaeology 6, Oxbow Books, Oxford, 2004, pp. 107-26.

Bichler, M., Exler, M., Peltz, C., Saminger, S., Thera ashes. In: M.W. Bietak (ed.), *The*

synchronisation of civilisations in the Eastern Mediterranean in the Second Millennium B.C. Proceedings of the SCIEM 2000-Euro Conference, Haindorf, 2-7 May 2001 (Contribution to the chronology of the Eastern Mediterranean 4). OAW, Vienna, 2003, pp. 11-21.

Bietak, M.W., Une citadelle royale à Avaris de la première moitié de la XVIII dinastie et ses liens avec le monde minoen. In A. Caubet (ed.), *L'acrobate au Taureau*, Documentation Française, Musée du Louvre, Paris, 1999, pp. 48-9.

Bietak, M.W., Seal Impressions from the Middle till the New Kingdom: A Problem for Chronological Research. In: M.W. Bietak, E. Czerny (eds.), *Scarabs of the Second Millennium BC from Egypt, Nubia, Crete and the Levant: Chronological and Historical Implications, Papers of a Symposium, Vienna, 10th – 13th of January 2002*. Contributions to the Chronology of the Eastern Mediterranean, vol. VII, OAW, Vienna, 2004, pp. 43-55.

Bietak, M.W., Antagonisms in Historical and Radiocarbon Chronology. In: A.J. Shortland, C. Bronk Ramsey (eds.), *Radiocarbon and the Chronologies of Ancient Egypt*, Oxbow Books, Oxford, 2013, pp. 76-109.

Bietak, M.W., Recent Discussions about the Chronology of the Middle and the Late Bronze Ages in the Eastern Mediterranean: Part I. *Bibliotheca Orientalis, LXXII*, N. 3-4, mei-augustus 2015, pp. 317-35.

Bietak, M.W., War Bates Island bei Marsah Matruh ein Piratennest? Ein Betrag zur Frühen Geschichte der Seevölker. In S. Nawracala (ed.), *ΠΟΛΥΜΑΘΕΙΑ – Festschrift für Hartmut Matthäus anlässlich seines 65. Geburtstages*. Shaker Verlag, Aachen, 2015, pp. 31-43.

Bietak, M.W., Sturt W. Manning, A Test of Time and A Test of Time Revisited: The Volcano of Thera and the Chronology and History of the Aegean and East Mediterranean in the mid-second Millennium BC. 2nd Edition (first edition 1999). *Bryn Mawr Classical Review* 2016.04.06 (http://bmcr.brynmawr.edu/2016/2016-04-06.html).

Bietak, M.W., A Thutmosid Palace Precinct at Peru Nefer/Tell el Dab'a. In M.W. Bietak, S. Prell (eds.), *Palaces in Ancient Egypt and the Ancient Near East vol. I: Egypt*, Contributions to the Archaeology of Egypt, Nubia and the Levant, No. V, OAW, Vienna, 2018, pp. 231-57.

Bietak, M.W., Dorner, J., Bagh, T., Czerny, E., Bartosek, J., Der Tempel und die Siedlung des Mittleren Reiches bei 'Ezbet Ruschdi: Grabungsvorbericht 1996. *Aegypten und Levante/Egypt and the Levant*, Vol. VIII, 1998, pp. 9-49.

Bietak, M.W., Marinatos, N., Avaris (Tell el Dab'a) and the Minoan World. In A. Karetsou (ed.), *Κρήτη – Αίγυπτος: πολιτισμικοί δεσμοί τριών χιλιετιών. Μελέτες*. Kapon, Athens, 2000.

Bietak, M.W., Hein, I., The Context of White Slip Wares in the Stratigraphy of Tell el-Dab'a and some Conclusions on Aegean Chronology. In V. Karageorghis (ed.), *The White Slip Ware of Late Bronze Age Cyprus*, *Proceedings of an International Conference Organized by the Anastasios G. Leventis foundation, Nicosia, in Honour of Malcolm Wiener, Nicosia, 29th-30th October 1998*, OAW, Vienna, 2001, pp. 171-94.

Bietak, M.W., Dorner, J., Jànosi, P., Ausgrabungen in dem Palastbezirk von Avaris, Vorbericht Tell el-Dab'a/'Ezbet Helmi 1993-2000, with a contribution by A. von den Driesch and J. Peters. *Aegypten und Levante/Egypt and the Levant*, Vol. XI, 2003, pp. 27-129.

Bietak, M.W., Höflmayer, F., Introduction: High and Low Chronology. In M.W. Bietak, E. Czerny (eds.), *The synchronisation of civilisations in the Eastern Mediterranean in the Second Millennium B.C. Proceedings of the SCIEM 2000-2nd Euro Conference, Vienna, 28 of May-1st of June 2003* (Contribution to the chronology of the Eastern Mediterranean 9), OAW, Vienna, 2007, pp. 13-23.

Bietak, M.W., Marinatos, N., Palyvou, C., *Taureador scenes from Tell el Dab'a and Knossos*. OAW, Vienna, 2007.

Bietak, M.W., Kopetzky, K., Stager, L.E., Voss, R., Synchronisation of Stratigraphies: Ashkelon and Tell el-Dab'a. *Aegypten und Levante/Egypt and the Levant*, Vol. XVIII, 2008, pp. 49-60.

Branigan, K., The genesis of the Household Goddes. *SMEA*, No. 8, 1969, pp. 28-38.

Breasted, J.H., *A History of Egypt from the Earliest Times to the Persian Conquest. Second*

Edition, Fully Revised. Charles Schribner's Sons, New York, 1948.

Bronk-Ramsey, C., Bayesian Analysis of Radiocarbon Dates. *Radiocarbon*, No. 51(1), 2009, pp. 337-60.

Bronk-Ramsey, C., Dee, M.W., Rowland, J.M., Higham, T.F.G., Harris, S.A., Brock, F., Quiles, A., Wild, E.M., Marcus, E.M., Shortland, A.J., Radiocarbon-BasedChronology for Dynastic Egypt. *Science*, No. 328, 2010, p. 1554.

Carinci, F.M., Western Mesara and Egypt during the Protopalatial period: a minimalist point of view. In A. Karetsou (ed.): *Κρήτη - Αίγυπτος: πολιτισμικοί δεσμοί τριών χιλιετιών. Μελέτες*. Kapon, Athens, 2000, pp. 31-9.

Cherubini, P., Humbel, T., Beeckman, H., Gärtner, H., Mannes, D., Pearson, C., Schoch, W., Tognetti, R., Lev-Yadun, S., Olive Tree-Ring Problematic Dating: A Comparative Analysis on Santorini (Greece). *PLoS ONE*, No. 8(1), 2013, https://doi.org/10.1371/journal. pone.0054730.

Clausen, B.H., Hammer, C.U., Hvidberg, C.S., Dhal-Jensen, D., Steffensen, J.P., Kipfstuhl, J, Legrand, M., A Comparison of the Volcanic Records over the past 4000 years from the Greenland Ice Core Project and DYE-3 Greenland Ice Cores. *Journal of Geophysical Research*, No. 102, 1997, pp. 707-23.

Cline, E.H., *Sailing the Wine-Dark Sea: International Trade and the Late Bronze Age Aegean*. BAR International Series 591, Oxford, 1994.

Crowley, J., Iconography and Interconnections. The Aegean and the Orient in the Second Millenium. In E.H. Cline, D. Harris-Cline (eds.), *The Aegean and the Orient in the Second Millenium. Proceedings of the 50th anniversary symposium*. *Aegaeum*, No. 18, Université de Liège, Liège, 1998, pp. 171-82.

Cultraro, M., *I Micenei*. Carocci, Roma, 2006.

Daressy, G., Les branches du Nil sous la XVIIIeme Dynastie. *BSGE*, No. 16, 1928/29, pp. 225-

54.

Dietz, S., *The Argolid at the transition to the Mycenaean age. Studies in the Chronology and Cultural Development in the Shaft Graves Period*. National Museum of Denmark, Copenaghen, 1991.

Doumas, C., *The Wall Paintings of Thera*. The Thera Foundation, Athens, 1992.

Duhoux, Y., *Des Minoens en Egypte?* Peeters, Leuven, 2003.

Easton, D., Weninger, B., A possible new Bronze Age period at Troy. *Anatolian Studies*, No. 68, 2018, pp. 33-73.

Ehrlich, Y., Regev, L., Boaretto, E., Radiocarbon analysis of modern olive wood raises doubts concerning a crucial piece of evidence in dating the Santorini eruption. *Nature Scientific Reports*, No. 8, 2018, article no. 11841, https://www.nature.com/articles/s41598-018-29392-9.

Eriksson, K.O., Late Cypriot I and Thera: Relative Chronology in the Eastern Mediterranean. In P. Aström (ed.), *Acta Cypria. Acts of an international congress on Cypriote archaeology held in Göteborg on 22-24 August 1991. Studies in Mediterranean Archaeology and Literature, Pocketbook 120*, Åströms förlag, Göteborg, 1992, pp. 152-223.

Eriksson, K. O., *Red Lustrous Wheel-made Ware*. SIMA 103, Åströms förlag, Jonsereds, 1993.

Eriksson, K. O., Cypriote Proto White Slip and White Slip I: Chronological Beacons on Relations between Late Cypriote I Cyprus and Contemporary Socities of the Eastern Mediterranean. In V. Karageorghis (ed.), *The White Slip Ware of Late Bronze Age Cyprus*, *Proceedings of an International Conference Organized by the Anastasios G. Leventis foundation, Nicosia, in Honour of Malcolm Wiener, Nicosia, 29th-30th October 1998*. OAW, Vienna, 2001, pp. 51-64.

Eriksson, K.O., Using Cypriot Red Lustrous Wheel-made Ware to establish Cultural and Chronological Synchronisms during the Late Bronze Age. In I. Hein (ed.), *The Lustrous Wares*

of Late Bronze Age Cyprus and the Eastern Mediterranean: Papers of a Conference, Vienna 5th-6th of November 2004. OAW, Vienna, 2007, pp. 61-70.

Evans, A.J., *The Palace of Minos: a comparative account of the successive stages of the early Cretan civilization as illustrated by the discoveries at Knossos*. Macmillan and Co., London, 1935.

Fantuzzi, T., The Debate on Aegean High and Low Chronologies: an Overview through Egypt. *Rivista di Archeologia*, XXXI, Bretschneider Editore, Padova-Venezia, 2007, pp. 53-65.

Fantuzzi, T., Antolini, F., Drawing the Line: Bayesian modelling and absolute chronology in the case-study of the Minoan eruption at Thera. In: G. Baldacci, I. Caloi, (eds.), *Rhadamanthys: Studies in Minoan archaeology in honour of Filippo Carinci in the occasion of his 70th Birthday*. BAR S2884, Oxford, 2018, pp. 247-54.

Faure, P., La pierre ponce en Crète, du Néolithique à nos jours. In A.G. Kalageropoulou (ed.), *Acta of the first scientific congress on the volcano of Thera*, Archaeological Services of Greece, 1971, pp. 422-29.

Feldman, M., *Diplomacy by Design: Luxury Arts and an "International Style" in the Ancient Near East 1400-1200 BCE*. Chicago University Press, Chicago-London, 2006.

Fischer, H.G., *Egyptian Titles of The Middle Kingdom: A Supplement to E. A. Ward's Index I-III*. Metropolitan Museum of Art, New York, 1985.

Fischer, P.M., White Slip I and II from Tell Abu al-Kharaz, Jordan Valley: Pottery Synchronism and Dating. In V. Karageorghis (ed.), *The White Slip Ware of Late Bronze Age Cyprus*, *Proceedings of an International Conference Organized by the Anastasios G. Leventis foundation, Nicosia, in Honour of Malcolm Wiener, Nicosia, 29th-30th October 1998*. OAW, Vienna, 2001, pp. 161-70.

Fischer, P.M., The Chronology of Tell el-'Ajjul, Gaza. In D.A. Warburton (ed.), *Time's Up! Dating the Minoan eruption of Santorini. Acts of the Minoan Eruption Chronology Workshop,*

Sandbjerg, November 2007 (Jan Heinemeier & Walter L. Friedrich). Vol. X, Monographs of the Danish Institute at Athens, Aarhus, 2009, pp. 253-65.

Forstner-Mueller, I., *Tell el Dab'a XVI: Die Graeber des Areals A/II von Tell el Dab'a*. UZK XXVIII, Vienna, 2008.

Foster, K.P., Sterba, J.H., Steinhauser, G., Bichler, M., The Thera eruption and Egypt: pumice, texts and chronology. In D.A. Warburton (ed.), *Time's Up! Dating the Minoan eruption of Santorini. Acts of the Minoan Eruption Chronology Workshop, Sandbjerg, November 2007 (Jan Heinemeier & Walter L. Friedrich)*. Vol. X, Monographs of the Danish Institute at Athens, Aarhus, 2009, pp. 171-80.

Friedrich, W.L., Kromer, B., Friedrich, M., Heinemeier, J., Pfeiffer, T., Talamo, S., Santorini Eruption Radiocarbon Dated to 1627-1600 B.C. *Science*, No. 312, 2006, p. 548.

Friedrich, W.L., Heinemeier, J., The Minoan eruption of Santorini radiocarbon dated to 1613±13 BC. In: D.A. Warburton (ed.), *Time's Up! Dating the Minoan eruption of Santorini. Acts of the Minoan Eruption Chronology Workshop, Sandbjerg, November 2007 (Jan Heinemeier & Walter L. Friedrich)*. Vol. X, Monographs of the Danish Institute at Athens, Aarhus, 2009, pp. 56-64.

Friedrich, W.L., Kromer, B., Friedrich, M., Heinemeier, J., The olive branch chronology stands irrespective of tree-ring counting. *Antiquity*, No. 88, Issue 339, 2014, pp. 274-7.

Gardiner, A., *Egyptian Grammar: Being an Introduction to the Study of Hieroglyphs, third edition Revised*. Griffith Institute, Ashmolean Museum, Oxford, 1957.

Gill, M., The Minoan Genius. *AM*, No. 79, 1964, pp. 1-21.

Glanville, S.R.K., Records of a Royal Dockyard of the Time of Tuthmosis III: Papyrus BM 10056, Part I. *Zeitschrift für Ägyptische Sprache und Altertumskunde*, Vol. LXVI, 1931, pp. 105-121.

Glanville, S.R.K., Records of a Royal Dockyard of the Time of Tuthmosis III: Papyrus BM 10056, Part II. *Zeitschrift für Ägyptische Sprache und Altertumskunde*, Vol. LXVIII, 1932, pp. 7-41.

Grimal, N., *Histoire de l'Égypte ancien*. Éditions Fayard, Paris, 1988.

Gundacker, R., Minoan Presence in the Pharaonic Naval Base of Peru-Nefer. In O. Krszyszkowska (ed.), *Cretan Offerings: Studies in Honour of Peter Warren*. BSA Studies 18, London, 2010, pp. 11-24.

Gundacker, R., Papyrus British Museum 10056: Ergebnisse einer Neukollationierung und Anmerkungen zur inhaltlichen Auswertung im Rahmen der militärischen Ausbildung Amenophis' II. *Aegypten und Levante/Egypt and the Levant*, Vol. XXVII, 2017, pp. 281-334.

Haider, P.W., Minoan Deities in an Egyptian Medical Text. In R. Laffineur, R. Hägg (eds.), *Potnia. Deities and Religion in the Aegean Bronze Age. Proceedings of the 8th International Aegean Conference, Göteborg University, 12-15 april 2000*. *Aegaeum*, No. 22, Université de Liège, Liege-Austin, 2001, pp. 479-82.

Hammer, C.U., Kurat, G., Hoppe, P., Grum, W., Clausen, H.B., Thera Eruption Date 1645 BC Confirmed by New Ice Core Data? In M.W. Bietak, E. Czerny (eds.), *The synchronisation of Civilisations in the Eastern Mediterranean in the Second millennium BC*. OAW, Vienna, 2003, pp. 87-94.

Hankey, V., Leonard, A., Aegean LB I-II Pottery in the East: "Who is the Potter, Pray, and Who is the Pot?". In E.H. Cline, D. Harris-Cline (eds.), *The Aegean and the Orient in the Second Millenium. Proceedings of the 50th anniversary symposium*. *Aegaeum*, No. 18, Université de Liège, Liège, 1998, pp. 29-39.

Hein, I., The Significance of the Lustrous Ware Finds from 'Ezbet Helmi/Tell el-Dab'a. In I. Hein (ed.), *The Lustrous Wares of Late Bronze Age Cyprus and the Eastern Mediterranean. Papers of a Conference, Vienna 5th–6th November 2004*, OAW, Vienna, 2007, pp. 79-106.

Hein, I., Second thoughts on Cypriot pottery and first appearances. In: I. Forstner-Müller, N. Möller (eds.), *The Hyksos Ruler Khayan and the Early Second Intermediate Period in Egypt. Problems and Priorities of Current Research. Proceedings of the Workshop of the Austrian Archaeological Institute and the Oriental Institute of the University of Chicago, Vienna, July 4–5, 2014*. OAW, Vienna, 2018, pp. 125-42.

Helck, W., Die Fahrt von Ägypten nach Kreta. *Mitteilungen des Deutschen Archäologischen Instituts Abteilung*, Deutsches Archäologisches Institut, Cairo, No. 39, 1983, pp. 81-92.

Höflmayer, F., The date of the Minoan Santorini Eruption: Quantifying the "Offset". *Radiocarbon*, No. 54 (3-4), 2012, pp. 435-48.

Höflmayer, F., An Early Date for Khayan and Its Implications for Eastern Mediterranean Chronologies. In I. Forstner-Müller, I., N. Möller (eds.), *The Hyksos Ruler Khayan and the Early Second Intermediate Period in Egypt: Problems and Priorities of Current Research*, *Proceedings of the Workshop of the Austrian Archaeological Institute and the Oriental Institute of the University of Chicago, Vienna, July 4–5, 2014*. OAW, Vienna, 2018.

Hornung, E., Krauss, R., Warburton, D.A., (eds.), *Ancient Egyptian Chronology*. Handbuch der Orientalistik 83, Brill, Leiden-Boston, 2006.

Kantor, H.J., *Plant Ornament in the Ancient Near East*. Chicago Oriental Institute, Chicago, 1948.

Kemp, B.J., Merrillees, R.S., *Minoan Pottery in Second millennium Egypt*. Philippe Von Zabern Verlag, Mainz am Rhein, 1980.

Kemp, B.J., The discovery of the painted plaster fragments from Malkata. In A. Karetsou (ed.), *Κρήτη – Αίγυπτος: πολιτισμικοί δεσμοί τριών χιλιετιών. Μελέτες*. Kapon, Athens, 2000, pp. 45-6.

Kempinsky, A., *Tel Kabri, the 1986-1993 Excavation Seasons*. Series 20, Tel Aviv University, Institute of Archaeology Monographs, Tel Aviv, 2002.

Kopetzky, K., *Datierung der Graeber der Grabungsflaesche F/I von Tell el Dab'a anhand der Keramik*. Unpublished Master script of the University of Vienna (in press), 1993.

Kopetzky, K., Typologhische Bemerkungen zur Siedlungskeramik von A/V-p/19. In I. Hein, P. Janosi (eds.), *Tell el Dab'a XI, Areal A/V, Siedlungsrelikte der spaeten 2. Zwischenzeit*. UZK XXI, Vienna, 2004, pp. 237-335.

Kopetzky, K., *Tell el Dab'a XX: Die Chronologie der Siedlungskeramik der Zweite Zwischenzeit aus Tell el Dab'a*. Part I-II. UZK XXXII, Vienna, 2010, pp. 165-7, 170.

Kutschera, W., Bietak, M.W., Wild, E.M., Bronk-Ramsey, C., Dee, M., Golser, R., Kopetzky, K., Stadler, P., Steier, P., Thanheiser, U., Weninger, F., The chronology of Tell el Dab'a: a crucial meeting point of ^{14}C dating, archaeology, and Egyptology in the 2nd Millennium BC. *Radiocarbon*, No. 54 (3-4), 2012, pp. 407-22.

Kyriakidis, E., Indications of the Nature of the Language of the Keftiu from Egyptian Sources. *Aegypten und Levante/Egypt and the Levant*, Vol. XII, 2002, pp. 211-9.

La Marche, V.C., Hirschboek, K.K., Frost Rings in Trees as Record of Major Volcanic Eruptions. *Nature*, No. 307, 1984, pp. 121-6.

Levi, D., Gli scavi a Festo nel 1956 e 1957. *Annuario della Scuola Archeologica Italiana di Atene e delle Missioni Italiane in Oriente*, No. 35/36, All'Insegna del Giglio, Firenze, 1957/58, pp. 193-361.

Libby, W.F., Anderson, E.C., Arnold, J.R., Age determination by radiocarbon content: World-wide assay of natural radiocarbon. *Science*, No. 109, 1949, pp. 227-8.

Lichtheim, M., *Ancient Egyptian Literature: A Book of Readings*. UCLA press, Berkeley-Los Angeles-London, 1976.

Lilyquist, C., *Egyptian Stone Vessels. Khyan to Thutmosi IV.* Metropolitan Museum of Art, New

York, 1995.

Lilyquist, C., Egyptian Stone Vases? Comments on Peter Warren's paper. In R. Laffineur, P.P. Betancourt (eds.), *TEXNH. Craftsmen, Craftswomen, and Craftmanship in the Aegean Bronze Age. Proceedings of the 6th International Aegean Conference, Philadelphia, Temple University 18-21 April 1996. Aegaeum*, No. 16, Université de Liège, Liège-Austin, 1997, pp. 225-7.

MacGillivray, A., A Minoan cup at Tell el Dab'a. *Aegypten und Levante/Egypt and the Levant*, Vol. V, 1995, pp. 81-4.

MacGillivray, A., *Knossos: Pottery Groups of the Old Palace Period*. British School at Athens Studies V, London, 1998.

Maguire, L.C., *The Cypriot Pottery and its Circulation in the Levant: Tell el Dab'a XXI*. OAW, Vienna, 2009.

Manning, S.W., *A test of Time: the volcano of Thera and the chronology and history of the Aegean and east Mediterranean in the mid-second millennium BC*. Oxbow Books, Oxford, 1999.

Manning, S.W., Clarifying the High versus Low Aegean/Cypriot Chronology for the Mid Second millennium BC: Assessing the Evidence, Interpretive Frameworks and Current State of the Debate. In M.W. Bietak, E. Czerny (eds.), *The Synchronisation of Civilisations in the II millennium BC, III.* OAW, Vienna, 2007, pp. 101-38.

Manning, S.W., *A test of Time. Revised edition.* Oxbow Books, Oxford, 2014.

Margueron, J-C., *Mari: Métropole de l'Euphrate au IIIéme et au Débout du IIéme Millénaire av. J-C*. Picard, Paris, 2004.

Marinatos, N., Lions from Tell el Dab'a. *Aegypten und Levante/Egypt and the Levant*, Vol. XX, 2010, pp. 325-55.

Marinatos, N., Morgan, L., The Dog Pursuit scenes from Tell el Dab'a and Kea. In: L. Morgan (ed.), *Aegean Wall Painting: a Tribute to Mark Cameron*. British School at Athens Studies 13, London, 2005, pp. 119-22.

Matthäus, H., Representation of Keftiu in Egyptian Tombs and the Absolute Chronology of the Aegean Late Bronze Age. *Bulletin of the Institute of Classical Studies*, No. 40, 1995, pp. 177-94.

Matthiae, P., *Ebla. Un impero ritrovato*. Einaudi, Torino, 1995 (3ª edizione).

Merrillees, R.S., Some Cypriote White Slip Pottery from the Aegean. In: V. Karageorghis (ed.), *The White Slip Ware of Late Bronze Age Cyprus*, *Proceedings of an International Conference Organized by the Anastasios G. Leventis foundation, Nicosia, in Honour of Malcolm Wiener, Nicosia, 29th-30th October 1998*. OAW, Vienna, 2001, pp. 89-100.

Merrillees, R.S., Chronological conundrums: Cypriot and Levantine imports from Thera. In D.A. Warburton (ed.), *Time's Up! Dating the Minoan eruption of Santorini. Acts of the Minoan Eruption Chronology Workshop, Sandbjerg, November 2007 (Jan Heinemeier & Walter L. Friedrich)*. Vol. X, Monographs of the Danish Institute at Athens, Aarhus, 2009, pp. 247-52.

Möller, N., Marouard, G., Discussion of Late Middle Kingdom and Early Second Intermediate Period History and Chronology in Relation to the Khayan Sealings from Tell Edfu. *Aegypten und Levante/Egypt and the Levant*, Vol. XXI, 2011, pp. 87-121.

Morgan, L., Feline Hunters in the Tell el Dab'a Paintings: Iconography and Dating. *Aegypten und Levante/Egypt and the Levant*, Vol. XIV, 2004, pp. 285-98.

Morgan, L., Art and International Relations: The Hunt Frieze at Tell el Dab'a. In E. Czerny, I. Hein, H. Hunger, D. Melman, A. Schwab (eds.), *Timelines. Studies in Honour of Manfred Bietak*, Peeters, Leuven-Paris-Dudley, 2006, pp. 249-58.

Morgan, L., An Aegean Griffin in Egypt: the Hunt Frieze at Tell el Dab'a. *Aegypten und Levante/Egypt and the Levant*, Vol. XX, 2010(a), pp. 303-23.

Morgan, L., A Pride of Leopards: a Unique Aspect of the Hunt Frieze from Tell el Dab'a. *Aegypten und Levante/Egypt and the Levant*, Vol. XX, 2010(b), pp. 263-302.

Müller, V., *Tell el Dab'a XVII. Opferdeponierungen in der Hyksoshauptstadt Auaris (Tell el Dab'a) vom spaeten Mittleren Reich bis zum fruehen Neuen Reich, 2 Vols*. UZK XXIX, Vienna, 2008.

Niemeier, W.D., Minoan Artisans travelling Overseas: The Alalakh Frescoes and the painted Plaster Floor at Tel Kabri, Western Galilee. In R. Laffineur (ed.), *Thalassa. L'Egée Prehistorique et la mer: actes de la troisième Rencontre égéenne internationale de l'Université de Liège, Station de recherches sous-marines et océanographiques (StaReSO), Calvi, Corse, 23-25 avril 1990*. *Aegeum*, No. 7, Université de Liège, Liège, 1991, pp. 189-201.

Niemeier, W.D., Niemeier, B., Minoan Frescoes in the Eastern Mediterranean. In E.H. Cline, D. Harris-Cline (eds.), *The Aegean and the Orient in the Second Millenium. Proceedings of the 50th anniversary symposium*. *Aegaeum*, No. 18, Université de Liège, Liège, 1998, pp. 69-98.

Niemeier, W.D., Niemeier, B., Minoan Frescoes in the Eastern Mediterranean. In S. Ahituv, E.D. Oren (eds.), *Aharon Kempinski Memorial Volume*. Ben-Gurion University of the Negev Press, Beer-Sheva, 2002, pp. 86-131.

Novak, M., Pfaelzner, P., Ausgrabungen in Tall Misrife-Qatna 2000: Vorbericht der deutschen Komponente des internationalen Kooperationsprojectes. *MDOG*, No. 133, 2001, pp. 157-98.

Oren, E.D., Early White Slip Pottery in Canaan: Spatial and Chronological Perspectives. In V. Karageorghis (ed.), *The White Slip Ware of Late Bronze Age Cyprus*, *Proceedings of an International Conference Organized by the Anastasios G. Leventis foundation, Nicosia, in Honour of Malcolm Wiener, Nicosia, 29th-30th October 1998*. OAW, Vienna, 2001, pp. 127-44.

Pearce, N.J.C., Westgate, J.A., Preece, S.J., Eastwood, W.J., Perkins, W.T., Hart, J.S., Reinterpretation of Greenland Ice-core Data Recognises the presence of the Late Holocene Aniakchak Tephra, not the Minoan Tephra (Santorini) at 1645BC. In M.W. Bietak, E. Czerny

(eds.), *The Synchronisation of Civilisations in the II millennium BC, III.* OAW, Vienna, 2007, pp. 139-48.

Petrie, W.M.F., *Ten Years Digging in Egypt, 1881-1891*. The Religious Tract Society, London, 1892.

Petrie, W.M.F., *Stone and Metal Vases*. British School of Archaeology in Egypt, London, 1937.

Phillips, J., Stone Vessel Production: New Beginnings and New Visions in New Palace Crete. In A.J. Shortland (ed.), *The Social Context of Technological Change. Egypt and the Near East, 1650-1550 BC. Proceedings of a Conference Held at St. Edmund Hall, Oxford 12-14 September 2000*. Oxbow Books, Oxford, 2001, pp. 73-91.

Phillips, J., Why?... and Why Not? Minoan Reception and Perception of Egyptian Influence. In E. Czerny, I. Hein, H. Hunger, D. Melman, A. Schwab (eds.), *Timelines. Studies in Honour of Manfred Bietak*, Vol. II, Peeters, Leuven-Paris-Dudley, 2006, pp. 293-300.

Phillips, J., *Aegyptiaca on the Island of Crete in their Chronological Context: A Critical Review*. OAW, Wien, 2008.

Pomerance, L., The Possible Role of Tomb Robbers and Viziers of the 18th Dynasty in Confusing Minoan Chronology. *Antichità Cretesi. Studi in Onore di Doro Levi*. Università di Catania, Istituto di archeologia, Catania, 1978, pp. 21-30.

Popham, M.R., *The Proto White Slip Pottery of Cyprus.* Appendix I. In P. Aström, G.R.H. Wright, Two Bronze Age Tombs at Dhenia in Cyprus. *Opuscola Atheniensa*, No. 4, 1962, pp. 277-97.

Poursat, J-C., Le Bronze Moyenne en Crete. In R. Treuil, P. Darcque, J-C. Poursat, G. Touchais, (eds.), *Le Civilisation Egéennes du Neolithique et de l'Age du Bronze*, 2nd/2éme éd., Presses Universitaires de France, Paris, 2008, pp. 136-68.

Pulak, C., Discovering a Royal Ship from the Age of King Tut: Uluburun, Turkey. In G. Bass

(ed.), *Beneath the Seven Seas*, Thames and Hudson, New York, 2005, pp. 34-47.

Rehak, P., Aegean Natives in the Theban Tomb Paintings: The Keftiu Revisited. In E.H. Cline, D. Harris-Cline (eds.), *The Aegean and the Orient in the Second Millenium. Proceedings of the 50th anniversary symposium*. *Aegaeum*, No. 18, Université de Liège, Liège, 1998, pp. 39-53.

Renaudin, L., Vases préhelléniques de Théra à l'Ecole française d'Athénes. *BCH*, No. 46, 1922, pp. 113-59.

Renfrew, A.C., *The Emergence of Civilisation*. Methuen, Oxford, 1972.

Rüden (Von), C., *Die Wandmalereien von Tell Mishrifeh/Qatna im Kontext Interregionaler Kommunikation (Dissertation, University of Freiburg, 2006). Mit Beiträgen von Ann Brysbaert und Ilka Weisser*. Qatna Studies vol. 2, Harrassowitz, Wiesbaden, 2011.

Rutter, J., *Prehistoric Archaeology of the Aegean*. Site of Dartmouth College. http://www.dartmouth.edu/~prehistory/aegean/.

Schiestl, R., *Tell el Dab'a XVIII, Die Palastnekropole von Tell el Dab'a. Die Graeber des Areals F/I der Straten d/2 und d/1*. UZK XXX, Vienna, 2010.

Shaw, M.C., Bull leaping Frescoes at Knossos and their Influence on the Tell el Dab'a Murals. *Aegypten und Levante/Egypt and the Levant*, Vol. V, 1995, pp. 91-120.

Steier, P., Rom, W., The Use of Bayesian Statistics for ^{14}C Dates of Chronologically Ordered Samples: A Critical Analysis. *Radiocarbon*, No. 42.2, 2000, pp. 183-98.

Sterba, J.H., Foster, K.P., Steinhauser, G., Bichler, M., New light on old pumice: the origins of Mediterranean volcanic material from ancient Egypt. *Journal of Archaeological Science*, No. 36, 2009, pp. 1738–44.

Stos-Gale, S., Minoan foreign relations and copper metallurgy in MMIII–LMIII Crete. In A. Shortland (ed.), *The Social Context of Technological Change: Egypt and the Near East, 1650-*

1550 BC. Proceedings of a Conference Held at St. Edmund Hall, Oxford 12-14 September 2000. Oxbow Books, Oxford, 2001, pp. 195-210.

Strange, J., *Caphtor/Keftiu. A New Investigation*. Brill Archive, Leyden, 1980.

Taraqji, A.F., Nouvelle découvertes sur les relations avec l'Egypte à Tell Sakka et à Keswé, dans la région de Damas. *BSFE*, No. 144, 1999, pp. 27-43.

Treuil, R., L'evolution de la Civilisation. In R. Treuil, P. Darcque, J-C. Poursat, G. Touchais, (eds.), *Le Civilisation Egéennes du Neolithique et de l'Age du Bronze*, 2nd/2éme éd., Presses Universitaires de France, Paris, 2008, pp. 63-83.

Vandersleyen, C., *Ouadj our w3d wr. Un autre aspect de la vallée du Nil*, Connaissance de l'Égypte Ancienne, Bruxelles, 1999.

Vandersleyen, C., *L'Egypte au temps de Moïse*. L'Harmattan, Paris, 2018.

Vercoutter, J., *L'Egypte et le monde Egéen Préhellenique*, Institut français d'archéologie orientale, Cairo, 1956.

Vermeule, E.D.T., Wolsky, F.Z., *Toumba tou Skourou: The Mound of Darkness. A Bronze Age Town on Morphou Bay in Cyprus*. Harvard University Press, Cambridge, 1990.

Vinther, B.M., Clausen, H.B., Johnsen, S.J., Rasmussen, S.O., Andersen, K.K., Bruchardt, S.L., Dahl-Jensen, D., Selerstad, I.K., Siggaard-Andersen, M.L., Steffensen, J.P., Svensson, A., A Synchronized dating of three Greenland Ice Cores throughout the Holocene. *Journal of Geophysical Research*, No. 111 (D13), 2005, https://pdfs.semanticscholar.org/d2d6/6e0786db6fbe47accb8f4ff9576385c8730a.pdf.

Wachsmann, S., *Aegeans in the Egyptian Tombs*. OLA 20, Peeters, Leuven, 1987.

Walberg, G., The finds at Tell el Dab'a and the Middle Minoan Chronology. *Aegypten und Levante/Egypt and the Levant*, Vol. II, 1991, pp. 115-20.

Ward, G.K., Wilson, S.R., Procedures for comparing and combining Radiocarbon Age Determinations: a Critique. *Archeaometry*, No. 20 (I), February 1978, pp. 19-31.

Warren, P. M., *Minoan Stone Vases*. Cambridge University Press, Cambridge, 1969.

Warren, P.M., Crete and Egypt: the transmission of relationship. In A. Karetsou (ed.), *Κρήτη – Αίγυπτος: πολιτισμικοί δεσμοί τριών χιλιετιών. Μελέτες*. Kapon, Athens, 2000, pp. 24-8.

Warren, P.M., The date of the Thera Eruption in Relation to Aegean-Egyptian Interconnections and the Egyptian Historical Chronology. In E. Czerny, I. Hein, H. Hunger, D. Melman, A. Schwab (eds.), *Timelines. Studies in Honour of Manfred Bietak*, Vol. II, Peeters, Leuven-Paris-Dudley, 2006, pp. 305-21.

Warren, P.M., The Date of the Late Bronze Age Eruption of Santorini. In D.A. Warburton (ed.), *Time's Up! Dating the Minoan eruption of Santorini. Acts of the Minoan Eruption Chronology Workshop, Sandbjerg, November 2007 (Jan Heinemeier & Walter L. Friedrich)*. Vol. X, Monographs of the Danish Institute at Athens, Aarhus, 2009, pp. 181-86.

Warren, P.M., Hankey, V., *Aegean Bronze Age Chronology.* Bristol Classical Press, London, 1989.

Watrous, L.W., Egypt and Crete in the Early Middle Bronze Age: A Case of Trade and Cultural Diffusion. In In E.H. Cline, D. Harris-Cline (eds.), *The Aegean and the Orient in the Second Millenium. Proceedings of the 50th anniversary symposium*. *Aegaeum*, No. 18, Université de Liège, Liège, 1998, pp. 19-28.

Weingarten, J., The transformation of Egyptian Taweret into the Minoan Genius: A study in cultural transmission in the Middle Bronze Age. *Studies in Mediterranean Archaeology*, Vol. LXXXVIII, 1991.

Weingarten, J., The transformation of Egyptian Taweret into the Minoan Genius. In A. Karetsou (ed.), *Κρήτη – Αίγυπτος: πολιτισμικοί δεσμοί τριών χιλιετιών. Μελέτες*. Kapon, Athens, 2000,

pp. 114-9.

Weninger, B.P., High-Precision Calibration of Radiocarbon Dates. In *NITRA: Papers of the Symposium held at the Institute of Archaeology of the Slovak Academy of Sciences, Nové Vozokany, October 28-31, 1985*, Acta Interdisciplinaria Archaeologica, Tomus IV, 1986, pp. 11-54.

Weninger, B.P., Clare, L., Jöris, O., Jung, R., Edinborough, K., Quantum Theory of Radiocarbon Calibration. *World Archaeology*, No. 47, Issue 4, 2015, pp. 543-66.

Wiener, M.H., The White Slip I of Thell el-Dab'a and Thera: Critical Challenge for the Aegean Long Chronology. In V. Karageorghis (ed.), *The White Slip Ware of Late Bronze Age Cyprus*, *Proceedings of an International Conference Organized by the Anastasios G. Leventis foundation, Nicosia, in Honour of Malcolm Wiener, Nicosia, 29th-30th October 1998*. OAW, Vienna, 2001, pp. 195-202.

Wiener, M.H., A point in Time. In O. Krzyszkowska (ed.), *Cretan Offerings: Studies in Honour of Peter Warren.* British School at Athens Studies, London, 2010, pp. 367-94.

Woolley, L., *Alalakh: An account of the Excavations at Tell Atchana in the Hatay, 1937-1949*. Society of Antiquaries, London, 1955.

Yon, M., White Slip Ware in the Northern Levant. In V. Karageorghis (ed.), *The White Slip Ware of Late Bronze Age Cyprus*, *Proceedings of an International Conference Organized by the Anastasios G. Leventis foundation, Nicosia, in Honour of Malcolm Wiener, Nicosia, 29th-30th October 1998*. OAW, Vienna, 2001, pp. 117-26.

Zielinsky, G.A., Mayevski, P.A., Meeker, L.D., Whitlow, S., Twickler, M.S., Morrison, M., Meese, D.A., Gow, A.J., Alley, L.B., Record of Volcanism since 7000 BC from the GISP2 Greenland Ice Core and Implications for the Volcano – Climate System. *Science*, No. 264, 1994, pp. 948-52.

Università
Ca'Foscari
Venezia

DEPOSITO ELETTRONICO DELLA TESI DI DOTTORATO

DICHIARAZIONE SOSTITUTIVA DELL'ATTO DI NOTORIETA'

(Art. 47 D.P.R. 445 del 28/12/2000 e relative modifiche)

Io sottoscritto TIZIANO FANTUZZI

nat o a CONEGLIANO (prov. TV) il 05/08/1984

residente a CONEGLIANO in VIA A. DIAZ n. 30

Matricola (se posseduta) 825926 Autore della tesi di dottorato dal titolo:

A REASSESSMENT OF THE DEBATE ON THE MINOAN I CHRONOLOGY THROUGH RADIOCARBON AND COMPARATIVE ANALYSIS

Dottorato di ricerca in SCIENZE DELL'ANTICHITÁ

(in cotutela con .....)

Ciclo XXXI

Anno di conseguimento del titolo 2018/2019

DICHIARO

di essere a conoscenza:

1) del fatto che in caso di dichiarazioni mendaci, oltre alle sanzioni previste dal codice penale e dalle Leggi speciali per l'ipotesi di falsità in atti ed uso di atti falsi, decado fin dall'inizio e senza necessità di nessuna formalità dai benefici conseguenti al provvedimento emanato sulla base di tali dichiarazioni;

2) dell'obbligo per l'Università di provvedere, per via telematica, al deposito di legge delle tesi di dottorato presso le Biblioteche Nazionali Centrali di Roma e di Firenze al fine di assicurarne la conservazione e la consultabilità da parte di terzi;

3) che l'Università si riserva i diritti di riproduzione per scopi didattici, con citazione della fonte;

4) del fatto che il testo integrale della tesi di dottorato di cui alla presente dichiarazione viene archiviato e reso consultabile via Internet attraverso l'Archivio Istituzionale ad Accesso Aperto dell'Università Ca' Foscari, oltre che attraverso i cataloghi delle Biblioteche Nazionali Centrali di Roma e Firenze;

5) del fatto che, ai sensi e per gli effetti di cui al D.Lgs. n. 196/2003, i dati personali raccolti saranno trattati, anche con strumenti informatici, esclusivamente nell'ambito del procedimento per il quale la presentazione viene resa;

6) del fatto che la copia della tesi in formato elettronico depositato nell'Archivio Istituzionale ad Accesso Aperto è del tutto corrispondente alla tesi in formato cartaceo, controfirmata dal tutor, consegnata presso la segreteria didattica del dipartimento di riferimento del corso di dottorato ai fini del deposito presso l'Archivio di Ateneo, e che di conseguenza va esclusa qualsiasi responsabilità dell'Ateneo stesso per quanto riguarda eventuali errori, imprecisioni o omissioni nei contenuti della tesi;

7) del fatto che la copia consegnata in formato cartaceo, controfirmata dal tutor, depositata nell'Archivio di Ateneo, è l'unica alla quale farà riferimento l'Università per rilasciare, a richiesta, la dichiarazione di conformità di eventuali copie;

Data 3/12/2018 **Firma** _____

NON AUTORIZZO

l'Università a riprodurre ai fini dell'immissione in rete e a comunicare al pubblico tramite servizio on line entro l'Archivio Istituzionale ad Accesso Aperto la tesi depositata per un periodo di 12 (dodici) mesi a partire dalla data di conseguimento del titolo di dottore di ricerca.

DICHIARO

1) che la tesi, in quanto caratterizzata da vincoli di segretezza, non dovrà essere consultabile on line da terzi per un periodo di 12 (dodici) mesi a partire dalla data di conseguimento del titolo di dottore di ricerca;
2) di essere a conoscenza del fatto che la versione elettronica della tesi dovrà altresì essere depositata a cura dell'Ateneo presso le Biblioteche Nazionali Centrali di Roma e Firenze dove sarà comunque consultabile su PC privi di periferiche; la tesi sarà inoltre consultabile in formato cartaceo presso l'Archivio Tesi di Ateneo;
3) di essere a conoscenza che allo scadere del dodicesimo mese a partire dalla data di conseguimento del titolo di dottore di ricerca la tesi sarà immessa in rete e comunicata al pubblico tramite servizio on line entro l'Archivio Istituzionale ad Accesso Aperto.

Specificare la motivazione:
□ motivi di segretezza e/o di proprietà dei risultati e/o informazioni sensibili dell'Università Ca' Foscari di Venezia.
□ motivi di segretezza e/o di proprietà dei risultati e informazioni di enti esterni o aziende private che hanno partecipato alla realizzazione del lavoro di ricerca relativo alla tesi di dottorato.
□ dichiaro che la tesi di dottorato presenta elementi di innovazione per i quali è già stata attivata / si intende attivare la seguente procedura di tutela:

.....;

√Altro (specificare):

ACCORDI DI PUBBLICAZIONE CON ENTE DI RICERCA (ÖAW)

.....

.....

A tal fine:
- dichiaro di aver consegnato la copia integrale della tesi in formato elettronico tramite auto-archiviazione (upload) nel sito dell'Università; la tesi in formato elettronico sarà caricata automaticamente nell'Archivio Istituzionale ad Accesso Aperto dell'Università Ca' Foscari, dove rimarrà non accessibile fino allo scadere dell'embargo, e verrà consegnata mediante procedura telematica per il deposito legale presso la Biblioteca Nazionale Centrale di Firenze;
- consegno la copia integrale della tesi in formato cartaceo presso la segreteria didattica del dipartimento di riferimento del corso di dottorato ai fini del deposito presso l'Archivio di Ateneo.

Data 3/12/2018 **Firma** .....

La presente dichiarazione è sottoscritta dall'interessato in presenza del dipendente addetto, ovvero sottoscritta e inviata, unitamente a copia fotostatica non autenticata di un documento di identità del dichiarante, all'ufficio competente via fax, ovvero tramite un incaricato, oppure a mezzo posta.

Firma del dipendente addetto .....

Ai sensi dell'art. 13 del D.Lgs. n. 196/03 si informa che il titolare del trattamento dei dati forniti è l'Università Ca' Foscari - Venezia.
I dati sono acquisiti e trattati esclusivamente per l'espletamento delle finalità istituzionali d'Ateneo; l'eventuale rifiuto di fornire i propri dati personali potrebbe comportare il mancato espletamento degli adempimenti necessari e delle procedure amministrative di gestione delle carriere studenti. Sono comunque riconosciuti i diritti di cui all'art. 7 D. Lgs. n. 196/03.

Estratto per riassunto della tesi di dottorato

L'estratto (max. 1000 battute) deve essere redatto sia in lingua italiana che in lingua inglese e nella lingua straniera eventualmente indicata dal Collegio dei docenti.

L'estratto va firmato e rilegato come ultimo foglio della tesi.

Studente: Tiziano Fantuzzi matricola: 825926

Dottorato: Scienze dell'antichità

Ciclo: XXXI

Titolo della tesi[1]: A Reassessment of the Debate on LM I and interlinked Chronologies through Radiocarbon and Comparative Analysis

Abstract:

The absolute chronology of the Late Minoan I A period and in particular the date of the Minoan eruption at Santorini is the object of a debate which is ongoing since the 1970's, and lead many scholars to speak of a "conflict" between archaeological and Radiocarbon dating. This study presents a collation of all the main arguments for the archaeological chronology in the bibliography, and a reanalysis of the radiocarbon datasets from Akrotiri on Santorini, Tell el Dab'a in Egypt and other relevant sites for the interlinked chronology. In particular, a critic approach to the accuracy of Bayesian chronology applied so far and a new possible approach to radiocarbon interpretation based on notions from Quantum mathematics are suggested. In addition, an open source package to perform the different analyses has been developed and uploaded on-line at the site http://c14.bpinfo.org

La cronologia assoluta del periodo Tardo Minoico I A, e in particolare la data dell'eruzione minoica di Santorini è stata – ed è tuttora – oggetto di un ampio dibattito che prosegue ininterrotto dagli anni '70, e ha portato svariati studiosi a parlare di un "conflitto" tra le scienze archeologiche e i dati derivati dalla datazioni al radiocarbonio. Il presente studio comprende una rianalisi di tutti gli argomenti disponibili in bibliografia riguardo alla cronologia archeologica, combinata con una rianalisi dei dati radiometrici disponibili per la datazione dei siti-chiave di Akrotiri a Santorini e Tell el Dab'a in Egitto. In particolare, si è inteso porre in evidenza alcune criticità legate all'utilizzo dell'analisi bayesiana nella forma in cui è stata applicata al caso-studio, criticità che possono essere superate tramite un nuovo approccio alla calibrazione delle date radiocarboniche improntato su concetti della teoria fisica dei quanti.

Firma dello studente

[1] Il titolo deve essere quello definitivo, uguale a quello che risulta stampato sulla copertina dell'elaborato consegnato.